THE ROLE OF COLLAGEN-DISCOIDIN DOMAIN RECEPTOR 1 IN HPV-POSITIVE AND –NEGATIVE HEAD AND NECK CANCER

LAI SOOK LING

FACULTY OF DENTISTRY
UNIVERSITY OF MALAYA
KUALA LUMPUR

2018

THE ROLE OF COLLAGEN-DISCOIDIN DOMAIN RECEPTOR 1 IN HPV-POSITIVE AND –NEGATIVE HEAD AND NECK CANCER

LAI SOOK LING

THESIS SUBMITTED IN FULFILMENT OF THE REQUIREMENTS FOR THE DEGREE OF DOCTOR OF PHILOSOPHY

FACULTY OF DENTISTRY
UNIVERSITY OF MALAYA
KUALA LUMPUR

2018

UNIVERSITY OF MALAYA

ORIGINAL LITERARY WORK DECLARATION

Name of Candidate: Lai Sook Ling

Matric No: DHA 130003

Name of Degree: Doctor of Philosophy

Title of Project Paper/Research Report/Dissertation/Thesis ("this Work"):

The Role of Collagen-Discoidin Domain Receptor 1 in HPV-positive and –negative Head and Neck Cancer

Field of Study: Oral Oncology

I do solemnly and sincerely declare that:

(1) I am the sole author/writer of this Work;
(2) This Work is original;
(3) Any use of any work in which copyright exists was done by way of fair dealing and for permitted purposes and any excerpt or extract from, or reference to or reproduction of any copyright work has been disclosed expressly and sufficiently and the title of the Work and its authorship have been acknowledged in this Work;
(4) I do not have any actual knowledge nor do I ought reasonably to know that the making of this work constitutes an infringement of any copyright work;
(5) I hereby assign all and every rights in the copyright to this Work to the University of Malaya ("UM"), who henceforth shall be owner of the copyright in this Work and that any reproduction or use in any form or by any means whatsoever is prohibited without the written consent of UM having been first had and obtained;
(6) I am fully aware that if in the course of making this Work I have infringed any copyright whether intentionally or otherwise, I may be subject to legal action or any other action as may be determined by UM.

Candidate's Signature Date:

Subscribed and solemnly declared before,

Witness's Signature Date:

Name:

Designation:

THE ROLE OF COLLAGEN-DISCOIDIN DOMAIN RECEPTOR 1 IN HPV-POSITIVE AND –NEGATIVE HEAD AND NECK CANCER

ABSTRACT

Head and neck squamous cell carcinoma (HNSCC) is the sixth most common cancer worldwide with oropharyngeal (OPSCC) and oral cavity (OSCC) tumours being the two major subtypes. The five year survival rate of patients with HNSCC has remained around 50% for the past four decades. The global incidence rate of HPV positive OPSCC is on the rise and, for reasons that are currently unclear, patients with HPV-related disease have a better prognosis. Molecular targeted therapies are not in routine use for the treatment of HNSCC and the identification of new therapeutic targets is highly desirable, but this will only be possible with a fuller understanding of the molecular events that drive the disease process. We now know that cancers are comprised of tumour cells and non-malignant cells within the tumour microenvironment (TME). Cancer-associated fibroblasts (CAFs) are predominant within the TME and are known to promote epithelial tumour progression in part via paracrine communication with cancer cells. This study examined the role of the collagen receptor, discoidin domain receptor 1 (DDR1), in the pathogenesis of HNSCC. The results demonstrated that two collagen subtypes, COL8a1 and COL11a1, were expressed by CAFs *in vitro* and that DDR1 was overexpressed in OPSCC and OSCC tissues. The expression of these proteins was further investigated in OPSCC and OSCC tissues and correlated to socio-demographic and clinico-pathological parameters, including HPV status and patient survival. Multiplex immunohistochemistry was used in conjunction with an automated pathology system to digitally quantify expression, with staining intensities, co-expression of proteins and single cell co-localisation analysed with digital imaging software. In OPSCCs from the United Kingdom, high expression of DDR1 was found to be significantly associated with non-smokers, patients within the moderate and high risk of death groups and lower survival rates. Low expression of

COL8a1 in tumours and CAFs was significantly associated with the low risk of death group and regional lymph node metastasis N2, whilst high expression was significantly associated with smoker. In OSCCs from Malaysia, COL8a1 in tumours was significantly associated with small primary tumour depth (1-10mm), bone invasion and deceased outcome. A significant association was found between high expression of COL11a1 in CAFs with traditional risk factors of OSCC, included female gender, Indian ethnicity and betel quid chewing. Collectively, these data show that DDR1 and its ligands are expressed in OPSCCs and OSCCs and high expression levels might negatively influence patient prognosis. Next, the functional role of collagen-DDR1 signalling was examined *in vitro* using HPV-negative and –positive HNSCC cell lines. Treatment of all cell lines with collagen enhanced cell proliferation, migration and invasion, and made the cells less sensitive to apoptosis induced by Cisplatin. Knockdown of DDR1 with shRNAs confirmed these effects were specific to DDR1. In conclusion, this study demonstrated for the first time that activation of DDR1 on HNSCC cells promotes the malignant phenotype and negatively impacts upon patient prognosis. DDR1 represents a novel therapeutic target for HPV-negative and –positive HNSCC.

Keywords: head and neck squamous cell carcinoma; human papillomavirus; discoidin domain receptor 1; Collagen 8a1; Collagen 11a1

PERANAN RESEPTOR 1 DOMAIN KOLAGEN-DISKOIDIN DALAM KANSER KEPALA DAN LEHER YANG HPV-POSITIF DAN –NEGATIF

ABSTRAK

Karsinoma sel skuamus kepala dan leher (HNSCC) adalah kanser yang ke-enam paling umum di dunia, yang mana tumor orofarinks (OPSCC) dan kaviti mulut (OSCC) merupakan dua subtip yang utama. Kadar kelangsungan hidup lima tahun bagi pesakit dengan HNSCC kini kekal pada 50% dalam tempoh empat dekad. Kadar insiden OPSCC yang HPV-positif didapati meningkat pada tahap global, tetapi dengan alasan yang pada ketika ini masih samar, pengidap penyakit yang berkait-HPV didapati mempunyai prognosis yang lebih baik. Terapi yang menyasarkan molekul bukanlah sesuatu yang rutin dalam rawatan HNSCC, oleh itu pengenalan kepada target terapi yang baru adalah diharapkan. Walaubagaimanapun ini hanya dapat berlaku setelah pelbagai interaksi molekul yang mendorong kepada penyakit tersebut difahami dengan jelas. Buat masa ini diketahui bahawa kanser merangkumi sel tumor dan sel bukan maglinan yang terdapat di persekitaran mikro tumor (TME). Fibroblas yang di kait-kanser (CAFs) adalah predominan dalam TME dan diketahui meransang perkembangan tumor epitelium yang mana sebahagiannya adalah melalui komunikasi parakrin bersama sel-sel kanser. Kajian ini meneliti peranan reseptor kolagen iaitu discoidin reseptor 1 (DDR1) dalam patogenesis HNSCC. Hasil kajian menunjukkan dua subtip kolagen iaitu COL8a1 dan COL11a1, di ekspres oleh CAFs secara *in vitro* manakala DDR1 pula di ekspres dengan melampau dalam kedua-dua tisu OPSCC dan OSCC. Ekspresi protein-protein ini diselidiki lebih lanjut dalam kedua-dua tisu dan dikaitkan kepada parameter sosio-demografi dan klinik-patologi, iaitu termasuk status HPV dan kelangsungan hidup pesakit. Kaedah *multiplex immunohistochemistry* telah digunakan disamping sistem patologi yang automatik untuk menentukan kadar ekspresi secara digital, berpandukan keamatan warna, ko-ekspresi protein serta analisis *co-localisation* sel tunggal dengan

menggunakan perisian pengimejan digital. Ekspresi DDR1 yang tinggi dalam kalangan OPSCC dari United Kingdom didapati berkorelasi secara signifikan dengan bukan-perokok dan para pesakit dalam kumpulan yang berisiko kematian sederhana dan tinggi, dengan kadar kelangsungan hidup yang rendah. Ekspresi COL8a1 yang rendah dalam tumor dan CAF pula didapati berkait secara signifikan dengan kumpulan berisiko kematian yang rendah dan metastasis N2 nod limfa serantau, manakala ekspresi melampau yang signifikan dikaitkan dengan perokok. Dalam kalangan OSCC dari Malaysia, COL8a1 dalam tumor berkait secara signifikan dengan kedalaman tumor primer yang kecil (1-10mm), invasi ke tulang dan penghasilan kematian. Perkaitan yang signifikan juga ujud di antara ekspresi COL11a1 yang tinggi dalam CAF dengan faktor-faktor risiko tradisi OSCC, termasuk gender wanita, etnik India dan pengunyahan sireh-pinang. Secara kolektif, data menunjukkan bahawa DDR1 dan ligannya diekspres dalam OPSCC dan OSCC, dan tahap ekspresinya yang tinggi mungkin memberi kesan negatif kepada prognosis pesakit. Seterusnya, peranan kolagen-DDR1 turut diselidik secara *in vitro* menggunakan sel-sel HNSCC yang HPV-negatif dan -positif. Rawatan semua sel dengan kolagen didapati menggalakkan proliferasi, migrasi dan invasi sel tumor, serta menjadikan sel-sel tersebut kurang sensitif terhadap apoptosis yang diransang oleh Cisplatin. DDR1 yang di *knockdown* dengan shRNA dapat mengesahkan bahawa kesan ini adalah khusus kepada DDR1. Kesimpulannya, kajian ini menunjukkan untuk pertama kalinya bahawa pengaktifan DDR1 pada sel HNSCC menggalakkan fenotip yang malignan, dan memberi impak yang negatif kepada prognosis pesakit. DDR1 adalah sasaran terapeutik yang novel untuk HNSCC yang negatif- dan positif-jangkitan HPV.

Kata kunci: karsinoma sel skuamus kepala dan leher; papillomavirus manusia; reseptor 1 domain diskoidin; Kolagen 8a1; Kolagen 11a1

ACKNOWLEDGEMENTS

Firstly, I would like to acknowledge University of Malaya Fellowship Scheme for providing me with financial support, University Malaya Research Grant and High Impact Research for funding the research. Next, I would like to heartily thank the following people who have contributed to this research.

PhD supervisors, Prof Ian Charles Paterson, Associate Prof Dr. Ivy Chung and Dr. Yap Lee Fah. I am thankful for the mentorship from all supervisors throughout my PhD study which greatly impacted my research life in these five years. It is with deepest gratitude that I acknowledge the help of Prof Ian in the development of this project, guiding me in scientific writing, checking every draft of my thesis and correcting my mistakes. Gratefully thanks to him for providing me the opportunity to undergo training in the UK as a student visitor during my candidature and giving me the chances to contribute to a few of research publications. I would like to thank Associate Prof. Dr. Ivy who took a chance on me when I had no experience in the lab and educated me with cell culture techniques and skills with patience. Further thanks to Dr. Yap whom I look up to her enthusiasm, perseverance and determination in doing research along my study.

Research collaborator, Prof Paul Murray. I would like to thank for the contributions of my fellow collaborator who supported the project in various aspects during my training in the University of Birmingham and thereafter. He encouraged me to grow into my strength and helped me see that I can be more. I learned many new techniques and grateful for the tremendous experience on new technologies and instruments hands-on opportunities which helps a lot in my study. I credit him with not only my continued passion in science, but also be more assertive and fearless about exploring new things in life.

Research partners and peers support. A big thanks to all fantastic fellows who have directly contributed to this research. My immense gratitude to Dr. Maha Ibrahim for her

professional advice and guidance in the clinical pathology aspect and thanks for her helps and cares during my training in Birmingham; Dr. Robert Hollows and Dr. Wei WenBin for their contributions in the bioinformatics study of this project; Dr. Katerina Vrzalikova, Dr. Navta Masand, Dr. Sandra Margielewska, Dr. Ezster Nagy and Jesinda Pauline for offering me their helps and wisdoms in times of need. A big thanks to all lab members past and present who created one of the best working environments I have ever experienced. I would especially like to say thanks to Suthashini for her helps in the OSCC patients profile collection, Sathya and Wee Lin who always supported me.

There are no words that can describe the appreciation I have for my parents and family for all their unconditional support, understanding and encouragement both emotionally and financially throughout the course of my PhD.

TABLE OF CONTENTS

LIST OF FIGURES

LIST OF TABLES

LIST OF SYMBOLS AND ABBREVIATIONS

ARCAGE	:	Alcohol-Related Cancers and Genetic susceptibility in Europe
ATP	:	Adenosine triphosphate
BSA	:	Bovine Serum Albumin
CAFs	:	Cancer-associated fibroblasts
Cdna	:	Complementary DNA
CM	:	Conditioned media
COL11a1	:	Collagen type XI alpha 1 chain
COL8a1	:	Collagen type VIII alpha 1 chain
cpm	:	counts-per-million
DAPI	:	4',6-diamidino-2-phenylindole
DDR	:	Discoidin Domain Receptor
DDR1	:	Discoidin Domain Receptor 1
dH_2O	:	Distilled water
DMEM	:	Dulbecco's Modified Eagle's Medium
DMEM/F12	:	Dulbecco's modified Eagle's medium and Hams F12
DMSO	:	dimethyl sulfoxide
DNA	:	Double-stranded deoxyribonucleic acid
dNTP	:	Deoxyribonucleotide triphosphate
DS	:	Discoidin homology
E6AP	:	Ubiquitin ligase E6-associated protein
ECACC	:	European Collection of Authenticated Cell Cultures
ECL	:	Enhanced chemiluminescence
ECM	:	Extracellular matrix
EGFR	:	Epidermal growth factor receptor

ERK1/2-MAPK	:	Extracellular signal regulated kinase 1/ 2 mitogen-activated protein kinase
FACS	:	Fluorescent Activated Cell Sorter
FBS	:	Fetal bovine serum
FFPE	:	Formalin-fixed paraffin embedded
FISH	:	Fluorescence *in-situ* hybridisation
GAS6	:	Growth arrest specific 6
HNSCC	:	Head and neck squamous cell carcinoma
HPV	:	Human papillomavirus
HR-HPV ISH	:	HR- HPV DNA *in-situ* hybridisation
HRP	:	Horse-radish peroxidase
IARC	:	International Agency for Research on Cancer
ICON-S	:	Oropharyngeal Cancer Network for staging
IGFBP3	:	Insulin like growth factor binding protein 3
IHC	:	Immunohistochemistry
INHANCE	:	International Head and Neck Cancer Epidemiology
ISH	:	*in situ* hybridisation
KD	:	Tyrosine kinase domain
LOH	:	Loss of heterozygosity
MEM	:	Minimum Essential Media
MMPs	:	Matrix metalloproteinases
MOCDTBS	:	Malaysian Oral Cancer Database and Tissue Bank System
MTT	:	3-(4, 5-Dimethylthiazol-2-yl)-2, 5-diphenyltetrazolium bromide
NA	:	Not applicable
NCR	:	National Cancer Registry
NF-κβ	:	Nuclear factor-κβ

NHOFs	:	Normal oral fibroblasts
OCRCC	:	Oral Cancer Research and Coordinating Centre
OPSCC	:	Oropharyngeal squamous cell carcinoma
OSCC	:	Oral squamous cell carcinoma
PCR	:	Polymerase chain reaction
PEI	:	Polyethylenimine
PI	:	Propidium Iodide
PRb	:	Retinoblastoma proteins
PTB	:	Phosphotyrosine binding
PVDF	:	Polyvinylidene difluoride
Q-PCR	:	Quantitative real-time PCR reactions
ROC		Receiver Operating Characteristic
RPMI	:	Roswell Park Memorial Institute
RTKs	:	Receptor tyrosine kinases
SA-β-gal	:	β-galactosidase
SH2	:	Src Homology 2
ShC1	:	SHC-transforming protein 1
STAT	:	Signal transducers and activators of transcription
TB	:	Toluidine blue
TBS	:	Tris-Buffered Saline
TCGA	:	The Cancer Genome Atlas
TERT	:	Telomerase reverse transcriptase
TF	:	Tissue factor
TGF-β1	:	Tumour growth factor 1
TMA	:	Tissue microarray
TNM	:	Tumour-Node-Metastasis

Tos	:	Overall survival time
Trfs	:	Recurrence free survival time
TSA	:	Tyramide Signal Amplification
UICC	:	Union for International Cancer Control
uPAR	:	Urokinase-type plasminogen activator receptor
URR	:	Upstream Regulatory Region
WHO	:	World Health Organisation
α-SMA	:	Alpha-smooth muscle

LIST OF APPENDICES

CHAPTER 1: INTRODUCTION

1.1. General Introduction

Head and neck squamous cell carcinoma (HNSCC) is the sixth most common cancer worldwide and the most common cancer in developing countries (P. Joshi *et al.*, 2014). It comprises a highly heterogeneous group of tumours that include oropharyngeal squamous cell carcinoma (OPSCC) and oral squamous cell carcinoma (OSCC). OPSCC is a tumour that arises in the posterior one-third of the tongue or known as base of tongue, soft palate and tonsils, as well as side and back wall of the throat (LeHew *et al.*, 2017; Rivera *et al.*, 2014) (Figure 1.1 A). OSCC arises in the anterior two-thirds of the tongue, floor of mouth, buccal mucosa, retromolar trigone, hard palate and gingivae (Kerawala *et al.*, 2016) (Figure 1.1 B).

OPSCC is common in the Western world, whilst the OSCC is the predominant HNSCC subtype in South and Southeast Asian countries (P. Joshi *et al.*, 2014; Vigneswaran & Williams, 2014). There are approximately 633,000 new cases of HNSCC diagnosed annually and 355,000 reported deaths worldwide every year (Chai *et al.*, 2015). The global incidence and mortality of HNSCC has remained high over the past 20 years, in part due to a lack of validated diagnostic and prognostic biomarkers (Patel *et al.*, 2017), as well as treatment failure due to resistance to primary or adjuvant chemotherapy (Puram & Rocco, 2015).

In recent years, there has been a decrease in the incidence of OSCC in developed countries that coincides with the reduced prevalence of smoking. In contrast, the incidence of OPSCC is on the rise and this has been attributed to infection with the human papillomavirus (HPV) (H Mehanna *et al.*, 2016; Vigneswaran & Williams, 2014). Interestingly, OPSCC is more than five times more likely to be HPV-related than OSCC

(Chai *et al.*, 2015). Latest statistics suggest that 70-90% of the OPSCC in Western countries are HPV-positive with 90% being associated primarily with high risk HPV serotype 16 (Puram & Rocco, 2015). One of the most significant breakthroughs in head and neck cancer research is the recent discovery and recognition that HPV-positive and HPV-negative HNSCC represent two completely distinct malignancies due to their differences in aetiology, genetic profiles, molecular pathogenesis and therapeutic response (Ravenda *et al.*, 2015; Vigneswaran & Williams, 2014). For example, in the case of OPSCC, patients with HPV-positive disease have a better prognosis and treatment response compared to their counterparts with HPV-negative tumours, but stand a higher rate of late distant metastasis (Vigneswaran & Williams, 2014). However, a complete understanding of the HPV-driven oncogenic signalling events that promote HNSCC pathogenesis remains to be determined.

Solid tumours are complicated structures comprising the malignant tumour cells surrounded by its tumour microenvironment that is made up of various cell types and a complex extracellular matrix (ECM). One of the cell types, fibroblasts, undergo unique phenotypic changes within the tumour microenvironment that make them distinguishable from normal fibroblasts and they are termed cancer-associated fibroblasts (CAFs). CAFs are the most prominent cells in the tumour microenvironment of HNSCCs and they have been intensively studies in recent years (M. Li *et al.*, 2016). Accumulating evidence has shown that the tumour microenvironment influences carcinogenesis by direct communication with the tumour cells via cell-cell contact (Ye *et al.*, 2014) or indirectly through paracrine (Chen *et al.*, 2014) and exocrine signalling (Ziaee *et al.*, 2015) and modulation of ECM (Giussani *et al.*, 2016). The ECM is a non-cellular dynamic network of proteins made up of fibronectins, laminins, elastins, proteoglycans and collagen, which are the major and most abundant component. The deregulation of ECM composition and

structure has been implicated in several pathologic diseases, including cancer (Theocharis *et al.*, 2016).

Discoidin Domain Receptor 1 (DDR1) is a specific receptor that interacts solely with collagen and plays an important role in cancer progression (Dong *et al.*, 2016). However, the role of collagen-mediated activation of DDR1 and the possible role of CAFs in this process has not been studied in HNSCC. Therefore, aims of the present study were to investigate collagen and DDR1 expression in HNSCC and to examine the role of collagen-mediated DDR1 signalling in disease pathogenesis.

1.2. General aims

Head and neck squamous cell carcinoma (HNSCC) is ranked the sixth most common cancer worldwide and OPSCC and OSCC are the most common subtypes (Prabhu & Pillai, 2017). The overall 5-year survival rate for patients with HNSCC has remained poor for the past two decades (Blatt *et al.*, 2016). Therefore, there is a compelling need to identify novel therapeutic targets that can improve the therapeutic management and survival outcome of patients. The starting point of this study was to identify proteins secreted by CAFs that could potentially regulate the HNSCC phenotype. COL8a1 and COL11a1 were identified as being more highly expressed in CAFs than normal fibroblasts, suggesting that DDR1 signalling in HNSCC cells might influence the pathogenesis of the disease. COL8a1 which is elevated in diseases of angiogenesis and vascular remodelling (N. U. B. Hansen *et al.*, 2016) has never been studied in head and neck cancers. COL11a1 was reported to be up-regulated in HNSCC (Meucci *et al.*, 2016), but its contribution particularly in the OPSCC or OSCC remains largely unknown. Although the contribution of DDR1 signalling has been reported in various types of cancers, its role in OPSCC and OSCC remains to be elucidated. Hence, the present study investigated the expression of DDR1, COL8a1 and COL11a1 in OPSCC and OSCC and

determined if their expression was associated with socio-demographic and clinico-pathological characteristics.

Having confirmed that DDR1, COL8a1 and COL11a1 were highly expressed in both OPSCC and OSCC tissues, it was hypothesised collagen-induced DDR1 signalling promoted the malignant phenotype of HNSCC cells. Hence, the last part of this study examined whether exogenous collagen would affect the proliferation, migration, invasion and chemo-sensitivity of HPV-positive and HPV-negative HNSCC cell lines *in vitro*. Subsequent experiments to knock down DDR1 expression were then performed to confirm its role in mediating the effects of collagen.

1.3. Specific objectives

The objectives of the present study were:

1. To identify extracellular proteins and receptors potentially involved in paracrine cross-talk between CAFs and HNSCCs.
2. To investigate the expression of DDR1, COL8a1 and COL11a1 in OPSCCs and OSCCs in United Kingdom and Malaysia cohorts.
3. To correlate the expression of DDR1, COL8a1 and COL11a1 with various socio-demographic and clinico-pathological characteristics of the OPSCC and OSCC patients.
4. To evaluate the biological significance of exogenous collagen and knockdown of DDR1 on the behaviour of HPV-positive and HPV-negative HNSCC cells *in vitro*.

A.

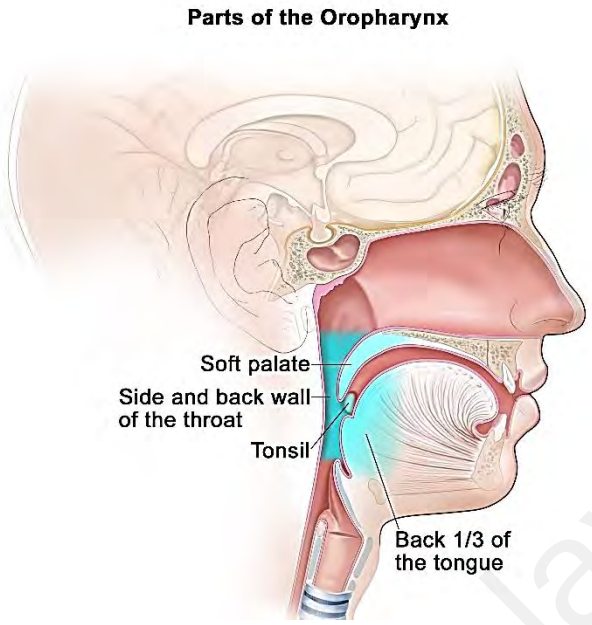

B.

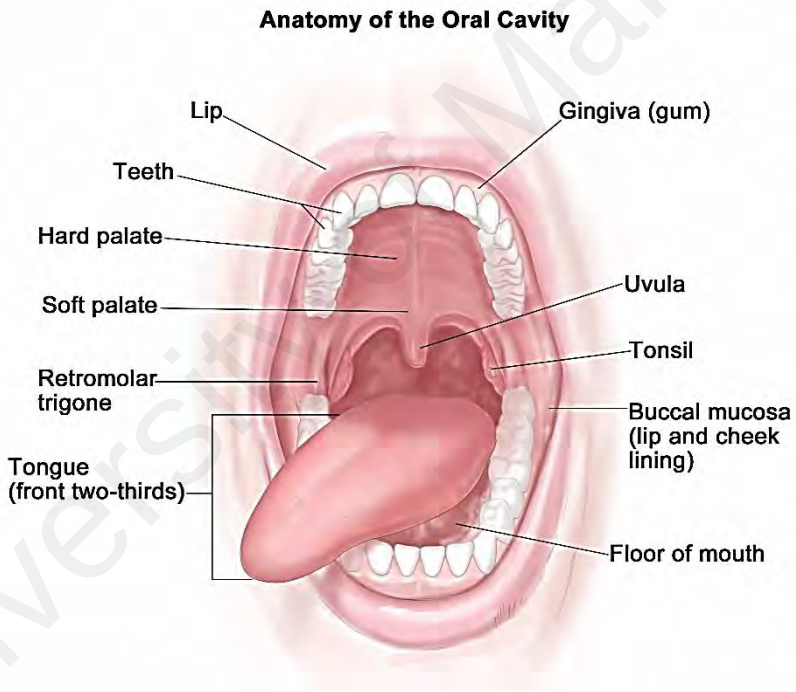

Figure 1.1: Anatomical sites of Oropharynx and Oral Cavity.

The location where **(A)** OPSCC (blue region) and **(B)** OSCC cancers arose is shown. Figures from https://www.cancer.gov/types/head-and-neck/patient/oropharyngeal-treatment-pdq and https://www.cancer.gov/types/head-and-neck/patient/lip-mouth-treatment-pdq

CHAPTER 2: LITERATURE REVIEW

2.1. Head and neck squamous cell carcinoma

Head and neck cancer is a heterogeneous group of malignancies, which technically refers to tumours that occur in the nasal cavity, paranasal sinuses, oral cavity, oropharynx, salivary glands, pharynx, and larynx (Bose *et al.*, 2013). More than 90% of head and neck malignancies are squamous cell carcinomas (SCC) that arise on the mucosal surfaces which is ranked the sixth most common cancer by incidence worldwide, with approximately 500,000 cases per year being diagnosed globally (Knopf *et al.*, 2017).

Tobacco, alcohol and betel quid chewing are the major traditional risk factors for head and neck cancer. During the past two decades, the overall global incidence of the majority of head and neck squamous cell carcinoma (HNSCC) subtypes has declined and this is thought to be associated with the cessation of these habits (Vigneswaran & Williams, 2014). However, there has been a marked increase in the incidence of oropharyngeal squamous cell carcinoma (OPSCC), which is believed to be attributable to human papillomavirus (HPV) infection (Garnaes *et al.*, 2015; Gillison *et al.*, 2015; Stein *et al.*, 2015). The infection by specific HPV subtypes has been suspected as a possible etiological factor for the development of HNSCC since the 19th century where 5% to 20% of HNSCCs were thought to be associated with HPV. However, in recent years it has been recognised that the majority of HPV-associated HNSCCs arise in the oropharynx and between 40% to 90% of OPSCCs are HPV-positive, whilst only a small proportion of tumours from other subsites are caused by HPV (Zaravinos, 2014).

2.2 Oropharyngeal Squamous Cell Carcinoma

2.2.1 Epidemiology of OPSCC

OPSCC has become a focus of attention worldwide as it has emerged as one of the most common malignancies of the head and neck (Williams *et al.*, 2014). Between 1988

and 2004, there was a 225% population-level increase in HPV-positive OPSCC, whilst a 50% decrease in HPV-negative cases were observed (K. B. Pytynia *et al.*, 2014). It has been estimated that by 2020, the incidence of HPV-positive OPSCC will be even higher than that of the other HPV-driven cancers, such as cervical cancer, and OPSCC is predicted to be the most common cancer caused by HPV and the most common cancer of the upper aero-digestive tract (Zevallos *et al.*, 2016).

According to the most recently available international population-based study by de Camargo Cancela *et al.* (2012), the highest rate of OPSCC in high income countries was in France for men and Switzerland for women. Among low-income countries, the highest rate was observed in India for men and Pakistan for women. In Malaysia, there were a total of 77 new cases of OPSCC recorded in 2012 and of these, 51 were male and 26 were female. This male: female ratio is similar to other developed and developing countries. The incidence rate is the highest in the age group between 60 and 64 years old in men (de Camargo Cancela *et al.*, 2012).

2.2.2 Histopathology of OPSCC

The anatomical sub-sites of the oropharynx include the boundary within the lateral and posterior pharyngeal wall, soft palate, uvula, pharyngoepiglottic folds, faucial tonsils, tonsillar pillars and base of tongue (R. Li *et al.*, 2015). A global database revealed that the cancers occur most frequently in the tonsils followed by the base of tongue, whilst the least frequent site was the soft palate (de Camargo Cancela *et al.*, 2012).

In current clinical settings, the key basis of diagnosis and prognosis of OPSCC is mainly on histopathological evaluation. Amongst the histopathological subtypes of OPSCC, basaloid squamous cell carcinoma has the worse prognosis. It has basaloid cells characteristics and palisading at the edge with high nuclei to cytoplasm ratio (Vigneswaran & Williams, 2014). There are keratinizing and non-keratinizing

morphologic variants of OPSCC. The formation of keratin pearls composed of cellular masses in several layers is called the keratinisation. What typically happens is that the cells die off and form small groups out-skirted by distinguishable non-keratinising basement membrane that are actively dividing (Woolgar & Triantafyllou, 2009).

World Health Organisation (WHO), Union for International Cancer Control (UICC) and Broder's grading systems classified OPSCCs into well differentiated (Grade 1), moderately differentiated (Grade 2) or poorly differentiated (Grade 3) according to the degree of nuclear abnormality, cellular variability in size and shape as well as keratinisation. This grading system is also used in conjunction with features such as tumour diameter and thickness, lymph node involvement, distant metastasis and invasiveness to give a more accurate Tumour-Node-Metastasis (TNM) staging in clinical settings (Shabestari *et al.*, 2017). This TNM staging system has been used for decades in clinical practice to predict clinical behaviour and help in therapy strategy for OPSCC patients. Interestingly, the latest edition of TNM system (Table 2.1) has been newly developed for HPV-related OPSCC by the International Collaboration on Oropharyngeal Cancer Network for staging (ICON-S) in 2017 based on adjusted hazard ratios for the patients' death risk (Taberna *et al.*, 2017).

Table 2.1: New 8th edition TNM staging system classification for HPV-related OPSCC patients developed by The International Collaboration on Oropharyngeal Cancer Network for Staging (ICON-S) (Taberna *et al.*, 2017)

Characteristics	7th edition TNM	8th edition TNM ICON-S
Stage classifications	Stage I (T1N0) Stage II (T2N0) Stage III (T3N0 or T1-T3N1) Stage IVa (T4aN0-1 or T1-T4aN2) Stage IVb (T4b or T1-T4bN3) Stage IVc (M1)	Stage I (T1-T2N0-N1) Stage II (T1-T2N2 or T3N0-N2) Stage III (T4 or N3) Stage IV (M1)
5 years OS by stage	NA	I: 88% II: 81% III: 65%
Main N (lymph node) differences	N1: metastasis in a single ipsilateral lymph nodes, <3 cm N2a: metastasis in a single ipsilateral lymph node >3 cm but <6 cm. N2b: metastasis in multiple ipsilateral lymph nodes,<6 cm N2c: metastasis in bilateral or contralateral lymph nodes, <6 cm	N1: ipsilateral metastasis in lymph node(s), <6 cm N2: bilateral or contralateral metastasis in lymph node(s), <6 cm[a]
Main T (tumor) differences	T4a: tumor invades the larynx, extrinsic muscle of tongue, medial pterygoid, hard palate or mandible T4b: tumor invades lateral pterygoid muscle, pterygoid plates, lateral nasopharynx, skull base or encases carotid artery	T4: tumor invades any of the following: larynx, deep/ extrinsic muscle of tongue, medial pterygoid, hard palate, mandible, lateral pterygoid muscle, pterygoid plates, lateral nasopharynx, skull base or encases carotid artery[b]

HPV, human papillomavirus; ICON-S: The International Collaboration on Oropharyngeal cancer Network for Staging; M: metastasis; N: lymph node; NA: Not applicable; OPSCC, oropharyngeal squamous cell carcinoma; OS, overall survival T, tumor.

[a] Because 5-years OS was similar among N1, N2a and N2b, they re-termed the N categories.

[b] Because 5-years OS was similar among T4a and T4b, they were no longer subdivided and it was re-termed as T4.

2.2.3 Aetiology of OPSCC

The exposure to tobacco and alcohol have been recognised as the traditional risk factors for OPSCC (Maasland *et al.*, 2014; Mathur *et al.*, 2015; Sarmento *et al.*, 2016; Sivasithamparam *et al.*, 2013). There is 35% higher risk for a smoker who smokes more than two packets of cigarettes and consumes more than four alcoholic beverages daily to develop OPSCC (Screening & Board, 2017). Studies have shown that there is 35% reduced risk in patients who quit smoking for 1 to 4 years and 40% reduced risk in patients who quit drinking for 20 years to develop OPSCC. The risk for an ex-smoker who has stopped smoking more than 20 years is similar to a non-smoker (Maasland *et al.*, 2014).

In recent years, the incidence of OPSCC has been increasing, especially in younger patients. This increment has been shown to be associated with an increase incidence in HPV related SCC, which is thought to be caused by changes in oral sexual behaviour and poor oral hygiene (Virdee & Kalavrezos, 2016). The association with HPV is particularly high in tumours originating from the tonsil and base of tongue (Wenig, 2015). Furthermore, the non-keratinizing OPSCC variant has been demonstrated to be strongly associated with HPV (Timothy Cooper *et al.*, 2015) and has better survival outcome (T Cooper *et al.*, 2014). In contrast, the keratinizing variant is more frequently associated with traditional risk factors such as smoking and alcohol.

There is a trend for patients with HPV-positive OPSCC to be non-drinkers or light drinkers, females, and the median age is lower than in HPV-negative cases. So, HPV-positive OPSCC is now thought to represent a new entity of HNSCC with distinct epidemiological, clinical, and molecular characteristics that differ from those of HPV-negative cancers (Kristen B Pytynia *et al.*, 2014).

2.2.4 Clinical presentation, treatment and prognosis of OPSCC

OPSCC patients often display the signs and symptom of persistent sore throat, hoarseness, weight loss, pain and difficulty in swallowing, inflammation of the ear and spasms of jaw muscles, change of voice, neck lump and blood-tinged sputum. It is not easily observed until the tumour presents as firm solid mass of larger than 2cm or ulcer with red and white shades.

Biopsy and histological assessment is always necessary for accurate diagnosis of OPSCC (Huber & Tantiwongkosi, 2014; McIlwain *et al.*, 2014). Clinical staging and evaluation of OPSCC are carried out by the use of nasopharyngoscopy, CT scan, MRI, panendoscopy and FDG-PET imaging approaches. Patients often present with advanced stage (Stage III-IV) at diagnosis and nodal involvement is common. Surgery and radiotherapy are the main treatment modalities for patients with early stage OSPCC (Stage I and II), whilst concurrent chemo-radiotherapy is used for locally advanced cases (Stage III and IV) (McIlwain *et al.*, 2014). The five-year survival rate of OPSCC patients has been shown to be higher than that of the oral cavity and larynx cancers, in which highlights the favourable outcome of HPV associated disease (Dahlstrom *et al.*, 2013; Posner *et al.*, 2011; Ritchie *et al.*, 2003; Stats, 2011). OPSCC patients are commonly categorised into low, moderate and high risk of death groups according to the prognostic factors of HPV status, smoking (pack years), nodal stage and tumour stage (A. Hay & Ganly, 2015) (Figure 2.1). The 3-year overall survival were reported to be 88.1% for low-risk group, 59.1% for moderate group and 33.5% for high risk group (Rietbergen *et al.*, 2013).

Moreover, regulators of immune activation (immune checkpoints) have been suggested as the prognostic factor in OPSCC where CD3+ and CD8+ T cells stromal infiltration was showed to be increased in HPV-positive OPSCC and significantly

improved the clinical outcome of patients (K Oguejiofor *et al.*, 2015). Similarly, better survival outcome was showed with CD8+ T cells infiltration in HPV-positive OPSCC and CD68 macrophages infiltration in HPV-negative OPSCC (Kenneth Oguejiofor *et al.*, 2017). Type I HPV 16-specific T cells were showed to be presence in more than two third of HPV16-positive tumours and strongly associated with better overall survival, less lymph node metastases and increased activated immune cells such as CD161+ T cells, CD103+ tissue resident T cells, dendritic cells and dendritic cells-like macrophages. Therefore, enhancement of HPV-16 specific reactivity was thought to be able to boost the favourable immune response to conventional therapy (Welters *et al.*, 2017).

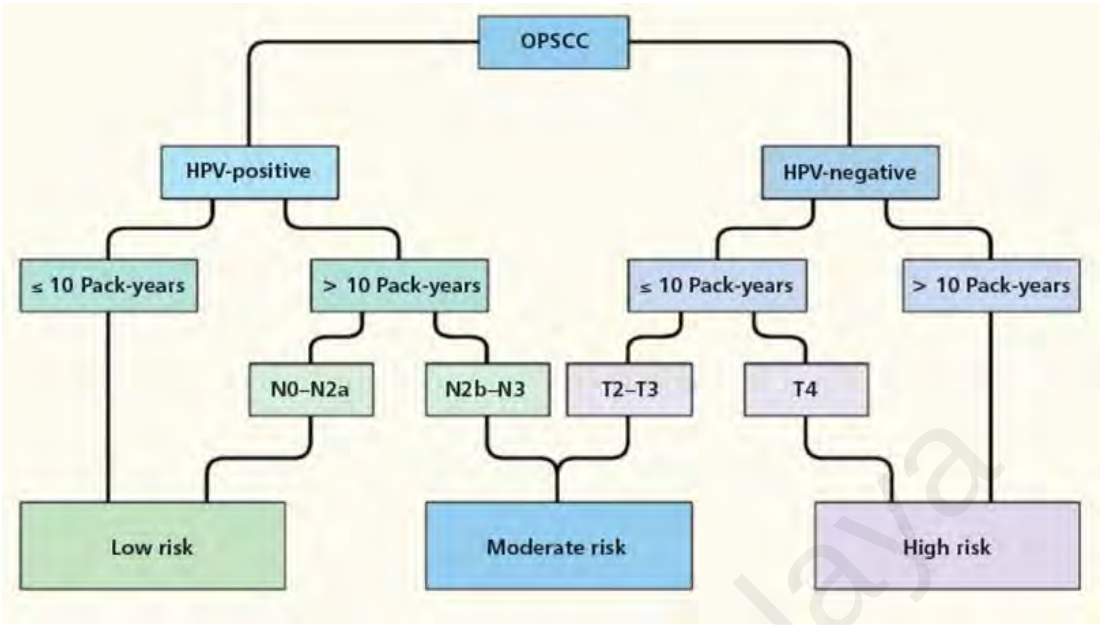

Figure 2.1: Classification of OPSCC according to risk of death groups.

HPV status, pack years, nodal stage and tumour stage segregate patients into low, moderate and high risk of death. HPV-negative, more than 10 pack-years or tumour Stage 4 amongst the patients less than 10 pack-years are important prognostic factors for high risk of death. In contrast, HPV-positive, more than 10 pack-years and nodal Stage N0-N2a are prognostic factors for low risk of death (A. Hay & Ganly, 2015).

2.3 Oral Squamous Cell Carcinoma (OSCC)

2.3.1 Epidemiology of OSCC

Oral squamous cell carcinoma (OSCC) comprises 95% of all head and neck cancers. According to the statistics based on the International Agency for Research on Cancer (IARC) in 2012, an estimated 300,400 new cases of oral cancer were diagnosed, resulting in 145,400 deaths worldwide. The highest incidence rate was found in Melanesia, South-Central Asia, and Europe, whilst the lowest was in the Western Africa and Eastern Asia (Johnson & Amarasinghe, 2016).

In Malaysia, as documented by the latest National Cancer Registry (NCR) data, oral cancer is the 21st most common cancer in the general population and ranked the 17th most common cancer in males and 16th in females of this country. The incidence of oral cancer is predominant among the Indian ethnic group where mouth and tongue cancers are among the 10 most common cancers among both genders.

2.3.2 Histopathology of OSCC

Cancers on the mucosal surfaces of the hard palate, tongue anterior to the circumvallate papillae, floor of mouth, gingival, buccal mucosa and the lips are categorised as OSCC (Tandon *et al.*, 2017). Among these, the buccal mucosa and gingiva are the most common sites for malignancy. Precancerous lesions such as leukoplakia and erythroplakia in the oral cavity transform into invasive carcinoma through a complex multi-step carcinogenic process. Histologically, lesions originate as epithelial hyperkeratosis, hyperplasia and dysplasia, which then transform into *in situ* or invasive carcinoma (Dost *et al.*, 2014; Lian *et al.*, 2013; Rivera, 2015).

According to the World Health Organisation, OSCCs are scored and graded based on their extent of differentiation, mitotic activity, site (S), tumour size (T), regional lymph node compromise (N), metastasis (M) and histopathology (P). This STNMP staging

system together with the patients' health status are useful to determine the prognosis and therapeutic strategy for patients (Rivera & Venegas, 2014; D. M. Walker *et al.*, 2003).

2.3.3 Aetiology of OSCC

Tobacco and alcohol are independent risk factors for the development of OSCC and also act synergistically to increase risk. They account for the majority of the deaths of OSCC in high-income countries. Approximately 75% of oral cancer cases are associated with tobacco, whilst alcohol drinkers have a six-fold higher of developing this malignancy. The synergistic effect of these two risk factors causes a fifteen-fold higher chance to develop the disease (Markopoulos, 2012). Over the past several decades, incidence rates for oral cancer have decreased significantly among both males and females in Asia (such as Philippines and Sri Lanka), Northern America, and Australia, and among males in Southern and Western Europe where the tobacco epidemic is gradually declining (Torre *et al.*, 2015).

In Asia, smokeless tobacco products and betel quid with or without tobacco are the major risk factors for OSCC, especially in India, Pakistan, Bangladesh, Taiwan and Thailand (Amtha *et al.*, 2014; Niaz *et al.*, 2017). Furthermore, patients with a positive history of betel quid chewing before surgery showed higher local recurrence rate than non-chewers (Liao *et al.*, 2014).

A meta-analysis comprising fourteen studies recently conducted in South-East Asia reported that 6.7% of the OSCC risk was accounted by smoking, 3.1% by drinking, 17.7% by chewing and 72.6% by the interaction effect of smoking-drinking-chewing (Petti *et al.*, 2013). Furthermore, the International Head and Neck Cancer Epidemiology (INHANCE) pooled seventeen European and American case control studies and reported that 64% of oral cavity cancer was due to combined effects of tobacco and alcohol (Hashibe *et al.*, 2009). This is consistent with the analysis from the Alcohol-Related

Cancers and Genetic susceptibility in Europe (ARCAGE) which stated that 61% of the oral cancer across the Europe is due to joint effect of tobacco and alcohol (Anantharaman *et al.*, 2011).

Apart from these well known risk factors, low socioeconomic status of patients and poor diets are also associated with OSCC. In particular, majority of the patients are unemployed or low monthly income (Anantharaman *et al.*, 2011), lower educational level (Anantharaman *et al.*, 2011) and belonged to lower and lower-middle class (Rao *et al.*, 2013). Dietary factors and vitamin deficiencies are also associated with increased risk of OSCC. For examples, iron, carotenoids, folate, Vitamin C and D and flavonoid (Chi *et al.*, 2015; Mostafa *et al.*, 2016).

2.3.4 Clinical presentation, prognosis and treatment of OSCC

The mean age of occurrence of OSCC is usually between 51-55 years in most countries. The overall five-year survival has remained unchanged at 53% for several decades (Rivera & Venegas, 2014).

The majority of OSCC lesions average between 2cm to 4cm at diagnosis. Those lesions less than 2cm are often asymptomatic (Bhattacharyya *et al.*, 2017). Patients often seek medical help only after the lesions have developed into significant mass which can cause discomfort and mild to severe pain. The general signs and symptoms of the OSCC are ulceration, swelling, difficulty in speech, swallowing and moving jaws, inner ear pain, bleeding and voice changes (Idahosa & Kerr, 2017). Erythroplakia is often present at diagnosis and the soft tissue is hard during palpation. As the lesion progresses into advance malignancy, it associated with certain typical features such as ulceration with irregular floor and margins, poorly defined boundaries lump, abnormal supplying blood vessels, weight loss and numbness of chin. Neck metastasis are frequently associated with the advance stages of OSCC (Hiraki *et al.*, 2016; Regezi *et al.*, 2016; Rivera, 2015).

As with all solid tumours, early detection is associated with a better prognosis and the detection of molecular and genetic changes linked to early carcinogenesis has potential in this regard for OSCC. For example, Toluidine blue (TB) staining which stains the nucleus of malignant lesions and lesions with loss of heterozygosity (LOH) (Petruzzi *et al.*, 2014); biomarkers such as Ki-67 indicative of proliferation and Bax/ Bcl-2 indicative of apoptosis (Schiegnitz *et al.*, 2017); DNA ploidy using automated image cytometry to measure gross genetic mutation (P. S. Joshi *et al.*, 2015); scanning and analysis of cytology samples collected by brush biopsy (Adami *et al.*, 2017); detection of histological and biochemical abnormalities that invisible to naked eyes by using optical spectroscopy system (Carvalho *et al.*, 2015) and computed tomography or magnetic resonance imaging (Wolff *et al.*, 2012); as well as saliva-based diagnostics for signature miRNAs that are up-regulated in OSCC patients (Momen-Heravi *et al.*, 2014).

Treatment options for OSCC patients depend on their clinical pathology staging and factors such as age and prognostic indicators. Multimodal treatments include oromaxillofacial surgery, chemotherapy, radiotherapy or combined radiochemotherapy (Kirita & Omura, 2015). Radiotherapy is often used with or without chemotherapy after surgery for advanced cases but in general, almost one fifth of the patients suffered from recurrence after two years from the first treatment and the five-year survival rate remained at 50% (Wang *et al.*, 2013). Patients have to undergo long term follow-up intervals of every three months in the first two years, every six months in the next two years and routinely undergo CT and MRI examination of the oral cavity and neck to screen for any recurrence or development second primary tumours after the five years follow-up (Wolff *et al.*, 2012). In recent years, targeted therapies are under the evaluation in the clinical settings to treat oral cancer patients. In particular, the addition of monoclonal antibody EGFR inhibitor to radiotherapy is carried out in clinical trials (S. H. Huang, 2013; RIBEIRO *et al.*, 2014). Furthermore, reactivation of T cells by using monoclonal

antibodies has been recently suggested as a promising immune checkpoint blockade therapy to treat the OSCC. For instance, B7-H4, which is a negative immune checkpoint of B7 gene family that regulated adaptive cellular immunity by T cells, was showed to overexpress in OSCC compared to normal oral mucosa and had poor overall survival thus has been suggested as one of the potential therapeutic target of OSCC (L. Wu *et al.*, 2016). B7-CD28 pathways immune checkpoint inhibition has been suggested as new version of anti-cancer strategies (Y. Zhu *et al.*, 2017).

2.4. Human Papillomaviruses (HPV)

The human papillomaviruses (HPV) are small, circular, non-enveloped and double-stranded deoxyribonucleic acid (DNA) epitheliotropic viruses which have approximately 7900 base pairs long. They infect the cutaneous and mucosal epithelium such as skin, mouth, anus and genitals but are absent in the lung and colon for unknown reasons (Bernard, 2013). More than 160 subtypes of HPV have been identified to infect squamous epithelia, which cause both cancers and benign lesions, including mucosal and epithelial warts (Fakhry & D'Souza, 2015).

Patients with HPV-associated cancers tend to be younger. There is global prevalence of HPV in women younger than 25 years old and the prevalence declines at older age after 40s (Forman *et al.*, 2012). Men has been shown to have significant higher prevalence of oral HPV than woman (Gillison *et al.*, 2012). The known risk factors for HPV related squamous cell carcinomas include sexual transmission of the virus via direct skin contact mainly due to early intercourse, multiple sexual partners, and oral sex activity (Candotto *et al.*, 2017; Walden & Aygun, 2013). The life-time transmission risk HPV in sexually active women, particularly cervical infection, is as high as approximately 80% (Zaravinos, 2014).

2.4.1 HPV genome and subtypes

The HPV genome comprises six early (E) and two late genes (L) which are named due to their relative expression during the viral life cycle (Figure 2.2). The early genes function during viral replication and transcription whilst the late genes encode for the structural proteins. Among the early genes, E6 and E7 are the main genes that encode for transforming proteins. The transcription is regulated by E2, replication is regulated by E1, viral release is regulated by E4 and immune invasion is controlled by E5. The Upstream Regulatory Region (URR) is made up of the viral origin of replication, promoter and enhancer elements that contribute to the transcription and replication activities carried out by the early genes. The two late genes, L1 and L2 code for the major and minor capsid proteins respectively (Taberna *et al.*, 2017).

Over 160 types of HPV have been identified based on at least 2% to 10% of their difference in the nucleotide sequence of the L1 open reading frame of their genome (Burk *et al.*, 2013). Not all HPV species are harmful but some cause common skin warts whilst certain species often cause cancer. In particular, genital warts are caused by HPV 6 and HPV 11 and skin warts are caused by HPV1, HPV2 and HPV4. Furthermore, the HPV genome is grouped into high-risk and low-risk with regard to their oncogenic potential in cancer. High-risk types (HPV 16, 18, 26, 31, 33, 34, 35, 39, 45, 51, 52, 56, 58, 59, 66, 68) are predominantly expressed in precancerous and cancerous lesions. The low-risk types (HPV 6 , 11, 40, 43, 44, 54, 69, 70, 71, 74) are expressed in benign and non-malignant lesions (Klingelhutz & Roman, 2012; Lingen *et al.*, 2013; Rautava & Syrjänen, 2012). High-risk HPV drives the fast proliferation of infected epithelial cells but low-risk HPV endures in slowly dividing epithelial cells (Doorbar, 2016).

HPV infects the basal cellular layer via microabrasion and remained outside the chromosome without viral reproducing activity (Klingelhutz & Roman, 2012; Tseng,

2016). During this initial HPV exposure, the viruses are at their non-productive state. They replicate together with the dividing host cells with viral copy number maintained at only 50 to 100 copies. The oncogenic viral genes and proteins (i.e. E6 and E7) block the normal regulation of host cells division but they are under strict controlled and their expression is still maintained at very low level at this stage. The E6 gene binds to p53 and the E7 gene binds to retinoblastoma proteins (pRb). They override the cell cycle checkpoints to allow replication of viral DNA in non-cycling cells. The infection at this stage is temporal and usually goes off naturally without any treatment (Rautava & Syrjänen, 2012; Stanley, 2012).

The risk of HPV infection to malignancy progression is depending on the host and viral genetics as well as the lifestyle and environmental factors (Figure 2.3). In particular, HPV 16 and 18 are most accountable to cause carcinogenesis than the other HPV subtypes (Crow, 2012; Schiffman & Wentzensen, 2013).

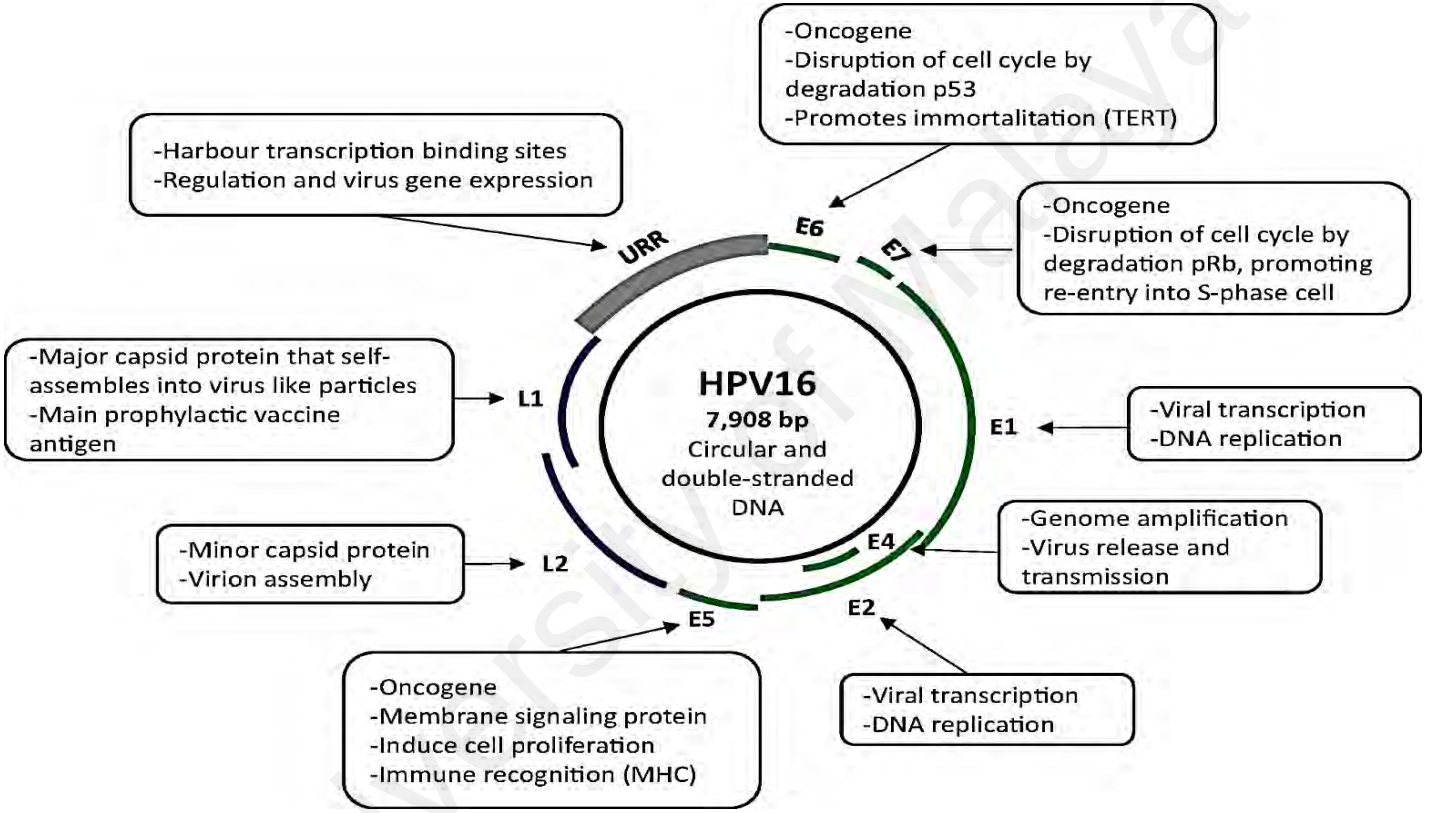

Figure 2.2: Typical genome of HPV and its main genes functions.

Diagram showing the position and transcription of HPV genes on the double-stranded viral DNA. There are six early genes (E1, E2, E4, E5, E6 and E7) and two late genes (L1 and L2). The early genes are responsible for viral replication and late genes are encoded for capsid protein (Taberna *et al.*, 2017).

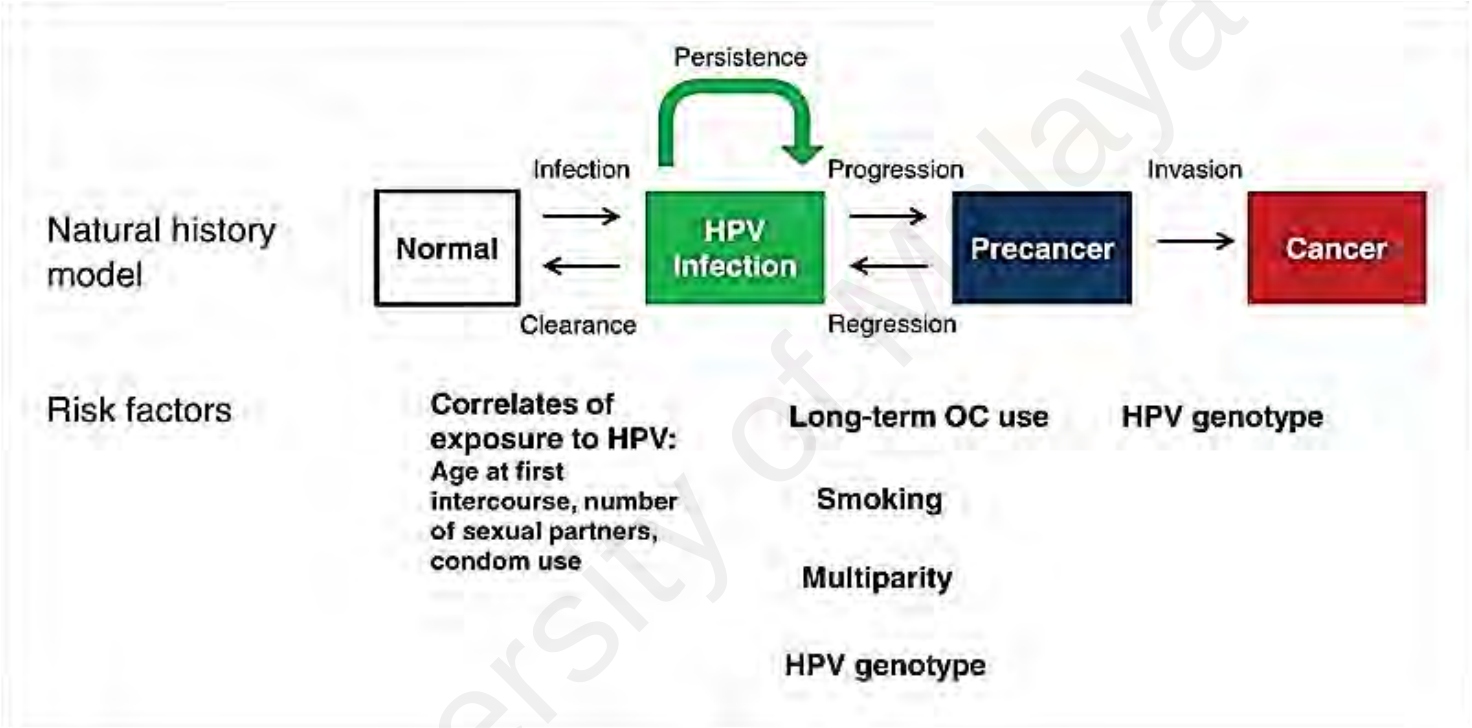

Figure 2.3: Natural history model of HPV oral infection and carcinogenesis process.

The role of persistence HPV infection and risk factors such as smoking leading to OPSCC progression and invasion. When the HPV infection persists and remained not cleared, it could lead to HPV-related precancerous oral mucosa lesion. If the precancerous lesion does not regress, it progress into invasive cancer. Image from Schiffman and Wentzensen (2013). Abbreviation: OC, oral contraceptives.

2.4.2 HPV vaccination and protection

Vaccines against HPV infection have been developed and introduced to induce persistent tumour-antigen specific immune responses that prevent the development of tumours (Zaravinos, 2014). There are two types of HPV vaccines available globally up-to-date. The first is a quadrivalent vaccine known as Gardasil, which is manufactured by Merck to prevent the infection of the low-risk type (i.e. HPV 6 and HPV 11) and the two high-risk types HPV 16 and HPV 18. The second type is bivalent vaccine known as Cervarix manufactured by GlaxoSmithKline Biologicals to protect from only the high-risk types HPV 16 and HPV 18 (Schiller & Lowy, 2012). However, high-risk HPV 16 and HPV 18 infections are not absolutely eradicated using existing vaccination strategies in most countries. As such, the development and improvement of HPV vaccination are still essentially on demand (Kawana *et al.*, 2012).

2.5 Role and molecular basis of HPV in HNSCC

High-risk HPV 16 is the HPV type which has been commonly proved to be involved in OPSCC carcinogenesis (Zaravinos, 2014), whereas low-risk HPV 6 and HPV 11 are responsible for benign laryngeal lesions (Nichols, Dhaliwal*, et al.*, 2013). HPV 16 has also been shown to persist the longest among all high-risk subtypes, with the higher likelihood of infection persistency found in middle aged adult and older men (Campbell *et al.*, 2015). Apart from this, a small proportion of 10% to 15% HPV-positive OPSCC have been found to be associated with the HPV 33, HPV 35, HPV 45 and HPV 58 but at lower frequencies and with less important role (Z. Deng *et al.*, 2012; Soria-Céspedes *et al.*, 2012; Zaravinos, 2014).

The majority of OPSCCs in developed countries, for example, 60% as reported in the United States, are associated with HPV 16 infections (Nguyen *et al.*, 2016). In contrast to the oropharynx, only minority of cancers arise in the oral cavity seem to be HPV related

even in young non-smoking and non-drinking patients (Mirghani, Amen, Moreau*, et al.*, 2015). However, the incidence rate of HPV-related OPSCC in middle-income developing countries, including Malaysia, is yet to be fully investigated and remains unknown.

Recent breakthrough in research has showed that HPV-positive OPSCC carries a more favourable prognosis than the HPV-negative OPSCC, which is characterised by histological poor squamous differentiation and often presenting with advanced regional nodal metastasis (Ng *et al.*, 2015). The overall 2-year and 5-year survival for HPV-positive OPSCC is significantly greater than for HPV-negative counterpart, likely caused by immune surveillance to viral antigens, absence of field cancerization (C. A. Fischer *et al.*, 2010a) and tendency of improved treatment response in patients (Young *et al.*, 2015). For instance, a meta-analysis reported by O'rorke *et al.* (2012) revealed significant lower mortality, lower progression and recurrence rates and higher survival rates in HPV-positive HNSCC than HPV-negative HNSCC.

The emerging epidemiologic evidence from case-series and case–control studies suggest that HPV-positive OPSCC risk factor profiles are distinguishable from their HPV-negative counterpart. HPV-positive OPSCC is characterized by a younger age at onset (3–5 years younger compared to HPV-negative OPSCC), male predominance (3:1 male: female ratio), strong associations with sexual behaviours, and inconsistent or weak associations with tobacco and alcohol consumptions but strongly associated with marijuana use. In contrast, HPV-negative OPSCC is characterized by older age at onset (typically at the age of 70's), male predominance (male to female ratio of 3:1), strong associations with tobacco and alcohol consumptions, and moderate associations with poor oral hygiene as well as low dietary intake of fruits and vegetables (Chaturvedi, 2012).

The major differences of HPV-positive and HPV-negative HNSCC are summarised in Table 2.2.

HPV-induced HNSCC show distinct molecular characteristics and suggests a different carcinogenesis pathway compared to HPV-negative HNSCC. The two viral oncoproteins, E6 and E7, are identified as the main mediators of HPV-induced oncogenesis in OPSCC. They play a major role in cell cycle control and the inhibition of the host cell innate immune response to HPV. Current research provides the understanding that the expression of the viral E6 and E7 oncoproteins inactivate the tumour-suppressor proteins (i.e. p53) and the retinoblastoma protein (i.e. pRb) respectively.

In particular, p53 is a transcription factor which plays vital role in tumour suppression. It is responsible to react towards DNA damage via ATM/ ATR/ CHk1/ CHk2-dependent homologous recombination DNA repair pathways (Serrano *et al.*, 2013). It is also stabilised in AFR-dependent manner for tumour suppression in response to oncogenic signals (Loughery & Meek, 2013). In the case of HPV-HNSCC, the wild-type p53 is ubiquitined by oncoprotein E6 with the host ubiquitin ligase E6-associated protein (E6AP) leading to p53 degradation by the proteasome and causing it to be malfunctioned (Rieckmann *et al.*, 2013). In addition to p53, another tumour suppressor protein named retinoblastoma, pRb, which essentially involved in cell cycle control is also being mutated in the HNSCC by HPV oncogene, E7. Wild-type pRb plays a role in G1-S phase progression by activation of Bax and mitochondrial apoptosis (Hilgendorf *et al.*, 2013). However, its function is disrupted by the E7 oncogene via binding to the pocket domain of pRb to the cyclic-AMP response element binding protein CBP/p300, causing the acetylation of pRb and loss of cell cycle control (Jansma *et al.*, 2014). The inactivation of pRb by E7 also causes the reciprocal release of E2F, Cyclin A and Cyclin E and promotes G1-S phase transition (Zaravinos, 2014).

As a result of these events, cyclin-dependent kinase inhibitors ($p16^{INK4a}$ and p21Cip1/WAF1) and MDM2 inhibitor (p14ARF) are up-regulated, further leading to the down-regulation of Cyclin D1 and inhibition of its complex formation with CDK4 (Mooren *et al.*, 2014). Eventually, these events deregulate host cell cycle control and inhibition of host cells apoptosis leading to uncontrollable high proliferation rate and maintain the favourable condition in host cell for viral genome replication and L1 as well as L2 genes expression for viral encapsidation (Zaravinos, 2014).

Biologically relevant HPV-associated OPSCCs can be identified by various molecular approaches. Despite the fact that no single 'gold standard' detection method has been globally recognised and accepted up-to-date, highly sensitive polymerase chain reaction (PCR)-based methods and highly specific fluorescence in-situ hybridisation (FISH) are widely used for detection of HPV-DNA in clinical diagnosis and research globally. However, both these methods have the drawbacks of high-risk of contamination and high probability of false-positive results (Moutasim *et al.*, 2015). In addition, these methods are relatively expensive and technically demanding compared to alternative immunohistochemistry detection of $p16^{INK4a}$ (C. A. Fischer *et al.*, 2010b). The detection of the $p16^{INK4a}$ protein is a consequence of its overexpression following the inhibition of the retinoblastoma protein by the E7 oncoprotein of HPV. The $p16^{INK4a}$ protein has been recognised worldwide to serve as a low specific (79-82%) yet highly sensitive (nearly 100%) surrogate and prognostic marker for HPV infection in formalin fixed paraffin embedded specimens (M. Robinson *et al.*, 2012). As such, the immunohistochemical detection of $p16^{INK4a}$ is considered to be a highly reliable and robust test and is now routinely performed in conjuction with HPV-DNA ISH detection or PCR-based methods in clinical-pathological settings (Ndiaye *et al.*, 2014a; Pannone *et al.*, 2012; Salazar *et al.*, 2014; Zaravinos, 2014).

Table 2.2: Clinico-pathological differences between HPV-negative and HPV-positive HNSCC patients (A. Hay & Ganly, 2015; Partlová *et al.*, 2015; Taberna *et al.*, 2017)

Characteristic	HPV-negative HNSCC	HPV-positive HNSCC
Risk factor	Alcohol, tobacco	Number of oral sex partners
Age	Older	Younger
Incident trends	Mostly decreasing	Increasing
Head and neck tumour location	Any	Base of the tongue, tonsil
Stage	Any	Smaller primary tumour, low T stage, large N involvement
Radiological image	Any	Cystic nodal involvement
Histopathological features	Keratinising	Basaloid, Non-keratinising
Tumour differentiation	Any	Undifferentiated
Prognosis	Poor	Better
Chemotherapy/ chemo-radiotherapy response rate	Lower	Higher
Outcomes	Worse OS and PFS	Better OS and PFS
Metastatic dissemination	Yes	Rarely
Comorbidity	Yes	No
Second primary tumours	Yes	No
Prevention strategies	Quitting smoking and drinking	Vaccination (in development)

Abbreviations: HNSCC, head and neck squamous cell carcinoma; HPV, human papillomavirus; OS, overall survival; PFS, progression-free survival

2.6 Molecular basis of HNSCC

Genetic and epigenetic changes in HNSCC have been studied in regards to the crucial signalling pathways involved in all hallmarks of cancer, including self-sufficiency in growth signals, limitless replicative potential, insensitivity to anti-growth signals, ability to metastasise, invasion, angiogenesis and evading apoptosis, evading immune response, gene instability, abnormal metabolic pathways and inflammation (Leemans *et al.*, 2018; Network, 2015a). In general, they can be discussed in terms of four major molecular alterations. Firstly, HNSCC possess unlimited cell cycling and replicative potential by inactivating p53 and pRb pathways. Tumour suppressor gene TP53 mutations occur in 80% HNSCC through somatic mutation in HPV-negative HNSCC or HPV 16 E6 in HPV-positive HNSCC. Significant association was found between decreased overall survival rate of patients and the disruptive mutation of TP53 (Leemans *et al.*, 2011). Together with p53 mutation, methylation of CDKN2A (encodes $p16^{INK4a}$) and amplification of CCND1 (encodes cyclin D1) changed the $p16^{INK4a}$-cyclin D1-CDK4-RB and the $p16^{INK4a}$-cyclin D1-CDK6-RB signalling cascades (Leemans *et al.*, 2011; C.-C. Li & Woo, 2014) and causes limitless cell replication. Secondly, overexpression of the EGFR was reported in HNSCC since the 19^{th} century. Its EGFRvIII mutant was found in almost half of the HNSCC, leading to tumour growth and proliferation via the Ras-MAPK and phospholipase C signalling pathways (Tafe, 2017). Treatment of EGFR-targeting antibodies was effectively improved the radiotherapy response of patients (Blaszczak *et al.*, 2017). However, the EGFR pathway alteration is rarely found in HPV-positive HNSCC but the HPV-negative counterpart (A. Hay & Ganly, 2015). Thirdly, another inhibitory growth factor pathway known to be down-regulated in HNSCC included the transforming growth factor-β (TGF-β) which coupling with the loss of SMAD3 and SMAD4 genes at the chromosome 18q (Park *et al.*, 2015). The abrogation of the TGF-β pathway was associated with the nuclear factor-κβ (NF-κβ) that leads to pro-survival of

cells (Leemans *et al.*, 2011). Fourthly, the PI3K-PTEN-AKT pathway mutation where activation of PI3K inactivates PTEN and activates AKT have been found in 30% HNSCC causing tumour cell migration and invasion (X. Zhang *et al.*, 2016), as well as the evasion of apoptosis via downstream molecules, such as Myc, mTOR and MDM2 (A. Hay & Ganly, 2015).

In addition to these four major pathways, HNSCC tumour cells have been shown to gain more mesenchymal and metastatic phenotypes through epithelial-to-mesenchymal transition. Examples of genes that induce EMT nclude NOTCH4-HEY1 (Fukusumi *et al.*, 2018), Snail (Ota *et al.*, 2016), TWIST 1, E-cadherin, N-cadherin, FOXC2, vimentin and fibronectin (Johansson *et al.*, 2016). Lastly, angiogenesis inducers such as vascular endothelial growth factor (VEGF) were found to be significantly associated with HNSCC poor prognosis (Mathew, 2017).

2.6.1 Molecular basis of HPV-positive HNSCC

The genetic landscape published in the most recent The Cancer Genome Atlas (TCGA) repositories characterised the distinct genomic and molecular alterations profile of HPV-negative and HPV-positive HNSCCs as summarised in Table 2.3 (Polo *et al.*, 2016). In a study published 2006 which compared the gene expression profiles of HPV-negative and HPV-positive HNSCC, genes encoded for cell cycle regulators, such as CDC7 and p18, and genes encoded for transcription factors, for example, RPA2, TFDP2 and TAF7L were identified to be up-regulated in HPV-positive HNSCC (Slebos *et al.*, 2006). Interestingly, another study reported that no significant differences in gene expression were observed between HPV-negative and HPV-positive OSCC but differential gene expression was found between HPV-negative and HPV-positive OPSCC, where 222 genes were up-regulated and 77 genes were down-regulated (Lohavanichbutr *et al.*, 2009). A few noteworthy up-regulated genes were those involved in DNA repair, included TOPBP1,

DDB2, XRCC1 and FANCG, and those involved in cell cycle and proliferation, such as Ki67, CDK2, NASP, CCNE2, CDC7, RBBP4, L1G1, RPA2, POLD1, and MCM2. Those genes involved in the cell cycle control, for example CCND1, HIPK2 and APC were found to be down-regulated. Interestingly, 21 genes were found to be up-regulated in HPV-positive OPSCC but down-regulated in HPV-negative normal controls. For example, FEZ2, EID1 and DHRS7 (Lohavanichbutr *et al.*, 2009). Recurrent loss of TRAF3 and ATM1 and amplification of E2F1 were also found in HPV-positive HNSCC (Aung & Siu, 2016; A. Hay & Ganly, 2015).

The mutation rate of HPV-positive HNSCC was found to be about half of that in HPV-negative HNSCCs (Stransky *et al.*, 2011). Recently, it has been reported that there are infrequent mutations of TP53 (i.e. mainly wild-type TP53) and CDKN2A in HPV-positive HNSCC compared to their HPV-negative counterparts (Hong *et al.*, 2016) but the crucial genes confidently known to be modulated by HPV E6 and E7 oncogenes are mainly those cell cycle regulatory genes encoding for proteins in the p53 and retinoblastoma pathways. For example, RB1, RBL1 encoded for p107 and RBL2 encoded for p130 (Martinez-Zapien *et al.*, 2016; Songock *et al.*, 2017). The role of increased ectopic expression of telomerase reverse transcriptase (TERT) was less important in HPV-positive HNSCC (Leemans *et al.*, 2011). In addition, a third mechanism of E7 instead of E6-dependent p53 impair mechanism was found, which is the p53-p21-DREAM-CDE/CHR pathway which impairs the cell cycle. It comprised of G_1/S and G_2/M cell cycle genes, included KIF23, Survivin (BICR5), CDC25C and PLK4 (M. Fischer *et al.*, 2017). These new data suggest that HPV overcomes cell cycle checkpoints by more than the accepted mechanisms.

H. Li and Grandis (2015) reviewed the gene mutation profiles of HPV-negative and HPV-positive HNSCC and those genes tend to be mutated predominantly in HPV-

positive HNSCC are PIK3CA, K-RAS, MAPK1 and FGER3. In contrast, CASP8, TP63 and NOTCH1 are less likely mutated in HPV-negative HNSCC. These data are in agreement with the evidence in a large-scale whole-exome sequencing study that showed that activating helical domain mutations of the oncogene PIK3CA is common in HPV-positive compared to HPV-negative HNSCC (Nichols, Palma*, et al.*, 2013), a next-generation sequencing study identified the driver genes that are higher in HPV-positive versus HPV-negative HNSCC such as the PIK3CA (30% versus 12%), KRAS (6% versus 1%) and NRAS (4% versus 0%) were associated with reduced survival (Tinhofer *et al.*, 2016), a novel proximity-based assay showed that total expression of HER2, HER3, HER2: HER3 heterodimer, HER3-PI3K complex was significantly up-regulated in HPV-positive HNSCC and inhibition of the phosphorylation of HER2 inactivated the MAPK pathway (Pollock *et al.*, 2015).

In addition, expression of programmed death 1 (PD1) and programmed death ligand-1 (PD-L1) was common in HPV-positive HNSCC compared to HPV-negative HNSCC (Mirghani, Amen, Blanchard*, et al.*, 2015). PD-L1 expression is found in 70% of HPV-positive OPSCC (Lyford-Pike *et al.*, 2013). It is in line with another study where PD-L1 is found in 49% of HPV-positive OPSCC but only 34% in HPV-negative counterpart (Ukpo *et al.*, 2013). The binding of PD-L1 to PD1 receptor was thought to cause immune evading by negative T-cell regulation and protect OPSCC cancer cell death (Mirghani, Amen, Blanchard*, et al.*, 2015).

The hypermethylation of DNA at promoter regions and global hypomethylation are two types of epigenetic changes (i.e. genetic alterations that occur without DNA sequence mutation) in HPV-positive compared to HPV-negative HNSCC as reviewed by van Kempen *et al.* (2014). Epigenetic alteration occurred at the sites where cytosine is followed by guanine (CpG dinucleotide) is called the methylation. There is a significantly

higher prevalence of hypermethylation at gene promoter regions in HPV-positive HNSCC which cause gene silencing. This is thought to be due to higher activated DNA methyltransferases resulting from p53 and pRb inhibition by HPV E6 and E7 oncoproteins (C. Zhang *et al.*, 2015). The CpG sites that are found to be methylated and significantly associated with HPV are TUSC3, CCNA1, CDH11, SYBL1, GRB7, SRFP4, TIMP3 and RUNX1T1, whilst those hypomethylated included JAK3, ESR2, SPDEF, RASSF1, MGMT, STAT5α and HSD17D12. Among the genes, MGMT promoter methylation was significantly associated with poor outcome in HPV-positive HNSCC. In addition, it is noteworthy that no methylation of p16 was found in HPV-positive HNSCC (van Kempen *et al.*, 2014). HPV-positive HNSCC showed higher methylation of genes involved in escaping growth suppression and activating invasion and metastasis. It has more global methylation and less genomic instability. In addition, another genome-wide DNA-methylation analysis also suggested that Polycomb repressive complex 2 target genes included cadherins responsible for tumour progression and metastasis were modulated by HPV in HNSCC (Lechner *et al.*, 2013). A deeper understanding of the methylation effects would give a better insight to the HPV-driven HNSCC carcinogenesis scheme.

2.6.2 Molecular basis of HPV-negative HNSCC

The understanding of the mutations and genetic aberrations in HPV-negative HNSCC is of utmost important in helping to identify biology and novel therapeutic targets for this disease entity. A recently published study had identified genes that are mutated in radiosensitive versus radioresistant HPV-negative HNSCC. In particular, phosphatidylinositol-4,5-bisphosphate 3-kinase-catalytic subunit alpha (PIK3CA), nuclear receptor binding SET domain protein 1 (NSD1) and tumour protein P63 (TP63) mutations were commonly found in radiosensitive tumours. On the other hand, down-

regulation of CCDC60, FAM81A, FGD2, HS3ST6, ITGB7, PRR15L, SCGB2A1, SCNN1A, ST6GALNAC1, VILL and up-regulation of CSTF3, ST3GAL5 and UFD1L were associated with radioresistant HPV-negative HNSCC both *in vitro* and in *vivo* (Foy *et al.*, 2017).

Smoking was thought to be the major risk factor for HPV-negative HNSCC (Polo *et al.*, 2016), thus tobacco smoke-related molecular alterations have been implicated in the carcinogenesis and pathogenesis of this entity. More than sixty smoke-related carcinogens were found to cause DNA adducts formation and KRAS, TP53 and RB were often mutated by the transitions and transversions at CpG sites (i.e. change of purine to another purine or pyrimidine to another pyrimidine nucleotides) in HPV-negative HNSCC (Hayes *et al.*, 2015). In contrast, mutations at the TpCp sites (i.e. mutation of cytosine-to-thymidine due to increased cytosine deaminase mutagenesis of APOBEC family of enzymes) were less common in the HPV-negative HNSCC compared to the HPV-positive HNSCC (Network, 2015a). Interestingly, several complex signalling cascades were activated upon binding of nicotine and its derivatives to the nicotinic acetylcholine receptor (nAChR). For example, JAK/STAT, Ras/Raf/MAPK and PI3K/AKT. These pathways are commonly seen in HPV-negative HNSCC. Furthermore, overexpression of cyclins and down-regulation of cyclin-dependent kinase (Cdk) inhibitors were showed to promote cell cycle progression and led to chemotherapy and radiotherapy resistance in HPV-negative patients who did not quit smoking during treatment (Schaal & Chellappan, 2014).

As far as smoke-related HPV-negative HNSCC is concerned, alterations and inactivation of the tumour suppressor genes, mainly TP53, CDKN2A and RB1 were commonly reported (Network, 2015a). In particular, mutations of the typical tumour suppressor TP53, are detected in most if not all of HPV-negative OSCC cases and

associated with increased genome instability (Samman *et al.*, 2015). Interestingly, TP53 mutant was frequently seen in late stage OSCC and had lower survival rates than those with TP53-positive OSCC (Al Salihi *et al.*, 2016; H.-J. Lee *et al.*, 2015) and the TP53 signalling alterations is nearly exclusive to HPV-negative HNSCC (Seiwert *et al.*, 2015). In addition, deregulation of G1/S modulators such as RB1 are early molecular deregulations in OSCC carcinogenesis and detected in 80% of potentially malignant oral lesions and OSCC (Monteiro & Warnakulasuriya, 2017; Rivera *et al.*, 2017). Apart from this, genes involved in oxidative stress pathways was found to be frequently mutated in HPV-negative HNSCC. For example, KEAPI, CUL3, and NFE2L2 (Seiwert *et al.*, 2015). Several other genes that responsible for cell squamous cell differentiation have also been showed to be mutated in HPV-negative HNSCC, such as FAT1 and NOTCH1 which inhibits Wnt/β-catenin signalling (Network, 2015b). However, NOTCH1 mutations do not occurred exclusively in HPV-negative HNSCCs but are found in both HPV-positive and HPV-negative tumours, which is similarly to PI3K signalling and SMAD network (Seiwert *et al.*, 2015).

Furthermore, somatic copy number alterations have been reported in HPV-negative HNSCC. For example, amplifications of 11q13 targeting CCND1, FADD and CTTN; 11q22 targeting BIRC2 and YAP1; 7p11 targeting EGFR and focal amplification of ERBB2 and FGFR1 receptor tyrosine kinases. These amplified genes lead to tumour growth and invasion (Kempen *et al.*, 2015). Notably, the amplification of 11q13 down-regulated CASP8 mutations and activated NF-κβ oncogenic pathways. Deletion of 3p targeting CDKN2A and focal deletion of NSD1 (Network, 2015a; Seiwert *et al.*, 2015) was also found to be predominantly occurred in HPV-negative HNSCC. Similarly to HPV-positive HNSCC, the HPV-negative HNSCC has also been showed to encounter amplification of the 3q26-28 targeting SOX2/TP63/PIK3CA (Seiwert *et al.*, 2015).

Table 2.3: Major genetic differences between HPV-negative and HPV-positive HNSCCs (A. Hay & Ganly, 2015; Partlová *et al.*, 2015; Taberna *et al.*, 2017)

Molecular genome	HPV-negative HNSCC	HPV-positive HNSCC
CDKN2A	Common	Rare
$p16^{INK4a}$ overexpression	Rare	Common
EGFR	Common (amplification)	Rare
p53	Common	Rare (p53 degradation by E6)
pRb	Rare	Rare (pRb degradation by E7)
PIK3CA	Common	Common (APOBEC)
TRAF3	Common	Rare
E2F1	Rare	Common
COX2	Rare	Common
PD1	Rare	Common
CCND1	Common	Rare
MYC	Common	Rare

Abbreviations: HNSCC, head and neck squamous cell carcinoma; HPV, human papillomavirus

2.7 The tumour microenvironment

Cancer comprises both the malignant cells and the tumour microenvironment. The tumour microenvironment refers to the surrounding non-malignant stromal cells within a scaffold of extracellular matrix (ECM) and a diverse composite of immune cells (such as macrophages and lymphocytes) as well as non-immune cells (such as vascular cells and cancer-associated fibroblasts, CAFs) (Theocharis *et al.*, 2016). It is now well recognised that stromal cells also play an important role in tumorigenesis, cancer progression, metastasis and treatment response whereby the malignant tumours are under a strict microenvironmental control (J. Zhang & Liu, 2013). However, the complex interactions between the malignant cells and the tumour microenvironment are yet to be fully understood and remained largely unexplored, particularly in HNSCC.

2.7.1 Cancer-associated fibroblasts (CAFs)

Fibroblasts are mesenchymal cells whose major function is to deposit and turnover ECM in normal tissues by secreting the ECM molecules, matrix metalloproteinases and metalloproteinases inhibitors (Darby *et al.*, 2014). However, in recent years, the structural and functional contributions of CAFs to carcinogenesis are beginning to emerge and they are now recognised as a potential target for cancer therapies (Ohshio *et al.*, 2015).

CAFs are the most abundant and prominent cell type in the tumour microenvironment (Kalluri, 2016). Locally quiescent fibroblasts, cancer epithelial cells, endothelial cells, mesenchymal stem cells from the bone marrow, pericytes, smooth muscle cells, adipocytes, and the inflammatory cells are all possible cellular precursors of CAFs (J. Zhang & Liu, 2013). In normal tissues, the quiescent fibroblasts undergo activation and become myofibroblasts during wound healing and fibrosis, which are then eventually removed by the granulation process. Considering that tumours are wounds that do not heal, CAFs share similarities with myofibroblasts but they are not eventually removed by

apoptosis and notably remain permanently activated (Bates, 2015; Pidelaserra Martí & Bassols Teixidó, 2015). CAFs are different from the normal fibroblasts as they proliferate faster and increased production of growth factors as well as ECM modulators such as matrix metalloproteinases (MMPs) and tumour growth factor 1 (TGF-β1) (Arcucci *et al.*, 2016; Dissmann *et al.*, 2015; Madar *et al.*, 2013; Van Bockstal *et al.*, 2014). As tumour cells begin to proliferate, they produce factors that activate fibroblasts and recruit CAFs. A fully exclusive marker for CAFs that distinguishes them from the normal fibroblasts has yet to be identified but alpha-smooth muscle (α-SMA) which tends to be over-expressed by CAFs compared with normal fibroblasts is most commonly used to denote CAFs (Berdiel-Acer *et al.*, 2014; Hsia *et al.*, 2016).

Apart from remodelling of ECM and suppressing immune responses, these activated CAFs are also involved in close crosstalk with tumour cells via paracrine secretion of growth factors, cytokines and extracellular proteins. These paracrine secretions regulate multiple signalling pathways that have been showed to be responsible for tumour cell growth and invasiveness, differentiation, angiogenesis and inflammatory responses (Arcucci *et al.*, 2016; Karagiannis *et al.*, 2012). Also, recent evidence has suggested that CAFs modulate drug sensitivity of malignant cells, specifically in breast (Paulsson *et al.*, 2017), prostate (Cheteh *et al.*, 2017), pancreatic (Quail & Joyce, 2013) and ovarian tumours (Thibault *et al.*, 2014).

2.7.2 Collagens

Collagens are the most abundant structural protein in humans which accounts for three-quarters of the dry weight of skin and are the major constituent of ECM. Collagens have defining structural motifs in which three parallel polypeptide α-chains (each contains repeating amino acid motif, Gly-X-Y) coil around one another by inter-strand hydrogen bonds to form a right-handed triple helix with all Glycine residue buried within the core

of the molecule and residues X and Y exposed on the surface. The α-chains can be either identical (homotrimeric) or genetically distinct (heterotypic) indicated by roman numerals (Figure 2.4) (Mienaltowski & Birk, 2014). In humans, there are at least twenty eight different types of collagens have been identified and they are expressed in unique tissue-specific patterns and exert different functional effects. They are grouped into subfamilies (e.g. COL11a1 is classical fibrillar collagen, and COL8a1 is short chain collagens). Fibrillar collagens are synthesized as soluble precursor molecules called procollagens, which then form the tripe helical tropocollagens and assemble into fibril bundles by removing the C-propeptide whilst extenting the N-terminal.

In addition to their structural function, recent studies have revealed other essential biological and physiological roles for collagens. For example, cell attachment, differentiation, chemotaxis, thrombosis, inflammation, regeneration and repair (Guo *et al.*, 2016; Nune *et al.*, 2017; Poundarik *et al.*, 2015; Somaiah *et al.*, 2015; Tangsadthakun *et al.*, 2017). Interestingly, many studies have reported that the expression of collagens is correlated with carcinoma cell proliferation, invasion, metastasis, *in vivo* tumorigenesis, and resistance to cell death (Barcus *et al.*, 2017; Gilkes *et al.*, 2013).

2.7.2.1 Collagen Type VIII Alpha 1 Chain (COL8a1)

Type VIII collagen is a non-fibrillar short chain homotrimer which is composed of alpha-1 (genomic localization: 3q12-q13.1) and alpha-2 (genomic localization: 1p34.3-p32.3) subunits, both with the similar molecular weight of approximately 60kDa (N. Hansen & Karsdal, 2016). It is the main component of Descemet's membrane and the highly expressed key component in vascular remodelling (Lopes *et al.*, 2013). COL8 has been reported to be involved in angiogenesis (N. U. B. Hansen *et al.*, 2016), facilitates smooth muscle cells migration (Adiguzel *et al.*, 2013) and movement of myofibroblasts in fibrosis (Skrbic *et al.*, 2015). However, little is known about the clinical implications

of COL8 expression in cancer and other diseases. What is known indicates that up-regulation of COL8 is detected in diabetic nephropathy (Van *et al.*, 2017) and caortic injury (Gil-Cayuela *et al.*, 2016) and it has also been demonstrated recently that the expression of COL8 is significantly correlated with hepatocarcinoma proliferation, invasion and reduced drug sensitivity (Ma *et al.*, 2012). COL8a1 is also found to be associated with epithelial-mesenchymal transition (Minafra *et al.*, 2014) and metastasis (Kanwar & Done, 2013) in breast cancer. However, there are no reports describing the expression of COL8 subunits in HNSCC and the role of this collagen in carcinogenesis remains to be elucidated.

2.7.2.2 Collagen Type XI Alpha 1 Chain (COL11a1)

Type XI collagen falls into the classical fibrillar group characterised by their ability to assemble into highly orientated staggered supramolecular fibrils. It is formed as a heterotrimer of three different alpha chains, alpha-1 (genomic localization 1p21), alpha-2 (genomic localization: 6p21.3), and alpha-3 (genomic localization: 12q13.11-q13.2) (Karaglani *et al.*, 2015; S.-J. Kim *et al.*, 2016; McAlinden *et al.*, 2014). It co-polymerises with Type II and Type IX collagens to largely contribute to the composition of cartilage which is important in tissue repair (Sok *et al.*, 2013b). Facial anomalies, cleft palate and hearing defects have been regarded as COLXI "collagenopathies" since the 19th century (Spranger, 1998). With regards tumorigenesis, COLXI specifically the α1 subtypes was reported to be over-expressed in colorectal (D. Zhang *et al.*, 2016), lung (Shen *et al.*, 2016), gastric (A. Li *et al.*, 2017) and pancreatic (García-Pravia *et al.*, 2013). It has also been shown to cause chemoresistance in ovarian cancer (Rada, Cha*, et al.*, 2017). Recently, COL11a1 was shown to be over-expressed in HPV-negative HNSCC and contribute to tumour proliferation, migration and invasion (Rada, Eldred*, et al.*, 2017; Sok *et al.*, 2013a), but the signalling mechanisms are still yet to be fully explained. To

date, there have been no studies investigating the influence and relation of COL11a1 to HPV-positive HNSCC.

A.

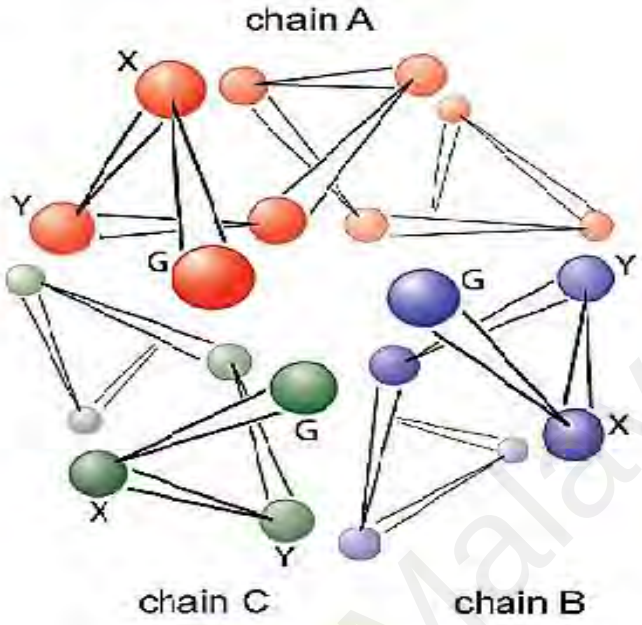

B.

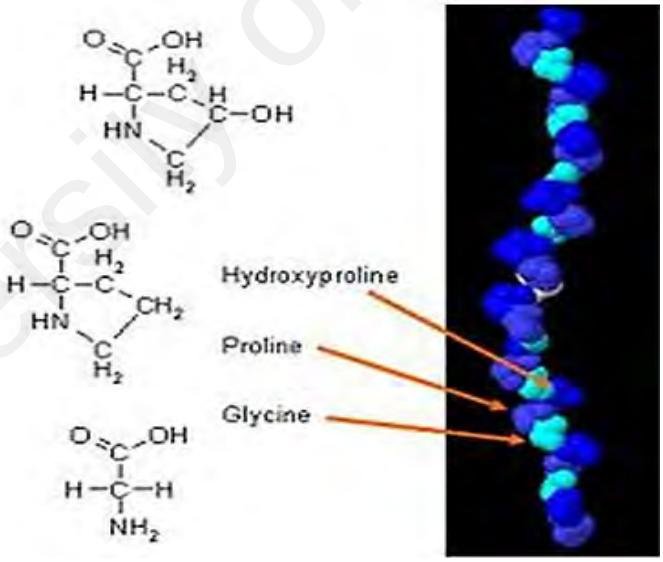

Figure 2.4: Diagram depicting the triple helix structure of collagens.

A. Location of residues in the Gly-X-Y triplets. **B.** Right-handed helical twist formed by polypeptides. Images and information from Fratzl (2008) and Wahyudi *et al.* (2016).

2.7.3 Cross-talk between tumour cells and the tumour microenvironment

There exists close crosstalk between CAFs and tumour cells during tumour progression. CAFs can become activated as a result of genetic or epigenetic alterations, which then results in an increase in ECM biosynthesis, angiogenesis, macrophage infiltration of epithelial tumours and secretion of growth factors and chemokines by tumour cells. This triggers signalling cues which in turn induce development of reactive fibroblasts (Krishnamachary *et al.*, 2017; Schoepp *et al.*, 2017; Tang *et al.*, 2016) and drives tumourigenesis (Attieh & Vignjevic, 2016; Dart, 2017; K. Miyake *et al.*, 2017). The interactions between cells and their microenvironment are mediated, in part, by the matrix receptors at the cellular surface. The matrix receptors play a crucial role to link the ECM to the behavioural response of cells, and this activates complex signalling pathways to regulate various biological processes, such as cell differentiation and survival (Bonnans *et al.*, 2014). Deregulated expression or function of many of these receptors has been implicated in tumour pathology, for example tumour development, differentiation, invasion and metastasis (Pickup *et al.*, 2014; Seguin *et al.*, 2015). For example, integrins have been identified as a primary receptor involved in cell-matrix adhesion and plays important role in regulating cancer stemness, metastasis and drug resistance (Seguin *et al.*, 2015); urokinase-type plasminogen activator receptor (uPAR), tissue factor (TF) and the epidermal growth factor receptor (EGFR) modulates angiogenesis, tumour growth and invasion via regulating ECM degradation and remodelling in OSCC (Christensen *et al.*, 2017).

2.8 Discoidin Domain Receptor 1 (DDR1)

2.8.1 DDR1 structure & isoforms

The Discoidin Domain Receptor (DDR) family is expressed in epithelial tissues and belong to the class of receptor tyrosine kinases (RTKs). The RTKs are single-pass trans-

membrane receptors characterised by conserved cytosolic kinase domains and structurally diverse extracellular ligand-binding regions. RTK-dependent signal transduction regulates cellular processes, such as proliferation and differentiation, cell survival, cell migration and cell cycle control (Chiasson-MacKenzie & McClatchey, 2017). Typical RTKs are activated by soluble peptide-like growth factors (Koschut *et al.*, 2016). It was therefore surprising that the DDRs are activated and could transmit signals in cells following binding to a number of collagens (Ruiz-Castro *et al.*, 2016).

There are only two members of the DDR family identified to date, namely DDR1 and DDR2. DDR1 was first identified in the *Dictyostelium discoideum* amoeba and was shown to mediate cell aggregation (Rammal *et al.*, 2016a). DDR1 and DDR2 share highly conserved sequence identity of discoidin homology (DS) in the extracellular region and DS-like domains with 59 and 51% of similarity, respectively (Carafoli & Hohenester, 2013). Both DDR1 and DDR2 receptors are activated upon binding to collagens. While DDR2 can only be activated by fibrillar collagen such as COL1 (C.-c. Zhu *et al.*, 2015) and COL3 (Lamandé *et al.*, 2017), DDR1 is known to be mostly activated by COL1 (Assent *et al.*, 2015) and COL4 collagens (Favreau *et al.*, 2014), whilst its activation by the COL8a1 and COL11a1 has rarely been described up to date and remains to be elucidated.

Structurally, DDR1 is known to have four distinct domains, i.e. a characteristic extracellular domain composed of the N-terminal DS domain and a DS-like domain (triple helical collagen and matrix metalloproteinase binding site); a single trans-membrane domain and an intracellular tyrosine kinase domain comprising both the juxta-membrane regulatory sequence of about 221 amino acids depending on the protein isoforms and a catalytic tyrosine kinase domain (KD) of about 300 amino acids, plus a C-terminal peptide of about 8 amino acids (Carafoli *et al.*, 2012; H.-L. Fu *et al.*, 2013).

The phosphorylation and activation of downstream signalling take place at the KD (Carafoli & Hohenester, 2013). The structure of DDR1 is shown in Figure 2.5A.

Alternative splicing around the juxta-membrane gives rise to five isoforms of DDR1 (DDR1a-e; Figure 2.5B) but only a single form for DDR2 (Nishida & Shimada, 2016; Rammal *et al.*, 2016a). The DDR1 gene is located on chromosome 6p21.3 in humans (Zum Gottesberge & Hansen, 2014). Among the five DDR1 isoforms, isoforms DDR1a, b and c are kinase-active whilst DDR1d and e isoforms are C-terminally truncated kinase-deficient forms due to a frame shift and truncation respectively. Specifically, frame-shift alterations of exons 11 and 12 in DDR1d causes a stop codon and premature termination of transcription, whereas exons 11, 12 and first half of exon 10 are lacking in DDR1e. The most abundant isoforms are DDR1a and DDR1b, whilst the longest isoform is DDR1c which is composed of 919 amino acids. DDR1a and DDR1b are closely related but DDR1b contains an additional sequence of 37 amino acids inserted into the juxta-membrane domain which is encoded by an exon that is spliced out of the DDR1a transcript. Importantly, it provides sites for downstream signalling at this LXNPXY motif and proline-rich stretch. The five isoforms of DDR1 have different tissue specific expression patterns, glycosylation, phosphorylation, protein interactions and functions (Borza & Pozzi, 2014; Carafoli & Hohenester, 2013; Birgit Leitinger, 2016).

The present study is focused on the DDR1 which expressed on the epithelial cells but not the DDR2 that often expressed on mesenchymal cells.

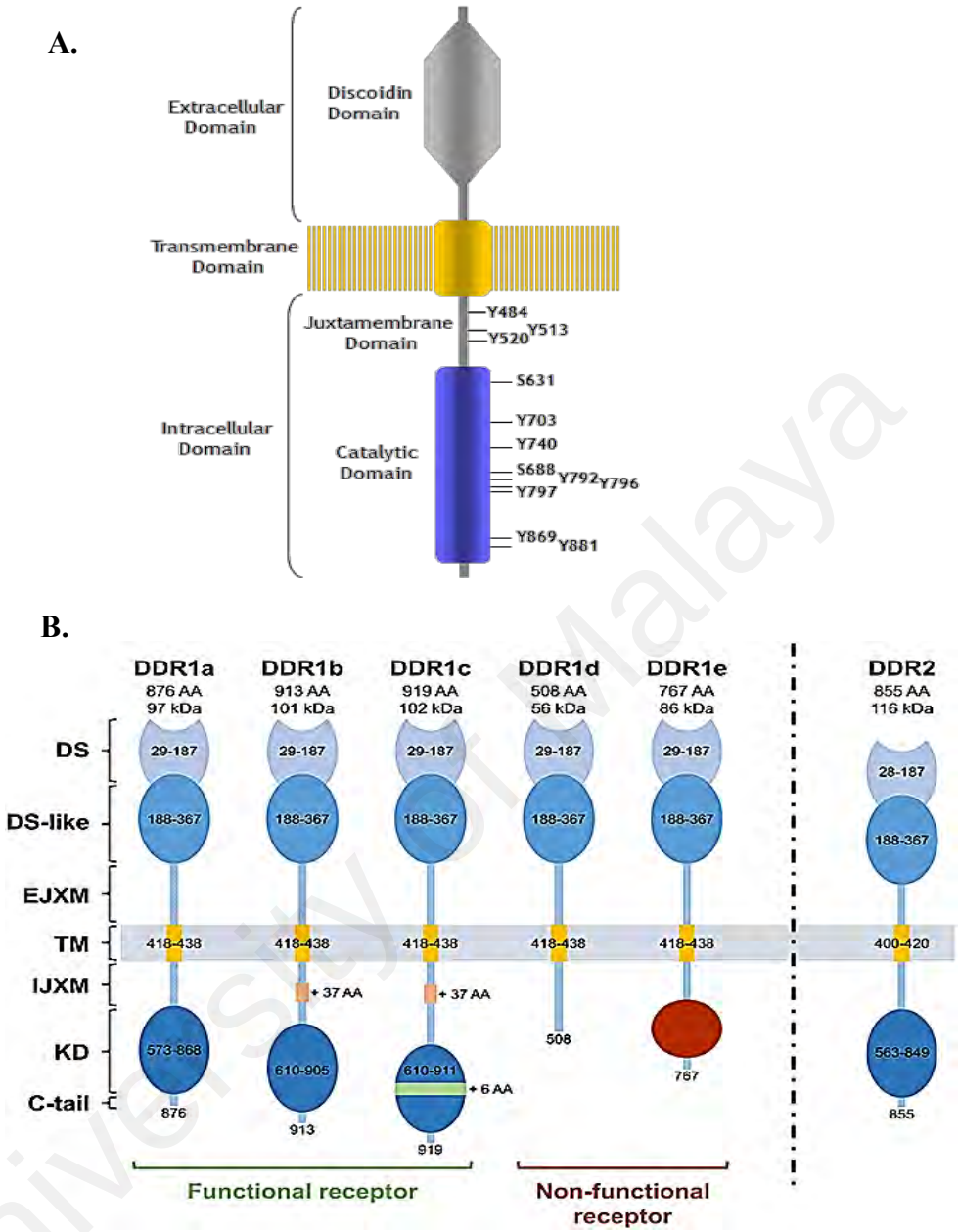

Figure 2.5: Diagrammatic representation of DDR1 isoforms.

A. DDR1 structure and localisation of phosphorylated site at intracellular domain.

B. Active and inactive kinase isoforms of DDR1. Images adapted from Atlas of Genetics and Cytogenetics in Oncology and Haematology; and Rammal *et al.* (2016a). Abbreviations: DS, discoidin domain; DS-like, discoidin-like domain; EJXM, extracellular juxtamembrane region; TM, transmembrane segment; IJXM, intracellular juxtamembrane region; KD, kinase domain; C-tail, C-terminal tail

2.8.2 Collagen-DDR1 signalling in cancer

The collagen-DDR1 axis is shown to modulate tumour-stromal interactions but defining the precise signalling mechanisms that regulate these interactions has always been challenging. DDR1 is unique in a way that binding to collagen results in delayed and sustained receptor phosphorylation (Rammal *et al.*, 2016a). Whilst other RTKs typically undergo receptor-ligand internalisation followed by dephosphorylation by phosphatase, DDR1 phosphorylation has been shown sustained up to 18 hours (Ju *et al.*, 2015). Upon binding of collagen, the tyrosine residue in the activation loop of DDR1 tyrosine kinase domain is phosphorylated. It brings about auto-phosphorylation of tyrosines at the juxta-membrane region. Next, docking and binding of several types of adaptor proteins or signalling molecules take place. For example, Src Homology 2 (SH2) (H. Huang *et al.*, 2016); phosphotyrosine binding (PTB) domain containing proteins (Vella *et al.*, 2017); extracellular signal regulated kinase mitogen-activated protein kinase (ERK1/2-MAPK) (El Azreq *et al.*, 2016), members of the signal transducers and activators of transcription (STAT) family of transcription factors (Ruiz-Castro *et al.*, 2016); cytoplasmic protein Nck2 (Iwai *et al.*, 2016); protein tyrosine phosphatase SHP-2 (Birgit Leitinger, 2016); Wnt5a/Frizzled (Rammal *et al.*, 2016a); and SHC-transforming protein 1 (ShC1) (H. Huang *et al.*, 2016). The binding of these proteins activates their downstream pathways and regulates various cellular processes. Recent studies have demonstrated a role of DDR1 in regulating various important cellular behaviours, such as adhesion and ECM remodeling (Chua *et al.*, 2016; Birgit Leitinger, 2016) but these functions are dysregulated in various human diseases, such as cancer (H. Gao *et al.*, 2016). However, DDR1 does not react with heat-denatured collagen (Birgit Leitinger, 2016) and is activated by the GVMGFO motif in native triple helix proteins (An *et al.*, 2016). Interestingly, unlike typical RTKs which are induced and phosphorylated by ligands within seconds, DDR1 is atypical and phosphorylation is much slower upon

ligand stimulation (Leitinger, 2015). Furthermore, unlike other RTKs where receptor dimerization happens upon ligand binding, DDR1 dimerization is necessary for collagen recognition prior to interaction (Juskaite *et al.*, 2017).

2.8.3 Role of DDR1 in cancer

Collagens are the only ligands known to interact with DDR1 (Juskaite *et al.*, 2017; Sarkar *et al.*, 2015) and DDR1 receptor activation regulates various cellular processes, including ECM remodelling, cell proliferation, differentiation, cell adhesion, cell migration, invasion and processes associated with tissue homeostasis (Justus *et al.*, 2016; Romayor *et al.*, 2017; Shitomi *et al.*, 2015; Yuge *et al.*, 2017). Mutation or overexpression of DDR1 expression has been implicated in numerous types of disease, including inflammation, tissue fibrosis, atherosclerosis and cancer (Kothiwale, Borza, Lowe*, et al.*, 2015). DDR1 expression is often de-regulated in cancer and has been reported to be overexpressed in lung cancer (Miao *et al.*, 2013), breast cancer (Badaoui *et al.*, 2017) and lymphoma (Fathima Zumla Cader *et al.*, 2013).

Recent publications have reported important roles of DDR1 in cancer progression via *in vitro* and *in vivo* studies. DDR1 silencing has been demonstrated to reduce the growth of tumour xenografts in human pancreatic adenocarcinoma (Rudra-Ganguly *et al.*, 2014); reduced motility and metastasis in colon carcinoma (Yuge *et al.*, 2017) and osteosarcoma (Zhaofeng Wang *et al.*, 2017); inhibited the cell proliferation, migration and invasion in myeloid leukemia (Favreau *et al.*, 2014); and decreased migrativeness and invasiveness of non-small cell lung carcinoma (Miao *et al.*, 2013). Furthermore, DDR1 overexpression has been showed to promote migration in breast cancer (Badaoui *et al.*, 2017; Reyes-Uribe *et al.*, 2015), pancreatic adenocarcinoma (H. Huang *et al.*, 2016) and myeloid leukemia (Favreau *et al.*, 2014). Interestingly, recent studies have showed that the activation of collagen receptors promotes tumour survival, particularly in lymphoma cells

(F. Z. Cader *et al.*, 2013) and breast cancer (Badaoui *et al.*, 2017). However, the underlying mechanisms of DDR1 activation and downstream molecular signalling are largely unknown.

The role of DDR1 in cancer is somewhat controversial and data exists to support both positive and negative regulation of cancers. It appears that these effects are cell type specific and context-dependent. DDR1 has been suggested as a positive regulator of epithelial-mesenchymal transition in human renal cancer (Song *et al.*, 2016), non-small cell lung carcinoma (Miao *et al.*, 2013), gastric cancer (R. Xie *et al.*, 2016) and pancreatic adenocarcinoma (H. Huang, 2016) but shown to be a negative regulator of epithelial-mesenchymal transition in human breast cancer (Koh *et al.*, 2015). It has also been shown to inhibit integrin mediated migration and spreading in Madin-Darby Canine Kidney cells (Borza & Pozzi, 2014) but promote cell migration and invasion in T helper cells (El Azreq *et al.*, 2016).

To date, little is known about the role of DDR1 in HNSCC and the expression and function of DDR1 in OPSCC and OSCC are currently unknown.

2.8.4 DDR1 inhibition and targeted therapy

As our understanding of the role of DDR1 in cancer has been advancing in recent years, this unique tyrosine kinase has been seen as a potential therapeutic target in cancer research. Examples of DDR1 targeted therapy in preclinical studies include the targeted delivery of miRNAs such as miR-199a-5p (Yingbin Hu *et al.*, 2014); use of monoclonal antibodies which bind to discoidin-like domain of DDR1 such as Fab 3E3, 48B3 and H-126; also inhibitors made against the DDR1 kinase (Rammal *et al.*, 2016a).

There are two types of DDR1 inhibitors that have been identified thus far, which are the Type 1 active inhibitors and Type 2 inactive inhibitors. Both types of inhibitors act

by preventing transfer of the terminal phosphate group of adenosine triphosphate to protein substrate, i.e. adenosine triphosphate (ATP) competitive inhibitors (Rammal *et al.*, 2016a). However, the mechanisms are different in that the Type 1 active inhibitors bind to the "open-configuration" of DDR1 kinase domain (i.e. Asp-Phe-Gly motif of the activation segment in open configuration of DDR1 activation loop) which is known as the DFG-in conformation, whereas the Type 2 inactive inhibitors bind to the "close-configuration" of DDR1 kinase domain known as the DFG-out conformation and stabilise DDR1 inactive kinase form. In addition, Type 1 active inhibitors inhibit a wide range of tyrosine kinases, whilst the Type 2 inactive inhibitors are more selective by inhibiting only a few tyrosine kinases (Kothiwale, Borza, Lowe Jr*, et al.*, 2015). Many potent small molecule inhibitors with effective IC_{50} have been designed by chemical and proteomic approaches. For instant, Dasatinib (IC_{50}= 0.5nM) of Type 1 active inhibitors, Imatinib (337nM), Nilotinib (43nM) and Ponatinib (9nM) of Type 2 inhibitors (Canning *et al.*, 2014).

Interestingly, *in vitro* studies showed that 3-(2-(pyrazolo[1,5-a]pyramidine-6-yl)-ethynyl) benzamides inhibited the kinase activity of DDR1 in Type 2 inhibitor mode with an IC_{50} of approximately 7nM. These potent compounds inhibited the proliferation of lung, breast and colon carcinoma cells that highly expressed DDR1 (M. Gao *et al.*, 2013). Additionally, another two Type 2 inhibitors, DDR1-IN-1 and DDR1-IN-2, have been shown to be able to induce significant inhibitory effects with the IC_{50} of 105nM and 47nM respectively (Rammal *et al.*, 2016b). Both the inhibitors have also been shown that they are able to inhibit DDR1 activation in U2OS cells even in the presence of collagen, with the EC_{50} of 86 and 9nM respectively (H.-G. Kim *et al.*, 2013). Apart from this, a series of pyrazolo-urea containing compounds such as 2a (IC_{50}= 69nM), 4a (IC_{50}= 235nM) and 4b (IC_{50}= 39nM) have also been identified as the new Type 2 inhibitors of DDR1

(Richters *et al.*, 2014). However, these DDR1 inhibitors have been used primarily as research tools and none are yet in clinical use or in clinical trials.

CHAPTER 3: MATERIALS AND METHODS

3.1 Materials

3.1.1 OPSCC tissues

The Astellas PredicTr Array 4 containing 38 cores of OPSCC tumours and 2 non-tumour cores and 56 OPSCC FFPE biopsy samples were obtained from the Institute of Head and Neck Studies and Education (InHANSE), Institute of Cancer and Genomic Sciences, University of Birmingham, United Kingdom. The tumours had been stratified by p16 and HPV DNA status previously. For the biopsy samples, additional information apart from the p16 and HPV DNA status such as age, gender, T stage, N stage, diagnostic biopsy date, date of first recurrence, date of death, survival months, date last seen, alive/ deceased outcome, smoking histories, overall survival time, recurrence free survival time and risk groups stratification were provided by Professor Hisham Mehanna [Director of the Institute of Head and Neck Studies and Education (InHANSE), University of Birmingham] and Professor Paul Murray (Professor of Molecular Pathology, Institute of Cancer and Genomic Medicine, University of Birmingham, United Kingdom). Ethical approval was obtained for this study (REC reference 10/H1210/9).

To examine the prevalence of HPV in Malaysian OPSCCs, 60 cases were obtained from four different hospitals in two major cities. Cases were identified by searching pathology databases for SCCs labelled as oropharynx, tonsil and soft palate and the patients were identified over a 12-year period (2004-2015). Formalin-fixed paraffin embedded (FFPE) tissue blocks were obtained from the relevant pathology tissue archives and clinico-pathological information were obtained from clinical databases and review of medical records. All patient information was de-identified. This study had ethical approval from the relevant institutional medical research and ethics boards (REC reference: NMRR-12-13577; UMMC 20164-2341; SDMC 201211.3).

3.1.2 OSCC tissues

For OSCCs, 60 biopsy samples of OSCCs from Malaysian patients were obtained from the Malaysian Oral Cancer Database and Tissue Bank System (MOCDTBS) managed by the Oral Cancer Research and Coordinating Centre (OCRCC), University of Malaya. Samples were collected from patients who visited University Malaya Medical Centre from 2004 to 2012. Ethical approval for this study was obtained from the Medical Ethics Committee, Faculty of Dentistry, University of Malaya [REC reference: DF OB1602/0026(U)].

3.1.3 HPV testing

The HPV status of OPSCCs tissues was assessed using p16 IHC and high risk HPV DNA in situ hybridisation. These tests were performed and interpreted by Dr Max Robinson (Honorary Consultant Oral Pathologist in Newcastle upon Tyne Hospitals NHS Foundation Trust; Senior Lecturer in Oral Pathology, University of Newcastle-upon-Tyne). The p16 immunohistochemistry (IHC) was performed using a proprietary kit (CINtec Histology, Roche mtm laboratories AG, Germany) on a Ventana Benchmark Autostainer (Ventana Medical Systems Inc, USA). Normal tonsil was used as a negative control and OPSCC with high p16 expression was used as a positive control. The p16 staining was assessed as positive when there was strong and diffuse nuclear and cytoplasmic staining present in greater than 70% of the malignant cells (Jordan *et al.*, 2012; Singhi & Westra, 2010). HR- HPV DNA in-situ hybridisation (HR-HPV ISH) was carried out using proprietary reagents (Inform HPV III Family 16 Probe (B), Ventana Medical Systems Inc, USA) on a Benchmark Autostainer (Ventana Medical Systems Inc, USA). The Inform HPV III Family 16 Probe (B) detects high risk genotypes HPV-16, -18, -31, -33, -35, -39, -45, -51, -52, -56, -58 and -66. Three control samples were used: FFPE CaSki cells (HPV-16 positive; 200-400 copies per cell), HeLa cells (HPV-18

positive; 10-50 copies per cell) and C-33A (HPV negative; Ventana Medical Systems Inc, USA). The HR- HPV ISH test was scored as positive if there was any blue reaction product that co-localised with the malignant cells (Thavaraj *et al.*, 2011).

3.1.4 Cell lines

A series of human oral fibroblasts cell lines were provided by Professor Ken Parkinson, Institute of Dentistry, Queen Mary University of London, United Kingdom. These included normal human oral fibroblasts (NHOF4, NHOF6, NHOF7), less senescent CAFs derived from genetically stable OSCC (BICR59F, BICR69F, BICR70F) and highly senescent CAFs derived from genetically unstable OSCC (BICR3F, BICR31F, BICR78F). The derivation and culture of these fibroblast strains has been described previously (Yazan Hassona *et al.*, 2013; Lim *et al.*, 2011a).

4 human OPSCC cell lines, SCC040 (UPCI-SCC-040), SCC154 (UPCI-SCC-154), VU040T (92-VU-040T) and VU147 (93-VU-147T), were provided by Dr Sally Roberts from the University of Birmingham, United Kingdom. Of these, 2 cell lines are HPV-positive (SCC154, VU147T) and 2 cell lines are HPV-negative (SCC040, VU040T). SCC040 is moderately differentiated tongue squamous cell carcinoma established from a 50-years old Caucasian male who was non-smoker who with alcohol intake history and died of disease (Shakir, 2014). SCC154 is derived from the tongue squamous cell carcinoma of a 54-years old Caucasian male with smoking and alcohol intake history. It has no TP53 mutations and no amplification of chromosomal band 11q13 (American Type Tissue Collection, 2018). VU040T is derived from tongue squamous cell carcinoma of a female (Hermsen *et al.*, 1996) (NCIthesaurus, 2018). VU147T is moderately differentiated floor of mouth squamous cell carcinoma established from a 58-years old male with the history of alcohol intake and smoking (Junaid, 2016). The HPV-negative status of SCC040 and VU040T and HPV-positive status of SCC154 and VU147T were

validated and confirmed by polymerase chain reaction using E6 and E7 primers sets (Figure 3.1).

A panel of 8 human OSCC cell lines (H103, H157, H314, H357, H376, H400, H413 and BICR31) originally derived by Prime et al. (1990) were obtained from European Collection of Authenticated Cell Cultures (ECACC) and confirmed negative for *Mycoplasma* infection. The cell lines have been characterised of p53, Ha-ras and CDKN2A mutations. In particular, all the cell lines showed p53 mutation (Burns *et al.*, 1993; Yeudall *et al.*, 1995), expressed wild-type Ha-ras except H357 (Clark *et al.*, 1993; Yeudall *et al.*, 1993), and all showed CDKN2A mutation or promoter methylation (Loughran *et al.*, 1996; C. L. Wu *et al.*, 1999).

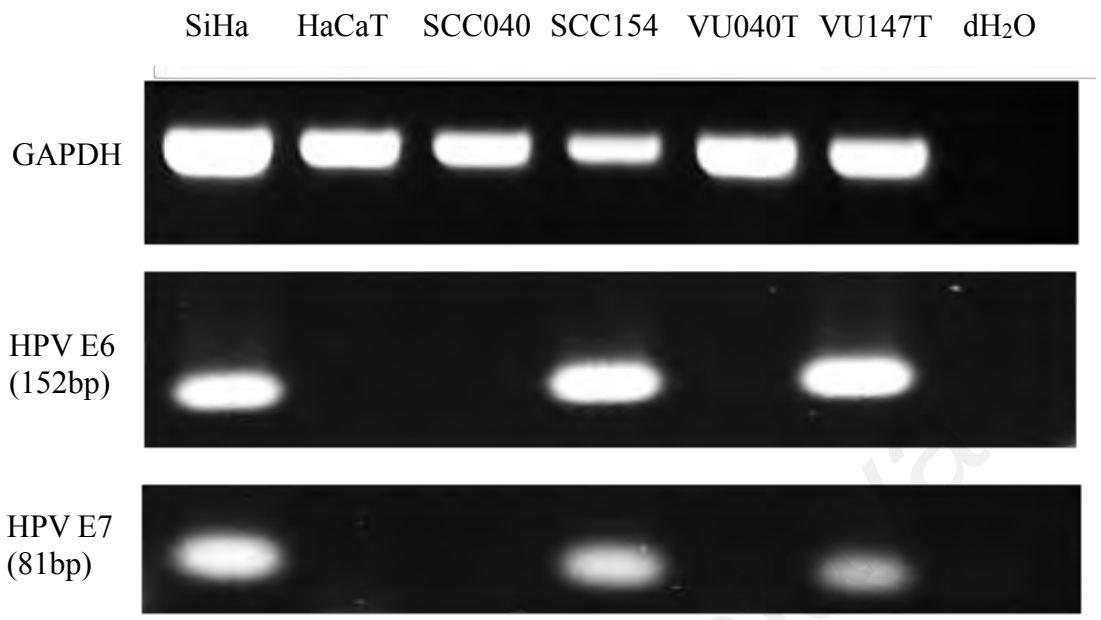

Figure 3.1: Validation of HPV status of OPSCC cell lines.

Absence and presence of E6 and E7 HPV viral oncogenes were confirmed in HPV-negative (SCC040 and VU040T) and HPV-positive (SCC154 and VU147T) OPSCC cell lines. Established HPV-positive cell line, SiHa, was used as the positive control; Distilled water, dH_2O was used as the negative control.

3.2 Immunohistochemistry (IHC) methods

3.2.1 Chromogenic immunohistochemistry

Chromogenic immunohistochemistry was carried out using the DAKO REAL™ EnVision Detection method. Tissue sections were removed from paraffin by immersing in Histo-Clear (National Diagnostic, UK) for 10 minutes and rehydrated by immersing the slides in 100% ethanol (Sigma-Aldrich, UK) for 10 minutes, 90% ethanol (Sigma-Aldrich, UK) for 5 minutes and 70% ethanol (Sigma-Aldrich, UK) for 10 minutes. The slides were rinsed with tap water for 10 minutes. Tissue sections were stained after low temperature antigen retrieval in Citrate buffer or overnight retrieval in EDTA solution. The endogenous peroxidase activity was blocked by hydrogen peroxide (Sigma-Aldrich, UK) for 10 minutes. Primary antibody diluted in PBS-Tween-20 (0.1%) was applied for 1 hour at temperature or overnight at 4^0C. The primary antibodies were discarded and the slides were washed with 1 X PBS for three times of 10 minutes each. Detection was performed with Streptavidin-HRP-conjugated goat anti-rabbit or goat anti-mouse secondary IgG (Dako, Agilent Technologies, US) for 30 minutes, followed by three times washing with 1 X PBS of 10 minutes each. The 3,3'-Diaminobenzidine (DAB) (Dako, Agilent Technologies, US) was added to the tissue sections and incubated at room temperature for 15 minutes. The Chromogen substrate solution was discarded from the slides. The tissue sections were rinsed under running tap water for 5 minutes. After counterstaining with Hematoxylin, the slides were mounted with aqueous mounting media using coverslips.

3.2.2 Antibody optimisation and validation for anti-CK AE1/AE3, -alpha-SMA, -COL8a1, -COL11a1 and -DDR1 antibodies

A panel of antibodies from different manufacturers were tested and validated for their specificities and sensitivity. They were optimised for the antigen retrieval buffer types,

pH, heating method and device, primary antibody concentration, types of diluents, incubation temperature and types of detection system. The optimal conditions of all the antibodies were assessed by Dr Maha Ibrahim (Pathologist, University of Birmingham, United Kingdom) and Professor Paul Murray (Professor of Molecular Pathology, University of Birmingham, United Kingdom) prior to use as listed in Table 3.1. Representative images of each optimised antibody were scanned and captured by Pannoramic Digital Slide Scanner (3DHISTECH Ltd, Hungary) are shown in Figure 3.2.

Table 3.1: Antibodies for immunohistochemistry assay

Antibody	Species	Dilution	Antigen retrieval	Manufacturer
Anti- pan-cytokeratin AE1/ AE3 (CK AE1/ AE3)	Mouse monoclonal	1:1000	Citrate buffer	Dako, Agilent Technologies, US
Anti- alpha-smooth muscle actin (α-SMA)	Rabbit polyclonal	1:1000	Citrate buffer	Dako, Agilent Technologies, US
Anti-fibroblasts-Specific Protein 1 (S100A4)	Rabbit polyclonal	1:1000	Citrate buffer	Sigma-Aldrich, US
Anti-fibroblasts Antibody, clone TE-7	Mouse monoclonal	1:500	EDTA buffer	Chemicon, Temecula, CA
Anti- collagen VIII alpha 1 (COL8a1)	Rabbit polyclonal	1:200	EDTA buffer	Sigma-Aldrich, US
Anti- Collagen XI alpha 1 (COL11a1) LS-C191996	Rabbit polyclonal	1:200	EDTA buffer	LifeSpan BioSciences, Inc, US
Anti- collagen XI alpha 1 (COL11a1) HPA052246	Rabbit polyclonal	1:200	EDTA buffer	Sigma-Aldrich, US
Anti- Discoidin Domain Receptor 1 (D1G6) XP®	Rabbit monoclonal	1:1000	Citrate buffer	Cell Signaling Technology, USA
Anti- Discoidin Domain Receptor 1 (C-20): SC532	Rabbit polyclonal	1:200	Citrate buffer	Santa Cruz Biotechnology, Inc, US
Anti- Discoidin Domain Receptor 1 (clone 2G4E12) LS-B3861	Mouse monoclonal	1:500	Citrate buffer	LifeSpan BioSciences, Inc, US

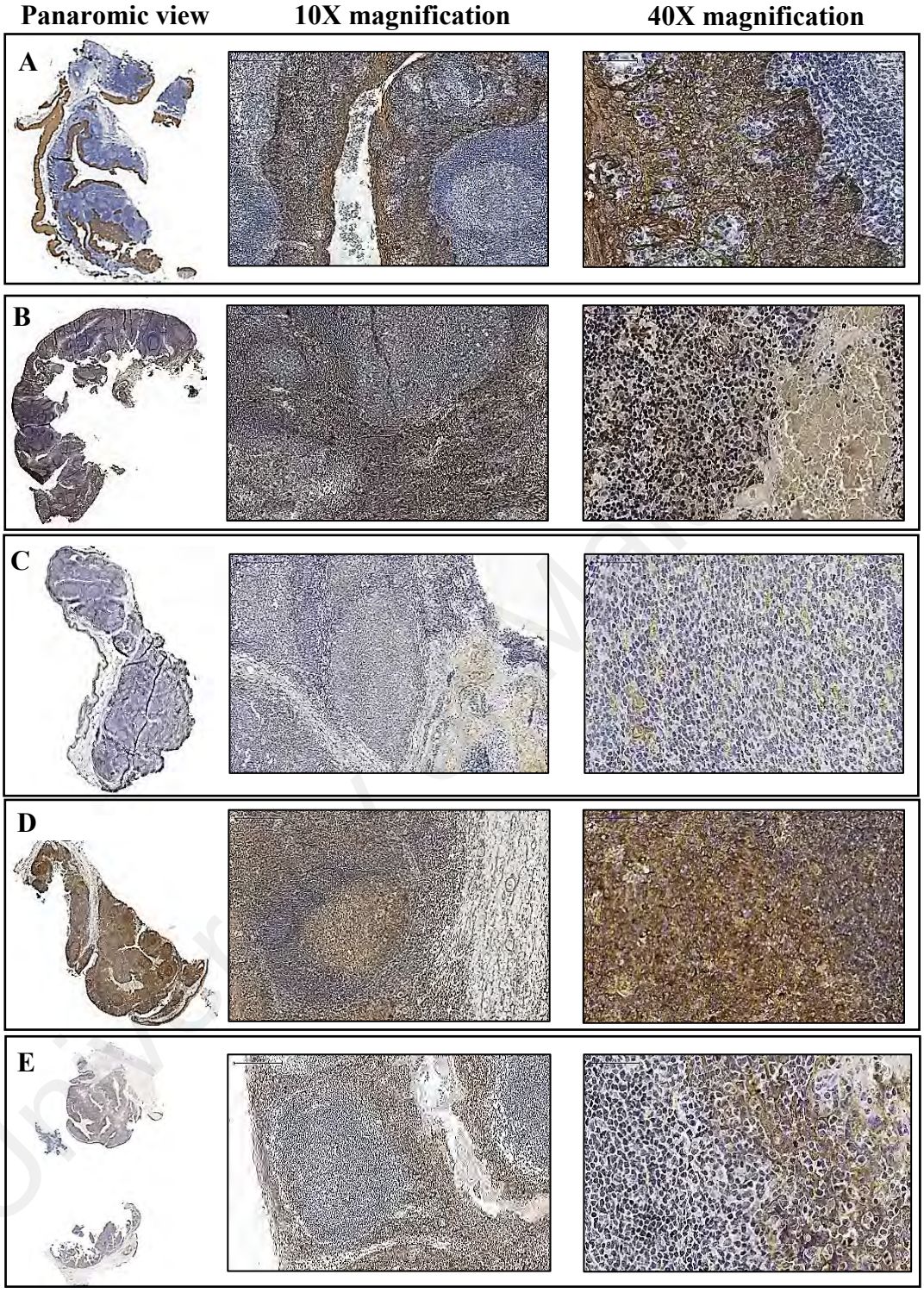

Figure 3.2: Representative images of optimised IHC staining using the selected antibodies in formalin fixed paraffin embedded human tonsil tissue.

Tonsils stained with antibodies targeting **(A)** CK AE1/ AE3 **(B)** α-SMA **(C)** COL8a1 **(D)** COL11a1 and **(E)** DDR1 and counterstained with haematoxylin under optimised condition and visualised at panaromic view; low power view at 10X magnification and high power view at 40X magnification.

3.2.3 Opal multiplex fluorescence staining

Tissues were de-waxed in Histo-Clear (AGTC Bioproducts t/a National Diagnostic, UK) for 10 minutes and rehydrated in 100% ethanol (Sigma-Aldrich, UK) and rinsed under running tap water for 5 minutes. The slides were blocked in 0.3% hydrogen peroxide (Sigma-Aldrich, UK) for 10 minutes to block the endogenous peroxidase activity and rinsed under running tap water for 5 minutes. The slides were microwaved in citrate buffer that contained 1.26g Sodium Citrate and 0.25g Citric Acid dissolved in 1L distilled water (pH6.0) at full power, moderate power and lower power for 10 minutes each. The slides were removed from the buffer after completely cooled and rinsed under running tap water. The slides were washed with 0.1% PBS-Tween-20 (PBST) for 5 minutes and incubated with 100µL of 5 X Casein Blocking System (Vector Laboratories Ltd., UK) at room temperature to avoid background signals.

The expression of DDR1 and COL11a1 in OPSCCs on the TMA were determined by dual immunohistochemistry using Opal TSA Plus Cyanine3/ Fluorescein immunofluorescence staining (NEL753001KT, PerkinElmer, Waltham, MA, US). Primary DDR1 antibody (rabbit mAb, 1:200 dilution, Cell Signaling) was used with anti-rabbit IgG (goat) HRP-conjugated secondary antibody prior to signal amplification with TSA Plus Cyanine 3. The primary-secondary-HRP complex was then removed by microwave treatment, the staining procedure repeated using primary COL11a1 antibody (rabbit pAb, 1:100 dilution, Sigma), anti-rabbit IgG (goat) HRP-conjugated secondary antibody and TSA Plus Fluorescein for detection.

The expression of CK AE1/ AE3, α-SMA, COL8a1, COL11a1 and DDR1 in primary OPSCC and OSCC tissue sections were examined. Primary cytokeratin AE1/AE3 antibody (mouse mAb, 1:1000 dilution, Dako Agilent Technologies, US) was used with anti-mouse IgG (goat) HRP-conjugated secondary antibody prior to signal amplification

with TSA Plus Cyanine 3. The primary-secondary-HRP complex was then removed by microwave treatment and the staining procedure repeated using primary DDR1 antibody (rabbit mAb, 1:200 dilution, Cell Signaling), anti-rabbit IgG (goat) HRP-conjugated secondary antibody and TSA Plus Fluorescein for detection. Serial sections were stained with primary α-SMA antibody (mouse mAb, 1:1000 dilution, Dako Agilent Technologies, US) and used with anti-mouse IgG (goat) HRP-conjugated secondary antibody prior to signal amplification with TSA Plus Cyanine 3. The primary-secondary-HRP complex was then removed by microwave treatment the staining procedure repeated using primary COL8a1 antibody (rabbit pAb, 1:100 dilution, Sigma) or COL11a1 antibody (rabbit pAb, 1:100 dilution, Sigma), anti-rabbit IgG (goat) HRP-conjugated secondary antibody and TSA Plus Fluorescein were used for detection of both collagens.

After counterstaining with DAPI, the slides were mounted with aqueous mounting media using coverslips. Their staining qualities and specificities were validated by pathologist. All the tissues on the TMA were scanned and captured by the Vectra Automated Quantitative Pathology Imaging System (PerkinElmer, Waltham, MA, US), whilst all the whole tissue sections were scanned and captured by the MetaMorph Microscopy Automation and Image Analysis Software (Molecular Devices, LLC, US).

3.2.4 Vectra Automated Quantitative Pathology Imaging System and InForm® Image Analysis software

Immunohistochemical stained slides were scanned and full tissue images were acquired using a fully automated quantitative pathology system, Vectra Version 2.0 (PerkinElmer, Waltham, MA, US). Single staining of each fluorophore was used to generate the spectral profile of unmixed emission spectra and auto-fluorescence spectrum was set up by using unstained slides. DAPI, FITC and Cy3 long pass filter cubes were optimised for maximum spectral resolution and to reduce cross-interference between

fluorophores. Whole slide scanning was performed where 10X and 40X pixel resolutions multispectral imaging were carried out and captured for every core. Identical exposure times were used for all slides to avoid variability. Epithelial staining in the nucleus and cytoplasm was scored and quantified digitally. The intensity of each fluorescent target was extracted from the multispectral data using linear unmixing.

The results were subsequently analysed using InForm® Analysis Software (PerkinElmer, Waltham, MA, US). Vectra multispectral images files were imported into the InForm software and converted into single layer TIFF format. The single layer TIFF files of each the TMA cores were loaded and analysed as 'maps' within a single 'scene' by using a customized import algorithm. Tissue and cellular segmentations were carried out in every core by the fluorescent intensity cut-offs determined by auto-adaptive threshold. Each core was segmented into epithelial cells and stroma, then further compartmentalized into cytoplasm and nuclei. Fields with artefactual staining, insufficient epithelial tissue or out-of-focus images were omitted prior to quantification. Each of the targets was interrogated specifically using fluorescent quantum dots and their intensities were quantitated on a per-pixel basis on every cell in a core, resulting in an algorithm-based absolute staining score for each core. Staining intensities for every marker were measured in the whole tissue core based on predetermined subcellular localization criteria. Pixel intensity of every marker in the predefined compartments was averaged across maps to yield a single value of double negative, single FITC, single Cy3, double positive, percentage of tissue category area and total number of cells for each core.

The entire process of scanning and analyses including the segmentation maps and scoring results of every core was assessed and validated for their accuracy and quality by Dr Maha Ibrahim (Pathologist, University of Birmingham) and Dr Neeraj Lal (Clinical Research Fellow, University of Birmingham).

3.2.5 MetaMorph® Microscopy Automation and Image Analysis

Multiplex fluorescent staining on tissue sections was quantitatively evaluated using a computerised image acquisition and analyser, the Metamorph® Microscopy Automation and Image Analysis (Molecular Device LLC, US). 5 random fields were captured for each slide. Auto threshold was used with manual adjustment to ensure the accuracy and validated by technical officer and pathologist. Regions of interest in every image were defined based on tissue structure and components, shape and size after image segmentation using the Integrated Morphometry Analysis. The active regions of interest were measured and analysed, whilst the regions outside the defined boundary were ignored. The total staining intensity, average intensity, maximum and minimum intensities were obtained by Region Statistics and Region Measurements. The image calibration and area measurement were carried out in microns and square microns. The area and co-localised integrated intensity of dual fluorescent probes in this study were measured quantitatively for the degree of overlap. H-scores were calculated as the product of the staining score and the percentage of cells showing positive staining. Means from random five fields were used in analyses for each case. The Data Log files of executed measurements were logging to Microsoft Excel for further analyses. Representative slides were imaged at magnification of (IV) 63X and (V) 100X oil immersion objectives captured by Confocal Laser Scanning Microscope (Zeiss). Constant laser settings, detector gain and offsets were used for all slides after the initial optimisation of each filter and slides. Confocal Z-stacks and flat images were acquired for each of the slides.

3.3 Cell culture methods

3.3.1 Maintenance of cell lines

Fibroblast cell lines were cultured in Dulbecco's Modified Eagle's Medium (DMEM) medium (Gibco Life Technologies, USA) supplemented with 20% fetal bovine serum

(FBS) (Gibco Life Technologies, USA). OPSCC cell lines were cultured in DMEM medium (Gibco Life Technologies, USA) supplemented with 10% FBS (Gibco Life Technologies, USA) and 10% Minimum Essential Media (MEM) Non-Essential Amino Acid Solution 10mM (100X) (Gibco Life Technologies, USA). The OSCC cells were cultured in Dulbecco's modified Eagle's medium and Hams F12 (DMEM/F12) (Gibco Life Technologies, USA) supplemented with 10% (v/v) FBS (Gibco Life Technologies, USA), 200 IU/mL Penicillin and 200µg/mL Streptomycin and 0.5µg/mL Hydrocortisone. The L428 (First Hodgkin cell line) and DG75 (Burkitt lymphoma cell line) controls were cultured in Roswell Park Memorial Institute (RPMI) 1640 medium (Gibco Life Technologies, USA) supplemented with 10% FBS (Gibco Technologies, USA). The breast cancer cell line T47D was cultured in DMEM medium (Gibco Life Technologies, USA) supplemented with 10% FBS (Gibco Life Technologies, USA).

3.3.2 Sub-culturing and cell number determination

All the cell lines used in this study were not beyond passage 10. Cells were sub-cultured at confluency of 70-80%.

To sub-culture the fibroblasts, OSCC and T47D control cell line, cells were washed with PBS (Gibco Life Technologies, USA) and trypsinised with 0.25% trypsin-EDTA (Gibco Life Technologies, USA). An equal volume of complete growth medium was added to neutralise the trypsin and cells were pelleted by centrifugation at 200 x g for 10 minutes. Cell pellets were resuspended in fresh medium and the cell number was determined using a Luna Automated Cell Counter (Logos Biosystems, Korea). To exclude cells and taken into account of viable cells, the cells were mixed 1:1 with Trypan Blue (Gibco Life Technologies, USA) and 10µL of the mixture was pipetted into compatible cell counting chamber (Logos Biosystem, Korea). The number of viable cells

was determined and cells were seeded at required densities according to the experimental designs.

To sub-culture OPSCC cell lines, the cells were trypsined with TrypLE Express Enzyme (1X), phenol red (Gibco Life Technologies, USA) for 10 minutes at 37^0C. Trypsinised cells were resuspended in equal volume of complete growth medium and pelleted as above.

For L428 and DG75 suspension control cell lines, cells were directly pelleted by centrifugation at 200 x g for 10 minutes without trypsinisation followed by the methods as mentioned above.

3.3.3 Cryopreservation and Recovery of Cells

Aliquots of 1 X 10^6 cells were resuspended in FBS containing 10% DMSO (Sigma Aldrich, USA) and transferred into cryovials (Nunc, USA). They were stored in Nalgene® Mr Frosty cryo container (Sigma Aldrich, UK) overnight at -80^0C and transferred to liquid nitrogen storage the next day.

To revive the cryopreserved cells, cells were thawed rapidly at 37^0C. Thawed cells were immediately resuspended in 5mL of fresh complete growth medium and centrifuged at 200 x g for 10 minutes. The supernatant was discarded and cell pellet was resuspended in 500µL of complete growth medium to ensure single cell suspension before grown in a 25cm^2 tissue culture flask in 5mL of fresh medium.

3.4 Stable knockdown of DDR1 in OPSCC cell lines

3.4.1 Transformation and propagation of competent bacteria (DH5α)

A 50µL aliquot of competent *Escherichia coli* cells (DH5α) was thawed on ice and mixed with 1µg shRNA construct from Sigma Aldrich (Table 3.2). The mixture was incubated on ice for 15 minutes, heat shocked at 42^0C in a thermomixer (Eppendorf, Germany) for exactly 45 seconds and promptly incubated on ice for 2 minutes. 250µL of

sterile Terrific Broth (Thermo Fisher Scientific, Waltham, MA, USA) was added to the cells and shaken in the thermomixer (Eppendorf™ Thermomixer, Thermo Fisher Scientific) at 200rpm and 37^{0}C for 1 hour prior to platting on 1.5% (w/v) Terrific Broth (TB) (Thermo Fisher Scientific, Waltham, MA, USA), 1.5% agar (Thermo Fisher Scientific, Waltham, MA, USA) plates and 50µg/ mL Carbenicillin (Thermo Fisher Scientific, Waltham, MA, USA). The bacteria cultures were incubated inverted at 37^{0}C for 16 hours. A single bacterial colony was then picked and inoculated into 5mL sterile TB medium containing 50µg/mL Carbenicillin and shaken overnight in 37^{0}C orbital shaker (SW22 Shaking Water Bath, Julabo GmbH, Germany) at 200r.p.m. 250uL of the overnight culture was inoculated into 500mL sterile TB medium containing 50µg/mL Carbenicillin and agitated for overnight in the 37^{0}C orbital shaker at 200r.p.m.

Table 3.2: shRNA constructs for stable DDR1 knock-down in cell lines

shRNA	DDR1
Clone 1	NM_001954/TRCN0000121293/pLKO
Clone 2	NM_001954/TRCN0000121163/pLKO
Clone 3	NM_001954/TRCN0000010084/pLKO

3.4.2 Purification of plasmid DNA

The resultant bacterial cell suspension from Section 3.4.1 was centrifuged at 5,300 x g for 10 minutes at 4^{0}C. The supernatant was discarded and plasmid DNA purification was performed using the Plasmid Maxiprep Kit (Qiagen Ltd, Manchester, UK). Cell pellets were resuspended in 10mL of 100µg/mL RNase containing Buffer P1. 10mL Buffer P2 was added and mixed thoroughly by inverting the tubes 6-8 times then incubated at room temperature for 5 minutes, followed by 10mL of cooled Buffer P3 and mixed gently by inverting the tubes again. The bacterial cells were lysed and the lysate were filtered through QIAfilter Maxi Cartridge into a 50mL tube after 10 minutes

incubation at room temperature. 2.5mL Buffer ER was added to the filtered lysates and mixed gently before incubating on ice for 30 minutes. The lysates were allowed to enter the resin of QIAGEN-tip 500 which had been pre-equilibrated with 10mL Buffer QBT. The tips were washed with 30mL of Buffer QC after the flow of lysates. The plasmids DNA were eluted with 15mL Buffer QN and precipitated with 0.7 volumes isopropanol at room temperature. The plasmid DNA was pelleted by centrifugation at 5,300 x g for 30 minutes at 4^0C and the supernatants were discarded. The pelleted plasmid DNA was then washed with 5mL of 70% (v/v) molecular grade ethanol (Sigma Aldrich, USA) by centrifugation at 5,300 x g for 10 minutes at 4^0C. After air-dried for 10 minutes at room temperature, the DNA pellets were dissolved in 500µL of 5mM Tris/HCl buffer. DNA concentration was quantitated using a NanoDrop 2000 spectrophotometer.

3.4.3 Generation of Puromycin kill curve

Appropriate densities of target cells were seeded in 6-well plates to be 60% confluence on the next day. Increasing concentrations of Puromycin (Sigma-Aldrich, USA) at 0, 0.25, 0.5, 1, 2.5 and 5µg/mL were added to the target cells. The cells were cultured at 30^0C at 5% CO_2 incubator and the percentage of alive cells were observed every subsequent day until Day-7. The minimum concentration of Puromycin that killed 90% of the target cells were chosen as the selection dose for subsequent experiments.

3.4.4 Lentiviral transfection and production of lentiviral supernatants

Lentiviral transfection and transduction system was used to generate stable knock down of DDR1 in HPV-negative (SCC040 and VU040T) and HPV-positive (SCC154 and VU147T) OPSCC cell lines. The DDR1 shRNA lentiviral plasmids and non-targeting shRNA (pLKO.1/NS) were prepared as described in Section 3.4.1 and 3.4.2. 12 X 10^6 HEK 293T cells were seeded in T150 flask until 80-90% confluent. A DNA mixture in OptiMEM contained 40µg Puromycin-resistant shRNA construct, 10µg envelope

plasmid pMD2.G and 30µg packaging plasmid psPAX2 were added to 5mL Opti-MEM® (Gibco Life Technologies, USA) and sterilised through a 0.2µm filter (Sartorius, Germany). Another 5mL of Opti-MEM® containing 1µL of 10mM polyethylenimine (PEI) (Sigma-Aldrich, USA) was sterilised through 0.2µm filter. These two solutions of plasmids DNA and PEI were mixed 1:1 ratio and incubated for 20 minutes at room temperature. The HEK 293T cells were washed with fresh Opti-MEM®. 10mL of the plasmids DNA and PEI mixtures were added to transfect the cells at 37^0C and 5% CO_2 for 4 hours. The media were then replaced with fresh complete DMEM and the cells were incubated for another 48 hours. The resulting viral supernatants were collected and filtered through a 0.45µm filter before aliquoting and storage at -80^0C until use.

3.4.5 Lentiviral transduction of OPSCC cells

1 X 10^6 target cells (SCC040, SCC154, VU040T and VU147T) were seeded in 100mm culture plates one day prior to transduction. The viral supernatants collected as described in Section 3.4.4 were reconstituted in 1:1 ratio with fresh DMEM and added to the target cells together with Polybrene (final concentration of 8µg/mL). The cells were incubated with the virus-containing medium at 37^0C and 5% CO_2 for 18 hours and the media then replaced with fresh DMEM. Puromycin (working concentration of 2µg/mL) was added in order to select for successfully transduced target cells. Fresh Puromycin-containing medium were changed every few days until the non-transduced cells being killed off. The selected transduced cells were being cultured and expanded for the used in subsequent experiments. The knock down efficiency of each construct lines was determined by Q-PCR and Western blotting methods, as described in Sections 3.5 and 3.6.

3.4.6 Collection of conditioned media and protein quantification

Fibroblasts were grown to 70-80% confluence in 100cm^2 dishes in DMEM complete medium. The media were changed to serum-free DMEM medium and the cells cultured

for an additional 3 days. Supernatants were collected on Day-4 and replaced with complete growth medium for cells recovery. The cells were incubated with fresh serum-free medium again on Day-7 and the supernatants were collected on Day-9. The collected supernatants were concentrated with Amicon® Ultra-15 Centrifugal Filter Devices (Merck Millipore, Germany). 12mL of the supernatants were loaded into the filter device and placed into fixed angle rotor with the membrane panel facing up and centrifuged at 5000 x g maximum speed for 30 minutes at 4°C. The protein concentrations of the concentrated solutes were determined by Bradford Protein Assay kit (Bio-Rad Laboratories, USA) as described in Section 3.6.2. The concentrated solutes were kept at -80°C until further use.

3.5 Molecular biology methods

3.5.1 RNA extraction from cell lines

Total RNA extraction was performed using QIAGEN RNeasy® Mini Kit (Qiagen Ltd, Manchester, UK). Cells were cultured to at least reach 1 X 10^6 cell number and trypsinised. The cells were washed and pelleted with ice cold PBS and dissolved in the recommended volume of RLT Buffer added with β-mercaptoethanol (Sigma Aldrich, USA) and vortexed. 700µL of the resuspended pellet was loaded into a QIAshredder spin column (Qiagen, Germany) and homogenised by centrifugation for 2 minutes at maximum speed of 20,238 x g in a micro-centrifuge (Eppendorf Centrifuge 5424). Equal volume of 70% (v/v) molecular grade Ethanol (Merck, Germany) was added to the lysates and mixture was loaded into an RNeasy® spin column. After washing with washing buffer, DNAse I incubation mix of RNAse Free DNAse set (QIAGEN, Germany) was loaded directly to the spin column membrane for on-column DNAse digestion. The column was washed with washing buffer for multiple times. RNA was eluted by loading 40µL of RNAse-free water onto the membrane. The quality and concentration of RNA

were determined by Nanodrop 2000 Spectrophotometer (Thermo Fisher Scientific, Waltham, MA, USA). The pure RNA with 260/230 ratios within 2.0-2.2 and 260/280 ratios close to 2 were used for subsequent experiments.

3.5.2 cDNA synthesis

Complementary DNA (cDNA) was synthesized using High-Capacity cDNA Reverse Transcription Kit (Applied Biosystem, California, US). 1µg of RNA was added with RNase-free water for final volume of 10µL. The RNA was mixed by centrifugation with a master mix containing 2µL of 10 X Reverse Transcriptase Random Primers, 2µL of 10 X Reverse Transcriptase Buffer, 0.8µL of 100mM deoxyribonucleotide triphosphate (dNTP) mix, 1µL of MultiSribe™ Reverse Transcriptase and 4.2µL of RNAse-free water. The mixtures were loaded to a thermal cycler (Applied Biosystems, USA) to convert the RNA into cDNA under the program of 10 minutes at 25°C, 2 hours at 37°C, 5 minutes at 85°C and hold at 4°C prior to storage at -20°C.

3.5.3 Reverse-Transcriptase Polymerase Chain Reaction (RT-PCR) and gel electrophoresis

The E6 and E7 oncogenes primers sequences were used for HPV detections and another five different DDR1 isoforms primers pairs were used to amplify the DDR1a to DDR1e as shown in Table 3.3. 1µL of the cDNA was mixed with 12.5µL of 2 X MM ET master mix, 2.5µL primer mix and 9µL nuclease-free water in 0.2mL PCR tube. The mixture in the tube was resuspended and vortexed before loaded to Veriti™ 96-Well Thermal Cycler (Applied Biosystem, California, US) and ran under different programs with the type of primers respectively (Table 3.4). After the RT-PCR, the DNA amplified product was loaded into 2% agarose gel and ran in 1 X TAE buffer for 30 minutes at 110V voltage. Bands were visualized by using MultiDoc-It™ Imaging System (UVP, LLC, US).

Table 3.3: Forward and reverse sequences of primers for RT-PCR

Gene	Sequences (5'--3')
E6	Forward primer: GCACCAAAAGAGAACTGCAATGTT
	Reverse primer: AGTCATATACCTCACGTCGCAGTA
E7	Forward primer: CAAGTGTGACTCTACGCTTCGG
	Reverse primer: GTGGCCCATTAACAGGTCTTCCAA
DDR1a	Forward primer: CCCCAATGGCTCTGCCTA
	Reverse primer: AACAATGTCAGCCTCGGCATA
DDR1b	Forward primer: GGCCAAACCCACCAACAC
	Reverse primer: AACAATGTCAGCCTCGGCATA
DDR1c	Forward primer: CCCTTTGCTGGTAGCTGTCAA
	Reverse primer: ACCAAGAATGCCAGCTTCTCC
DDR1d	Forward primer: GCAGGCTCCTCAGCAAGG
	Reverse primer: CCTTTGCTGGTAGCTGTCAAGA
DDR1e	Forward primer: GTCCCCAATGGCTCTGGT
	Reverse primer: TTCCTGAAAGAGGTGAAGATCAT
GAPDH	Forward primer: GAAGGTGAAGGTCGGAGTC
	Reverse primer: GAAGATGGTGATGGGATTTC

Table 3.4: Reverse transcription PCR programmes

Gene	Stage	Cycle	Step	Temperature	Time
E6 & E7	1	1	Initial denaturation	95°C	15 min
	2	45	Denaturation	94°C	30 sec
			Annealing	56°C	40 sec
			Elongation	72°C	40 sec
	3	∞	Hold	4°C	∞
GAPDH	1	1	Initial denaturation	94°C	2 min
	2	25	Denaturation	94°C	30 sec
			Annealing	58°C	45 sec
			Elongation	72°C	1 min
	3	1	Final elongation	72°C	10 min
	4	∞	Hold	4°C	∞
DDR1	1	1	Initial denaturation	96°C	1 min
	2	40	Denaturation	96°C	10 sec
			Annealing	50°C	5 sec
			Elongation	60°C	4 min
	3	1	Final elongation	72°C	5 min
	4	∞	Hold	4°C	∞

3.5.4 Quantitative Real-Time Polymerase Chain Reaction (Q-PCR)

Quantitative real-time PCR reactions (Q-PCR) was performed using Fast Start Universal Probe Master (ROX; Roche Molecular Diagnostics, California, US) and Taqman ® Gene Expression Assay probes (Applied Biosystems, California, US) labelled with FAM reporter dye at the 5' end. The following TaqMan ® Gene Expression Assay probes were used to investigate the expression levels of different target mRNAs: COLVIIIa1 (Hs00156669_m1), COLXIa1 (Hs01097664_m1), DDR1 (Hs01058430_m1) and GAPDH (4326317E). The cDNA was diluted at 1:20x ratio with nuclease-free water. 5µL of the diluted cDNA, 10µL of FastStart Universal Probe Master (Rox), 1µL of TaqMan® Gene Expression Assay, 1µL of GAPDH probe and 3µL of nuclease-free water were mixed and loaded into each well. The expression levels of target genes mRNA were detected in triplicate wells and read by StepOnePlus 7500 Fast Real-Time PCR system (Applied Biosystem, California, US). Quantification of the Q-PCR results was performed using the 7500 Software v2.0.5 (Applied Biosystems, California, US). Data of delta-delta Ct (ΔΔCt) were expressed either as relative gene expression normalized to endogenous control (GAPDH) which was amplified in the same reactions in the case where reference sample was not applicable or relative to the baseline value in reference sample to obtain the absolute fold change in the case where reference sample was applicable.

3.6 Western blotting protein analysis

3.6.1 Protein extraction

Cells were grown in 60mm dishes until 80% confluent. The cells were lysed on ice for 15 minutes using NP40 lysis buffer containing [1.5M NaCl, 1% IGEPAL® CA-630 (Sigma-Aldrich, USA), 50mM Tris-HCl (pH8.0), 1:100 Protease Inhibitor Cocktail Set III (Calbiochem, Merck Millipore, Darmstadt, Germany) and 1:100 Halt Phosphatase

Inhibitor Cocktail (Thermo Fisher Scientific, Waltham, MA, USA). The cells were scraped and incubated on ice for another 15 minutes. The lysates were then centrifuged at maximum speed (20,238 x g) for 30 minutes at 4^0C on a refrigerated centrifuge (Eppendorf, Hamburg, Germany) and the protein lysates stored at -80°C.

3.6.2 Protein concentration quantification

Protein concentrations were measured using a Bradford assay kit (Bio-Rad, CA, US). Bovine Serum Albumin (BSA) standard set (Bio-Rad, USA) was used to create a standard curve of 7 increasing BSA concentrations at 0.125, 0.250, 0.500, 0.750, 1.000, 1.500 and 2.000mg/mL). 250uL of 1 X Bradford reagent (Bio-Rad Laboratories, USA) was added to 5µL of protein samples diluted at 1:10 ratio with PBS or the BSA standards in a 96-well plate and incubated at room temperature for 5 minutes. The absorbance was measured at 595nm using a Tecan Microplate Reader (Infinite® 200 PRO, Switzerland). A standard curve was plotted using the BSA standards readings to determine the protein concentration of the samples.

3.6.3 Sodium dodecyl sulphate-polyacrylamide gel electrophoresis

50µg protein was mixed with 2 X Laemmli buffer (Bio-rad, USA) containing 5% β-mercaptoethanol (Bio-basic, Canada). The sample was heated at 90°C for 10 minutes to denature the proteins. Bio-rad apparatus was used for SDS-PAGE. 6% resolving gel was prepared and poured into the gel cassettes. Once the gel had set, 4% gel stacking gel was casted on top of the resolving gel with the gel comb inserted. The gel was placed in the electrophoresis tank containing 1 X Running Buffer (Thermo Scientific, USA) and the denatured protein lysates and 5µL of Precision Plus Protein All Blue standard (Bio-rad, USA) were loaded into wells after removing the gel comb. Electrophoresis was performed at 70V for 20 minutes to allow the protein lysates ran down the stacking gel followed by 90V for 90 minutes to run down the resolving gel.

3.6.4 Transfer, immunoblotting and visualisation of proteins

0.45µm pore size polyvinylidene difluoride (PVDF) membranes (Merck Milipore, Germany) were hydrated in methanol (Merck Milipore, Germany) for 15 seconds, ultrapure water for 2 minutes and 1 X Transfer Buffer (Bio-rad, USA) containing 20% methanol for 5 minutes. Protein transfer was carried out using a Trans-Blot® Turbo Transfer System (Bio-Rad, CA, USA) at 25V for 30 minutes. The membrane was subsequently blocked in 5% non-fat milk or 5% BSA (Bio-basic, Canada) in Tris-Buffered Saline (TBS) [150mM NaCl, 50mM Tris-HCl (pH7.6)] with 0.1% Tween 20 (TBST) for 1 hour at room temperature and then incubated with primary antibodies overnight at various optimal dilutions as listed in Table 3.5. The membrane bound protein-antibody complexes were incubated with 1:5000 dilution of horse-radish peroxidase (HRP)-conjugated secondary antibodies (goat anti-rabbit or goat anti-mouse antibodies, Sigma-Aldrich) at room temperature for 1 hour after washed three times for 10 minutes each in TBST. The membrane was washed with TBST again for three times of 10 minutes each and followed by enhanced chemiluminescence (ECL) detection using Odyssey Fc Imaging System (LI-COR Biosciences, USA) after incubated with Western Bright™ Sirius ECL reagent (Advansta, CA, USA).

Table 3.5: Primary antibodies details and working dilutions for Western blotting

Antibody	Species	Dilution	Blocking buffer	Manufacturer
Anti-DDR1 (D1G6) XP®	Rabbit monoclonal	1:1000	5% w/v BSA/ TBST	Cell Signaling Technology, USA
Anti-DDR1 (C-20): SC532	Rabbit polyclonal	1:200	5% w/v BSA/ TBST	Santa Cruz Biotechnology, Inc, US
Anti-DDR1 (clone 2G4E12) LS-B3861	Mouse monoclonal	1:500	5% w/v BSA/ TBST	LifeSpan BioSciences, Inc, US
Anti-GAPDH ab37168	Rabbit polyclonal	1:1000	5% w/v non-fat milk/ TBST	Abcam, UK

3.7 Ribonucleic acid-Sequencing (RNA-seq) and bioinformatics

DDR1 transcript expression in H376 cells was analysed by RNAseq, which was performed as part of a related study (Yap *et al.*, 2016). Briefly, Total RNA was extracted and strand specific library preparation and paired-end RNA sequencing (Illumina HiSeq 4000) was performed by BGI Tech Solutions (Hong Kong) Co Ltd. Sequence reads were aligned to human ensemble transcripts database using star aligner. Bioinformatic analyses were performed by Dr Wenbin Wei (Senior Bioinformatician, University of Birmingham). Differentially expressed 58 splice variants of DDR1 were identified and transcript quantification was performed using RSEM (RNA-seq by Expectation-Maximization). Percentages of transcript isoforms were also calculated and reported by RSEM. The data was normalized using TMM (trimmed mean of M values) method, and then analysed to identify the major DDR1 transcripts isoforms. The raw data was background subtracted using normexp method and normalized using quantile method of limma package. Differentially expressed probe sets were identified using limma (Smyth, 2004)with the criteria of absolute fold change greater than 1.5 and limma p value< 0.01.

3.8 Analysis of DDR1 expression in The Cancer Genome Atlas HNSCC data set

The Cancer Genome Atlas (TCGA) analyses were performed by Dr Robert Hollows (Bioinformatician, University of Birmingham). Data from TCGA were downloaded using the "Data matrix" option within the TCGA data portal (Network, 2015a). Level 3 RNA-sequencing data based on the Illumina HiSeq 2000 RNA Sequencing platform (Version 2) were downloaded along with all available clinical data in the "Biotab" format". Tumour samples were categorized as either "HPV-negative" or "HPV-positive" according to the data item "HPV status" provided in TCGA's clinical data. In total there were 400 HPV-negative tumour samples (282 male, 118 female) and 94 HPV-positive samples (84 male, 10 female) for which RNA-seq data were also available. In addition,

RNA-seq data were available for 44 "normal" samples, 37 of which were matched to HPV-negative tumour samples and 6 to HPV-positive tumour samples.

The RNA-seq files labelled "rsem.genes.results" contained unnormalised read counts for over 20,000 genes. Read counts were normalized between samples and converted to counts-per-million (cpm) reads for each gene using the edgeR package (M. D. Robinson *et al.*, 2010) in R (Team, 2016). Differential expression analysis was also performed using edgeR. Kaplan-Meier and Cox proportional hazards analyses of overall survival based on normalised cpm values for DDR1 were performed using the "Survival" package in R. Log-rank statistical tests were performed for Kaplan-Meier analyses, with samples split into groups using the modal DDR1 cpm value and also into the top and bottom thirds by DDR1 expression. Wald tests were used for the Cox analyses. A significance level of 5% was used in all statistical tests.

3.9 *In vitro* assays of cell behaviour and apoptosis

3.9.1 Senescence detection assay

8 X 10^4 cells were seeded into 12-well plates and senescence-associated beta-galactosidase (SA-β-Gal) activity measured using a Senescence Detection kit (BioVision, Mountain View, CA). Cells were washed thoroughly with 1mL of 1 X PBS and fixed with 500µL of Fixative Solution for 15 minutes at room temperature. The cells were washed twice in 1mL of 1 X PBS and incubated in a dark environment for overnight in 500 µL staining solution mixture consisted of 470µL Staining Solution, 5µL Staining Supplement and 25µL of 20mg/ml X-gal in dimethyl sulfoxide (DMSO). The staining solution was removed and the cells were overlaid with 70% glycerol. The development of blue staining was detected and captured by using a Nikon inverted microscope equipped with a colour CCD camera (Nikon Instruments, Inc., Lewisville, US) under 20X

magnification. Senescent cells with positive dark blue staining were counted in random 10 microscope fields and the percentage of senescent cells calculated.

3.9.2 Cell proliferation assay

Cells were cultured in 75cm^2 flasks until 80% confluence. Cells were trypsinised with TrypLE Express (Gibco® Thermo Fisher Scientific, US) and centrifuged at 200 x g for 8 minutes. Pellets were resuspended in fresh complete medium and 1 X 10^5 cells were seeded into 60mm dish. Media were changed every 4 days over a period of 14 days. To examine the effect of collagen, the cells were treated with 100µg/mL of collagen (Merck Millipore, Germany) the next day and fresh collagen added at each media change. Cell numbers were determined at 4-day intervals by trypsinisation and cell counting using a Luna Automated Cell Counter (Logos Biosystems, Korea).

3.9.3 Clonogenic assay

50 cells were seeded into triplicate 60mmes dish in 3mL complete medium. Media were changed every 4 days over a period of 14 days. On Day-14, the cells were washed twice with 1 X PBS, fixed and stained with 0.5% crystal violet (Merck Millipore, Germany) contained 0.4% formaldehyde (Merck Millipore, Germany) and 20% methanol (Merck Millipore, Germany) for 2 hours at room temperature. The cells were washed under running tap water and air-dried for overnight. Colonies were counted by bright field microscope where islands of more than 50 cells were considered as one colony.

3.9.4 Wound healing assay

Cells were seeded into 6-wells plate at a density that reached 90% confluence in monolayer after 24 hours. The monolayer of cells was gently scratched with a sterilised pipette tip across the centre of the well in a straight line direction. The cells were washed gently with PBS to remove dead cells and replenished with fresh complete medium containing with or without collagen (Merck Millipore, Germany) or gelatin (Sigma-

Aldrich, US). Closure of the wound was monitored every 24 hours over a period of 72 hours using a Nikon inverted microscope equipped with a colour CCD camera (Nikon Instruments, Inc., Lewisville, US) under 20X magnification.

3.9.5 Transwell migration assay

Cells were grown in 75cm^2 flasks to reach 80% confluence and incubated with or without collagen (Merck Millipore, Germany) or gelatin (Sigma-Aldrich, US) for 24 hours. The next day, cells were treated with a final concentration of 10µg/mL mitomycin C (Merck Millipore, Germany) at 37°C for 2 hours to negate the effects of cell proliferation. Polycarbonate inserts of 8µm pore size (Transwell, Corning, USA) in 24-well plates were coated with 200µL of 10µg/mL fibronectin (Gibco Life Technologies, US) at 37°C for 2 hours prior used. 1 X 10^6 cells in 200µL medium were seeded into the upper chambers and 500µL of medium enriched with 20% FBS was loaded into the lower chamber. The cells were allowed to migrate for 19 hours and the cells in the upper chamber were then removed with a cotton bud and the migrated cells in the lower chamber were fixed and stained with 0.5% crystal violet (Merck Millipore, Germany) contained 0.4% formaldehyde (Merck Millipore, Germany) and 20% methanol (Merck Millipore, Germany) for 2 hours at room temperature. The cells were washed with distilled water and allowed to air-dry for overnight before counting five random fields at 20X magnification for each triplicate by using a Nikon inverted microscope equipped with a colour CCD camera (Nikon Instruments, Inc., Lewisville, US).

3.9.6 Transwell invasion assay

Cell invasion assays were performed using Corning® Matrigel® Invasion Chamber (8µm pore size; Discovery Labware, Inc, US) in 24-well plates. Cells were grown in 75cm^2 flasks to reach 80% confluence and serum-starved for overnight prior to the experiment. The next day, cells were treated with a final concentration of 10µg/mL

mitomycin C (Merck Millipore, Germany) at 37°C for 2 hours invasion chambers rehydrated in 500µL of serum-free medium at 37°C and 5% CO_2 for 2 hours. 1 X 10^6 or 0.5 X 10^6 cells depending on the cell line to be used, in 500µL media were seeded into the upper chambers and 750µL of media enriched with 20% FBS was pipetted into the lower chamber. The cells were allowed to invade for 48 hours at 37°C and 5% CO_2. The non-invaded cells in the upper chamber were then removed with a cotton bud and the invaded cells in the lower chamber were fixed, stained and counted, as described in Section 3.9.6.

3.9.7 MTT cell viability assay

Cell viability was determined by colorimetric 3-(4, 5-Dimethylthiazol-2-yl)-2, 5-diphenyltetrazolium bromide (MTT) assay. Cells were seeded in triplicate wells of 96-well plates (Costar, Washington, DC, USA) and incubated at 37°C for 24 hours before treatment with Cisplatin (Tocris, UK) for a period of 72 hours. Then a 10% volume of 5mg/mL MTT (Merck, Germany) was added to the wells and incubated for 4 hours and the crystal blue formazan was solubilized overnight in 10% sodium dodecyl sulphate (SDS; Thermo Scientific, USA)/0.01M hydrochloric acid (Merck, Germany). The absorbance was measured at a wavelength of 575nm with a reference wavelength of 650nm using a Tecan Infinite M200 Pro Multiplate Reader (Tecan, Switzerland) with Magellan Data Analysis Software (Tecan, Switzerland). Viability curves were plotted to determine the IC_{50} which was the concentration of the drug at which 50% of cells were killed by Cisplatin.

3.9.8 Annexin V-FITC/ Propidium Iodide (PI) apoptotic assay

Cells treated with Cisplatin (Tocris, UK) with or without Collagen (Merck Millipore, Germany) pre-treatment were collected using Accutase Cell Detachment Reagent (BD Biosciences, CA, US) together with the dead cells in the medium. Cells were pelleted by

centrifugation at 200 x g for 10 minutes and resuspended in 1 X Binding Buffer (BD Pharmingen™, CA, US) at a final concentration of 1 X 10^6 of cells after washing with cold 1 X PBS and filtered with cell strainer (BD Biosciecnes, CA, US). 1 X 10^5 cells in 100µL of the suspension was transferred to a 5mL round bottom polypropylene tube (BD Biosciences, CA, US). The cells were incubated in 5µL each of Annexin V-FITC and Propidium Iodide (PI) supplied in the FITC Annexin V Apoptosis Detection Kit I (BD Pharmingen™, CA, US) for 15 minutes in the dark at room temperature. The cells were immediately analysed using BD FACS Canto II Flowcytometer (BD Biosciences, CA, US) and BD FACSDIVA software (BD Biosciences, CA, US) after diluted with 400µL of 1 X Binding Buffer. Cells treated with 1mM of Cisplatin were used as positive controls and untreated cells were used to define the cell debris.

3.10 Statistical analysis

All the statistical analyses were carried out using GraphPad PRISM 5.0 software (Graphpad, USA) and SPSS Version 22. The associations and correlations of protein expression in tissues with socio-demographic and clinico-pathological background data in OPSCC and OSCC were studied using Pearson Chi Square, Spearman Correlation, One-way ANOVA, Bonferroni Post Hoc, Univariate Logistic Regression and Multiple Logistic Regression tests. Differences between the groups were evaluated by ANOVA, followed by the Dunnett's test for post hoc analysis. A p-value less than 0.05 was considered as statistically significant.

CHAPTER 4: IDENTIFICATION AND VALIDATION OF SECRETED PROTEINS UP-REGULATED BY CAFS AND EXPRESSION OF COLLAGENS AND DDR1 IN OPSCC AND OSCC

4.1 Introduction

It has been reported previously that CAFs from head and neck cancer are often prematurely senescent and secrete more proteins than normal oral fibroblasts (NHOFs) (Y Hassona *et al.*, 2014; Lim *et al.*, 2011b). Conditioned media (CM) from these CAFs has been shown to enhance the invasive capacity of malignant epithelial cells (Lim *et al.*, 2011b), but there are limited published data describing the precise mechanisms underlying the communication between CAFs and tumour cells in HNSCC.

To identify the proteins secreted by CAFs that might contribute to crosstalk with HNSCC cells, a previously published microarray gene expression data set Lim *et al.* (2011b) was reanalysed and it was shown that senescent CAFs expressed higher levels of COL8a1 and COL11a1 than non-senescent CAFs and NHOFs. These observations led to the hypothesis that collagens secreted, at least in part, by CAFs might affect tumour cell behaviour.

Extracellular collagens are known to bind to various collagen receptors. In particular, collagens act as ligands to bind and interact with a unique family of receptor tyrosine kinases named Discoidin Domain Receptors (DDRs) (H. L. Fu *et al.*, 2013). Overexpression of one of its isoforms, DDR1, has been reported recently in several cancer types, such as lymphocytic leukemia (Barisione *et al.*, 2017), colorectal cancer (Y. Hu *et al.*, 2014), and lung cancer (Valencia *et al.*, 2012). However, its expression has not been reported in head and neck cancer. Therefore, the present study examined the expression of collagens and DDR1 in human OPSCC and OSCC cell lines and tissues.

4.2 Verification of the senescence state of CAFs and NHOFs

A series of normal fibroblasts (NHOF4, NHOF6 and NHOF7), non-senescent CAFs (BICR59F, BICR69F and BICR70F) and senescent CAFs (BICR3F, BICR31F and BICR78F) were used in this study. To confirm that these fibroblast strains exhibited similar phenotypes to those reported previously (Lim *et al.*, 2011b), the degree of senescence was first measured by assaying for senescence-associated β-galactosidase (SA-β-gal) activity. In agreement with Lim *et al* (2011), the results showed that the level of senescence in CAFs derived from head and neck tumours was variable and that the senescence level in NHOFs was low (Table 4.1), indicating that the senescent phenotypes were stable over time. Representative images of the SA-β-gal staining are shown in Figure 4.1A demonstrating a higher degree of senescence in CAFs.

In order to confirm that the senescence state of CAFs is associated with a protein secretory phenotype, the amount of protein secreted by representative fibroblast strains (NHOF7, BICR59F and BICR78F) was measured. The protein concentrations in the CM were measured using Bradford assays over the incubation periods of 4 and 9 days. The results showed that the highly senescent CAF (BICR78F) secreted comparably higher concentration of proteins than non-senescent CAFs (BICR59F) and normal fibroblasts (Figure 4.1 B).

Table 4.1: Level of senescence in NHOFs and CAFs derived from head and neck measured by SA-β-gal activity. The senescence level was variable in CAFs but generally higher compared to NHOFs.

Fibroblast types	Fibroblast strains	Senescence percentage (%)
Normal	NHOF-4	7.14
	NHOF-6	1.69
	NHOF-7	5.21
CAFs	BICR59F	9.38
	BICR66F	19.08
	BICR69F	16.53
	BICR73F	26.18
	BICR3F	63.14
	BICR31F	66.41
	BICR63F	48.79
	BICR78F	49.6

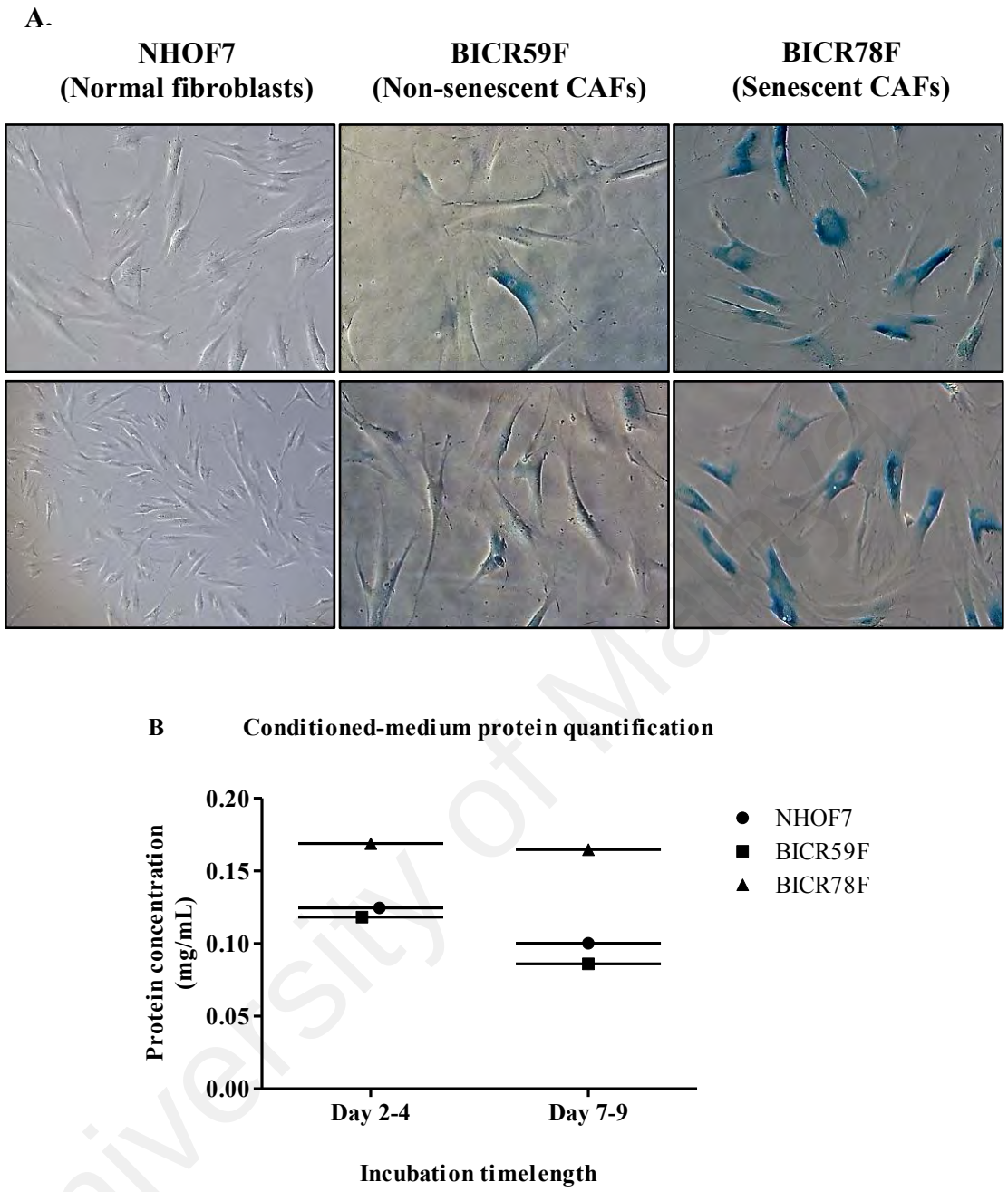

Figure 4.1: Highly senescent CAFs (BICR78F) secrete more proteins than moderately senescent CAFs (BICR59F) and normal fibroblasts (NHOF7).

A. Bright-field images of SA-β-gal staining (blue) in representative fibroblast strains (magnification 20X) demonstrated higher senescence state in CAFs. **B.** The protein content of conditioned media was quantified by Bradford assay. Senescent CAFs contained more secreted proteins than CAFs from GS-OSCC and NHOF. Line, mean of triplicates; error bars, SD of triplicates.

4.3 Validation of CAFs transcriptomic expression profiles

In a genome-wide transcriptomic study conducted by Lim *et al.* (2011b) which comprised fibroblast strains of 6 NHOFs, 8 non-senescent CAFs and 10 senescent CAFs derived from primary tissue samples, it was demonstrated that gene expression profiles could distinguish senescent CAFs, non-senescent CAFs and normal oral fibroblasts. In order to identify the secreted proteins which could potentially play a role in head and neck cancer pathogenesis, the microarray data from this study was reanalysed to identify secreted proteins up-regulated in senescent CAFs.

121 genes were up-regulated in senescent but not in non-senescent CAFs. To identify the possible genes responsible for mediating tumour-stroma crosstalk, these 121 genes were manually ranked in terms of cytoplasmic localisation and extracellular secretion characteristics. 74 genes amongst the 121 up-regulated genes were identified as coding for soluble secreted proteins (Appendix A). Out of these 74 shortlisted genes, four candidate genes relevant to cell survival, apoptosis, migration and invasion, namely insulin like growth factor binding protein 3 (IGFBP3), growth arrest specific 6 (GAS6), collagen type VIII alpha 1 chain (COL8a1) and collagen type XI alpha 1 chain (COL11a1), were selected for validation of their expression in independent NHOF and CAF lines (Figure 4.2). Notably, genes encoding two specific subtypes of collagen, COL8a1 and COL11a1, were up-regulated in highly senescent CAFs relative to non-senescent CAFs and NHOFs. These results validated the genome-wide transcription profiles and COL8a1 and COL11a1 were selected further investigation in the present study.

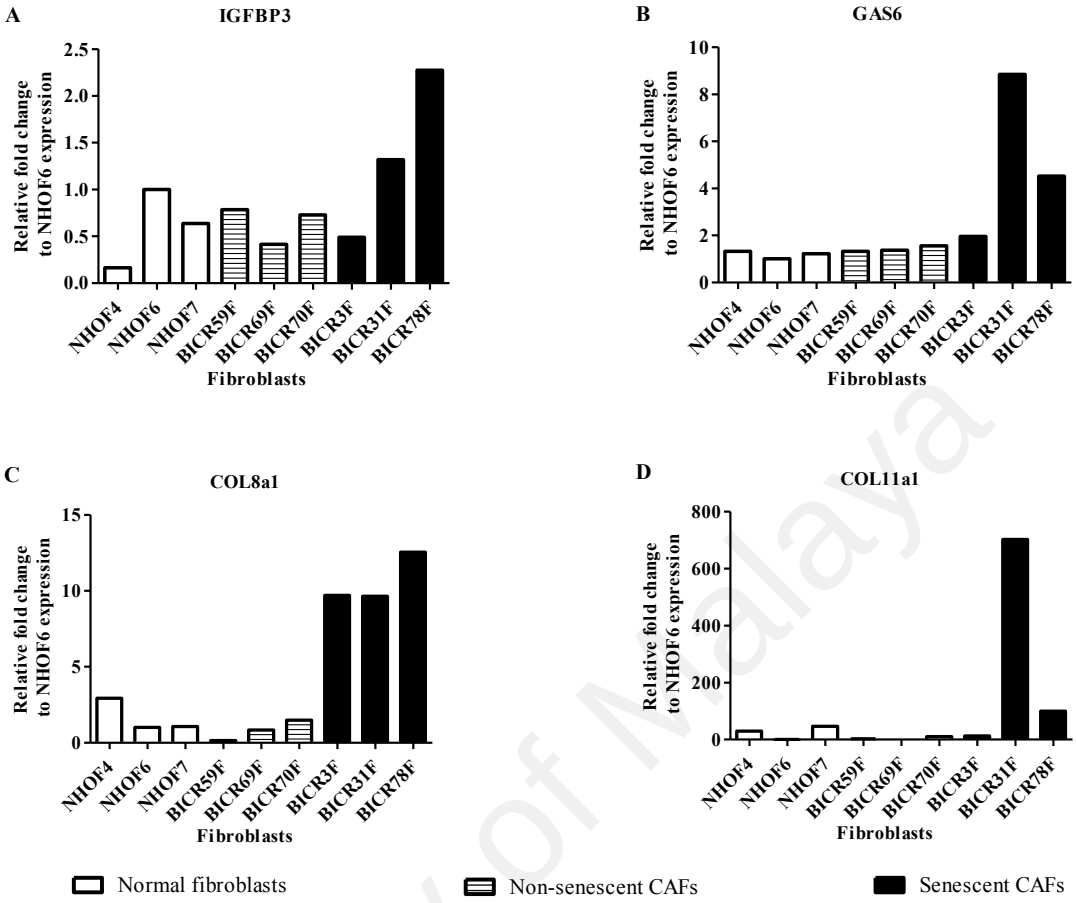

Figure 4.2: Expression of genes encoding soluble secreted proteins IGFBP3, GAS6, COL8a1 and COL11a1 in NHOFs and CAFs.

The fibroblasts cell lines were processed to obtain cDNA and QPCR was performed subsequently. The results show mRNA expression of the indicated genes relative to NHOF6. All the genes were up-regulated in senescent CAFs compared to normal fibroblasts and the other counterparts. Results represent data obtained from triplicate samples. Bars, mean of triplicates.

4.4 Expression of collagens and DDR1 in fibroblasts and HNSCC cell lines

Q-PCR using a Taqman probe which amplified a common "core" sequence within all DDR1 isoforms revealed that DDR1 mRNA was expressed at very low levels in both NHOFs and CAFs (Figure 4.3). By contrast, a high level of expression was observed in a panel of OPSCC (Figure 4.4 A) and OSCC (Figure 4.5 A) cell lines at the mRNA level. The mRNA levels of COL8a1 and COL11a1 were also determined by Q-PCR in OSCC (H376) and OPSCC (SCC040, SCC154, VU040T and VU147T) human cell lines. There was heterogeneity in the expression of both the COL8a1 and COL11a1 across the epithelial tumour cell lines. In particular, COL11a1 was expressed at very low levels in all the epithelial tumour cell lines and low expression of COL8a1 was detected only in 3 out of 5 cell lines (Figure 4.6).

In order to detect DDR1 protein, three antibodies from different manufacturers were validated for their specificity and sensitivity, namely Santa Cruz Biotechnology (SC532, rabbit polyclonal IgG), LifeSpan Biosciences (LSB3861, mouse monoclonal IgG) and Cell Signaling Technology (CST; D1G6 XP®, rabbit monoclonal IgG). Firstly, the specificity of the DDR1 antibodies was compared by Western blotting. The human cell line, DG75, which does not express DDR1 was used as the negative control and L428 cells which over-expresses DDR1 was used as the positive control (Fathima Zumla Cader *et al.*, 2013). DDR1 protein was detected at its expected molecular size of 125kDa by the antibodies from LSBio and CST, but couldn't be detected by the antibody from SCBT (Figure 4.7). Therefore, further evaluation was carried out to compare the sensitivity of the first two antibodies by immunocytochemistry (ICC).

Next, the LSBio and CST antibodies were further validated in DG75 cells transfected with a DDR1 expression plasmid or the empty vector as the negative control. No staining was observed with the LSBio antibody in either the cells transfected with DDR1 (Figure

4.8A) or the empty vector (Figure 4.8B). By contrast strong staining was observed in the cells transfected with DDR1 (Figure 4.8C) when incubated with the CST antibody, whilst no staining was seen in the vector controls (Figure 4.8D). Therefore, the CST antibody was used in all further experiments in this study.

DDR1 protein was detected in the panel OPSCC (Figure 4.4 B) and OSCC (Figure 4.5 B) cell lines by Western blotting. The DDR1 Western blot results were in concordance with the DDR1 mRNA levels, confirming its expression in tumour cells.

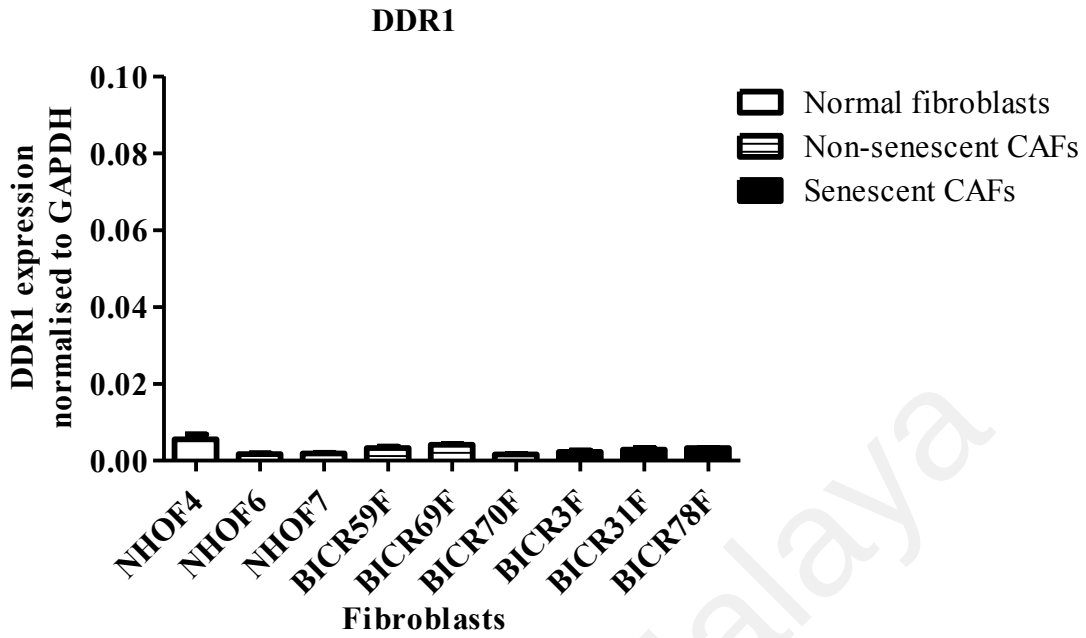

Figure 4.3: DDR1 mRNA expression in fibroblast cell lines.

Q-PCR analysis showed that all normal fibroblasts, senescent CAFs and non-senescent CAFs expressed very low level of DDR1 mRNA. Results are the DDR1 mRNA expression in fibroblast cell lines normalised to GAPDH as determined by Q-PCR. The result represent data obtained from triplicate samples. Bars, mean of triplicates; error bars, SD of triplicates.

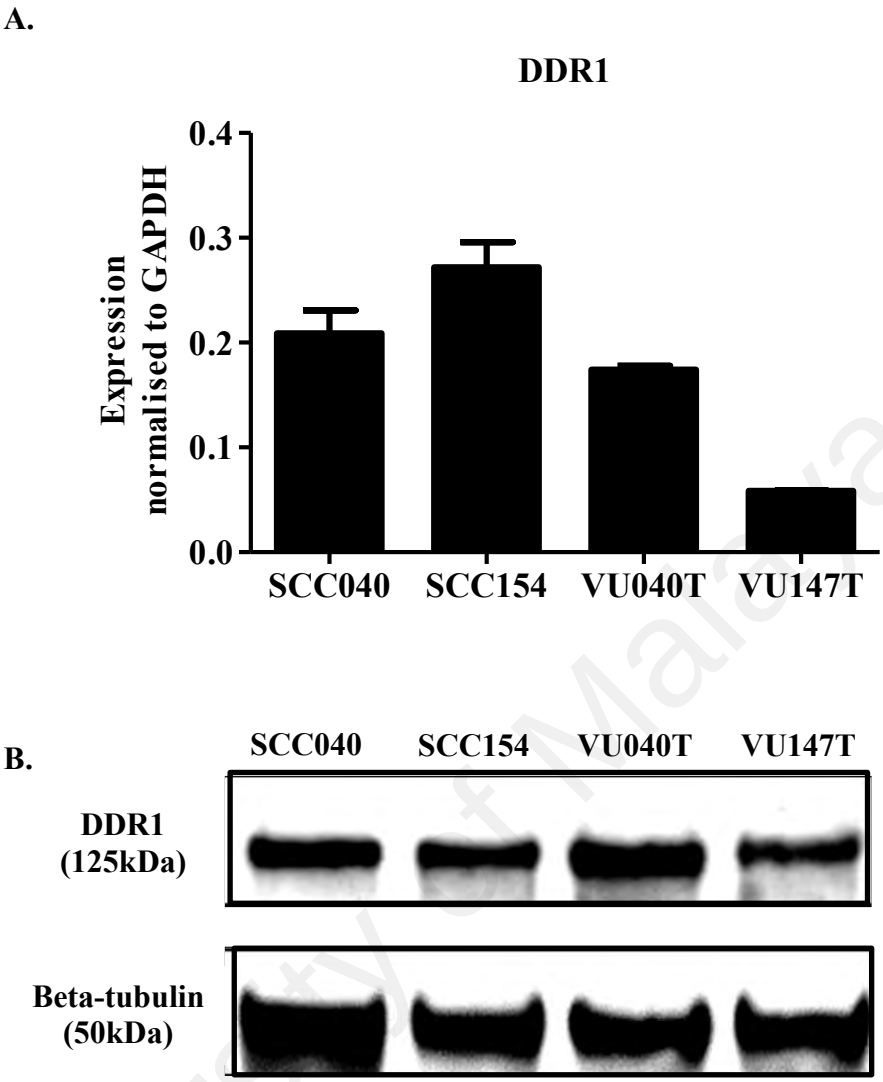

Figure 4.4: DDR1 mRNA and protein expression in OPSCC cell lines.

A. Graph shows the mRNA expression of DDR1 (normalised to GAPDH) in two HPV negative (SCC040 and VU040T) and HPV positive (SCC154 and VU147T) OPSCC cell lines as determined by Q-PCR analysis. DDR1 was expressed in all the OPSCC cell lines to different extent. Bars, mean of triplicates; error bars, SD of triplicates. **B.** Western blot analysis of the OPSCC cell lines with beta-tubulin as the loading control. Result showed a distinct band corresponding to the predicted molecular weight of DDR1 (125kDa) in parallel with the mRNA expression pattern.

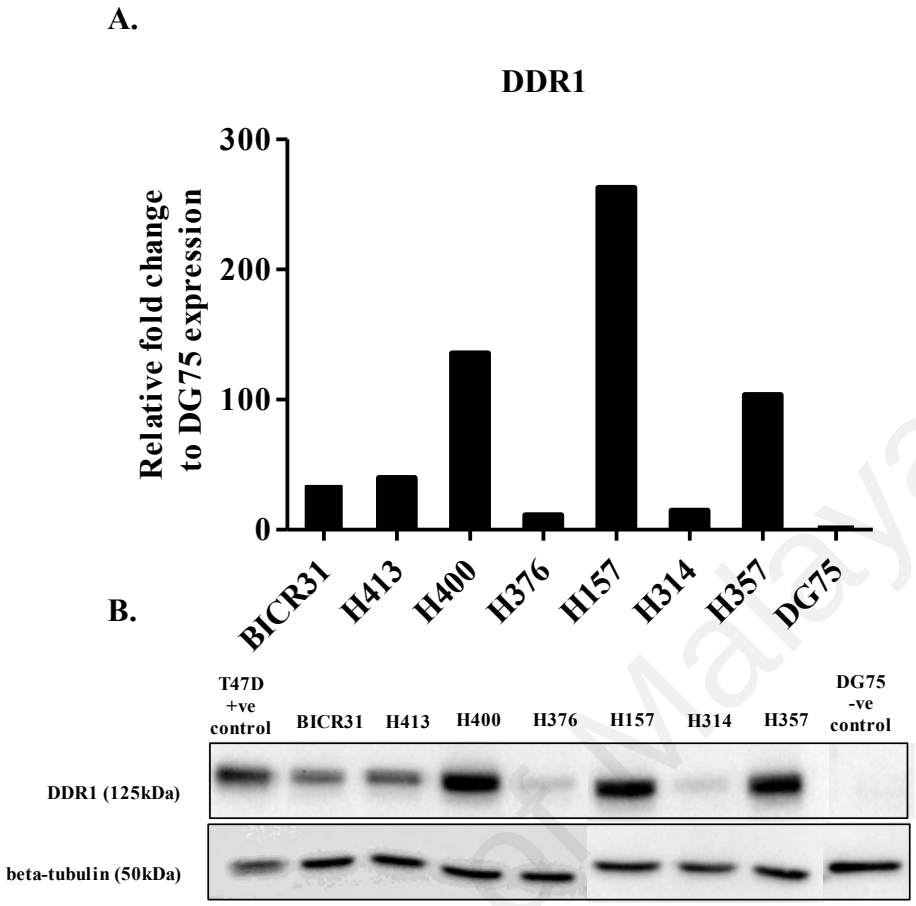

Figure 4.5: DDR1 mRNA and protein expression in OSCC cell lines.

A. Graph shows the mRNA expression of DDR1 as determined by Q-PCR. DG75 cell line was the negative control for DDR1 expression. Data are the fold change of DDR1 expression in OSCC cell lines relative to DG75. DDR1 was markedly expressed in all the OSCC cell lines to different extent. Bars, mean of triplicates; error bars, SD of triplicates. **B.** Western blot analysis of the OSCC cell lines. The T47D breast cancer cells served as the positive control (Ono *et al.*, 2017), DG75 served as the negative control and beta-tubulin as the loading control. A distinct band corresponding to the predicted molecular weight of DDR1 (125kDa) was detected.

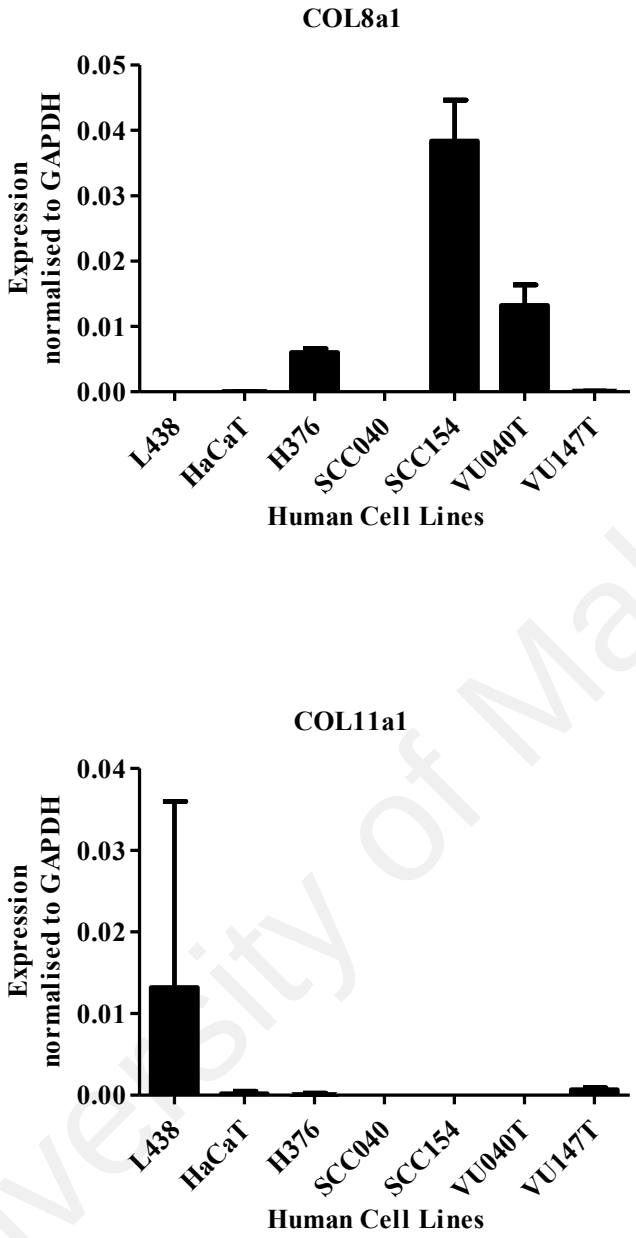

Figure 4.6: Expression of the COL8a1 and COL11a1 in OPSCC cell lines.

Graph shows the mRNA expression determined by Q-PCR of the indicated genes (normalised to GAPDH) in immortal keratinocyte cell line from adult human skin (HaCaT), Hodgkin cell line as the positive control (L428), OSCC cell lines (H376) and OPSCC cell lines which are HPV-positive (SCC154 and VU147T) and HPV-negative (SCC040 and VU040T). Bars, mean of triplicates; error bars, SD of triplicates.

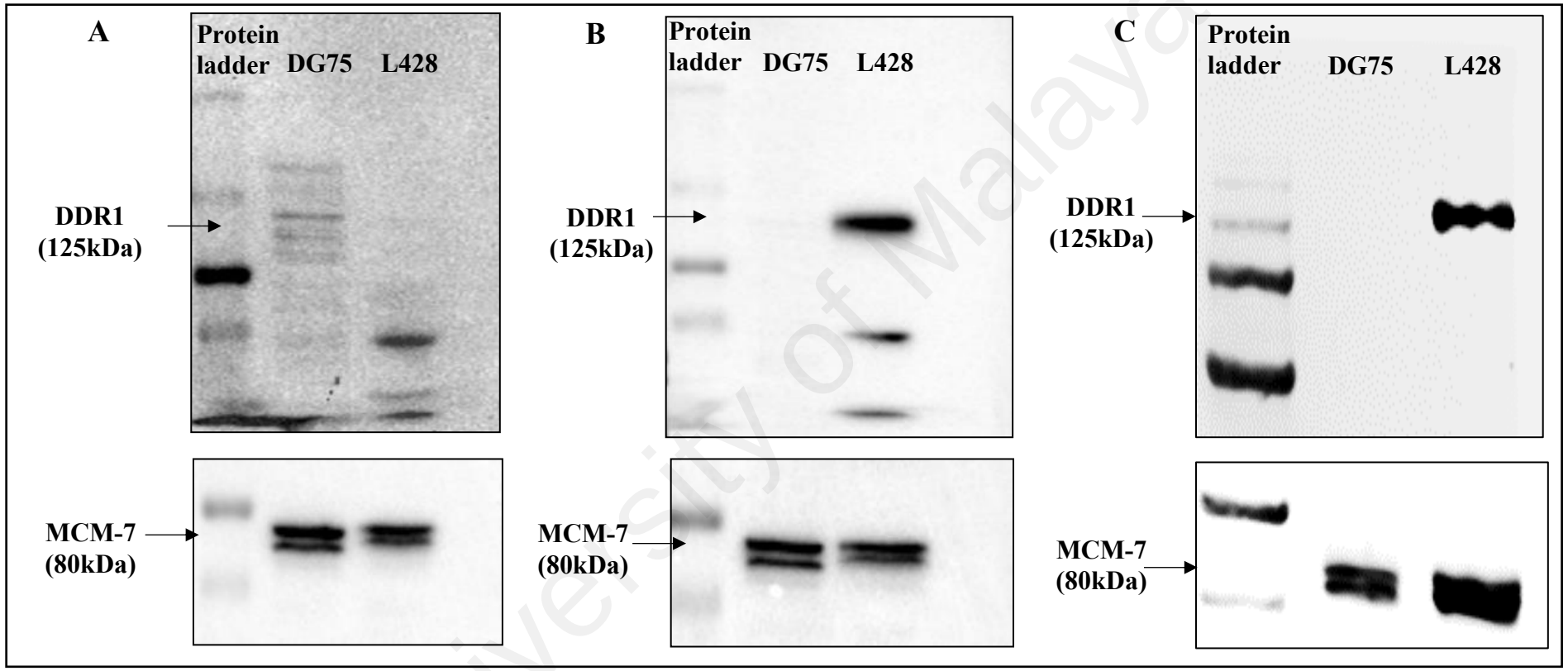

Figure 4.7: Validation of the specificity of antibodies against DDR1 protein in Western blot analyses.

L428 cells which was reported to over-express DDR1 showed a distinct band corresponding to the expected molecular weight of DDR1 (125kDa) in both **(B)** LifeSpan BioSciences and **(C)** Cell Signaling Technology, except **(A)** Santa Cruz Biotechnology. The protein was absent in all negative control, DG75 cells. MCM-7 protein was used as the loading control of the same amount of lysates.

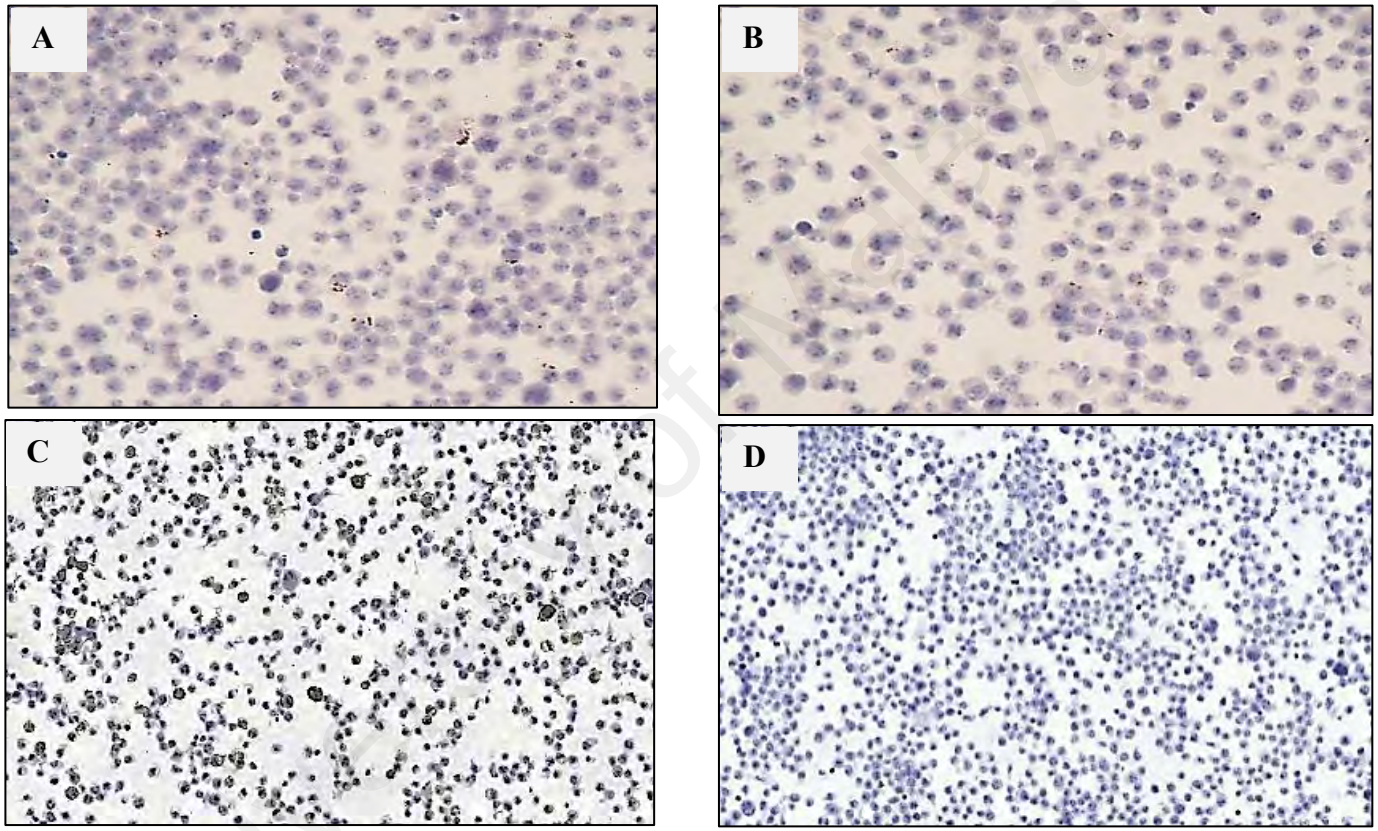

Figure 4.8: Validation of the sensitivity of antibodies from LifeSpan BioSciences and Cell Signaling Technology against DDR1 protein in immunocytochemistry analyses.

DG75 cell line showed negative staining in both **(A)** DDR1-transfected and **(B)** empty vector by LSBio. Positive staining was detected in **(C)** DDR1-transfected but not **(D)** empty vector by CST. Result confirmed the sensitivity of CST antibody.

4.5 Expression of DDR1 mRNA and expression in OPSCC and OSCC tissues

The results of Section 4.4 demonstrated that DDR1 was expressed in OPSCC and OSCC cell lines. However, before studying the expression and function of this collagen receptor in more detail, it was important to confirm its expression in tumour tissues. This part of the study examined the expression of DDR1 mRNA in the The Cancer Genome Atlas (TCGA) head and neck cancer data set and a pilot immunohistochemistry (IHC) study was carried out using OPSCC and OSCC tissues.

4.5.1 DDR1 expression in TCGA HNSCC database

The TCGA HNSCC expression data for DDR1 stratified by HPV status in tumours and normal tissues is shown in Figure 4.9. DDR1 was significantly over-expressed in tumours relative to normal samples, and this is the case for both HPV-negative ($p=0.0001$) and HPV-positive tumours ($p=0.0008$). There were a lot fewer normal samples (37 relating to HPV-negative patients and only 6 to HPV-positive patients), so the matched analysis (i.e. only using tumour samples for which there is a matched normal sample) for HPV-positive cases was not statistically significant ($p=0.1151$) but it was statistically significant for HPV-negative cases ($p<0.0001$). There was no statistically significant difference in DDR1 expression between HPV-negative and HPV-positive tumours ($p=0.8529$).

The median DDR1 expression of each respective HPV group was used as the cut-off value for the Kaplan-Meier analyses (Figure 4.10A). The distribution of values was unimodal. The medians aren't exactly the same as the modal values, so the plots have been reproduced based on splits at the modal values (Figure 4.10B). Cox proportional hazards analysis was also carried out for both HPV groups and in both cases this was clearly not significant. Also, comparing the cases in the top 1/3 by DDR1 expression with

those in the bottom 1/3 hints at a weak association for HPV-negative cases, but it was still not statistically significant (Figure 4.10C). Hence, it implies that there is no statistically significant association between DDR1 expression and overall survival in the HPV-negative or HPV-positive tumours combined. However, for female HPV-negative cases, high DDR1 expression was strongly associated with impaired survival (Cox p-value = 0.0055; Figure 4.11A), although this was not evident for female HPV-positive (only 10 cases; data not show), males HPV-negative (Figure 4.11B) and male HPV-positive (Figure 4.11C).

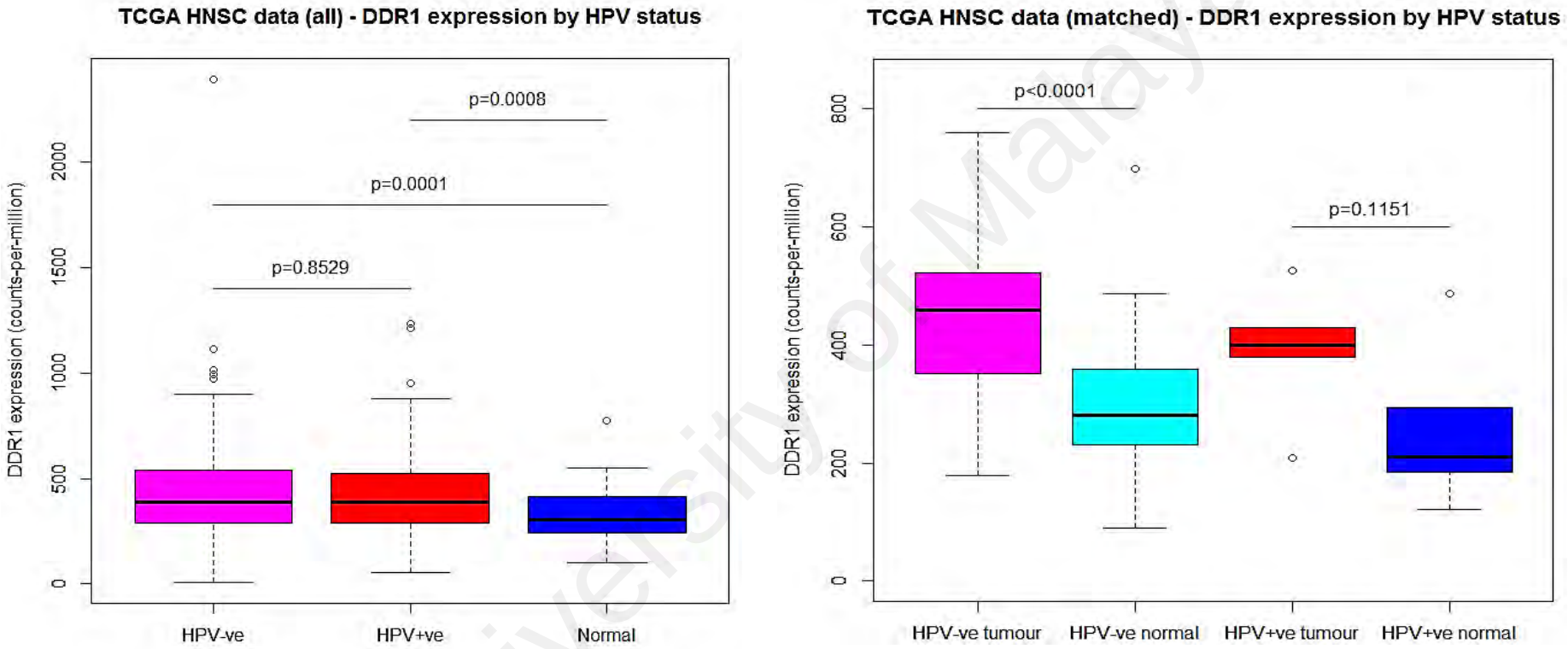

Figure 4.9: TCGA data on DDR1 expression in HPV-negative and HPV-positive HNSCC tumours versus normal tissues.

DDR1 is significantly over-expressed in tumours relative to normal samples. There are a lot fewer normal samples (37 relating to HPV-negative patients and only 6 to HPV-positive patients), so the matched analysis (i.e. only using tumour samples for which there is a matched normal sample) for HPV-positive cases is not statistically significant but it is statistically significant for HPV-negative cases There is no statistically significant difference in DDR1 expression between HPV-negative and HPV-positive tumours.

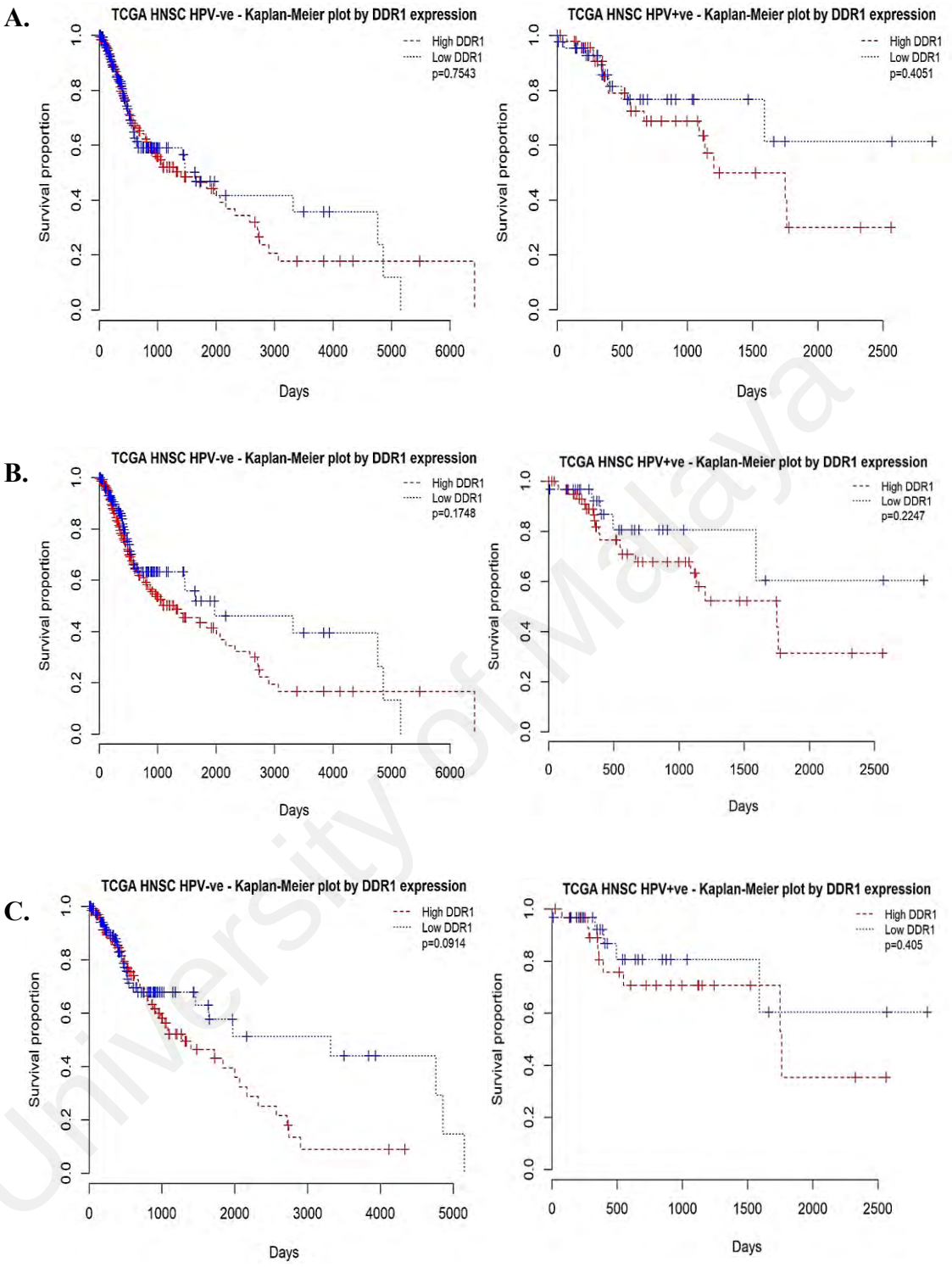

Figure 4.10: TCGA data of Kaplan-Meier plots on DDR1 expression in HPV-negative (left panel) and HPV-positive (right panel) HNSCC.

No statistically significant association between DDR1 expression and overall survival in either HPV-negative or HPV-positive tumours when the cut-off values was based on A. median B. modal split and C. comparing the cases in the top 1/3 by DDR1 expression with those in the bottom 1/3.

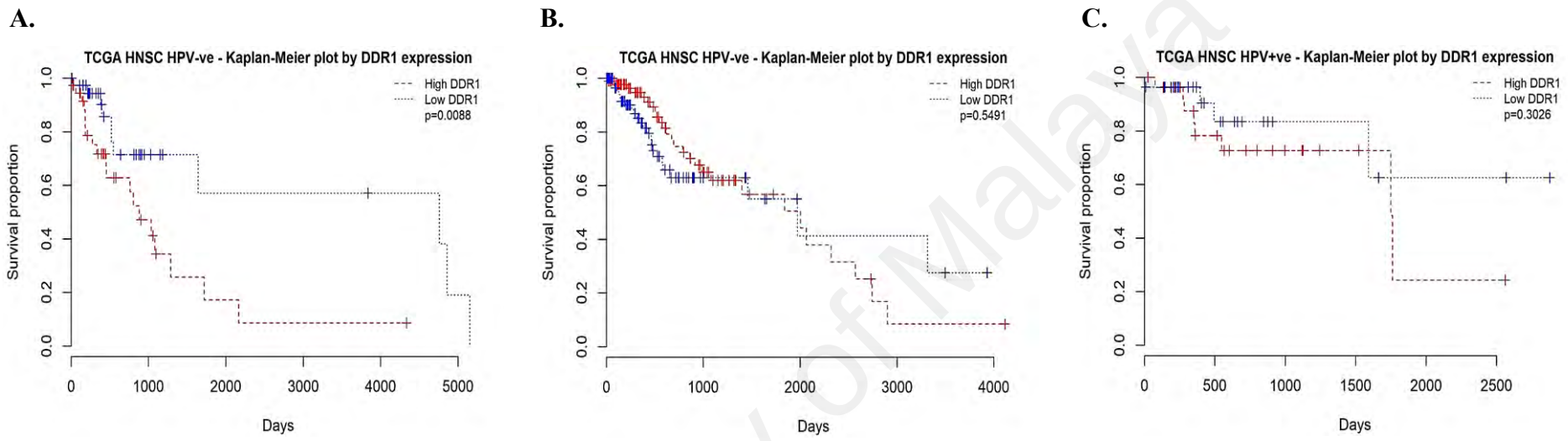

Figure 4.11: TCGA data of Kaplan-Meier plots on DDR1 expression in female HPV-negative (left panel), male HPV-negative (middle panel) and male HPV-positive (right panel) HNSCC.

A. Impaired survival was significantly associated with high expression of DDR1 in female HPV-negative cases. No significant association between high and low expression of DDR1 in **B.** male HPV-negative and **C.** male HPV-positive cases.

4.5.2 DDR1 protein expression in HNSCCs

Five cases of normal oral mucosa, 6 cases of OPSCC and 6 cases of OSCC were used in a pilot study to determine the expression of DDR1 protein in SCCs compared to normal epithelium. DDR1 protein was detected using chromogenic immunohistochemistry. DDR1 protein levels were evaluated by a consultant head and neck pathologist (Dr Max Robinson, University of Newcastle, UK) based on the proportion of tissues stained and the overall staining intensity (overall scoring grade ranging from 0 to 3).

DDR1 was found predominantly in the squamous cell carcinoma where the staining was generally stronger than normal epithelium. In the normal epithelium, DDR1 staining was weak and appeared to be cytoplasmic and occasionally membranous. In contrast, 5 out of the 6 OPSCC and 3 out of the 6 OSCC showed higher expression of DDR1 in the tumour than the adjacent morphologically normal epithelium. The positive staining was homogenous and showed moderate to strong cytoplasmic staining (Table 4.2). Figure 4.12 illustrates the comparison of DDR1 staining in normal and squamous carcinoma tissue sections.

Table 4.2: Scoring of DDR1 in OPSCC and OSCC full tissue sections analysed by chromogenic immunohistochemistry. The DDR1 intensity was higher in the squamous cell carcinoma compared to the adjacent epithelium. The scoring denoted by ascending numeric 1 to 3 represented low, medium to high intensity.

Path no.	Site	Epithelium intensity	Tumour intensity
10893/09	Lip mucosa	1	N/A
11877/09	Buccal mucosa	1	N/A
1293/10	Tongue dorsum	1	N/A
32648/11	Palate	1	N/A
7881/16	Pharyngeal tonsil	1	N/A
36638/15	Oropharyngeal SCC	1	3
36765/15	Oropharyngeal SCC	1	2
37916/15	Oropharyngeal SCC	2	3
38819/15	Oropharyngeal SCC	1	2
38887/15	Oropharyngeal SCC	2	2
40400/15	Oropharyngeal SCC	1	3
9013/01	Oral cavity SCC	1	1
21811/02	Oral cavity SCC	1	1
13551/04	Oral cavity SCC	1	2
19075/04	Oral cavity SCC	1	2
34670/04	Oral cavity SCC	2	2
23710/05	Oral cavity SCC	1	2

Abbreviation: N/A, not available.

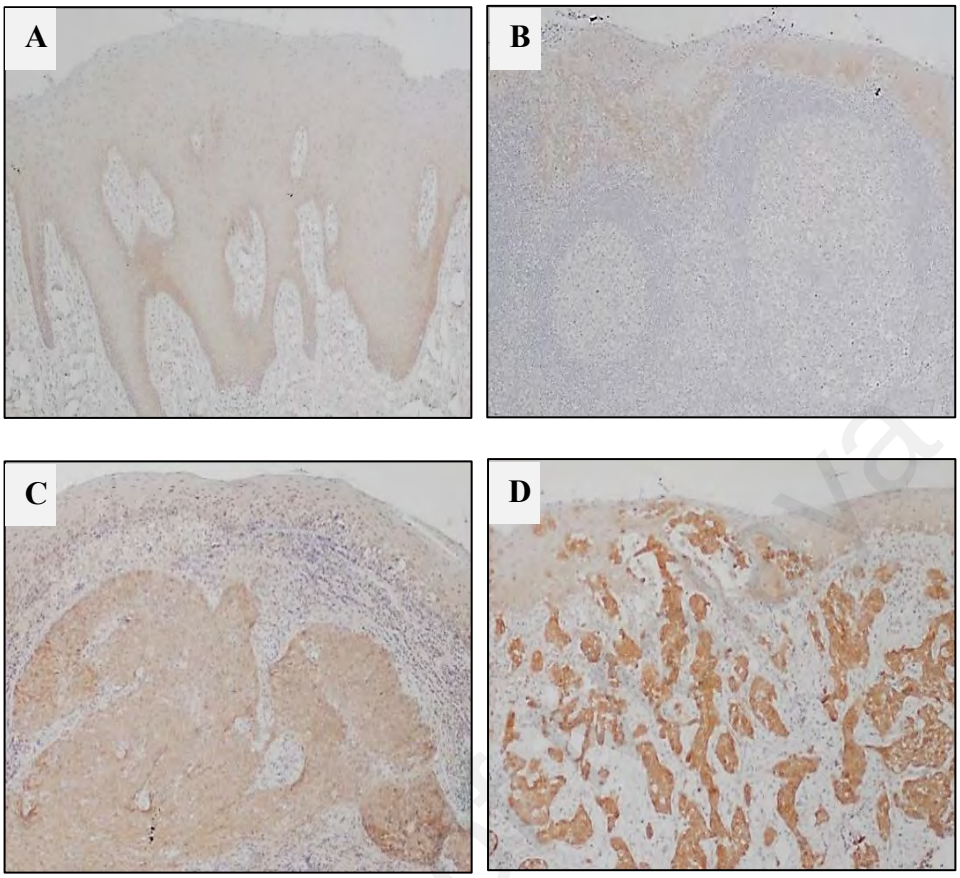

Figure 4.12: Photomicrographs of DDR1 protein expression in squamous cell carcinoma.

Chromogenic immunohistochemistry revealed normal epithelium showed weak cytoplasmic staining **(A & B)**. The OPSCC **(C & D)** showed increased DDR1 expression by comparison to normal epithelium. Images showed 100X magnification.

4.6 HPV status of Malaysian OPSCCs and association with clinico-pathological parameters

The results of Section 4.5 indicate that DDR1 might be over-expressed in OPSSCs. The incidence of OPSCC has been increasing in recent years and this has been attributed to HPV infection (Garnaes *et al.*, 2015; Kristen B Pytynia *et al.*, 2014; Stein *et al.*, 2015). Most of the data relating to the increase in HPV-positive OPSCCs has come from Western countries. There are only limited data on the prevalence of HPV-related OPSCC in South East Asia and no data are available from Malaysia. To determine whether studies on the pathogenesis of OPSCC using cohorts of Western patients might also be relevant to Malaysia, the present study was initiated to examine the HPV status in Malaysian OPSCCs.

OPSCCs from 60 patients were identified from four hospitals in two major cities in Malaysia. 15 cases showed p16 expression, but only 10 of the p16 positive tumours (16.7%) showed evidence of high risk HPV DNA by *in situ* hybridisation. Samples from all 4 hospitals were collected between 2009 and 2015 and for these years 13 of 37 (35.1%) cases where positive for p16 expression (Table 4.3; Figure 4.13).

Complete demographic data were available for 54 of the patients; the gender and age for 6 of the patients were not available. The clinico-pathological profile of the patients is shown in Table 4.4. The overall mean age of patients (n = 54) was 65.44 years (± 12.16) at diagnosis and ranged from 36 to 93 years of age. There was no statistically significant difference in age between patients who had high risk-HPV negative and high risk-HPV positive OPSCC (p=0.543). However, the two youngest patients in this cohort at 36 and 41 years of age had p16 positive disease.

The overall male to female ratio was 2.4:1 and the ratio was similar in HPV negative cases (2.75:1), however the ratio was much lower in HPV positive cases (1.25:1). Most patients in this cohort were of Chinese ethnicity (53.3%) followed by Indians (35.0%). All the Indian patients had HPV negative disease, whilst 80% of the HPV positive cases were Chinese; this finding was statistically significant ($p = 0.046$). Overall, most of the OPSCC were classified as being moderately differentiated (MD) SCC (40.0%) and this was similar in cases of HPV negative disease. However, in HPV positive cases, 70% were classified as being poorly differentiated (PD) SCC; this finding was statistically significant ($p = 0.011$).

Table 4.3: Demographics of patients with OPSCCs demonstrating p16 expression

Case	Year of diagnosis	p16 - IHC	HR-HPV ISH	Ethnicity	Age	Sex	Hospital
1	2015	+	+	Chinese	54	M	UMMC
2	2014	+	+	Chinese	72	F	Penang
3	2014	+	-	Chinese	72	M	Penang
4	2013	+	+	Chinese	NK	NK	HKL
5	2013	+	+	Malay	74	M	Penang
6	2013	+	+	Malay	36	M	SDMC
7	2013	+	+	Chinese	53	M	SDMC
8	2013	+	-	Chinese	70	M	SDMC
9	2012	+	-	Chinese	56	M	UMMC
10	2012	+	+	Chinese	56	M	UMMC
11	2012	+	+	Chinese	67	F	SDMC
12	2010	+	+	Chinese	64	F	UMMC
13	2009	+	-	Chinese	41	F	HKL
14	2006	+	+	Chinese	88	F	UMMC
15	2005	+	-	Malay	NK	NK	HKL

Abbreviations: UMMC, University Malaya Medical Center; HKL, Hospital Kuala Lumpur; SDMC, Sime-Darby Medical Center

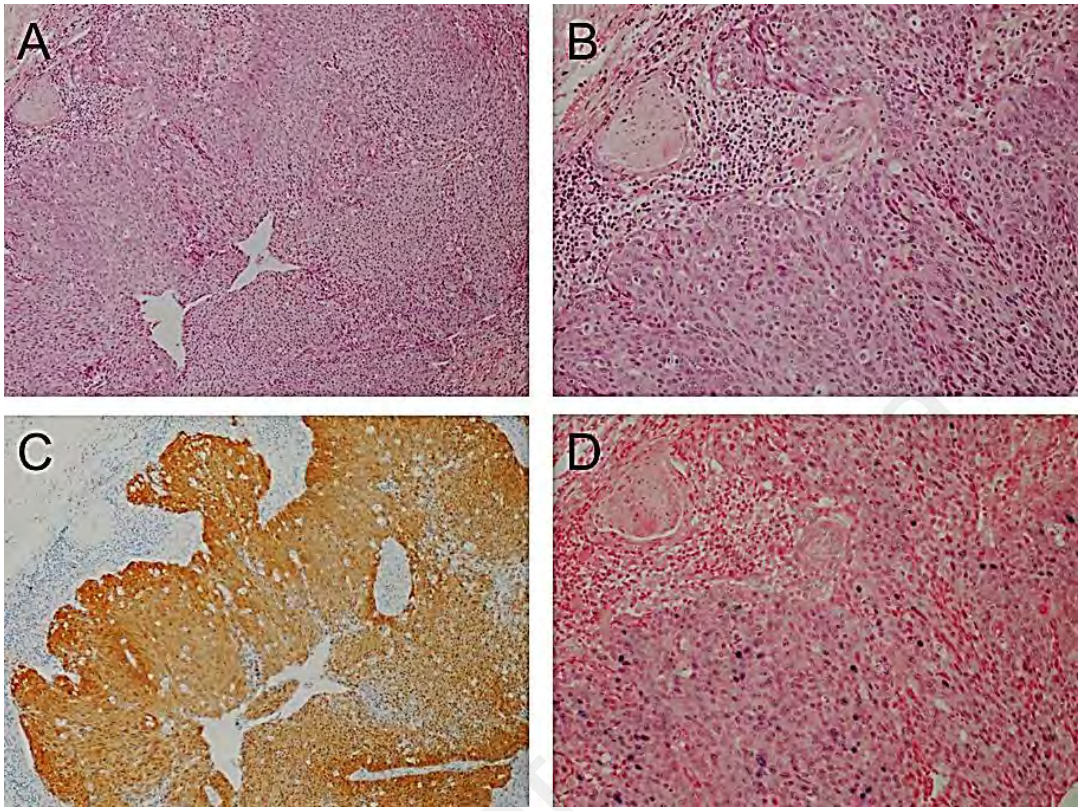

Figure 4.13: Representative photomicrographs showing positive p16 staining and HPV ISH in Malaysian OPSCCs.

HPV-related oropharyngeal squamous cell carcinoma (**A&B**; H&E stain) showing high levels of p16 expression by immunohistochemistry **(C)** and evidence of high risk HPV DNA by in situ hybridisation **(D)**. Images showed magnification at 100X (A & C) and 200X (B & D). Images provided by Dr Max Robinson, University of Newcastle, United Kingdom.

Table 4.4: Clinico-pathological characteristics of patients

Clinico-pathological Characteristics	All Patients n=60 (100%)	HR-HPV (-ve) n=50 (83.3%)	HR-HPV(+ve) n=10 (16.7%)	p-value
Age at diagnosis (Years) [n = 54] Mean (±SD)	65.44 (±12.16)	66.00 (±11.63)	62.67 (±15.01)	¥0.543
Gender (n = 54)				*0.505
Male	38 (70.4%)	33 (73.3%)	5 (55.6%)	
Female	16 (29.6%)	12 (26.7%)	4 (44.4%)	
Ethnicity				*0.046
Malay	7 (11.7%)	5 (10%)	2 (20%)	
Chinese	32 (53.3%)	24 (48%)	8 (80%)	
Indian	21 (35.0%)	21 (42%)	0 (0%)	
Histopathological differentiation/grading				*0.011
WD	16 (26.7%)	14 (28.0%)	2 (20.0%)	
MD	24 (40.0%)	23 (46.0%)	1 (10.0%)	
PD	17 (28.3%)	10 (20.0%)	7 (70.0%)	
Others	3 (5.0%)	3 (6.0%)	0 (0%)	

¥Independent sample's t-test
* Pearson's Chi-Square test

WD = well differentiated; MD = moderately differentiated; PD = poorly differentiated

4.7 Summary

In this chapter, the senescent and non-senescent phenotypes of normal fibroblasts and CAFs were first demonstrated *in vitro* and found to correspond to an increase secretory capacity of senescent CAFs. Next, the re-analyses of a published microarray dataset (Lim *et al.*, 2011b) revealed up-regulation of genes in senescent CAFs compared to their non-senescent counterparts. COL8a1 and COL11a1 were shown to be more highly expressed in senescent CAFs compared to NHOFs and non-senescent CAFs. By contrast, the expression of the collagen receptor, DDR1, was very low in all fibroblasts but was highly expressed in the malignant tumour cells. Analyses from the latest available TCGA's head and neck dataset showed that DDR1 is over-expressed in tumours relative to normal samples. There were no differences in expression between HPV-negative and HPV-positive HNSCC or and DDR1 expression was not associated with overall survival in these groups. However, high DDR1 expression was significantly associated with impaired survival in female HPV-negative cases. The DDR1 expression data were further confirmed in a pilot study using immunohistochemistry, which showed moderate to strong cytoplasmic staining of DDR1 protein in OPSCC and OSCC tissues compared to weak staining in normal epithelium.

The results from the present study also suggest that the occurrence of HPV-related OPSCC in Malaysia may not be as high as those reported in developed nations such as the USA and the UK, but the proportion of OPSCCs that are HPV-positive appears to be increasing, particularly in patients of Chinese ethnicity. Further studies will be required to determine how these observations might impact upon Malaysian communities and the national healthcare system in the future.

Taken together, these data confirm that COL8a1 and COL11a1 were highly expressed in CAFs but not normal fibroblasts. Interestingly, their corresponding tyrosine kinase

receptor DDR1 was highly expressed in OPSCC and OSCC cells, indicating that aberrant DDR1 signalling might affect tumour behaviour. These novel findings suggest that DDR1 signalling contributes to the malignant phenotype in HPV-negative and HPV-positive HNSCC and that some of the collagen required to activate DDR1 could result from paracrine cross-talk between CAFs and malignant epithelial cells. Further investigations to examine the expression of DDR1, COL8a1 and COL11a1 in HPV-negative and HPV-positive OPSCC and OSCC are therefore warranted.

CHAPTER 5: THE EXPRESSION OF COLLAGENS AND DDR1 IN OPSCC

5.1 Introduction

The results of Chapter 4 demonstrated that two subtypes of collagen, COL8a1 and COL11a1, were expressed by CAFs from head and neck tumours. Further, the expression of the tyrosine kinase receptor, DDR1, was shown to be low in CAFs but readily detectable in HNSCC cell lines and tissues; a small pilot study suggested that DDR1 protein was over-expressed in OPSCCs compared to normal oral mucosa. COL8a1 and COL11a1 are soluble proteins secreted into the extracellular matrix. COL8a1 has been shown to serve as prognostic marker to predict the survival of gastric cancer (Zhiqiang Wang *et al.*, 2017) and its expression correlates with poor survival of renal cancer (Joanna Boguslawska *et al.*, 2016; J Boguslawska *et al.*, 2014). COL11a1 expression was also previously reported as a marker of CAFs and correlates with invasive cancer progression and metastasis in high-grade glioblastomas (Vázquez-Villa *et al.*, 2015) and breast cancer (Freire *et al.*, 2014). Evidence is accumulating to show that DDR1 plays an important role in cancer progression. Inhibition of DDR1 was reported to reduce gastric cancer cell migration and metastasis (Yuge *et al.*, 2017), as well as breast cancer proliferation and invasion (Palladino *et al.*, 2016). Taken together, these data suggest that DDR1 signalling induced by COL8a1 and COL11a1might play a role in the pathogenesis of OPSCC, but the expression and functional significance of these molecules has yet to be examined in this disease.

The aim of the present study was to examine the expression of the COL8a1, COL11a1 and DDR1 in OPSCC tissues and to correlate their expression with socio-demographic and clinico-pathological parameters.

5.2 Expression of COL11a1 and DDR1 in OPSCC tissue microarray (TMA)

The starting point of the present study was to examine the expression of COL11a1 and DDR1 in an OPSCC tissue microarray by Opal multiplex fluorescence immunohistochemistry and analysis using a Vectra Automated Pathology System and inFORM® image analysis software.

5.2.1 Tissue microarray construction and HPV screening

The TMA (Astellas PredicTr Array 4) consisted of a total of 44 cores extracted from 35 formalin-fixed paraffin embedded tissues taken from 28 OPSCC patients. In some cases duplicate cores from different parts of the same tumour block were included to avoid sampling bias. The TMA array was screened by using p16 immunohistochemistry (CINtec histology) and high risk HPV *in situ* hybridisation (ISH) automated assay (DeEscalate SOP) in order to obtain the p16 and high risk-HPV DNA profile of the tumours (Appendix B).

The p16 IHC and HPV DNA ISH screening results were evaluated by Dr Max Robinson (Honorary Consultant Pathologist, Newcastle upon Tyne Hospitals NHS Foundation Trust and senior lecturer in Oral Pathology, Newcastle University). In cases where there were duplicate cores from the same tumour, data were averaged for subsequent analyses. The 2 non-tumour cores (6.7%) were negative for p16 and high risk HPV DNA. 13 tumours (43.3%) were negative for both p16 and high risk HPV DNA, 5 tumours (16.7%) were positive for p16 but negative for high risk HPV DNA and 10 cases (33.3%) were positive for both p16 and high risk HPV DNA (Figure 5.1).

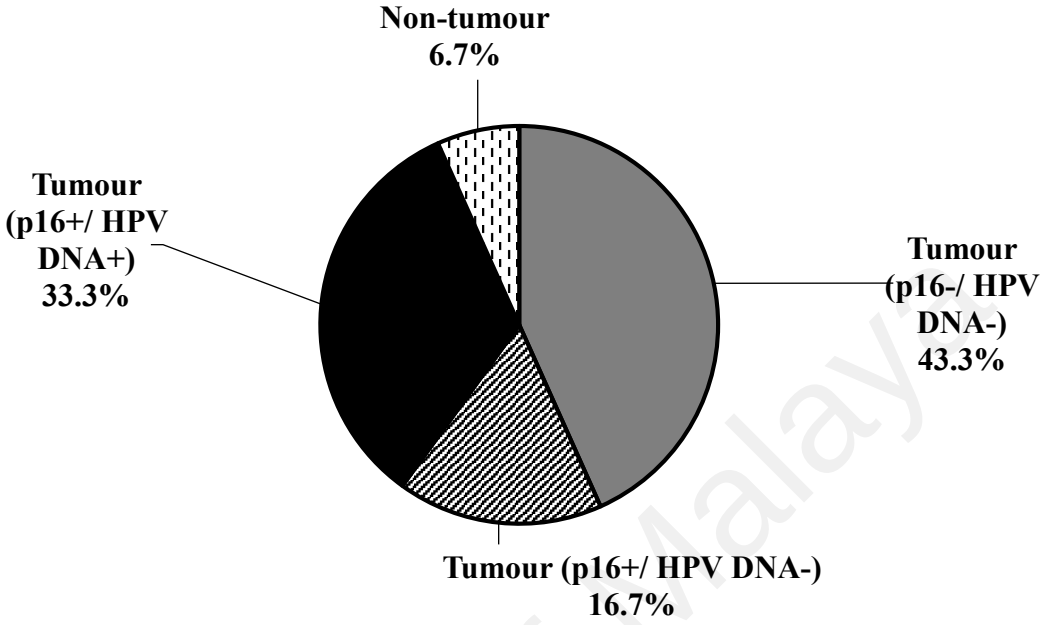

Figure 5.1: Pie chart summarizing the HPV status of the Astellas PredicTr Array 4. Non-tumour (n=2, 6.7%); HPV-negative tumour (n=13, 43.3%); p16-positive but HR-HPV DNA-negative tumour (n=5, 16.7%); and HPV-positive tumour (n=10, 33.3%). Abbreviations: -, negative; +, positive.

5.2.2 Expression of COL11a1 and DDR1 on the Astellas PredicTr Array

The expression of COL11a1 and DDR1 in the tissues on the Astellas PredicTr Array 4 was examined by Opal multiplex fluorescent staining (PerkinElmer, MA), which facilitated the simultaneous staining and analysis of both proteins either alone or co-expressed within a single cell. COL11a1 was labelled using an anti-COL11a1 antibody and Tyramide Signal Amplification (TSA) Plus Cyanine 3 (Red), whilst DDR1 was labelled with an anti-DDR1 antibody and TSA Plus Fluorescein (Green). The slides were scanned and analysed using a Vectra Automated Pathology System. Unstained and control slides single stained with each of fluorescein, Cyanine 3 and DAPI were used to build for non-mixed signals in order to determine the signal threshold for each fluorescent signal. Multispectral visualisation and imaging (8-bit image cubes) of the entire stained TMA were successfully acquired with 40X objective lens using a full CCD frame at 1 x 1 binning (1360 x 1024 pixels) for analysis. The multispectral images were then aligned with the TMA core co-ordinates to identify the donor tissue blocks (Figure 5.2).

COL11a1 and DDR1 expression were readily detected in the tissues and a heterogeneous staining pattern was observed for both proteins. The detection of co-expression of COL11a1 and DDR1 within a single cell could be assessed and, therefore, COL11a1 and DDR1 staining was quantified digitally on an individual cell basis using inFORM® image analysis software.

Section 1

Section 2

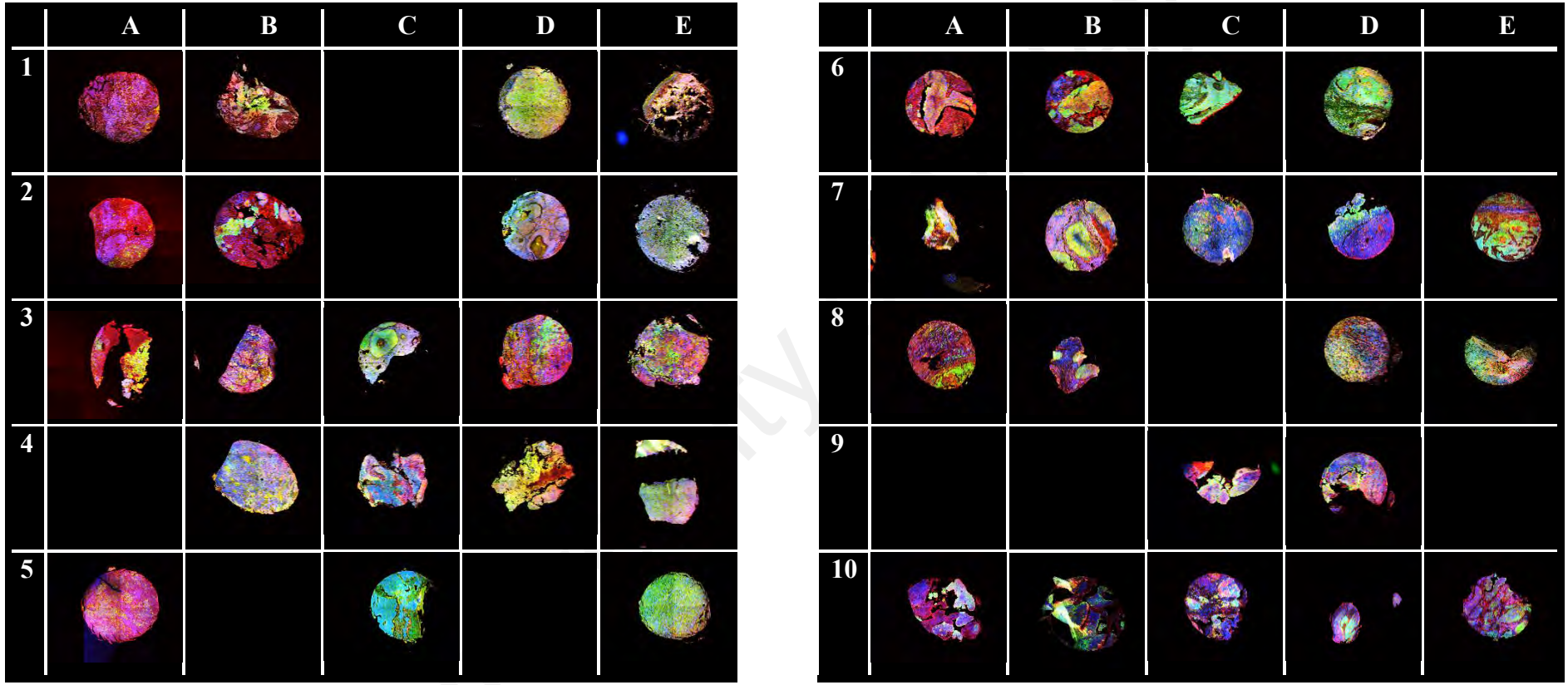

Figure 5.2: Automated TMA scanning and acquisition of mosaic 40 cores normal tissue and OPSCC.
Composite images on the Astellas PredicTr Array 4 stained using fluorescent TSA reagents to detect COL11a1 (TSA Plus Cyanine3, red), DDR1 (TSA Plus Fluorescein, green) and nuclear counterstain (DAPI, blue). Imaged with a Vectra Automated Quantitative Pathology Imaging System at 40X magnification. The position of each core was indicated by alphabets which denoted the column and numbers which denoted the row.

5.2.3 Digital quantitation of COL11a1 and DDR1 expression

After the acquisition of the multiplexed immunofluorescence images, COL11a1 and DDR1 expression was measured using inForm® analysis software. By using the trainable pattern-recognition-based algorithm of inForm® Tissue Finder, the tumour areas and every cell within those areas were successfully identified. The segmentation map of every core on the TMA was reviewed by a trained pathologist, Dr Maha Ibrahim (Pathologist, University of Birmingham, United Kingdom).

The green Fluorescein (excitation wavelength 494nm, emission wavelength 517nm, FITC filter) signal was mixed with red Cyanine3 (red; excitation wavelength 550nm, emission wavelength 570nm, TRITC filter) in the cellular compartments where co-localisation occurred. Successful multispectral unmixing was performed, such that the COL11a1 signal could be distinguished from the DDR1 signal and the background signal was eliminated. A representative example is presented in Figure 5.3. In this study, linear unmixing of each fluorophore was performed on the multispectral data obtained and analysed on an individual cell basis in the areas of interests (Appendix C).

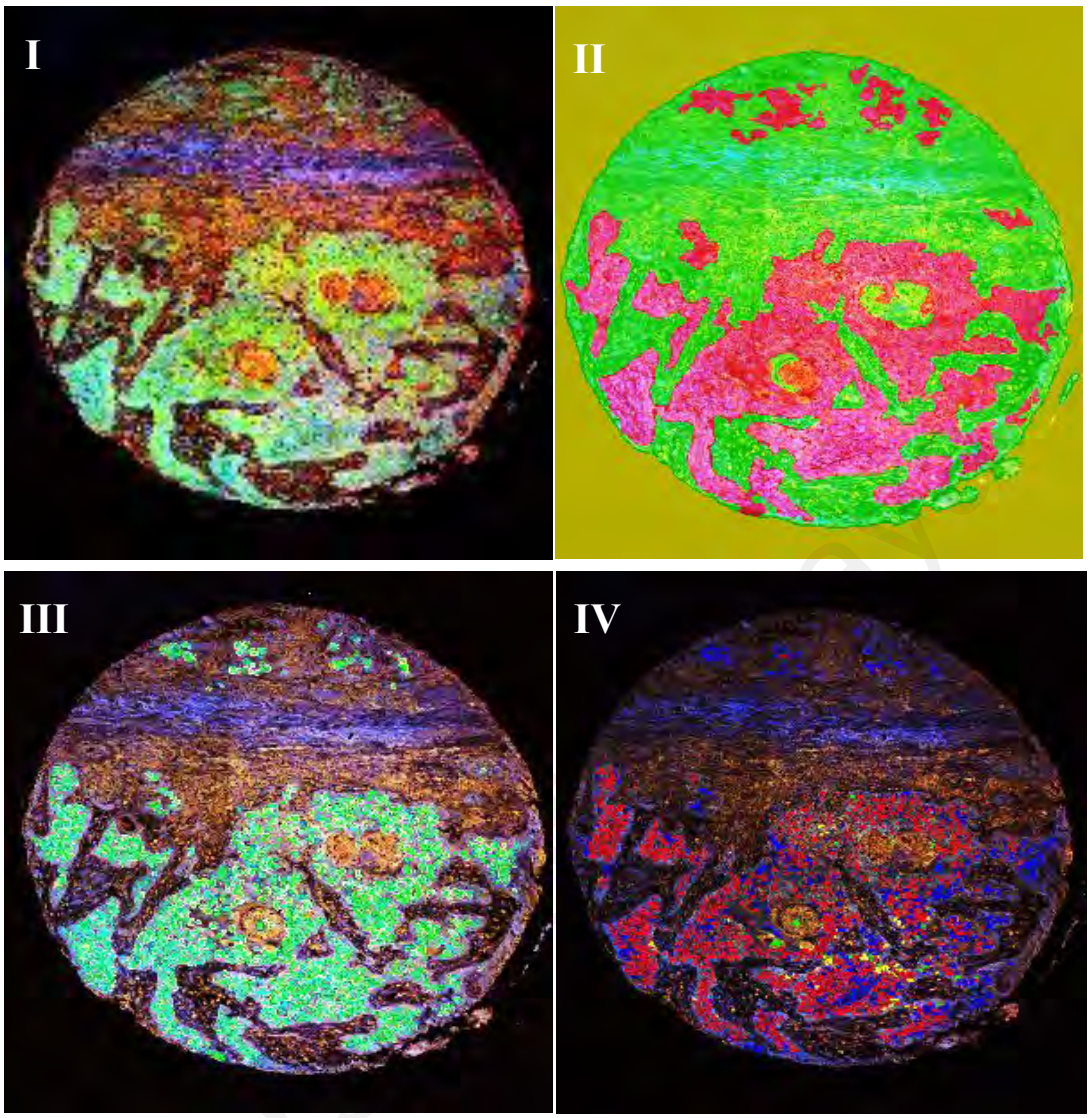

Figure 5.3: Representative core subjected digitally scored using the Vectra Automated Quantitative Pathology System.

(I) Spectrally unmixed composite image showing nuclei (DAPI, blue), COL11a1 (TRITC, red) and DDR1 (FITC, green). **(II)** Tissue segmentation of epithelial (red) and stromal (green) compartments. **(III)** Cell segmentation of nuclear and membranous compartments. Cells positive for only DDR1 are displayed in green, cells double positive for COL11a1 and DDR1 are displayed in yellow, and cells negative for both markers are displayed in blue. **(IV)** The scoring map of per-cell protein expression generated by the digital workflow algorithm. Cells positive for only DDR1 are displayed in red, cells positive for COL11a1 are displayed in green, cells double positive for COL11a1 and DDR1 are displayed in yellow, and cells negative for both markers are displayed in blue.

5.2.4 Statistical analyses of DDR1 and COL11a1 differential expression

The expression of DDR1 and COL11a1 were analysed for their correlation with HPV in the tumours stratified into p16-positive and p16-negative groups. This is because p16 is a recognised surrogate marker of oncogenic HPV infection and there is now an international precedent for classifying HPV positive OPSCCs by p16 status alone (Holmes *et al.*, 2015; Jouhi *et al.*, 2017). Taking into consideration the importance of HPV DNA status in addition to p16 (Bussu *et al.*, 2014; C. H. Chung *et al.*, 2014; Qureishi *et al.*, 2017), the samples were also sub-divided into three discordant groups based on high risk HPV DNA and p16 combined status [i.e. HPV-negative; intermediate (i.e. p16-positive but HPV DNA-negative) and HPV-positive]. The data from the 28 tumours were analysed in subsequent statistical tests. The 2 non-tumours were removed from the comparison due to the limited number of cases.

5.2.4.1 Differential expression in samples classified by p16 alone

DDR1 protein was detected in the majority of OPSCC samples. Some of the tissues expressed only DDR1 and some expressed only COL11a1. In some cases, DDR1 and COL11a1 expression was detected within single cells. For single positive staining, there was no significant differential expression of DDR1 between p16-negative and p16-positive tumours, but the percentage of cells expressing COL11a1 was significantly higher in the p16-negative group ($p<0.05$). There were no significant differences between the p16-negative and p16-positive groups in the percentage of cells co-expressing DDR1 and COL11a1, or in the total number of cells expressing overall (singly and co-expressed) DDR1 or that of COL11a1 (Figure 5.4).

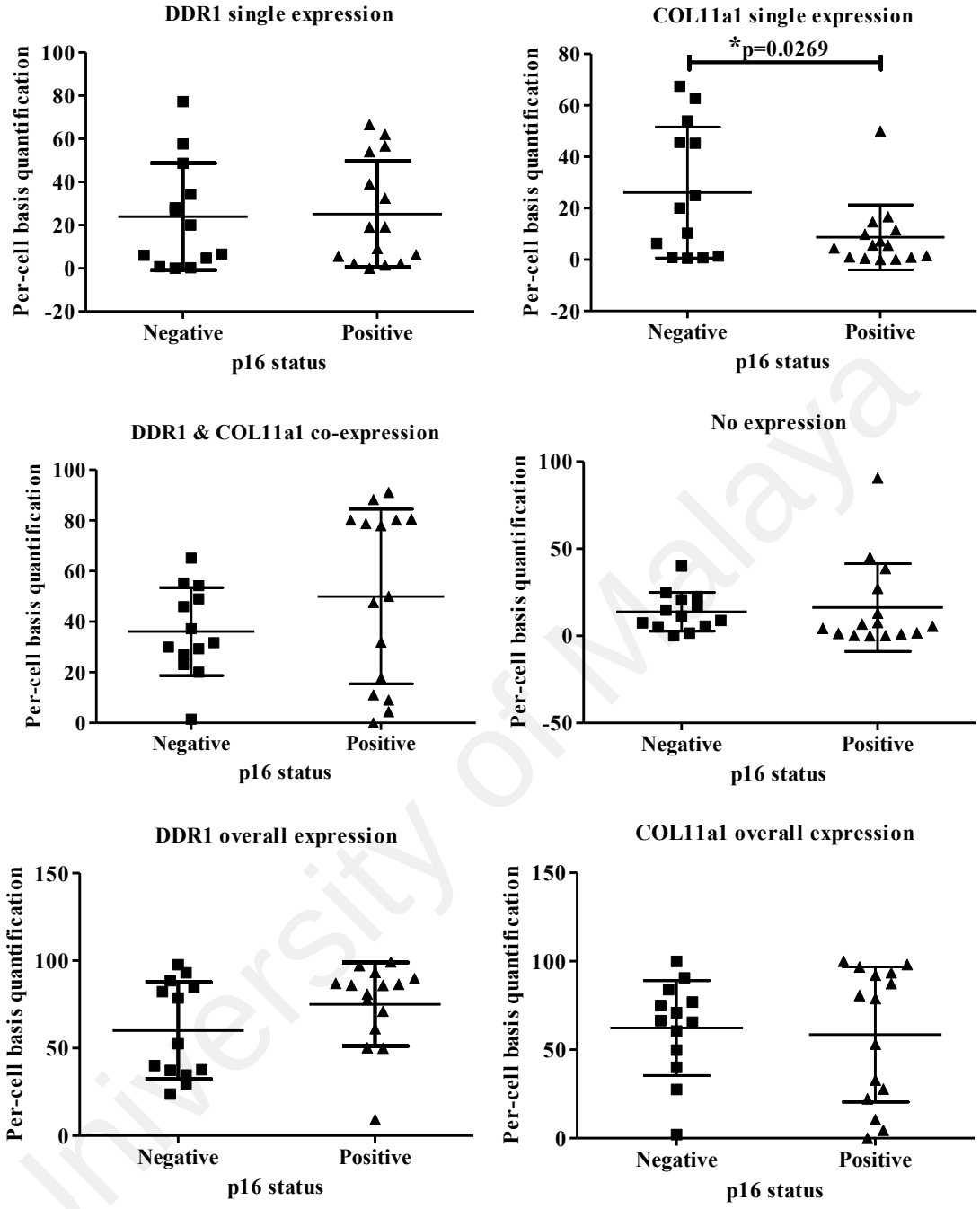

Figure 5.4: Unpaired T-test analyses on differential expression of DDR1 and COL11a1 in p16-negative and p16-positive OPSCC TMA.

Expression was scored as percentage of total cells within the tumour regions which shown positive staining. Per cell basis quantification of the expression was plotted against p16 status of tumours. COL11a1 was significantly down-regulated in HPV-positive tumour cells not expressing DDR1 but no significant difference of COL11a1 in overall (i.e. single cum double expression). * denotes $p<0.05$.

5.2.4.2 Differential expression in samples classified by combined status of p16 and HPV DNA

The tumours from 28 patients were stratified into 3 discordant groups of HPV status [i.e. p16-negative/HPV DNA-negative (n=13, 46.4%); p16-negative/HPV DNA-positive (n=5, 17.9%); p16-positive/HPV DNA-positive (n=10, 35.7%)]. Similar to the results in Section 5.2.4.1, there was no significant difference in percentage of cells that showed DDR1 single expression between the three HPV discordant groups. Although higher expression of COL11a1 single expression was observed in the p16-negative/HPV DNA-negative tumours, it was not statistically significant. In addition, there was no significant difference between the three discordant groups in the percentage of cells expressing concomitant double positive staining of DDR1 and COL11a1, COL11a1 overall expression (singly and co-expressed with DDR1), DDR1 overall expression (singly and co-expressed with COL11a1) and double negative staining.

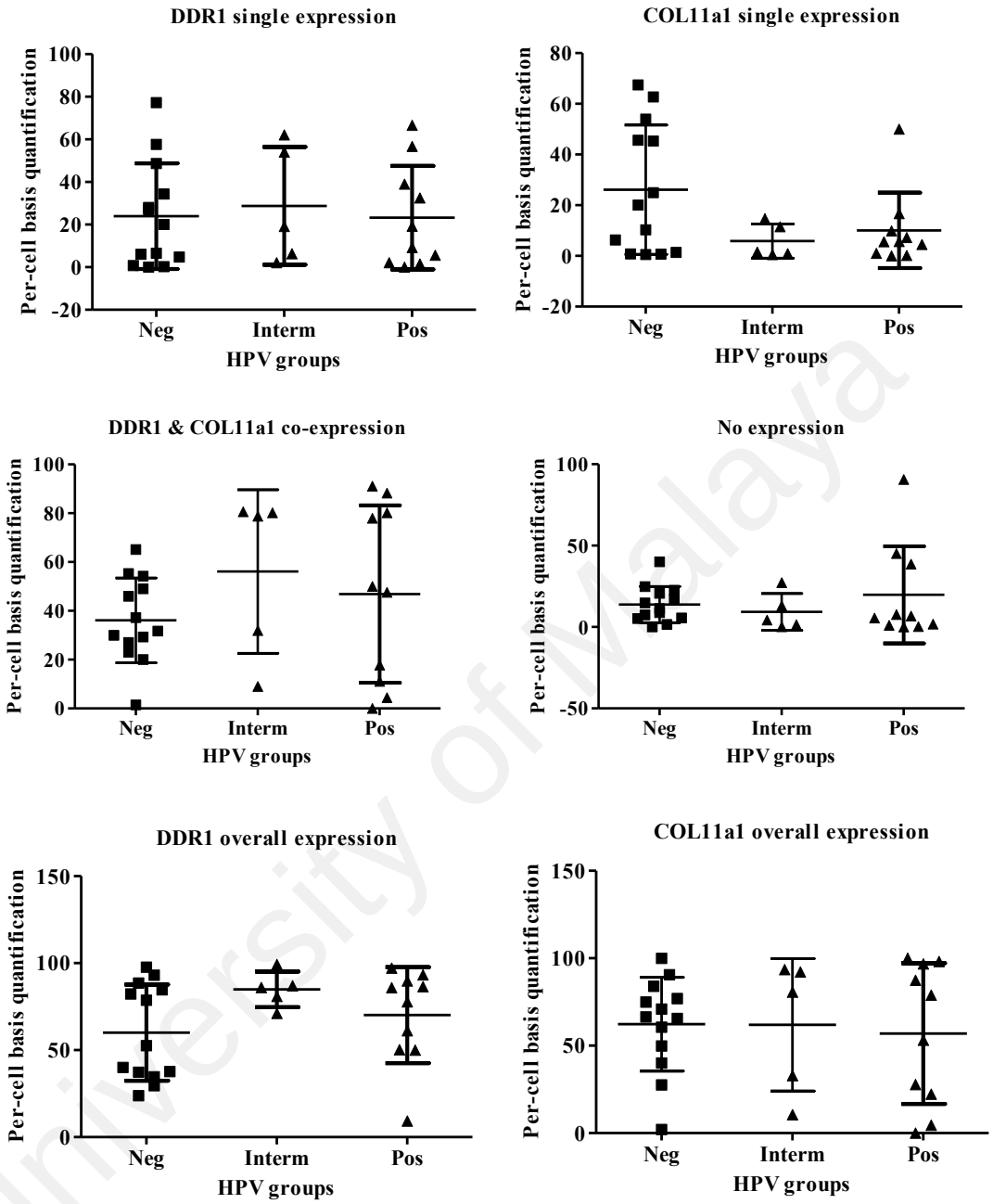

Figure 5.5: Unpaired T-test analyses on differential expression of DDR1 and COL11a1 in OPSCC TMA of three discordant groups of HPV status.

Expression was scored as percentage of total cells within the tumour regions which shown positive staining. Per cell basis quantification of the expression was plotted against three groups stratified by HPV status. None of the differential was biostatical significant. Abbreviation, Neg, negative; Interm, intermediate group which was p16-positive but high risk HPV DNA-negative; Pos, positive.

5.2.5 Association and correlations of DDR1 and COL11a1 expression with HPV status

Potential correlations between DDR1 and COL11a1 expression and HPV status were next analysed. Expression was analysed in terms of cells that showed single expression and in terms of cells that showed single cell co-expression of both proteins. The associations and correlations between DDR1 and COL11a1 with the HPV status of tumours on the TMA are summarised in Table 5.1. Non-tumour controls were excluded in these analyses and only tumours were studied.

For DDR1 single expression, the area under curve of ROC was below 0.6, skewness divided by standard deviation (skewness/SD=1.64) and kurtosis divided by standard deviation (kurtosis/SD=-0.95) were lower than 1.96, so it was assumed to be normally distributed. The cut-off value determined by mean (μ= 24.57). Crosstabs of the dataset (N= 28) showed that 16 samples (57.1% of total cohort) displayed low expression whilst 12 samples (42.9% of total cohort) displayed high expression of DDR1. Of the high expressing samples, equivalent percentage (21.4% of total cohort) of the OPSCC was p16-negative and p16-positive. It is not statistically significant in Pearson Chi Square, Spearman correlation, Univariate ANOVA, Univariate Logistic Regression and after Multiple Logistic Regression analyses was applied to adjust the p16 and HPV DNA as confounders. When grouping the HPV status by HPV DNA, 66.7% within high expression group (28.6% of total cohort) was HPV DNA-negative and 33.3% within high expression group (14.3% of total cohort) was HPV DNA-positive. No statistical significance was found. When grouping the HPV status by three discordant groups using the combined status of p16 and HPV DNA, 50% within the high expression group (21.4% of total cohort) was p16-negative/HPV DNA-negative, 16.7% within the high expression group (7.1% of total cohort) was p16-positive/HPV DNA-negative and 33.3% within the

high expression group (14.3% of total cohort) was p16-positive/HPV DNA-positive. However, no significant differences were found.

For COL11a1 single expression, the area under curve of ROC was below 0.6, skewness divided by standard deviation (skewness/SD=2.97) and kurtosis divided by standard deviation (kurtosis/SD=0.39) were lower than 1.96, so it was assumed to be skewed distributed. The quantitated percentage of cells showing positive staining of COL11a1 was transformed into low and high classifications by median (cut-off value=6.78). Crosstabs of the dataset (N= 28) showed that equivalent percentage of samples (50% of total cohort) displayed low expression and high expression of COL11a1 respectively. Within the COL11a1 high expressing group, 57.1% within high expression was p16-negative (28.6% of total cohort) and 42.9% within high expression group was p16-positive (21.4% of total cohort). The association and correlation were not statistically significant in Pearson Chi Square, Spearman Correlation, Univariate ANOVA and Univariate Logistic Regression and after Multiple Logistic Regression analyses was applied to adjust the p16 and HPV DNA as confounders. Majority (71.4% within high expression) of the COL11a1 high expression samples were within the HPV DNA-negative group (35.7% of total cohort) whilst 28.6% within high expression group (14.3% of total cohort) was HPV DNA-positive but the difference did not reach statistical significance. Also, when COL11a1 was analysed according to three discordant groups of HPV status combined of p16 and HPV DNA, 57.1% within the high expression group (28.6% of total cohort) was p16-negative/HPV DNA-negative, 14.3% within the high expression group (7.1% of total cohort) was p16-positive/HPV DNA-negative and 28.6% within the high expression group (14.3% of total cohort) was p16-positive/HPV DNA-positive. This association was not statistically significant.

Lastly, the dataset was analysed on the concomitant co-expression of DDR1 together with COL11a1 in single cells. The area under curve of ROC was above 0.6 (AUC= 0.621). The quantitated percentage of cells showing concomitant double-positive staining was transformed into low and high co-expression classifications by the cut-off value determined by its maximum sensitivity and specificity (cut-off= 71.53) of 46.7% sensitivity and 100% specificity (Appendix D). Crosstabs of the dataset (N=28) showed that 21 cases (75% of total cohort) were classified in the low co-expression group whilst 7 cases (25% of total cohort) fell in the high co-expression group. Of the high expressing samples, 100% was p16-positive (25% of total cohort). Majority of the tumours (46.4% of total cohort) was p16-negative showing low co-expression (61.9% within low expression group). It was statistically significant in Pearson Chi Square (p= 0.004), Spearman Correlation (p=0.003), Univariate ANOVA (p=0.003) but not significant in Univariate Logistic Regression and after Multiple Logistic Regression analyses was applied to adjust the p16 and HPV DNA as confounders. Majority (71.4% within low co-expression) of the low co-expression samples were within the HPV DNA-negative group (53.6% of total cohort) whilst 28.6% within low co-expression group (21.4% of total cohort) was HPV DNA-positive but the difference did not reach statistical significance. Also, when the co-expression was analysed according to three discordant groups of HPV status combined of p16 and HPV DNA, none of high co-expression tumours was p16-negative/HPV DNA-negative, 42.9% within the high expression group (10.7% of total cohort) was p16-positive/HPV DNA-negative and 57.1% within the high expression group (14.3% of total cohort) was p16-positive/HPV DNA-positive. This association was statistically significant in Pearson Chi Square (p= 0.012), Spearman Correlation (p=0.017), Univariate ANOVA (p=0.009) but not significant in Univariate Logistic Regression and after Multiple Logistic Regression analyses was applied to adjust the p16 and HPV DNA as confounders.

Table 5.1: Association and correlation between DDR1 and COL11a1 protein expression with p16, HPV DNA and combined status of OPSCC patients.

Proteins	Parameters	Characteristics	Expression (% of total cohort)		Pearson Chi Square	Spearman	Univariate ANOVA	Logistic Regression			Multiple Logistic Regression		
			Low	High	p-value	p-value	p-value	Odd ratio	95% CI	p-value	Odd ratio	95% CI	p-value
Single expression of DDR1	p16	Neg	25.0	21.4	0.743	0.754	0.754	1.286	(0.29,5.77)	0.743	1.286	(0.16,10.45)	0.814
		Pos	32.1	21.4				1.000	-	-	1.000	-	-
	HPV DNA	Neg	35.7	28.6	0.820	0.828	0.828	1.200	(0.25,5.77)	0.820	1.000	(0.11,8.95)	1.000
		Pos	21.4	14.3				1.000	-	-	1.000	-	-
	HPV group	Neg	25.0	21.4	0.948	0.769	0.953	1.286	(0.24,6.83)	0.768	-	-	-
		Interm	10.7	7.1				1.000	(0.11,8.95)	1.000	-	-	-
		Pos	21.4	14.3				1.000	-	-	-	-	-
Single expression of COL11a1	p16	Neg	17.9	28.6	0.256	0.272	0.272	2.400	(0.52,10.99)	0.259	2.400	(0.29,19.78)	0.416
		Pos	32.1	21.4				1.000	-	-	1.000	-	-
	HPV DNA	Neg	28.6	35.7	0.430	0.449	0.449	1.875	(0.39,9.01)	0.433	1.000	(0.11,8.95)	1.000
		Pos	21.4	14.3				1.000	-	-	1.000	-	-
	HPV group	Neg	17.9	28.6	0.524	0.304	0.554	2.400	(0.44,12.98)	0.309	-	-	-
		Interm	10.7	7.1				1.000	(0.11,8.95)	1.000	-	-	-
		Pos	21.4	14.3				1.000	-	-	-	-	-

Table 5.1, continued.

Proteins	Parameters	Characteristics	Expression (% of total cohort)		Pearson Chi Square	Spearman	Univariate ANOVA	Logistic Regression			Multiple Logistic Regression		
			Low	High	p-value	p-value	p-value	Odd ratio	95% CI	p-value	Odd ratio	95% CI	p-value
Single cell co-expression of DDR1 and COL11a1	p16	Neg	46.4	0.0	*0.004	*0.003	*0.003	0.000	(0.00,-)	0.998	0.000	(0.00,-)	0.999
		Pos	28.6	25.0				1.000	-	-	1.000	-	-
	HPV DNA	Neg	53.6	10.7	0.172	0.185	0.185	0.300	(0.05,1.76)	0.183	-	-	-
		Pos	21.4	14.3				1.000	-	-	-	-	-
	HPV group	Neg	46.4	0.0	*0.012	*0.017	*0.009	0.000	(0.00,-)	0.999	-	-	-
		Interm	7.1	10.7				2.250	(0.25,20.13)	0.468	2.250	(0.25,20.13)	0.468
		Pos	21.4	14.3				1.000	-	-	1.000	-	-

Multivariate Logistic Regression analyses was applied to adjust the confounders of p16 and HPV DNA for single expression of DDR1 or COL11a1 and applied to adjust the confounders of p16 and HPV group for single cell co-expression of both DDR1 and COL11a1.

Abbreviation: Neg, negative; Interm, intermediate; Pos, positive

*Indicated significant p-value ($p<0.05$).

5.3 Investigation of DDR1, COL8a1 and COL11a1 in tissue sections

The results of Section 5.2 demonstrated that DDR1 and COL11a1 were expressed in OPSCCs and that COL11a1 expression associated with p16-negative status in this small cohort. Low single cell co-expression of DDR1 and COL11a1 was associated with p16-negative tumours and the HPV discordant group that was p16-negative/ HPV DNA-negative. However, one of the disadvantages of using TMAs is that protein expression within the tumour microenvironment cannot be assessed. Therefore, this study was extended to examine DDR1 and COL11a1 in a larger series of whole tissue sections, using Opal Multiplex Fluorescent Immunohistochemistry (PerkinElmer, MA). COL8a1 was also examined, as it was also shown to be expressed by CAFs (Chapter 4).

5.3.1 OPSCC full tissue serial sections with socio-demographic and clinico-pathological parameters

Serial sections from 55 independent cases of formalin-fixed paraffin embedded primary OPSCC tissue blocks (REC reference 10/H1210/9) were used for fluorescence multiplex immunohistochemistry. Due to the potential 'field' effects, morphologically 'normal' epithelial adjacent to the tumours were excluded from this study. The socio-demographic and clinico-pathological characteristics of the cases are shown in Table 5.2. In addition, the patients were grouped into three discordant risk groups (i.e. low, moderate and high risk) with regards to the risk of death from disease where the classification was based on the HPV status, pack-years, lymph node metastasis and tumour size.

Table 5.2: Summary of the socio-demographic and clinico-pathological characteristics of OPSCCs used in this study.

Characteristic		N=55 (%)	Characteristic		N=55 (%)
Age (years old)	20-40	2 (3.6)	**Gender**	Male	37 (67.3)
	41-50	13 (23.6)		Female	18 (32.7)
	51-60	22 (40.0)	**T stage**	T0	1 (1.8)
	61-70	14 (25.5)		T1	33 (60.0)
	71-90	4 (7.3)		T2	18 (32.7)
Smoking	Never	19 (34.5)		NA	3 (5.5)
	Past	8 (14.5)	**N stage**	N1	30 (54.5)
	Current	27 (49.1)		N2	22 (40.0)
	NA	1 (1.8)		NA	3 (5.5)
Tos (years)	0-2	17 (30.9)	**HPV DNA ISH**	Negative	38 (69.1)
	2.1-4	15 (27.3)		Positive	16 (29.1)
	4.1-6	11 (20.0)		No record	1 (1.8)
	6.1-8	3 (5.5)	**p16**	Negative	24 (43.6)
	8.1-10	1 (1.8)		Positive	30 (54.5)
	NA	8 (14.5)		NA	1 (1.8)
Trfs (years)	0-2	18 (32.7)	**HPV RNAscope**	Negative	20 (36.4)
	2.1-4	16 (29.7)		Positive	25 (45.5)
	4.1-6	9 (16.4)		No record	10 (18.2)
	6.1-8	4 (7.3)	**Outcome**	Alive	20 (36.4)
	8.1-10	1 (1.8)		Deceased	32 (58.2)
	NA	7 (12.7)		NA	3 (5.5)
Risk of death group	Low	19 (34.5)			
	Moderate	19 (34.5)			
	High	16 (29.1)			
	NA	1 (1.8)			

Abbreviation: Tos, Overall Survival Time; Trfs, Recurrence Free Survival Time; T stage, Primary tumour stage; N stage, extent of regional lymph node metastasis; HPV DNA ISH, High Risk HPV DNA *in situ* hybridisation; HPV RNAscope, HPV RNA *in situ* hybridisation; NA, not available.

5.3.2 DDR1, COL8a1 and COL11a1 expression in OPSCC tissue sections

The tissue sections were first double-stained for CK AE1/ AE3 (Cy3, red) to highlight the epithelia and DDR1 (Fluorescein, green). Five random hotspots of each case were visualised using a confocal laser scanning microscope (CLSM, Zeiss). The results showed that DDR1 was expressed in all OPSCC tissues examined and the staining was found to be cytoplasmic (Figure 5.6) and focally membranous (Figure 5.7).

To examine whether COL8a1 is expressed by OPSCC CAFs *in vivo*, sections were dual-stained for COL8a1 and alpha-smooth muscle actin (α-SMA), which is a marker of fibroblast activation. COL8a1 was found to be expressed in both the OPSCC tumour cells (Figure 5.8) and CAFs (Figure 5.9). However, the expression of COL8a1 in tumour cells was heterogeneous from strong to weak positively stained. COL8a1 protein was predominantly detected in the cytoplasm of tumour cells and CAFs.

The OPSCC tissue sections were also dual-stained for the presence of another collagen subtype, COL11a1 and α-SMA. COL11a1 was found to be expressed in both the OPSCC tumour cells (Figure 5.10) and CAFs (Figure 5.11). The expression of COL11a1 in tumour cells and CAFs was strong and COL11a1 protein was predominantly localised in the cytoplasm of tumour cells, whilst the staining in CAFs was also predominantly cytoplasmic and nuclear.

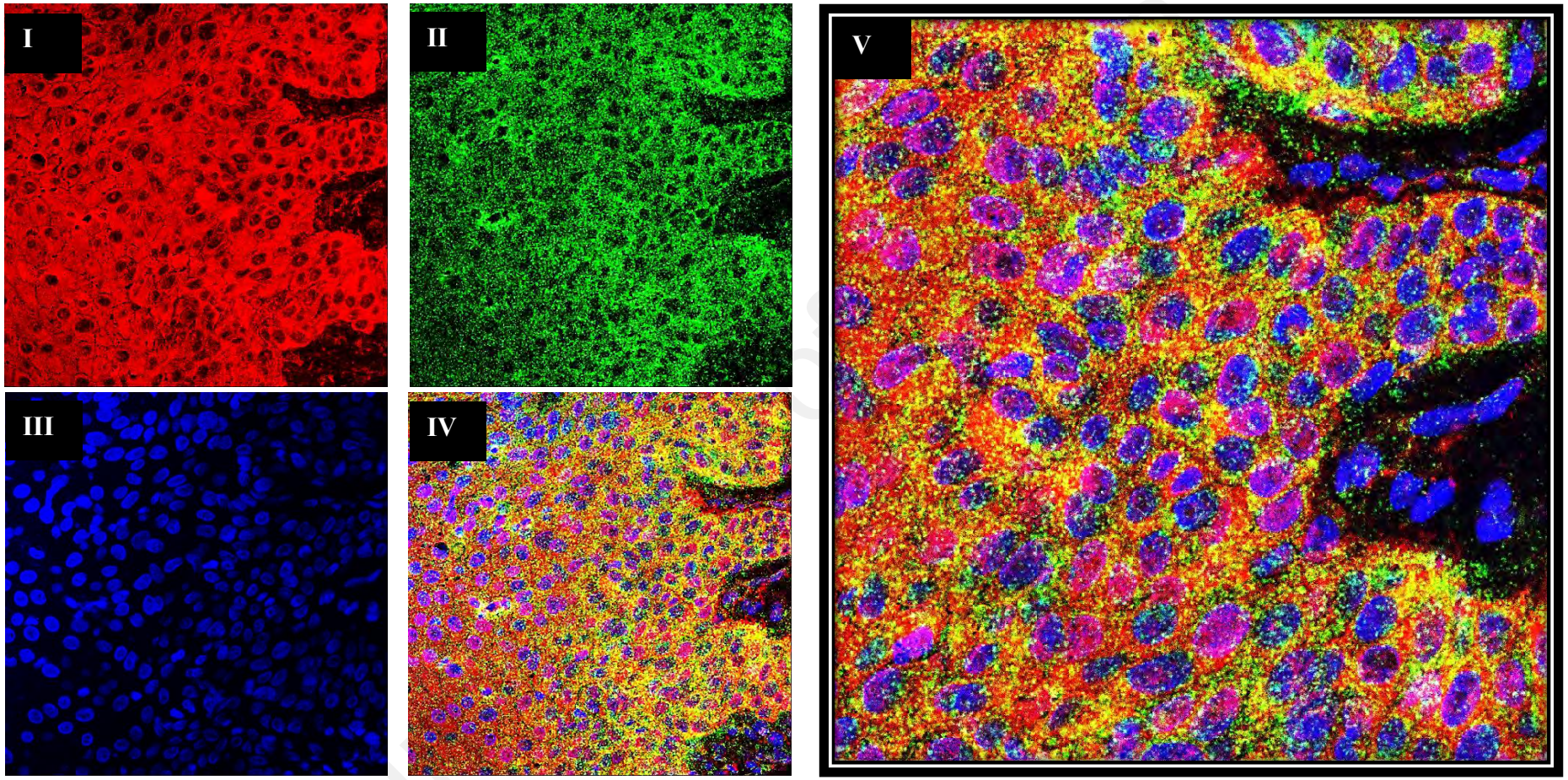

Figure 5.6: Representative images showing cytoplasmic DDR1 protein expression in OPSCC tumour cells.
Tissues were multiplex-stained with **(I)** CK AE1/ AE3 (Cy3, red), **(II)** DDR1 (fluorescein, green) antibodies and **(III)** DAPI (blue) nuclear counterstain. Strong DDR1 staining was shown in malignant epithelium at magnification of **(IV)** 63X and **(V)** 100X captured by confocal laser scanning microscope (Zeiss).

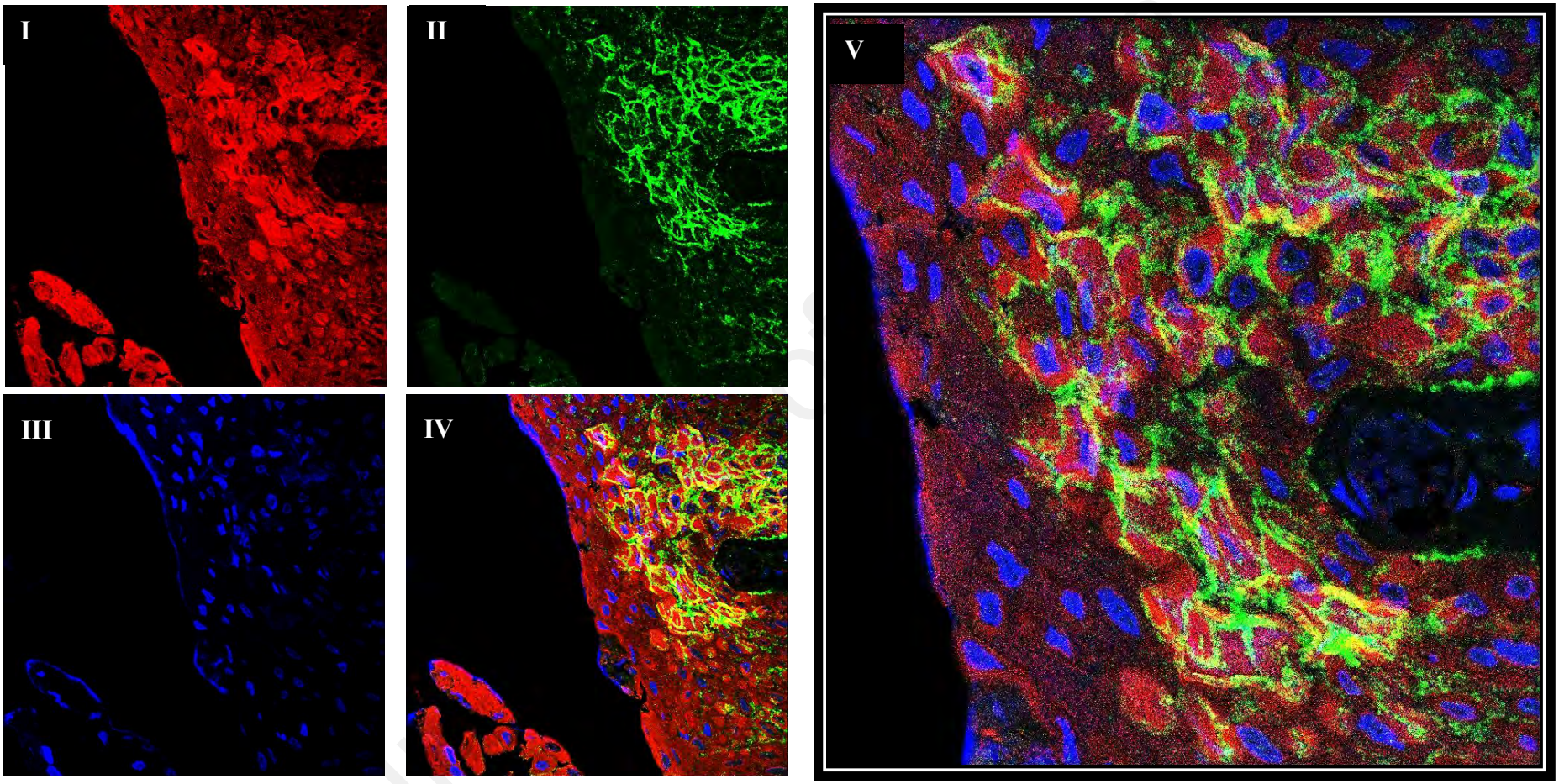

Figure 5.7: Representative images showing focal membranous DDR1 protein expression in OPSCC tumour cells.
Tissues were multiplex-stained with **(I)** CK AE1/ AE3 (Cy3, red), **(II)** DDR1 (fluorescein, green) antibodies and **(III)** DAPI (blue) nuclear counterstain. Strong DDR1 staining was shown in malignant epithelium at magnification of **(IV)** 63X and **(V)** 100X captured by confocal laser scanning microscope (Zeiss).

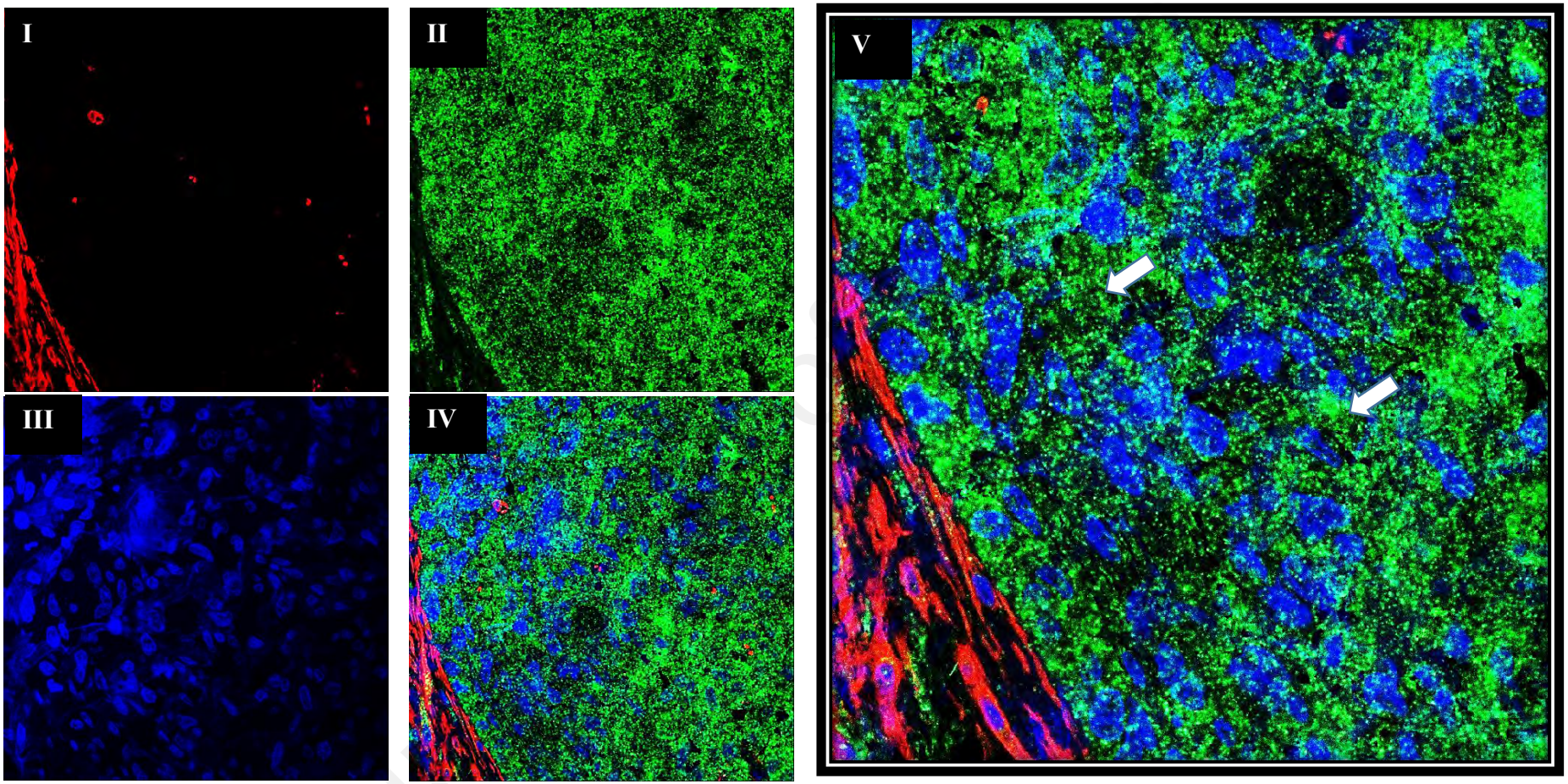

Figure 5.8: Representative images showing cytoplasmic COL8a1 protein expression in OPSCC tumours.
The tumour cells (region indicated by arrows) expressed **(II)** COL8a1 (Fluorescein, green) when multiplex-stained with **(I)** activated-CAF marker, α-SMA (Cy3, red) and **(III)** DAPI (blue) nuclear counterstain. Images showed magnification at **(IV)** 63X and **(V)** 100X captured by confocal laser scanning microscope (Zeiss).

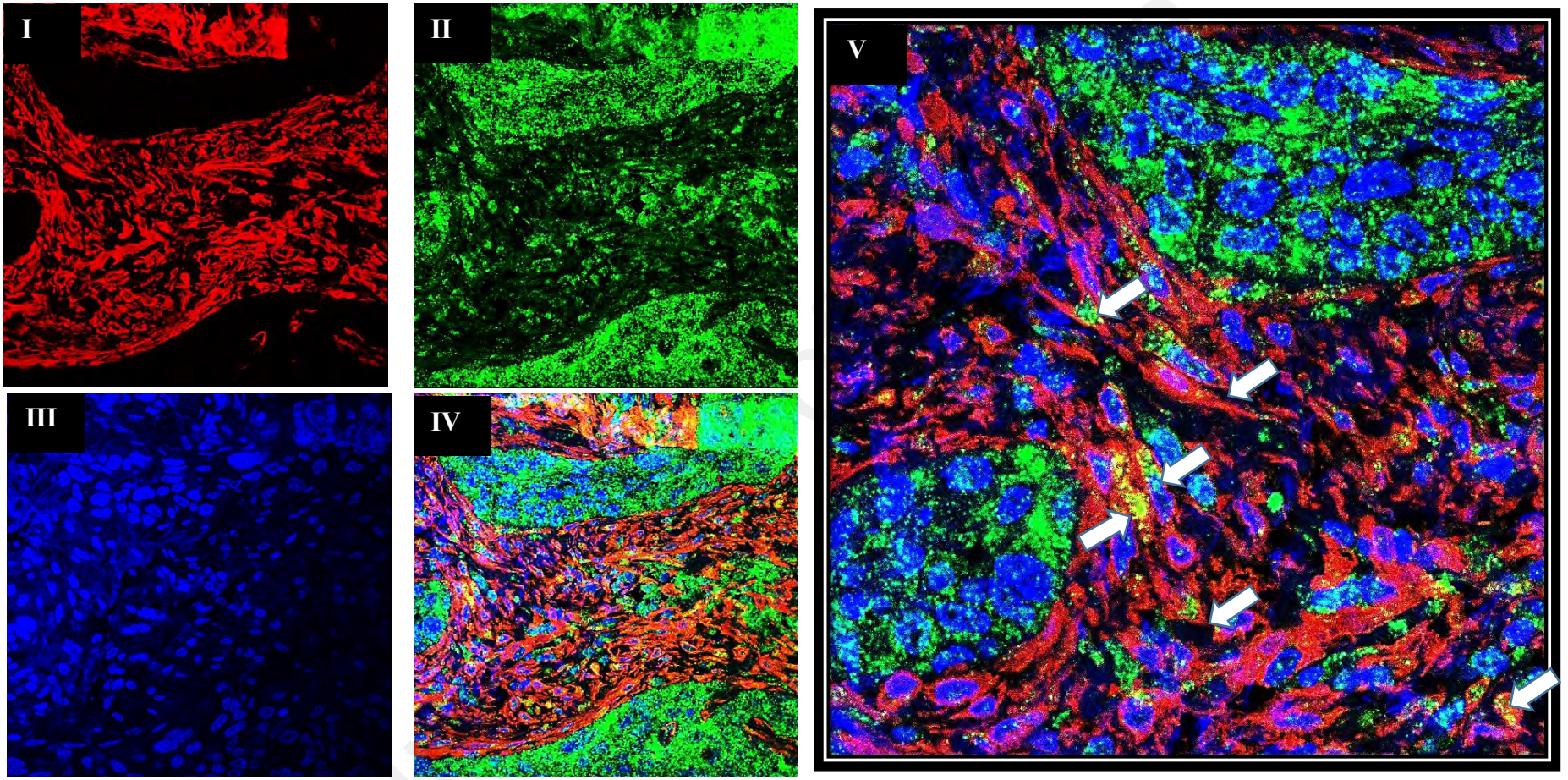

Figure 5.9: Representative images showing cytoplasmic and nuclear COL8a1 expression in OPSCC CAFs.
Tissues were multiplex-stained with **(I)** activated-CAF marker, α-SMA (Cy3, red), **(II)** COL8a1 (fluorescein, green) antibodies and **(III)** DAPI (blue) nuclear counterstain. Arrows indicate COL8a1 protein in activated-CAFs at magnification of **(IV)** 63X and **(V)** 100X captured by confocal laser scanning microscope (Zeiss).

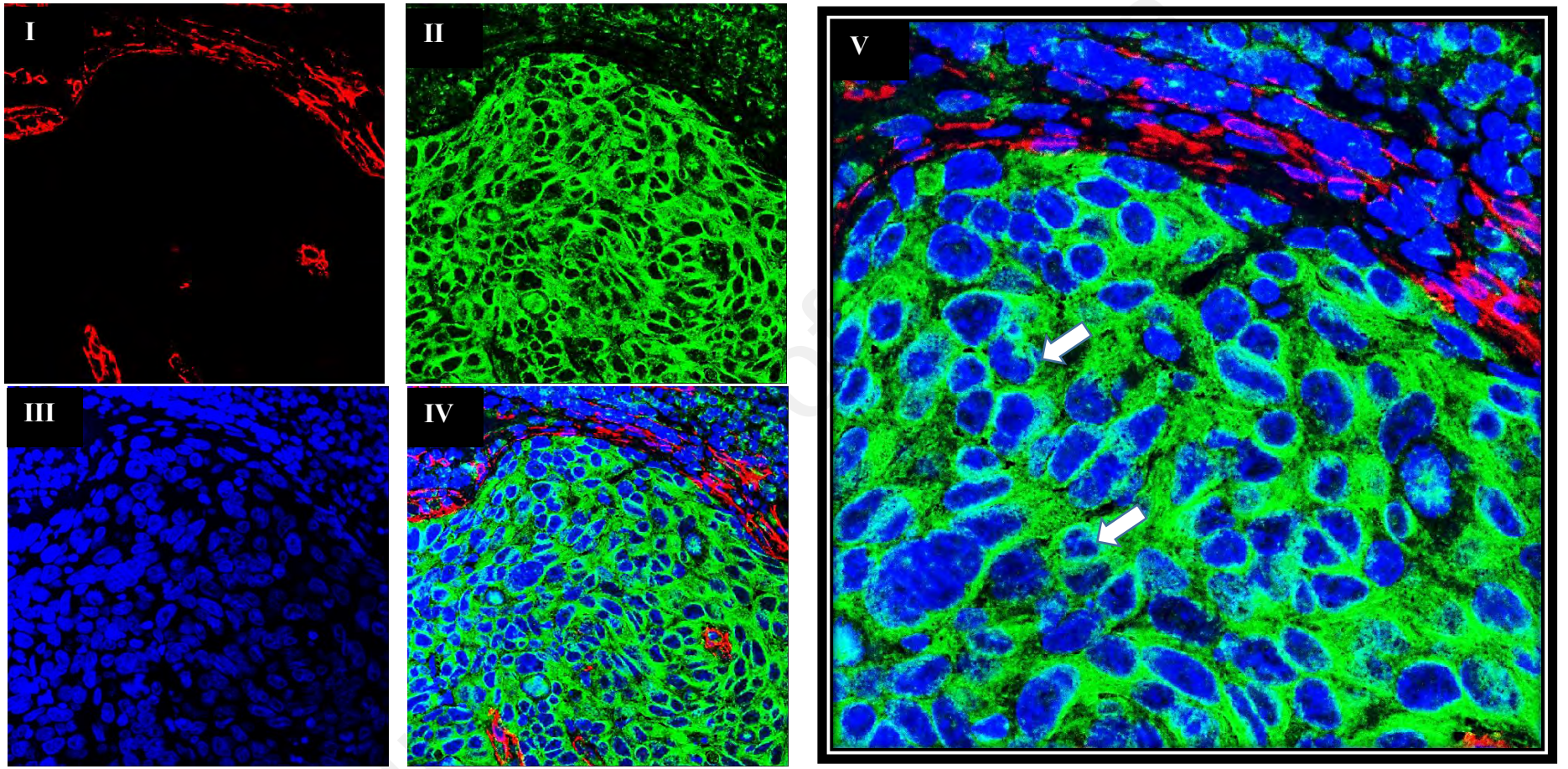

Figure 5.10: Representative images showing cytoplasmic COL11a1 protein expression in OPSCC tumours.
The tumour cells (region indicated by arrows) expressed **(II)** COL11a1 (Fluorescein, green) when multiplex-stained with the **(I)** activated-CAF marker, α-SMA (Cy3, red) and **(III)** DAPI (blue) nuclear counterstain. Images showed magnification at **(IV)** 63X and **(V)** 100X captured by confocal laser scanning microscope (Zeiss).

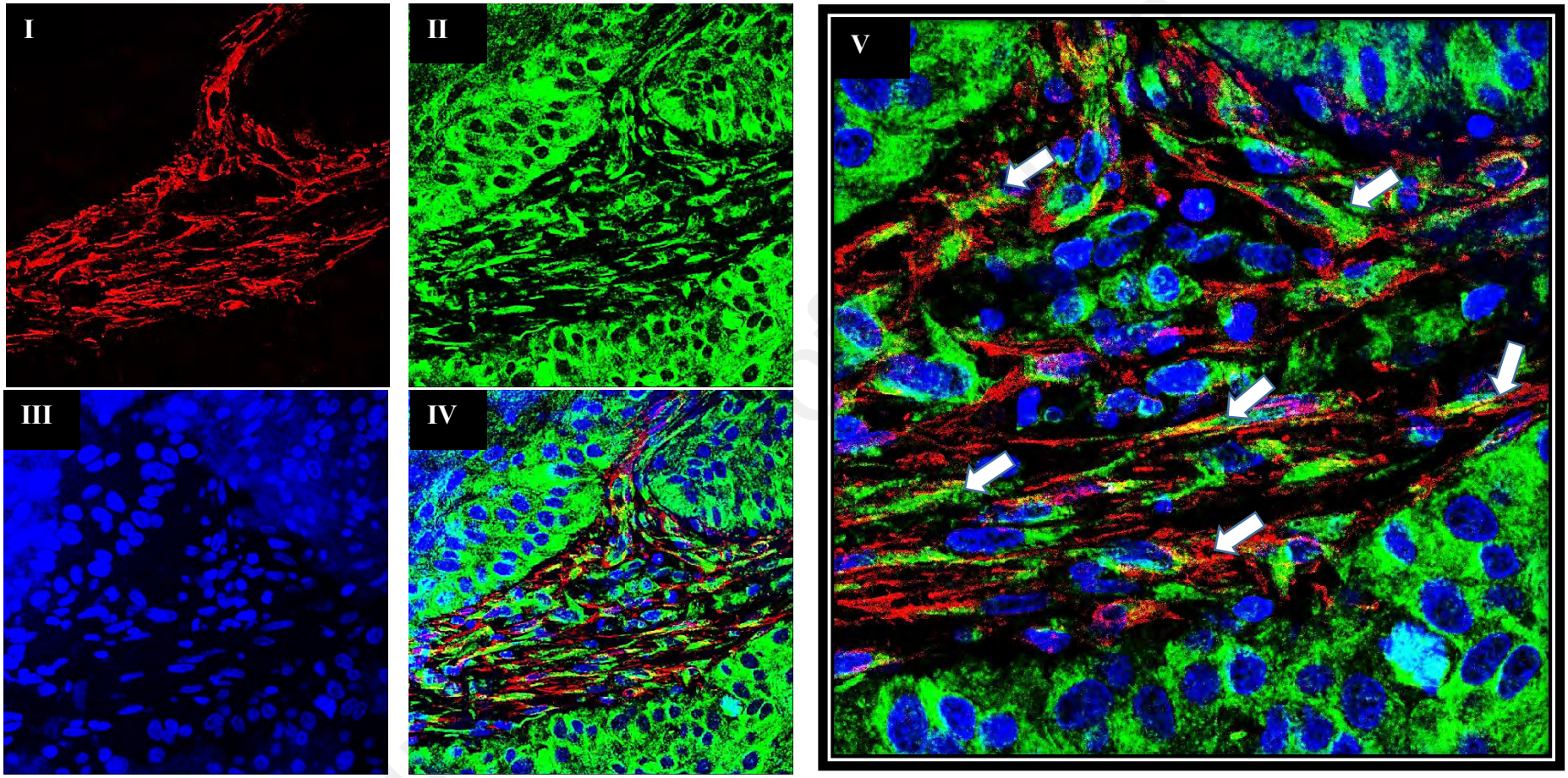

Figure 5.11: Representative images showing cytoplasmic and nuclei COL11a1 protein expression in OPSCC CAFs.
Tissues were multiplex-stained with **(I)** activated-CAF marker, α-SMA (Cy3, red), **(II)** COL11a1 (fluorescein, green) antibodies and **(III)** DAPI (blue) counterstain. Arrows indicate COL11a1 protein in activated-CAFs at magnification of **(IV)** 63X and **(V)** 100X captured by confocal laser scanning microscope (Zeiss).

5.3.3 Quantification of DDR1, COL8a1 and COL11a1 expression and correlation with socio-demographic and clinico-pathological characteristics

The DDR1, COL8a1 and COL11a1 staining intensities were scored quantitatively using Metamorph Pathology Analysis Software on an individual cell basis. The tumour regions of interest of each case were identified by a trained pathologist (Dr Anand Ramanathan, Department of Oro-Maxillofacial Surgical and Medical Science, Faculty of Dentistry, University of Malaya). The expression was quantified as the number of positive staining cells multiplied by the staining intensity above local background in an average of random five hotspots for each case.

5.3.3.1 DDR1 expression

The correlation between DDR1 expression in CK AE1/ AE3 positive cells with socio-demographic and clinico-pathological parameters was examined and is summarised in Table 5.3. The area under curve of a Receiver Operating Characteristic (ROC) Curve was below 0.6 and the skewness divided by standard deviation was less than 1.98 (skewness/SD=2.82) indicating that the population was not normally distributed. Therefore, median (Med= 118 386.24) was used as the cut-off value in transforming the DDR1 expression scales into low and high expression groups. Among the 55 cases, 28 cases (50.9% of total cohort) were assigned to the low expression group, whilst 27 cases (49.1% of total cohort) fell in the high expression group.

Crosstabs of DDR1 expression demonstrated that its high expression was significantly associated (Pearson Chi Square, p= 0.023) and correlated (Spearman Correlation, p= 0.029) with non-smokers. Within the total cohort of 55 patients, 19 patients (34.5% of total cohort) were non-smokers, 35 patients (63.6% of total cohort) were past and current smokers; and the record of 1 patient (1.8% of total cohort) was unavailable. In addition, Univariate ANOVA and Logistic Regression were carried out to study and validate the significance of the association. Both the tests showed significant p-values (Univariate

ANOVA, p= 0.021; Univariate Logistic Regression, p= 0.013), which support the finding that DDR1 high expression was strongly associated and correlated with non-smoking behaviour in OPSCC. Further analyses were carried out by Multiple Logistic Regression. However, the association between DDR1 protein expression and smoking behaviour became not significant (p= 0.052) in the Multiple Logistic Regression analyses after adjusting for the confounding factors including age, gender, p16, HPV DNA ISH, HPV RNAscope, risk group, smoking, T stage, N stage, outcome, overall survival time and recurrence free survival time.

Although high DDR1 expression was not significantly associated with risk group under Pearson Chi Square (p= 0.056), Spearman Correlation (p= 0.056) and Univariate ANOVA (p= 0.055), significant p-value was found using Univariate Logistic Analysis (p= 0.036) indicating that DDR1 high expression was associated with risk group. Within the high expression group, 14 patients (25.5% of total cohort) have moderate risk of death, 7 patients (12.7% of total cohort) have high risk of death and the records from 6 patients (10.9% of total cohort) were unavailable. Of note, all the patients from low risk group (100% within low risk; i.e. 9.1% of total cohort) have low expression of DDR1. However, the association between DDR1 protein expression and risk of death characteristic became not significant (p= 0.052) in the Multiple Logistic Regression analyses after adjusting for the confounding factors including age, gender, p16, HPV DNA ISH, HPV RNAscope, risk group, smoking, T stage, N stage, outcome, overall survival time and recurrence free survival time.

These quantitative results were in agreement with the observations from images captured by the multi-spectral unmixed composite imaging which showed differential expression of DDR1 in the risk of death and smoking groups. Higher expression of DDR1 was observed in non-smokers (Figure 5.12) and moderate and high risk groups (Figure 5.13).

Table 5.3: Association and correlation between DDR1 protein expression with socio-demographic and clinico-pathological characteristics of OPSCC patients

Variables	Categories	DDR1 Expression (% of total cohort)		Pearson Chi Square	Spearman	Univariate ANOVA	Univariate Logistic Regression			Multiple Logistic Regression		
		Low	High	p-value	p-value	p-value	Odd ratio	95% CI	p-value	Odd ratio	95% CI	p-value
Age	20-40	1.8	1.8	0.993	0.889	0.994	1.000	-	-	1.000	-	-
	41-50	10.9	12.7				1.167	(0.06,22.94)	0.919	1071939542	(0.00,-)	0.999
	51-60	21.8	18.2				0.833	(0.05,15.09)	0.902	373799069.6	(0.00,-)	0.999
	61-70	12.7	12.7				1.000	(0.05,19.36)	1.000	2296674518	(0.00,-)	0.999
	71-90	3.6	3.6				1.000	(0.03,29.81)	1.000	405411434.4	(0.00,-)	0.999
Gender	Male	36.4	30.9	0.504	0.513	0.513	1.000	-	-	1.000	-	-
	Female	14.5	18.2				1.471	(0.47,4.56)	0.504	3.125	(0.33,29.55)	0.320
p16	Neg	23.6	20.0	0.527	0.796	0.542	1.000	-	-	1.000	-	-
	Pos	25.5	29.1				1.351	(0.46,3.97)	0.584	0.263	(0.00,16.00)	0.524
	NA	1.8	0.0				0.000	(0.00,-)	1.000	-	-	-
HPV DNA ISH	Neg	36.4	32.7	0.512	0.780	0.527	1.000	-	-	1.000	-	-
	Pos	12.7	16.4				1.429	(0.44,4.63)	0.552	4.758	(0.29,78.30)	0.275
	NA	1.8	0.0				0.000	(0.00,-)	1.000	0.000	(0.00,-)	0.999
HPV Group	Neg	23.6	20.0	0.706	0.908	0.723	1.000	-	-	-	-	-
	Interm	12.7	12.7				1.182	(0.316,4.424)	0.804	-	-	-
	Pos	12.7	16.4				1.519	(0.425,5.426)	0.519	-	-	-
	NA	1.8	0.0				0.000	(0.00,-)	1.000	-	-	-
HPV RNAscope	Neg	18.2	18.2	0.379	0.499	0.393	1.000	-	-	1.000	-	-
	Pos	20.0	25.5				1.273	(0.39,4.14)	0.689	0.369	(0.01,24.14)	0.640
	NA	12.7	5.5				0.429	(0.09,2.15)	0.303	0.430	(0.02,8.84)	0.584
Risk of death Group	Low	9.1	0.0	0.056	0.056	0.055	4.667	(1.11,19.65)	*0.036	60.374	(0.97,3762.5)	0.052
	Moderate	21.8	25.5				0.972	(0.25,3.85)	0.968	2.556	(0.12,54.54)	0.548
	High	18.2	12.7				1.000	-	-	1.000	-	-
	NA	1.8	10.9				0.000	(0.00,-)	1	-	-	-

Table 5.3, continued.

Variables	Categories	DDR1 Expression (% of total cohort)		Pearson Chi Square	Spearman	Univariate ANOVA	Univariate Logistic Regression			Multiple Logistic Regression		
		Low	High	p-value	p-value	p-value	Odd ratio	95% CI	p-value	Odd ratio	95% CI	p-value
Smoking	No	9.1	25.5	*0.023	*0.029	*0.021	4.738	(1.39,16.21)	*0.013	60.374	(0.97,3762.5)	0.052
	Yes	40.0	23.6				1.000	-	-	1.000	-	-
	NA	1.8	0.0				0.000	(0.00,-)	1	0.000	(0.00,-)	1.000
T stage	T0	0.0	1.8	0.111	0.618	0.113	1.000	-	-	1.000	-	-
	T1	29.1	30.9				0.000	(0.00,-)	1	0.000	(0.00,-)	1.000
	T2	21.8	10.9				0.000	(0.00,-)	1	0.000	(0.00,-)	1.000
	NA	0.0	5.5				1615478896	-	1	49690208	(0.00,-)	1.000
N stage	N1	30.9	23.6	0.455	0.461	0.470	1.000	-	-	1.000	-	-
	N2	16.4	23.6				1.889	(0.62,5.76)	0.264	0.993	(0.12,8.14)	0.995
	NA	3.6	1.8				0.654	(0.05,8.02)	0.740	0.000	(0.00,-)	0.999
Outcome	Alive	32.7	25.5	0.446	0.455	0.461	1.000	-	-	1.000	-	-
	Deceased	14.5	21.8				1.929	(0.62,6.00)	0.257	9.414	(0.90,98.29)	0.060
	NA	3.6	1.8				0.643	(0.05,7.83)	0.729	16.540	(0.23,1206.91)	0.200
Tos	0-6	43.6	38.2	0.720	0.961	0.731	0.656	(0.13,3.28)	0.608	0.195	(0.01,5.83)	0.350
	6-12	5.5	7.3				1.000	-	-	1.000	-	-
	NA	1.8	3.6				1.500	(0.09,25.39)	0.779	6.787E23	(0.00,-)	0.999
Trfs	0-3	20.0	23.6	0.354	0.177	0.368	1.719	(0.57,5.22)	0.339	1.799	(0.30,10.75)	0.523
	3.1-9	29.1	20.0				1.000	-	-	1.000	-	-
	NA	1.8	5.5				4.364	(0.40,47.61)	0.227	0.000	(0.00,-)	1.000

Multivariate Logistic Regression analyses was applied to adjust the confounders of age, gender, p16, HPV DNA ISH, HPV RNAscope, risk group, smoking, T stage, N stage, outcome, Tos and Trfs.

Abbreviation: Neg, negative; Pos, positive; Interm, intermediate; NA, not available; HPV DNA ISH, HPV DNA *in situ* hybridisation; HPV RNAscope, HPV RNA *in situ* hybridisation; Tos, overall survival time; Trfs, recurrence free survival time; *Indicated significant p-value ($p<0.05$).

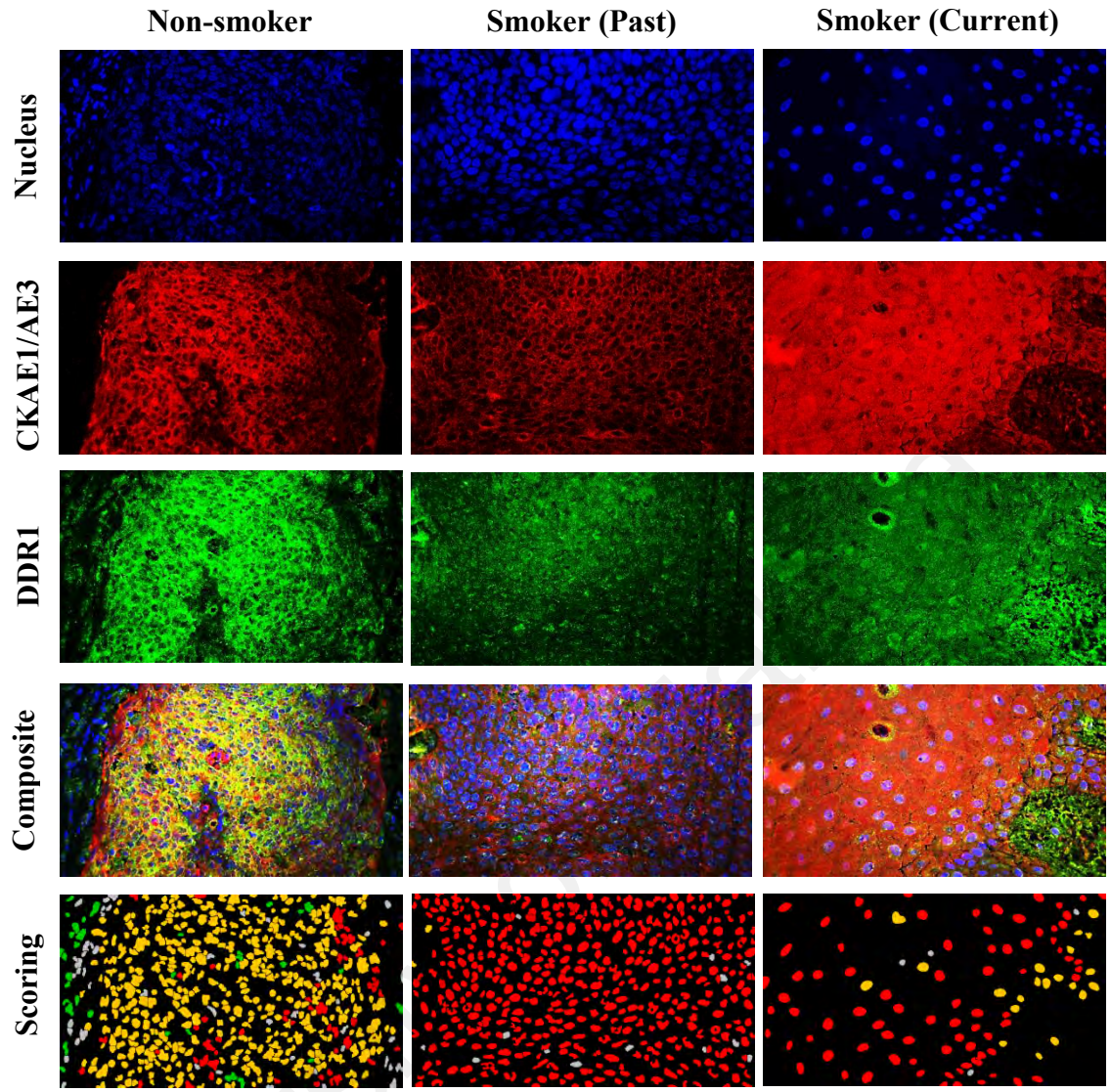

Figure 5.12: Multi-spectral unmixed composite imaging and quantitative digital scoring showed high DDR1 expression in non-smokers compared to smokers.

Tissues were simultaneously multiplex-stained with epithelium marker, CK AE1/AE3 (Cy3, red), DDR1 (fluorescein, green) and DAPI (blue) nuclear counterstain. The scoring map of per-cell DDR1 expression generated by the digital workflow algorithm. Cells positive for only CK AE1/AE3 are displayed in red, cells positive for DDR1 are displayed in green, cells double positive for CK AE1/AE3 and DDR1 are displayed in yellow, and cells negative for both markers are displayed in white.

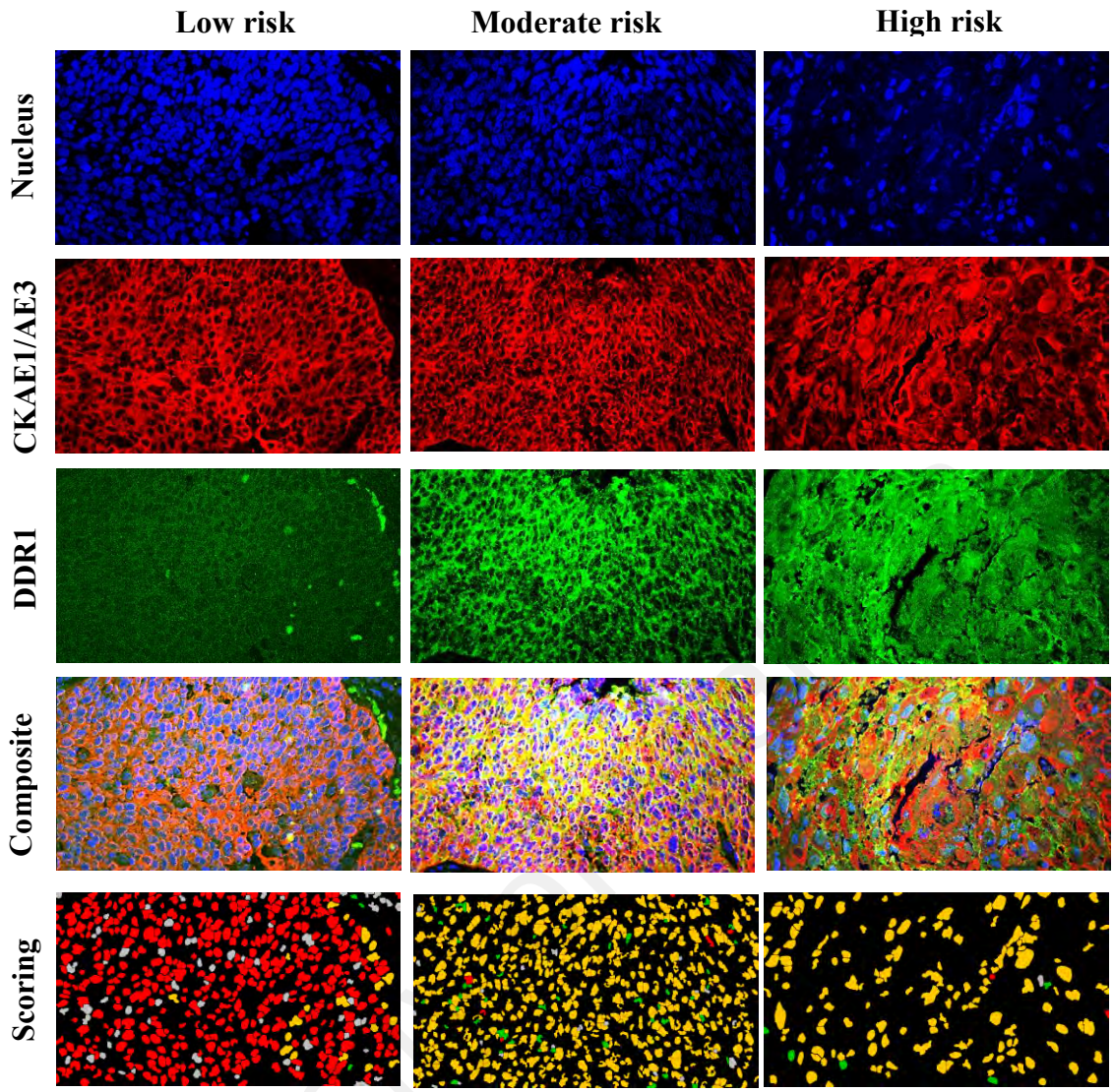

Figure 5.13: Multi-spectral unmixed composite imaging and quantitative digital scoring showed high DDR1 expression in moderate and high risk compared to low risk group.

Tissues were simultaneously multiplex-stained with epithelium marker, CK AE1/AE3 (Cy3, red), DDR1 (fluorescein, green) and DAPI (blue) nuclear counterstain. The scoring map of per-cell DDR1 expression generated by the digital workflow algorithm. Cells positive for only CK AE1/AE3 are displayed in red, cells positive for DDR1 are displayed in green, cells double positive for CK AE1/AE3 and DDR1 are displayed in yellow, and cells negative for both markers are displayed in white.

5.3.3.2 COL8a1 expression

The expression of COL8a1 in tumour cells was analysed for association and correlation with socio-demographic and clinico-pathological parameters. The area under curve of ROC Curve was above 0.6 (AUC= 0.715). The cut-off value determined by its maximum sensitivity and specificity (cut-off= 9385.18) of 63% sensitivity and 81.3% specificity was used for transforming the obtained COL8a1 expression scales into low and high expression groups of (Appendix E). Among the 55 cases, 23 cases (41.8% of total cohort) were classified in the low expression group whilst 21 cases (38.2% of total cohort) fell in the high expression group. The remaining 11 cases (20% of total cohort) were excluded for technical reasons after staining.

Crosstabs of the COL8a1 expression in tumour cells demonstrated that low expression of COL8a1 was significantly associated and correlated with low risk-group (Pearson Chi Square, p= 0.012; Spearman Correlation, p= 0.006; Univariate ANOVA= 0.009) and N2 lymph nodes metastasis (Spearman Correlation, p=0.042), whilst high expression was significantly associated with smoking behaviour (Pearson Chi Square, p= 0.011; Spearman Correlation, p= 0.002; Univariate ANOVA= 0.009). Further analyses by Univariate Logistic Regression were carried out and supported the results that COL8a1 expression in tumour cells were significantly associated and correlated with smoking behaviour (Univariate Logistic Regression= 0.008) and risk group (Logistic Regression, p= 0.004) but its association with the lymph node metastasis was not significant. However, none of these associations were significant after adjusted to the confounder factors in Multiple Logistic Regression (Table 5.4).

These quantitative results were in agreement with the observations from images captured by the multi-spectral unmixed composite imaging which showed differential expression of COL8a1 in which lower expression of COL8a1 was showed in low risk

(Figure 5.14) and N2 lymph node metastasis groups (Figure 5.15) while higher expression was observed in smokers (Figure 5.16).

Table 5.4: Association and correlation between COL8a1 protein expression in tumour cells with socio-demographic and clinico-pathological characteristics of OPSCC patients

Variables	Categories	COL8a1 expression in tumour cells (n,% of total cohort)		Pearson Chi Square	Spearman	Univariate ANOVA	Univariate Logistic Regression			Multiple Logistic Regression		
		Low	High	p-value	p-value	p-value	Odd ratio	95% CI	p-value	Odd ratio	95% CI	p-value
Age	20-40	0.0	2.3	0.391	0.442	0.416	1.000	-	-	1.000	-	-
	41-50	15.9	11.4				0.000	(0.00,0.00)	1.000	6.17E+260	(0.00,-)	0.992
	51-60	15.9	22.7				0.000	(0.00,0.00)	1.000	1.518E+295	(0.00,-)	0.992
	61-70	15.9	11.4				0.000	(0.00,0.00)	1.000	1.135E+212	(0.00,-)	0.993
	71-90	4.5	0.0				0.000	(0.00,-)	0.999	1.741E+203	(0.00,-)	0.994
Gender	Male	36.4	27.3	0.392	0.404	0.404	1.000	-	-	1.000	-	-
	Female	15.9	20.5				1.714	(0.50,5.92)	0.394	0.000	(0.00,-)	0.990
p16	Neg	15.9	25.0	0.246	0.116	0.259	1.000	-	-	1.000	-	-
	Pos	34.1	22.7				0.424	(0.12,1.47)	0.175	3.013E+117	(0.00,-)	0.989
	NA	2.3	0.0				0.000	(0.00,-)	1.000	-	-	-
HPVISH	Neg	31.8	34.1	0.540	0.424	0.559	1.000	-	-	1.000	-	-
	Pos	18.2	13.6				7.000	(0.19,2.53)	0.586	0.000	(0.00,-)	0.989
	NA	2.3	0.0				0.000	(0.00,-)	1.000	5.016E+269	(0.00,-)	0.993
RNAscope	Neg	11.4	20.5	0.319	0.168	0.335	1.000	-	-	1.000	-	-
	Pos	29.5	20.5				0.385	(0.10,1.54)	0.176	0.000	(0.00,-)	1.000
	NA	11.4	6.8				0.333	(0.06,2.02)	0.232	0.000	(0.00,-)	1.000
HPV Group	Neg	15.9	22.7	0.530	0.425	0.554	2.286	(0.52,10.01)	0.273	-	-	-
	Interm	15.9	13.6				1.371	(0.29,6.54)	0.692	-	-	-
	Pos	18.2	11.4				1.000	-	-	-	-	-
	NA	2.3	0.0				0.000	(0.00,-)	1.000	-	-	-
Risk Group	Low	29.5	6.8	*0.012	*0.006	*0.009	0.069	(0.01,0.42)	*0.004	-	-	-
	Moderate	15.9	15.9				0.300	(0.06,1.58)	0.156	0.000	(0.00,-)	0.999
	High	6.8	22.7				1.000	-	-	1.000	-	-
	NA	0.0	2.3				484642459.3	(0.00,-)	1.000	-	-	-

Table 5.4, continued.

Variables	Categories	COL8a1 expression in tumour cells (n,% of total cohort)		Pearson Chi Square	Spearman	Univariate ANOVA	Univariate Logistic Regression			Multiple Logistic Regression		
		Low	High	p-value	p-value	p-value	Odd ratio	95% CI	p-value	Odd ratio	95% CI	p-value
Smoking	No	29.5	6.8	*0.011	*0.002	*0.009	1.000	-	-	1.000	-	-
	Yes	22.7	38.6				7.367	(1.68,32.31)	*0.008	1.026E+231	(0.00,-)	0.999
	NA	0.0	2.3				700391085	(0.00,-)	1.000	1.922E+15	(0.00,-)	1.000
T stage	T1	27.3	34.1	0.423	0.202	0.441	1.000	-	-	1.000	-	-
	T2	20.5	11.4				0.444	(0.12,1.68)	0.232	0.000	(0.00,-)	0.989
	NA	4.5	2.3				0.400	(0.03,4.96)	0.476	0.000	(0.00,-)	0.997
N stage	N1	18.2	31.8	0.107	*0.042	0.111	1.000	-	-	1.000	-	-
	N2	29.5	13.6				0.264	(0.07,0.97)	*0.045	6.009E+055	(0.00,-)	0.990
	NA	4.5	2.3				0.286	(0.02,3.67)	0.336	0.000	(0.00,-)	0.996
Outcome	Alive	34.1	25.0	0.282	0.294	0.297	1.000	-	-	1.000	-	-
	Deceased	18.2	18.2				1.364	(0.39,4.77)	0.627	1.000	(0.01,92.42)	1.000
	NA	0.0	4.5				2202920270	(0.00,-)	0.999	0.000	(0.00,-)	0.999
Tos	0-6	40.9	45.5	0.221	0.098	0.233	1.000	-	-	1.000	-	-
	6-12	6.8	2.3				0.300	(0.03,3.15)	0.316	0.000	(0.00,-)	1.000
	NA	4.5	0.0				0.000	(0.000,-)	0.999	0.000	(0.00,-)	0.997
Trfs	0-3	20.5	22.7	0.787	0.887	0.799	0.600	(0.05,7.63)	0.694	35609215277	(0.00,-)	1.000
	3.1-9	27.3	22.7				1.000	-	-	1.000	--	-
	NA	4.5	2.3				1.333	(0.39,4.57)	0.647	1.237E+041	(0.00,-)	0.990

Multivariate Logistic Regression analyses was applied to adjust the confounders of age, gender, p16, HPV DNA, RNAscope, risk group, smoking, T stage, N stage, outcome, Tos and Trfs.

Abbreviation: Neg, negative; Pos, positive; Interm, intermediate; NA, not available; Tos, overall survival time; Trfs, recurrence free survival time; *Indicated significant p-value ($p<0.05$).

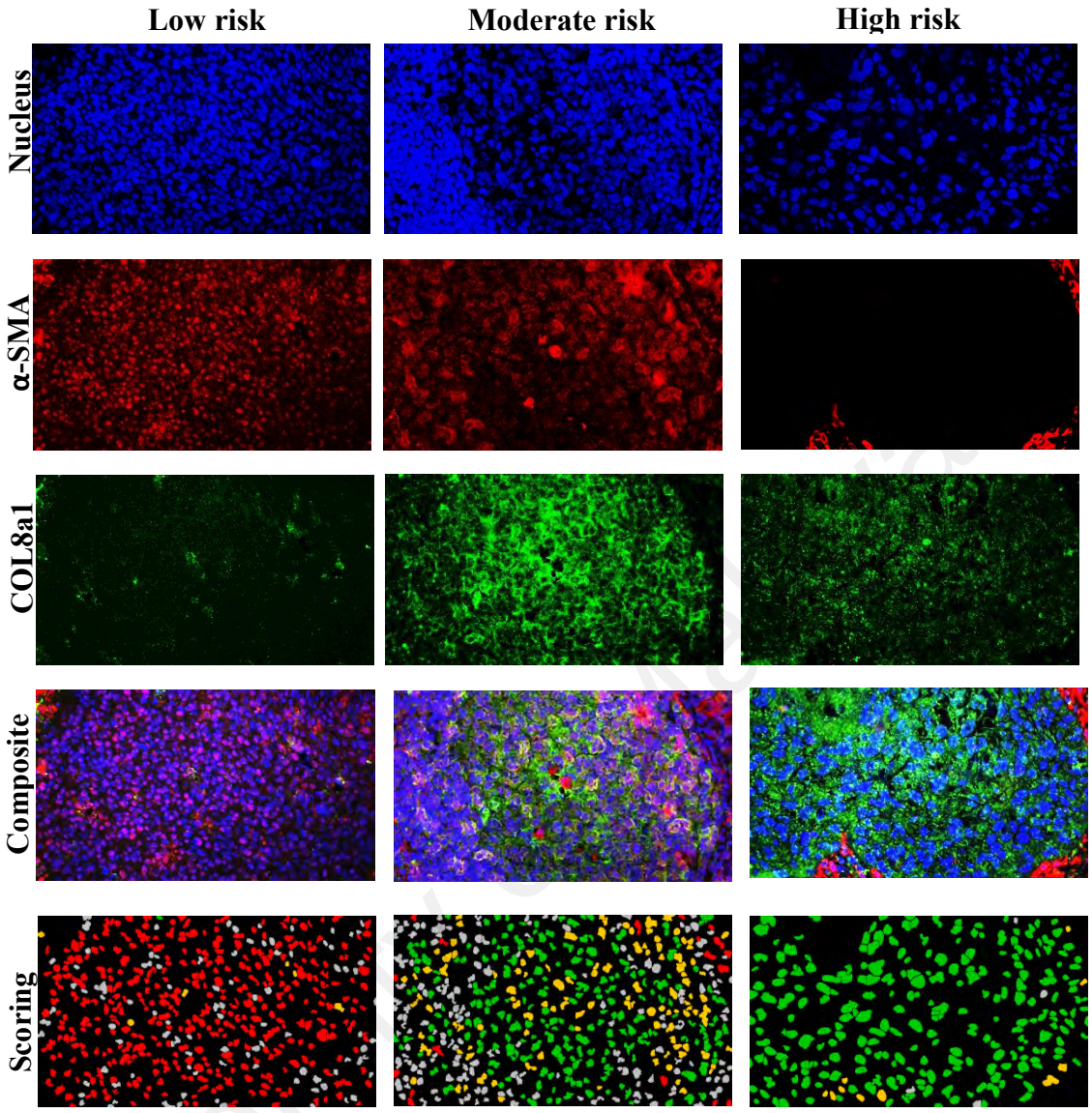

Figure 5.14: Multi-spectral unmixed composite imaging and quantitative digital scoring showed low expression of COL8a1 in tumours from low risk of death group compared to the counterparts.

Tissues were simultaneously multiplex-stained with the CAF marker, α-SMA (Cy3, red), COL8a1 (fluorescein, green) and DAPI (blue) nuclear counterstain. The scoring map of per-cell COL8a1 expression generated by the digital workflow algorithm. Cells positive for only α-SMA are displayed in red, cells positive for COL8a1 are displayed in green, cells double positive for α-SMA and COL8a1 are displayed in yellow, and cells negative for both markers are displayed in white.

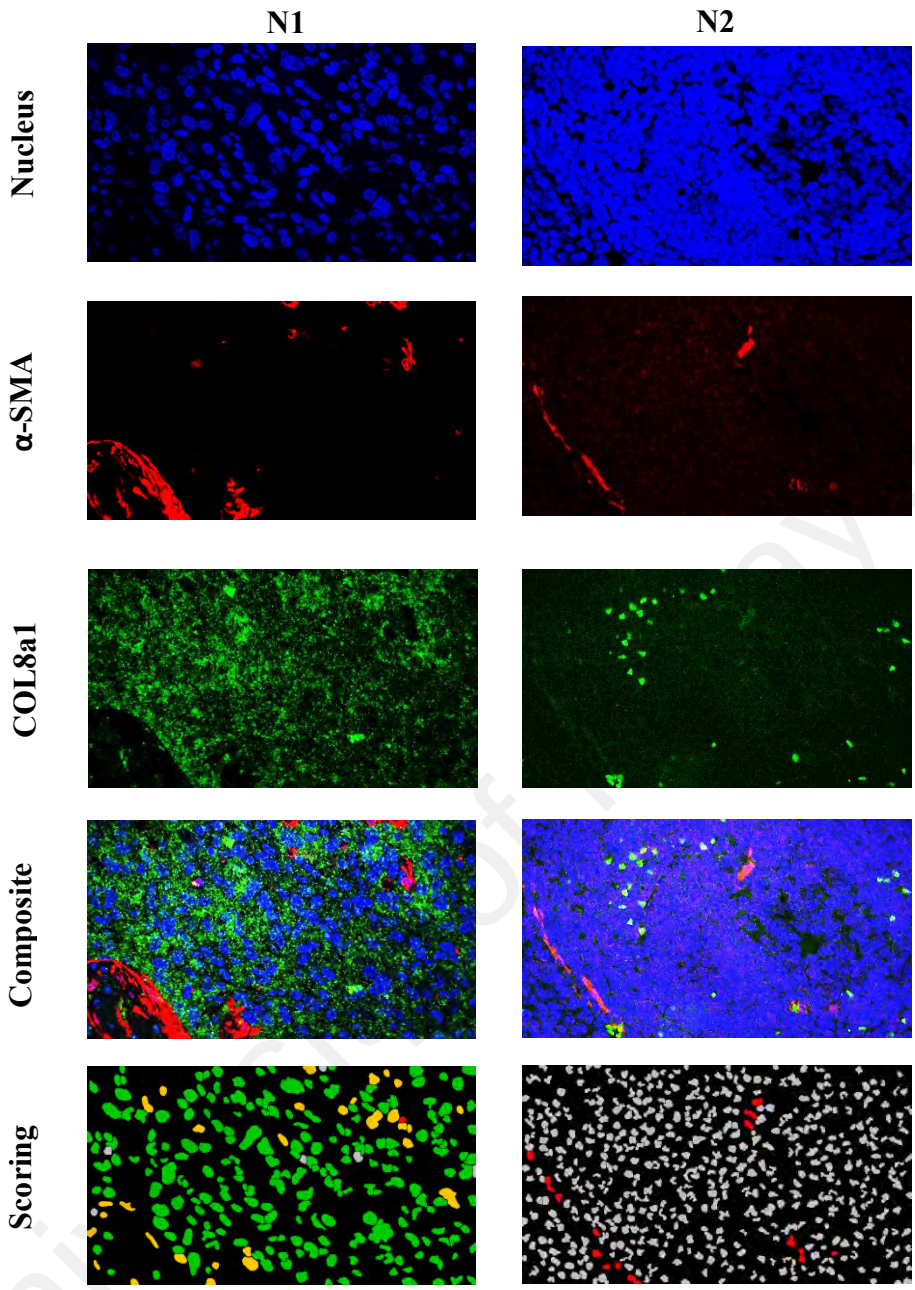

Figure 5.15: Multi-spectral unmixed composite imaging and quantitative digital scoring showed low expression of COL8a1 in tumours from N2 lymph node metastasis group compared to the counterparts.

Tissues were simultaneously multiplex-stained with CAF marker, α-SMA (Cy3, red), COL8a1 (fluorescein, green) and DAPI (blue) nuclear counterstain. The scoring map of per-cell COL8a1 expression generated by the digital workflow algorithm. Cells positive for only α-SMA are displayed in red, cells positive for COL8a1 are displayed in green, cells double positive for α-SMA and COL8a1 are displayed in yellow, and cells negative for both markers are displayed in white.

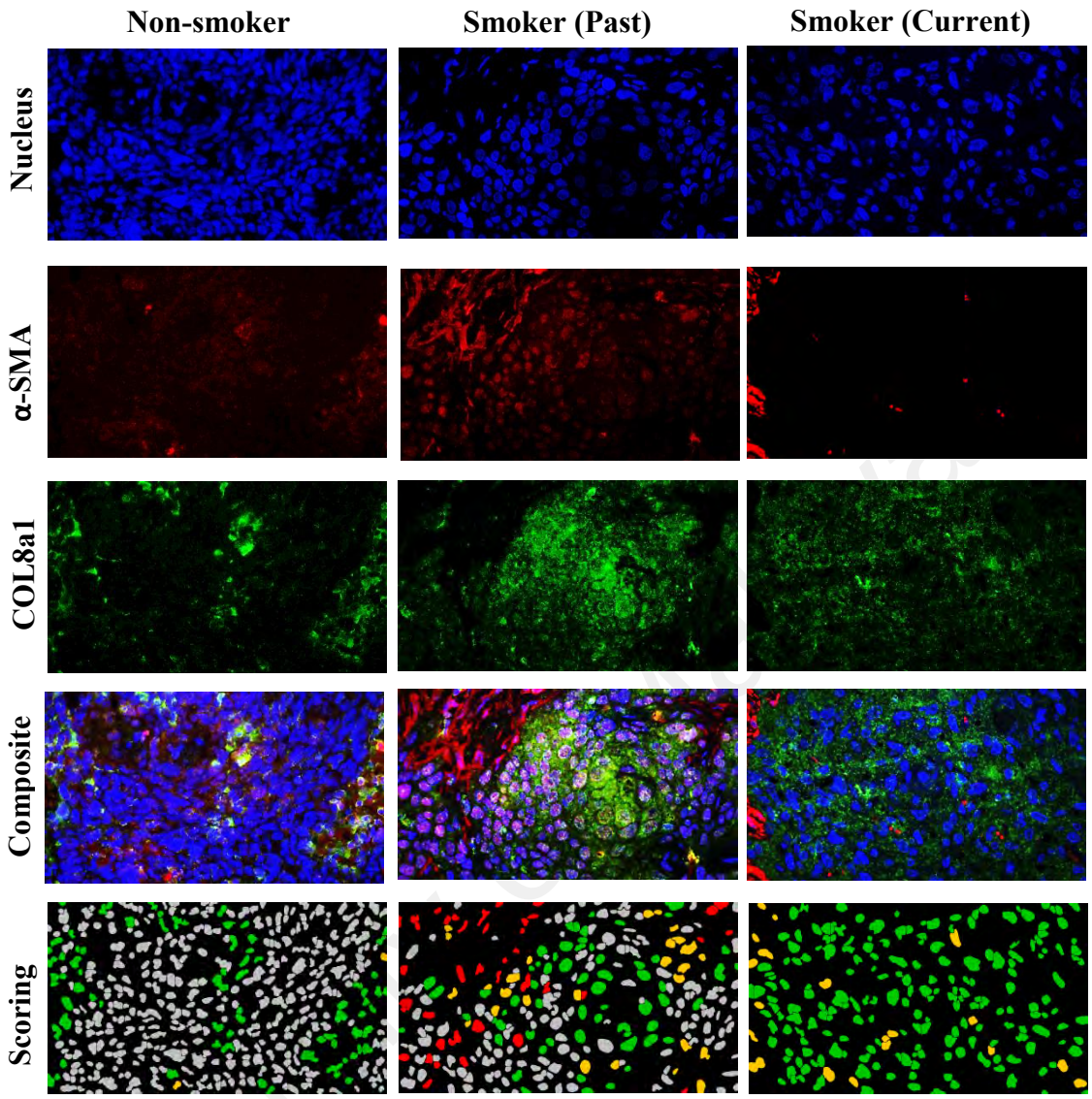

Figure 5.16: Multi-spectral unmixed composite imaging and quantitative digital scoring showed high expression of COL8a1 in tumours from smoker compared to non-smoker.

Tissues were simultaneously multiplex-stained with CAF marker, α-SMA (Cy3, red), COL8a1 (fluorescein, green) and DAPI (blue) nuclear counterstain. The scoring map of per-cell COL8a1 expression generated by the digital workflow algorithm. Cells positive for only α-SMA are displayed in red, cells positive for COL8a1 are displayed in green, cells double positive for α-SMA and COL8a1 are displayed in yellow, and cells negative for both markers are displayed in white.

The expression of COL8a1 in CAFs (co-expression with α-SMA) was also analysed for association and correlation with patients' socio-demographic and clinico-pathological parameters. The area under curve of ROC was above 0.6 (AUC= 0.646). The cut-off value determined by its maximum sensitivity and specificity (cut-off= 12850.67) of 63% sensitivity and 68.8% specificity was used for transforming the obtained COL8a1 expression in CAFs into low and high expression groups (Appendix F). Among the 55 cases, 22 cases (40% of total cohort) were assigned to both the low and high expression groups. 11 cases (20% of total cohort) were excluded for technical reasons after staining.

Similar to the expression of COL8a1 in tumour cells, crosstabs of the COL8a1 expression in CAFs demonstrated correlation of low expression with the low risk group (Spearman Correlation, p= 0.023; Univariate Logistic Regression, p= 0.048) and N2 lymph node metastasis (Univariate Logistic Regression, p= 0.045) whilst there was high expression of COL8a1 in CAFs with smoking behaviour (Univariate Logistic Regression, p= 0.049). However, similar to the expression of COL8a1 in tumour, none of these associations was significant after adjusted to the confounder factors in Multiple Logistic Regression (Table 5.5).

These quantitative results were in agreement with the observations from images captured by the multi-spectral unmixed composite imaging which showed differential expression of COL8a1 in which lower expression was showed in low risk (Figure 5.17) and N2 lymph node metastasis groups (Figure 5.18) while higher expression was showed in smoker in CAFs (Figure 5.19).

Table 5.5: Association and correlation between COL8a1 protein expression in CAFs with socio-demographic and clinico-pathological characteristics of OPSCC patients

Variables	Categories	COL8a1 expression in CAFs (n,% of total cohort)		Pearson Chi Square	Spearman	Univariate ANOVA	Univariate Logistic Regression			Multiple Logistic Regression		
		Low	High	p-value	p-value	p-value	Odd ratio	95% CI	p-value	Odd ratio	95% CI	p-value
Age	20-40	0.0	2.3	0.605	0.421	0.635	1.000	-	-	1.000	-	-
	41-50	18.2	9.1				0.000	(0.00,-)	1.000	0.000	(0.00,-)	1.000
	51-60	18.2	20.5				0.000	(0.00,-)	1.000	0.000	(0.00,-)	1.000
	61-70	11.4	15.9				0.000	(0.00,-)	1.000	0.000	(0.00,-)	1.000
	71-90	2.3	2.3				0.000	(0.00,-)	1.000	0.000	(0.00,-)	1.000
Gender	Male	31.8	31.8	1.000	1.000	1.000	1.000	-	-	1.000	-	-
	Female	18.2	18.2				1.000	(0.29,3.42)	1.000	0.060	(0.00,9.58)	0.277
p16	Neg	13.6	27.3	0.135	0.053	0.142	1.000	-	-	1.000	-	-
	Pos	34.1	22.7				0.333	(0.09,1.18)	0.089	0.000	(0.00,-)	0.998
	NA	2.3	0.0				0.000	(0.00,-)	1.000	-	-	-
HPVISH	Neg	29.5	36.4	0.450	0.312	0.469	1.000	-	-	1.000	-	-
	Pos	18.2	13.6				0.609	(0.17,2.21)	0.451	5.821	(0.04,817.10)	0.485
	NA	2.3	0.0				0.000	(0.00,-)	1.000	0.000	(0.00,-)	0.999
RNAscope	Neg	11.4	20.5	0.402	0.194	0.420	1.000	-	-	1.000	-	-
	Pos	27.3	22.7				0.463	(0.11,1.84)	0.273	6568597378	(0.00,-)	0.999
	NA	11.4	6.8				0.333	(0.06,2.02)	0.232	0.001	(0.00,74.67)	0.228
HPV Group	Neg	13.6	25.0	0.356	0.268	0.377	2.933	(0.66,13.09)	0.159	-	-	-
	Interm	15.9	13.6				1.371	(0.29,6.54)	0.692	-	-	-
	Pos	18.2	11.4				1.000	-	-	-	-	-
	NA	2.3	0.0				0.000	(0.00,-)	1.000	-	-	-
Risk Group	Low	25.0	11.4	0.141	*0.023	0.147	0.202	(0.04,0.98)	*0.048	-	-	-
	Moderate	13.6	18.2				0.593	(0.12,2.89)	0.517	5402.903	(0.45,6469E+4)	0.073
	High	9.1	20.5				1.000	-	-	1.000	-	-
	NA	2.3	0.0				0.000	(0.00,-)	1.000	-	-	-

Table 5.5, continued.

Variables	Categories	COL8a1 expression in CAFs (n,% of total cohort)		Pearson Chi Square	Spearman	Univariate ANOVA	Univariate Logistic Regression			Multiple Logistic Regression		
		Low	High	p-value	p-value	p-value	Odd ratio	95% CI	p-value	Odd ratio	95% CI	p-value
Smoking	No	25.0	11.4	0.079	0.113	0.082	1.000	-	-	1.000	-	-
	Yes	22.7	38.6				3.740	(1.01,13.92)	*0.049	0.239	(0.00,873.19)	0.732
	NA	2.3	0.0				0.000	(0.00,-)	1.000	1783.246	(0.00,-)	1.000
T stage	T1	25.0	36.4	0.301	0.131	0.316	1.000	-	-	1.000	-	-
	T2	20.5	11.4				0.382	(1.00,1.45)	0.158	0.595	(0.01,52.40)	0.820
	NA	4.5	2.3				0.344	(0.03,4.27)	0.406	16.993	(0.00,1438E+3)	0.625
N stage	N1	18.2	31.8	0.103	0.142	0.107	1.000	-	-	1.000	-	-
	N2	29.5	13.6				0.264	(0.07,0.97)	*0.045	0.026	(0.00,8.04)	0.212
	NA	2.3	4.5				1.143	(0.09,14.68)	0.918	1.842	(0.00,2232E+2)	0.919
Outcome	Alive	29.5	29.5	0.325	0.810	0.341	1.000	-	-	1.000	-	-
	Deceased	20.5	15.9				0.778	(0.22,2.72)	0.694	0.040	(0.00,2.77)	0.137
	NA	0.0	4.5				1615E+6	(0.00,-)	0.999	696940.421	(0.00,-)	1.000
Tos	0-6	38.6	47.7	0.110	0.099	0.114	1.000	-	-	1.000	-	-
	6-12	9.1	0.0				0.000	(0.00,-)	0.999	0.000	(0.00,-)	0.998
	NA	2.3	2.3				0.810	(0.05,13.92)	0.884	1.377E+20	(0.00,-)	0.999
Trfs	0-3	20.5	22.7	0.824	0.887	0.835	1.111	(0.33,3.80)	0.867	0.041	(0.00,1.88)	0.102
	3-9	25.0	25.0				1.000	-	-	1.000	-	-
	NA	4.5	2.3				0.500	(0.04,6.35)	0.593	0.000	(0.00,-)	0.999

Multivariate Logistic Regression analyses was applied to adjust the confounders of age, gender, p16, HPV DNA, RNAscope, risk group, smoking, T stage, N stage, outcome, Tos and Trfs.

Abbreviation: Neg, negative; Pos, positive; Interm, intermediate; NA, not available; Tos, overall survival time; Trfs, recurrence free survival time; *Indicated significant p-value ($p<0.05$).

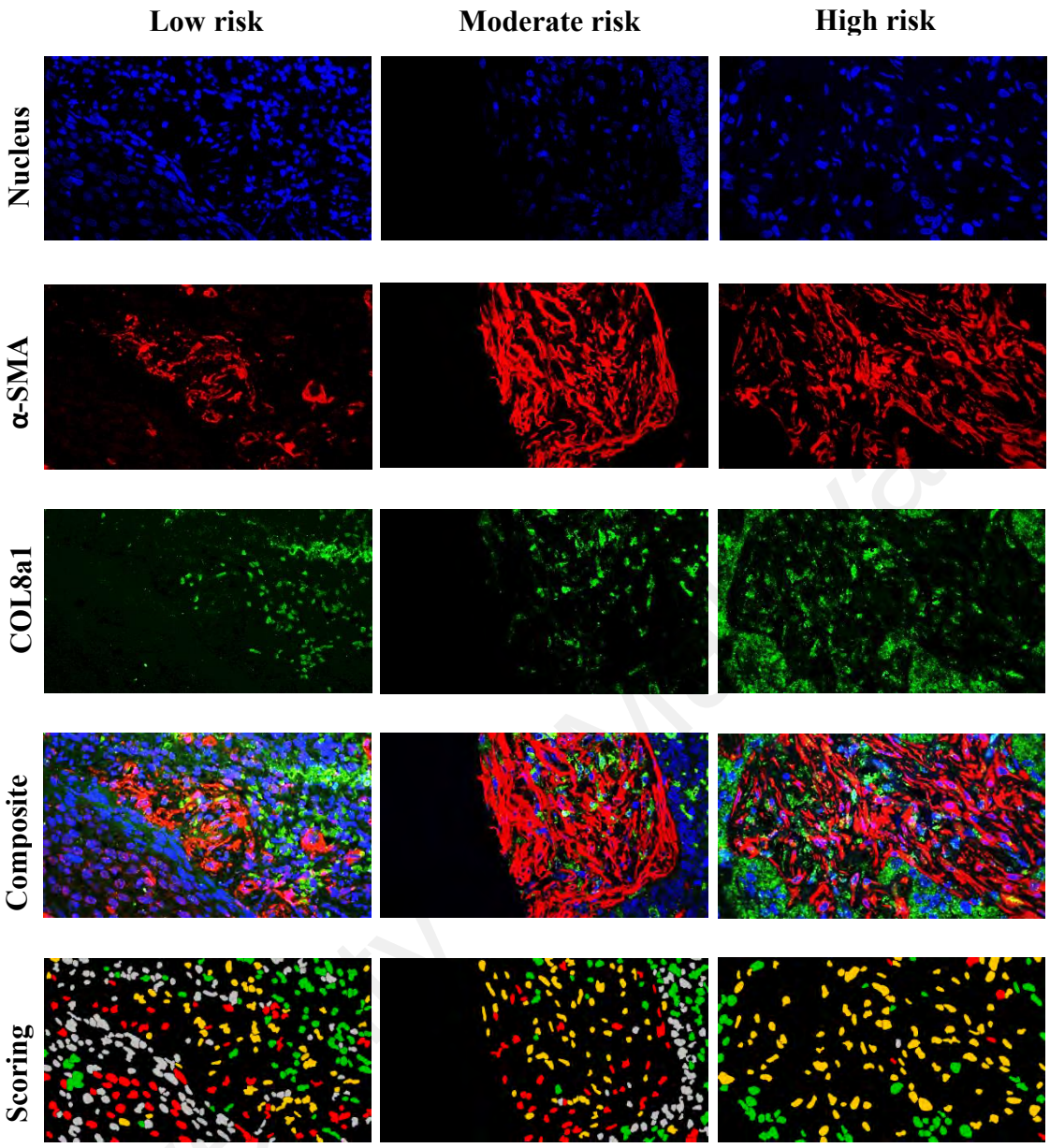

Figure 5.17: Multi-spectral unmixed composite imaging and quantitative digital scoring showed low expression of COL8a1 in CAFs from low risk of death group compared to the counterparts.

Tissues were simultaneously multiplex-stained with CAF marker, α-SMA (Cy3, red), COL8a1 (fluorescein, green) and DAPI (blue) nuclear counterstain. The scoring map of per-cell COL8a1 expression generated by the digital workflow algorithm. Cells positive for only α-SMA are displayed in red, cells positive for COL8a1 are displayed in green, cells double positive for α-SMA and COL8a1 are displayed in yellow, and cells negative for both markers are displayed in white.

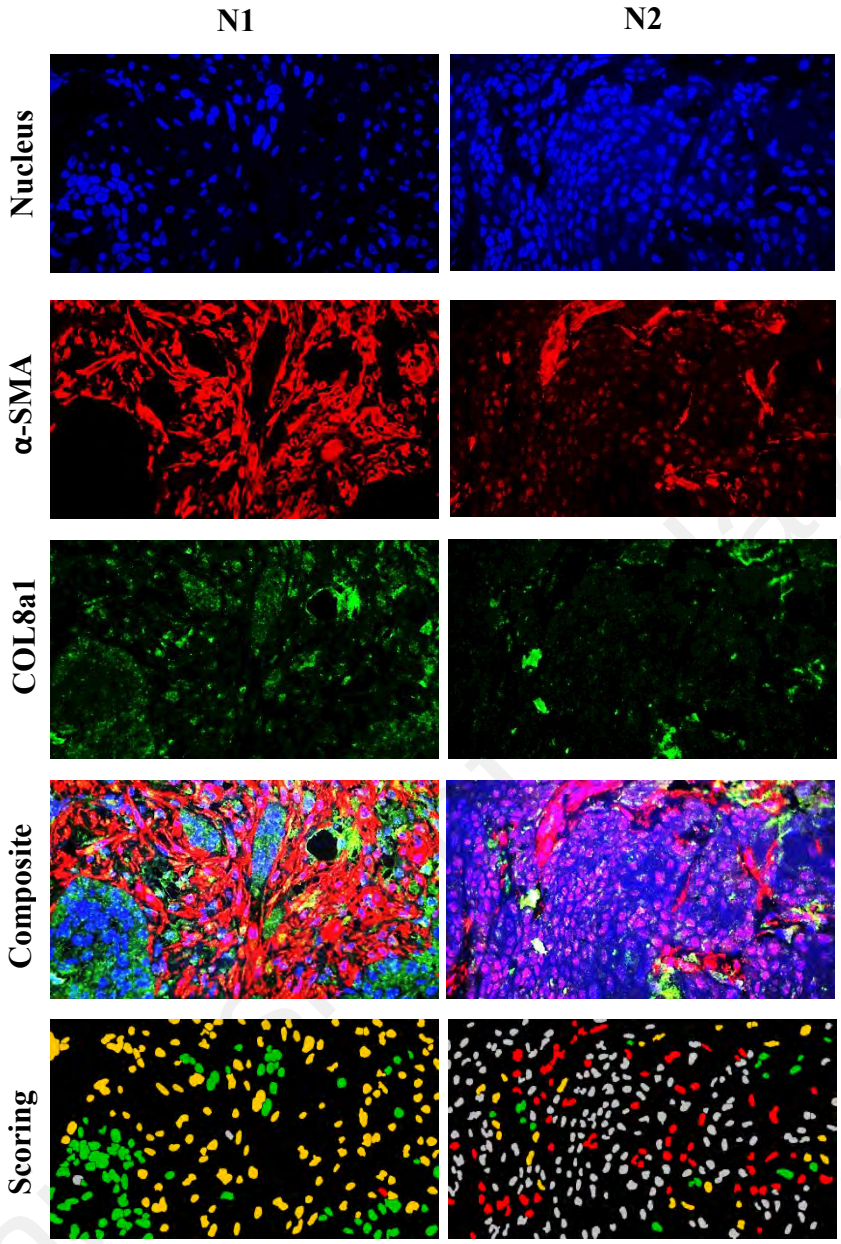

Figure 5.18: Multi-spectral unmixed composite imaging and quantitative digital scoring showed low expression of COL8a1 in CAFs from N2 lymph node metastasis group compared to the counterparts.

Tissues were simultaneously multiplex-stained with CAF marker, α-SMA (Cy3, red), COL8a1 (fluorescein, green) and DAPI (blue) nuclear counterstain. The scoring map of per-cell COL8a1 expression generated by the digital workflow algorithm. Cells positive for only α-SMA are displayed in red, cells positive for COL8a1 are displayed in green, cells double positive for α-SMA and COL8a1 are displayed in yellow, and cells negative for both markers are displayed in white.

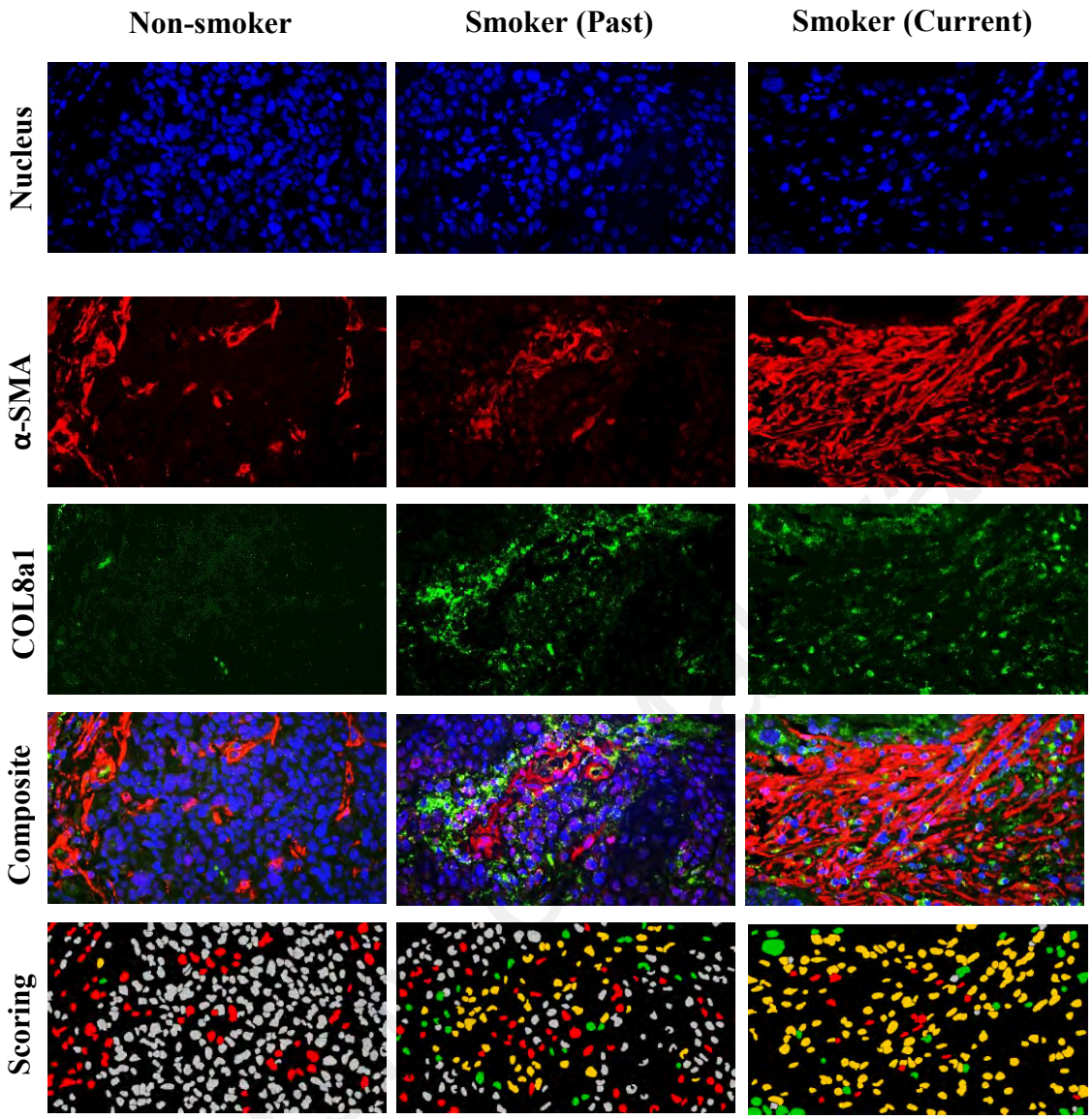

Figure 5.19: Multi-spectral unmixed composite imaging and quantitative digital scoring showed high expression of COL8a1 in CAFs from smoker compared to non-smoker.

Tissues were simultaneously multiplex-stained with CAF marker, α-SMA (Cy3, red), COL8a1 (fluorescein, green) and DAPI (blue) nuclear counterstain. The scoring map of per-cell COL8a1 expression generated by the digital workflow algorithm. Cells positive for only α-SMA are displayed in red, cells positive for COL8a1 are displayed in green, cells double positive for α-SMA and COL8a1 are displayed in yellow, and cells negative for both markers are displayed in white.

5.3.3.3 COL11a1 expression

The correlation between COL11a1 in tumour cells with socio-demographic and clinico-pathological parameters were examined. The area under curve of ROC was below 0.6 and the skewness divided by standard deviation was less than 1.98 (skewness/SD=2.20) indicating that the population was not normally distributed. Therefore, median (median= 214483.45) was used as the cut-off value in transforming COL11a1 expression scales into low and high expression groups. Among the 55 cases, equal numbers of 27 cases (49.1% of total cohort) were assigned to the low and high expression group respectively. The remaining 1 case (1.8% of total cohort) was excluded due to the tissues damage during staining.

The expression of COL11a1 in CAFs was also analysed for association and correlation with patients' socio-demographic and clinical-pathological parameters. The area under curve of ROC was below 0.6 and the skewness divided by standard deviation was less than 1.98 (skewness/SD=1.78) indicating that the population was normally distributed. Therefore, mean (mean= 107200.2852) was used as the cut-off value in transforming COL11a1 expression scales into low and high expression groups. Among the 55 cases, 28 cases (50.9% of total cohort) were assigned to low expression group, whilst 26 cases (47.3% of total cohort) were assigned to high expression group. The remaining 1 case (1.8% of total cohort) was excluded for technical reasons after staining.

Crosstabs of the COL11a1 expression in tumour and CAFs demonstrated no significant association and correlation of COL11a1 expression in tumour cells (Table 5.6) and CAFs (Table 5.7) with any of the socio-demographic and clinico-pathological parameters using Pearson Chi Square, Spearman Correlation, Univariate ANOVA, Univariate Logistic Regression and Multiple Logistic Regression analyses.

Table 5.6: Association and correlation between COL11a1 protein expression in tumour cells with socio-demographic and clinico-pathological characteristics of OPSCC patients

Variables	Categories	COL11a1 expression in tumour cells (n,% of total cohort)		Pearson Chi Square	Spearman	Univariate ANOVA	Univariate Logistic Regression			Multiple Logistic Regression		
		Low	High	p-value	p-value	p-value	Odd ratio	95% CI	p-value	Odd ratio	95% CI	p-value
Age	20-40	1.9	1.9	0.466	0.315	0.489	1.000	-	-	1.000	-	-
	41-50	7.4	16.7				2.250	(0.11,45.72)	0.598	4.124	(0.08,220.16)	0.485
	51-60	22.2	18.5				0.833	(0.05,15.09)	0.902	0.915	(0.02,37.37)	0.963
	61-70	16.7	9.3				0.556	(0.03,10.93)	0.699	0.379	(0.01,16.16)	0.613
	71-90	1.9	3.7				2.000	(0.05,78.25)	0.711	2.801	(0.03,270.82)	0.659
Gender	Male	33.3	33.3	1.000	1.000	1.000	1.000	-	-	1.000	-	-
	Female	16.7	16.7				1.000	(0.32,3.10)	1.000	0.381	(0.06,2.47)	0.311
p16	Neg	24.1	20.4	0.548	0.504	0.563	1.000	-	-	1.000	-	-
	Pos	25.9	27.8				1.266	(0.43,3.74)	0.670	4.190	(0.12,147.02)	0.430
	NA	0.0	1.9				19091E+5	(0.000,-)	1.000	-	-	-
HPVISH	Neg	35.2	33.3	0.598	0.493	0.613	1.000	-	-	1.000	-	-
	Pos	14.8	14.8				1.506	(0.33,3.41)	0.928	0.993	(0.13,7.49)	0.995
	NA	0.0	1.9				17052E+5	(0.00,-)	1.000	1602965417	(0.00,-)	1.000
RNAscope	Neg	18.5	16.7	0.782	0.598	0.792	1.000	-	-	1.000	-	-
	Pos	24.1	22.2				1.026	(0.31,3.39)	0.967	0.075	(0.00,4.08)	0.204
	NA	7.4	11.1				1.667	(0.35,7.88)	0.519	0.241	(0.01,4.21)	0.330
HPV Group	Neg	24.1	22.2	0.506	0.614	0.526	1.477	(0.38,5.79)	0.576	-	-	-
	Interm	11.1	16.7				2.400	(0.52,11.0)	0.259	-	-	-
	Pos	14.8	9.3				1.000	-	-	-	-	-
	NA	0.0	1.9				25847E+5	(0.00,-)	1.000	-	-	-
Risk Group	Low	13.0	22.2	0.414	0.452	0.433	1.959	(0.49,7.77)	0.339	-	-	-
	Moderate	20.4	14.8				0.831	(0.21,3.25)	0.790	0.711	(0.06,8.92)	0.791
	High	14.8	13.0				1.000	-	-	1.000	-	-
	NA	1.9	0.0				0.000	(0.00,-)	1.000	-	-	-

Table 5.6, continued.

Variables	Categories	COL11a1 expression in tumour cells (n,% of total cohort)		Pearson Chi Square	Spearman	Univariate ANOVA	Univariate Logistic Regression			Multiple Logistic Regression		
		Low	High	p-value	p-value	p-value	Odd ratio	95% CI	p-value	Odd ratio	95% CI	p-value
Smoking	No	13.0	22.2	0.248	0.124	0.259	1.000	-	-	1.000	-	-
	Yes	35.2	27.8				0.461	(0.15,1.46)	0.187	0.579	(0.03,12.03)	0.724
	NA	1.9	0.0				0.000	(0.00,-)	1.000	0.000	(0.00,-)	1.000
T stage	T0	0.0	1.9	0.207	0.641	0.216	1.000	-	-	1.000	-	-
	T1	31.5	29.6				0.000	(0.00,-)	1.000	0.000	(0.00,-)	1.000
	T2	13.0	18.5				0.000	(0.00,-)	1.000	0.000	(0.00,-)	1.000
	NA	5.6	0.0				0.000	(0.00,-)	0.999	0.000	(0.00,-)	0.999
N stage	N1	27.8	27.8	0.827	0.907	0.835	1.000	-	-	1.000	-	-
	N2	18.5	20.4				1.100	(0.36,3.36)	0.867	2.064	(0.28,15.08)	0.475
	NA	3.7	1.9				0.500	(0.04,6.12)	0.588	1.043	(0.01,81.49)	0.985
Outcome	Alive	24.1	35.2	0.250	0.102	0.261	1.000	-	-	1.000	-	-
	Deceased	22.2	13.0				0.399	(0.12,1.29)	0.124	0.555	(0.09,3.57)	0.535
	NA	3.7	1.9				0.342	(0.03,4.18)	0.401	0.348	(0.01,21.65)	0.617
Tos	0-6	40.7	40.7	0.788	0.950	0.798	1.000	-		1.000	-	-
	6-12	7.4	5.6				0.750	(0.15,3.75)	0.726	0.044	(0.00,1.29)	0.070
	NA	1.9	3.7				2.000	(0.17,23.70)	0.583	0.019	(0.00,-)	1.000
Trfs	0-3	22.2	20.4	0.943	0.942	0.948	1.000	-	-	1.000	-	-
	3.1-6	16.7	20.4				1.333	(0.40,4.44)	0.639	2.502	(0.45,13.98)	0.296
	6.1-9	7.4	5.6				0.818	(0.15,4.51)	0.818	-	-	-
	NA	3.7	3.7				1.091	(0.13,9.12)	0.936	29.039	(0.00,-)	1.000

Multivariate Logistic Regression analyses was applied to adjust the confounders of age, gender, p16, HPV DNA, RNAscope, risk group, smoking, T stage, N stage, outcome, Tos and Trfs.

Abbreviation: Neg, negative; Pos, positive; Interm, intermediate; NA, not available; Tos, overall survival time; Trfs, recurrence free survival time; *Indicated significant p-value ($p<0.05$).

Table 5.7: Association and correlation between COL11a1 protein expression in CAFs with socio-demographic and clinico-pathological characteristics of OPSCC patients

Variables	Categories	COL11a1 expression in CAFs (n,% of total cohort)		Pearson Chi Square	Spearman	Univariate ANOVA	Univariate Logistic Regression			Multiple Logistic Regression		
		Low	High	p-value	p-value	p-value	Odd ratio	95% CI	p-value	Odd ratio	95% CI	p-value
Age	20-40	1.9	1.9	0.628	0.829	0.489	1.000	-	-	1.000	-	-
	41-50	9.3	14.8				1.600	(0.08,31.77)	0.758	4.838	(0.09,254.51)	0.436
	51-60	25.9	14.8				0.571	(0.03,10.44)	0.706	1.203	(0.03,46.74)	0.921
	61-70	13.0	13.0				1.000	(0.05,19.36)	1.000	1.466	(0.04,60.84)	0.841
	71-90	1.9	3.7				2.000	(0.05,78.25)	0.711	5.759	(0.06,564.87)	0.454
Gender	Male	35.2	31.5	0.847	0.851	1.000	0.895	(0.29,2.78)	0.847	1.000	-	-
	Female	16.7	16.7				1.000	-	-	0.586	(0.12,2.90)	0.512
p16	Neg	25.9	18.5	0.443	0.335	0.563	1.000	-	-	1.000	-	-
	Pos	25.9	27.8				1.500	(0.50,4.46)	0.466	23.910	(0.65,885.66)	0.085
	NA	0.0	1.9				2261664810	(0.00,-)	1.000	-	-	-
HPVISH	Neg	37.0	31.5	0.557	0.582	0.613	1.000	-	-	1.000	-	-
	Pos	14.8	14.8				1.176	(0.36,3.80)	0.786	0.608	(0.09,4.14)	0.611
	NA	0.0	1.9				1900558666	(0.00,-)	1.000	2781408156	(0.00,-)	1.000
RNAscope	Neg	18.5	16.7	0.991	0.904	0.792	1.000	-	-	1.000	-	-
	Pos	24.1	22.2				1.026	(0.31,3.39)	0.967	0.068	(0.00,2.76)	0.155
	NA	9.3	9.3				1.111	(0.24,5.14)	0.893	0.148	(0.01,2.14)	0.161
HPV Group	Neg	25.9	20.4	0.461	0.797	0.526	1.257	(0.32,4.94)	0.743	-	-	-
	Interm	11.1	16.7				2.400	(0.52,10.99)	0.259	-	-	-
	Pos	14.8	9.3				1.000	-	-	-	-	-
	NA	0.0	1.9				2584759786	(0.00,-)	1.000	-	-	-
Risk Group	Low	16.7	18.5	0.777	0.914	0.433	1.270	(0.33,4.93)	0.730	-	-	-
	Moderate	18.5	16.7				1.029	(0.27,3.99)	0.968	0.690	(0.07,7.03)	0.754
	High	14.8	13.0				1.000	-	-	1.000	-	-
	NA	1.9	0.0				0.000	(0.00,-)	1.000	-	-	-

Table 5.7, continued.

Variables	Categories	COL11a1 expression in CAFs (n,% of total cohort)		Pearson Chi Square	Spearman	Univariate ANOVA	Univariate Logistic Regression			Multiple Logistic Regression		
		Low	High	p-value	p-value	p-value	Odd ratio	95% CI	p-value	Odd ratio	95% CI	p-value
Smoking	No	16.7	18.5	0.578	0.528	0.259	1.000	-	-	1.000	-	-
	Yes	33.3	29.6				0.800	(0.26,2.46)	0.697	1.547	(0.08,29.55)	0.772
	NA	1.9	0.0				0.000	(0.00,-)	1.000	0.000	(0.00,-)	1.000
T stage	T0	1.9	0.0	0.259	0.662	0.216	1.000	-	-	1.000	-	-
	T1	29.6	31.5				17164E+5	(0.00,-)	1.000	2171E+5	(0.00,-)	1.000
	T2	14.8	16.7				18174E+5	(0.00,-)	1.000	2001E+5	(0.00,-)	1.000
	NA	5.6	0.0				1.000	(0.00,-)	1.000	0.020	(0.00,-)	1.000
N stage	N1	29.6	25.9	0.802	0.907	0.835	1.000	-	-	1.000	-	-
	N2	18.5	20.4				1.257	(0.41,3.84)	0.688	1.499	(0.25,9.12)	0.660
	NA	3.7	1.9				0.571	(0.05,7.00)	0.662	2.675	(0.05,155.62)	0.635
Outcome	Alive	29.6	29.6	0.855	0.693	0.261	1.000	-	-	1.000	-	-
	Deceased	18.5	16.7				0.900	(0.29,2.80)	0.856	1.725	(0.29,10.16)	0.547
	NA	3.7	1.9				0.500	(0.04,6.08)	0.587	0.433	(0.01,16.33)	0.651
Tos	0-6	40.7	40.7	0.461	0.649	0.798	1.000	-	-	1.000	-	-
	6-12	9.3	3.7				0.400	(0.07,2.29)	0.303	0.130	(0.01,2.78)	0.192
	NA	1.9	3.7				2.000	(0.17,23.70)	0.583	0.221	(0.00,-)	1.000
Trfs	0-3	20.4	22.2	0.739	0.497	0.948	1.000	-	-	1.000	-	-
	3.1-6	18.5	18.5				0.917	(0.28,3.04)	0.887	1.271	(0.27,5.94)	0.760
	6.1-9	9.3	3.7				0.367	(0.06,2.29)	0.283	-	-	-
	NA	3.7	3.7				0.917	(0.11,7.67)	0.936	4.114	(0.00,-)	1.000

Multivariate Logistic Regression analyses was applied to adjust the confounders of age, gender, p16, HPV DNA, RNAscope, risk group, smoking, T stage, N stage, outcome, Tos and Trfs.

Abbreviation: Neg, negative; Pos, positive; Interm, intermediate; NA, not available; Tos, overall survival time; Trfs, recurrence free survival time; *Indicated significant p-value ($p<0.05$).

5.3.4 Kaplan-Meier analysis of DDR1, COL8a1 and COL11a1 expression with patient survival

Survival data were available for 53 of the 55 patients. The follow-up period ranged from 3-140 months with a mean of 41.47 months and a median of 38 months. The DDR1 scores from fluorescence multiplex staining were transformed and recoded into low and high expression of DDR1 by using the cut-off value (cut-off= 104 126.455) obtained from ROC curve with the highest value of specificity and sensitive (AUC= 0.622, 80% sensitivity and 55.6% specificity) based on patients' outcome whether alive or deceased (Appendix G). Among the 53 patients, 23 patients (43.4% of total cohort) had low expression of DDR1, whilst 30 patients (56.6% of total cohort) had high DDR1 expression. At last follow-up, 20 patients out of total 53 total patients (37.7% of total cohort) were dead, whilst 33 patients (62.3% of total cohort) were alive. More specifically, within the low DDR1 expression group, 4 patients (17.4% within low expression) were dead whilst the remaining 19 patients (82.6% within low expression) were alive and within the high DDR1 expression group, 16 patients (53.3% within high expression) were dead whilst 14 patients (46.7% within high expression) were alive. High DDR1 expression showed the trend of lower overall survival compared to low DDR1 expression. Using Kaplan-Meir Survival Analysis, the Log-Rank (Mantel Cox) (p= 0.022), Breslow (Generalised Wilcoxon) (p= 0.020) and Tarone-Ware (p= 0.017) overall comparisons were strongly significant (Figure 5.20). Patients with high DDR1 expression also have a significantly lower 5-years survival rate (5yr survival rate= 33%) than that of patients with low DDR1 expression (5yr survival rate= 78%). Importantly, the Cox Regression Multivariate model revealed that DDR1 remained significantly (p= 0.049) associated with survival outcome after adjusted for other major risk factors that are associated with OPSCC survival, such as age, HPV DNA, p16, HPV RNAscope, risk of

death group, smoking habit, N stage, T stage, overall survival time, and recurrence free survival time (Table 5.8). Hence, high DDR1 expression was significantly associated with poor overall survival of OPSCC patients.

In addition, the association of survival time with COL8a1 expression in tumour cells (median= 8913.26) and CAFs (median= 13202); and COL11a1 in tumour (median= 209017.20) and CAFs (mean= 107248.1182, skewness/ SD= 1.82) were analysed using Log-Rank (Mantel Cox), Breslow (Generalised Wilcoxon) and Tarone-Ware tests. The survival measurement revealed that patients with higher expression of COL8a1 in tumour cells and CAFs have lower survival rate, but this was not significant under Kaplan-Meier analyses. Patients with higher and lower expression of COL11a1 in tumour cells have no difference in terms of overall survival rate under Kaplan-Meier analyses. The 5-years survival rate measurement also showed that patients with higher expression of COL11a1 in CAFs have lower survival rate than that of patients with lower expression of COL11a1, but the difference was not significant under the Kaplan-Meier analyses.

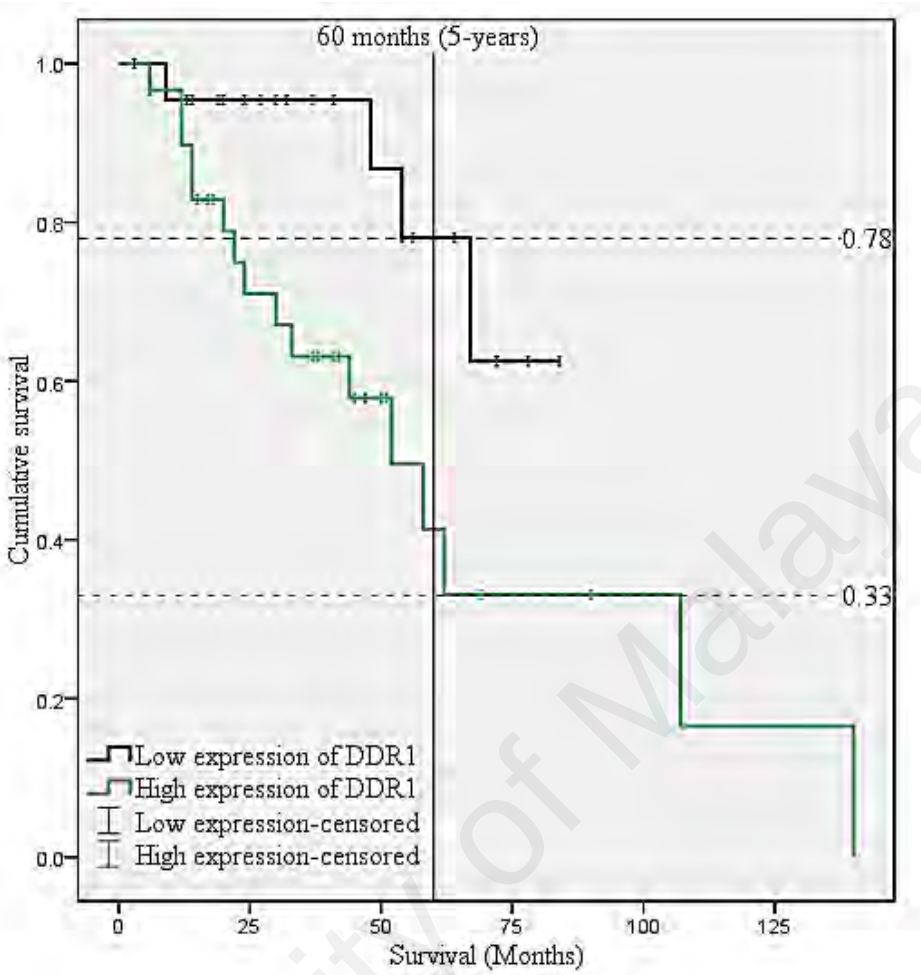

	p-value
Log Rank (Mantel-Cox)	*0.022
Breslow (Generalized Wilcoxon)	*0.020
Tarone-Ware	*0.017

Figure 5.20: The Kaplan-Meir plot for overall survival of low and high DDR1 expression in OPSCC patients.

Patients with high DDR1 expression have lower 5-years survival rate (33%) than that of patients with low DDR1 expression (78%). Strong significance was found between the expression of DDR1 with the patients overall survival in Log Rank (Mantel-Cox) (p=0.022), Breslow (Generaliased Wilcoxon) (p=0.020) and Tarone-Ware test (p=0.017). Blue line represents low DDR1 expression whilst green line represents high DDR1 expression. Crosses indicate censored patients. * denotes significant p-value (p<0.05).

Table 5.8: Multivariate Cox regression analysis of overall survival for DDR1 expression

Variables	Category	Multivariate Cox Regression		
		HRR	95% CI	p-value
DDR1 protein expression	Low	1.000	-	-
	High	3.444E+16	(1.226,9.670E+32)	*0.049
Age group	20-40	1.000	-	-
	41-50	5.801E+33	(0.00,1.470E+088)	0.224
	51-60	2.909E+21	(0.00,9.106E+061)	0.299
	61-70	56831133.21	(0.00,1.391E+22)	0.291
	71-90	1.271E+25	(0.00,1.932E+068)	0.255
HPV DNA ISHHR	Neg	1.000	-	-
	Pos	0.000	(0.00,28365218.96)	0.475
	NA	5.768E+32	(0.00,2.579E+079)	0.169
p16	Neg	1.000	-	-
	Pos	8.534	(0.00,1.599E+20)	0.925
	NA	-	-	-
HPV RNAscope	Neg	1.000	-	-
	Pos	69.522	(0.00,7.751E+15)	0.797
	NA	0.000	(0.00,10621165.83)	0.316
Smoking	No	0.000	(0.00,5381135286)	0.154
	Yes	1.000	-	-
	NA	-	-	-
Gender	Male	1.000	-	-
	Female	0.000	(0.00,115702.312)	0.257
	NA	-	-	-

Table 5.8, continued.

Variables	Category	Multivariate Cox Regression		
		HRR	95% CI	p-value
Risk group	Low	1.000	-	-
	Moderate	0.000	(0.00,1.938)	0.055
	High	-	-	-
	NA	-	-	-
Tstage	T0	1.000	-	-
	T1	0.000	(0.00,2.922E+35)	0.613
	T2	0.000	(0.00,9.863E+038)	0.708
	NA	1299.961	(0.00,2.637E+044)	0.883
Nstage	N1	1.000	-	-
	N2	33.036	(0.001,943281.571)	0.504
	NA	0.000	(0.00,4.371)	0.064
Tos	0-6	5.938E+22	(0.00,3.957E+053)	0.148
	6-12	1.000	-	-
	NA	-	-	-
Trfs	0-3	4.946E+26	(0.00,2.906E+064)	0.166
	3.1-9	1.000	-	-
	NA	3.177E+13	(0.00,1.808E+042)	0.357

Multivariate logistic regression analyses was applied to adjust the confounders of age, gender, p16, HPV DNA, RNAscope, risk group, smoking, T stage, N stage, Tos and Trfs

Abbreviation: Neg, negative; Pos, positive; Interm, intermediate; NA, not available; Tos, overall survival time; Trfs, recurrence free survival time; HRR= Hazard rate ratio; *Indicated significant p-value ($p<0.05$).

5.4 Summary

This study examined the expression of DDR1, COL8a1 and COLL11a1 in OPSCC tissues using Opal Multiplex Immunohistochemistry. Firstly, the expression of COL11a1 and DDR1 was examined in OPSCCs on the Astellas PredicTr Array 4 and their expression correlated with p16 expression alone, followed by combined status of p16 and HPV DNA. Co-expression of both proteins was detected in tumours. Significantly higher expression of COL11a1 was found in p16-negative OPSCCs. In addition, all the tumours that showed high single cell co-expression of DDR1 and COL11a1 were p16-positive, whilst low single cell co-expression of DDR1 and COL11a1 was significantly associated with p16-negative tumour when samples were stratified by p16 HPV surrogate marker alone. Similarly, the low single cell co-expression of DDR1 and COL11a1 was significantly associated with p16-negative/ HPV DNA-negative tumours when samples were stratified by both p16 and HPV DNA status. No significant difference or association of DDR1 expression was found across with groups.

The expression of DDR1, COL8a1 and COL11a1 was examined in an independent cohort of OPSCC tissues and correlations made with the socio-demographic and clinico-pathological characteristics of the tumours. DDR1 was detected in the malignant epithelium and high expression of DDR1 was found to be significantly associated with non-smokers, and patients within the moderate and high risk of death groups. Further, COL8a1 and COL11a1 were detected in both tumours and CAFs. Low expression of COL8a1 in tumours and CAFs was significantly associated with the low risk of death group and non-smokers, whilst high expression was significantly associated with regional lymph node N1. No significant associations were found between COL11a1 expression in tumours or CAFs with the clinico-pathological parameters.

Lastly, significantly a lower survival rate was found in patients whose tumours highly expressed DDR1. Higher expression of COL8a1 in tumours and CAFs was also observed in patients with a lower survival rate, but the association was not statistically significant. There was no significant association of COL11a1 with patient survival.

CHAPTER 6: THE EXPRESSION OF COLLAGENS AND DDR1 IN OSCC

6.1 Introduction

The present study is the first to examine the expression of DDR1 and two of its ligands, COL8a1 and COL11a1, in HNSCC. In the previous chapter, DDR1 as well as COL8a1 and COL11a1 were shown to be expressed in OPSCC. To date, there are no published data describing the expression of these three proteins in another HNSCC entity, OSCC. The results of Chapter 4 demonstrated that DDR1 was up-regulated at both the mRNA and protein levels in OSCC cell lines and primary tissues. Notably, The Cancer Genome Atlas (TCGA) data also implies that DDR1 is found to be highly expressed at the mRNA level in OSCC. Therefore, the present study was extended to examine the expression of DDR1, COL8a1 and COL11a1 in a Malaysian OSCC cohort and to investigate potential clinical correlation and associations, including risk and prognosis factors, clinico-pathological parameters and patient survival.

6.2 Study design and cohort details

A total of 44 biopsies from OSCC patients were obtained from the Malaysian Oral Cancer Database and Tissue Bank System (MOCDTBS) managed by the Oral Cancer Research and Coordinating Centre (OCRCC), University of Malaya. The socio-demographic and clinico-pathological information, including age, gender, risk factor exposure, stage, pattern of invasion and metastasis, and patient survival are shown in Table 6.1.

Opal multiplex immunofluorescence staining was performed and the staining intensities were digitally scored using the computer-assisted Metamorph Pathology Analysis Software and validated by a head and neck pathologist, Dr. Anand Ramanathan

(OCRCC, University of Malaya). The H-scores were then used to determine potential clinical associations and/or correlations.

Table 6.1: Socio-demographic and clinico-pathological parameters of OSCC samples

Parameters	Characteristic	N=44 (%)	Parameters	Characteristic	N=44 (%)	Parameters	Characteristic	N=44 (%)
Age	30-50	9 (20.5)	Betel chewing status	No	15 (34.1)	Extent of the primary tumour	T1	6 (13.6)
	51-70	25 (56.8)		Yes	20 (45.5)		T2	12 (27.3)
	71-90	10 (22.7)		No record	9 (20.5)		T3	9 (20.5)
Gender	Male	13 (29.5)	Stage	I	2 (4.5)		T4	14 (31.8)
	Female	31 (70.5)		II	11 (25.0)		No record	3 (6.8)
Ethnic	Malay	8 (18.2)		III	0 (0.0)	Extent of regional lymph node metastasis	N0	13 (29.5)
	Chinese	9 (20.5)		IV	26 (59.1)		N1	5 (11.4)
	Indian	27 (61.4)		V	0 (0.0)		N2	1 (2.3)
Smoking	No	29 (65.9)		No record	5 (11.4)		N2B	18 (40.9)
	Yes	3 (6.8)	Vascular invasion	No	26 (59.1)		N2C	1 (2.3)
	No record	12 (27.3)		Yes	14 (31.8)		N3	1 (2.3)
Survival	Alive	8 (18.2)		No record	4 (9.1)		No record	5 (11.4)
	Deceased	15 (34.1)	Perineural invasion	Yes	14 (31.8)	Extra-capsular spread	Yes	14 (31.8)
	Not follow up	2 (4.5)		No	28 (63.6)		No	28 (63.6)
	No record	19 (43.2)		No record	2 (4.5)		No record	2 (4.5)

Table 6.1, continued.

Parameters	Characteristic	N=44 (%)	Parameters	Characteristic	N=44 (%)	Parameters	Characteristic	N=44 (%)
Drinking	No	30 (68.2)	Bone invasion	Yes	15 (34.1)	Skip metastasis	Yes	9 (20.5)
	Yes	2 (4.5)		No	22 (50.0)		No	33 (75)
	No record	12 (27.3)		No record	7 (15.9)		No record	2 (4.5)
Grade	Well	11 (25.0)	Survival months	0-20	21 (47.7)	Tumour depth	1-10mm	15 (34.1)
	Moderate	27 (61.4)		21-40	2 (4.5)		11-20mm	8 (18.2)
	Moderate to poor	1 (2.3)		41-70	2 (4.5)		21-30mm	4 (9.1)
	Poor	3 (6.8)		No record	19 (43.2)		31-40mm	2 (4.5)
	No record	2 (4.5)					No record	15 (34.1)
Invasive	Non-cohesive	42 (95.5)						
	Cohesive	1 (2.3)						
	No record	1 (2.3)						

Abbreviations: N0 (no regional lymph node metastasis); N1 (metastasis in single ipsilateral lymph node, ≤3cm); N2 (metastasis in single ipsilateral lymph node, 3-6cm); N2B (metastasis in single ipsilateral lymph node, ≤6cm); N2C (metastasis in bilateral/ contralateral lymph node, ≤6cm); N3 (metastasis in lymph node >6cm); T1 (tumour ≤2cm); T2 (tumour 2-4cm); T3 (tumour >4cm); T4 (tumour invades adjacent structures such as tongue, skin of neck and through cortical bone).

6.3 Expression of DDR1 in OSCCs and association with socio-demographic and clinico-pathological parameters

The OSCC tissue sections were first double-stained for Cytokeratin AE1/ AE3 and DDR1. Five random hotspots of each case were visualised and the expression at the cellular level were scored quantitatively using Metamorph Pathology Analysis Software. The results showed that DDR1 was expressed in all OSCC malignant tissues examined. Strong positive staining was found to be cytoplasmic and membranous (Figure 6.1).

The analyses of the expression of DDR1 in Cytokeratin AE1/ AE3 positive cells for their association and correlation with socio-demographic and clinico-pathological parameters is shown in Table 6.2. The area under curve of a Receiver Operating Characteristic Curve (ROC) was above 0.6 (AUC= 0.726). Therefore, the distinct value (cut-off= 89189) obtained from the highest specificity and sensitivity ROC (100% sensitivity and 46.2% specificity) was used in transforming the obtained DDR1 scoring into low and high expression groups (Appendix H). Among the 44 cases, 18 cases (40.9% of total cohort) were assigned to the low expression group, whilst 24 cases (54.5% of total cohort) fell into the high expression group. 2 cases (4.5% of total cohort) were excluded due to defects during staining.

Cross-tabulation of the DDR1 expression demonstrated higher expression in females, Indians, non-smokers, non-drinkers, betel quid chewers, moderate histological grade, tumour depth of 1-10mm, no vascular invasion, no perineural invasion and no bone invasion, no extracapsullar spread, no skip metastasis and higher expression was found in the majority of deceased cases. However, no statistically significant associations and/or correlations were found when the relationship between the DDR1 staining with the socio-demographic and clinico-pathological parameters when tested by statistical approaches

including Pearson Chi Square, Spearman Correlation comparisons, Univariate ANOVA, Univariate Logistic Regression and Multiple Logistic Regression (Table 6.2).

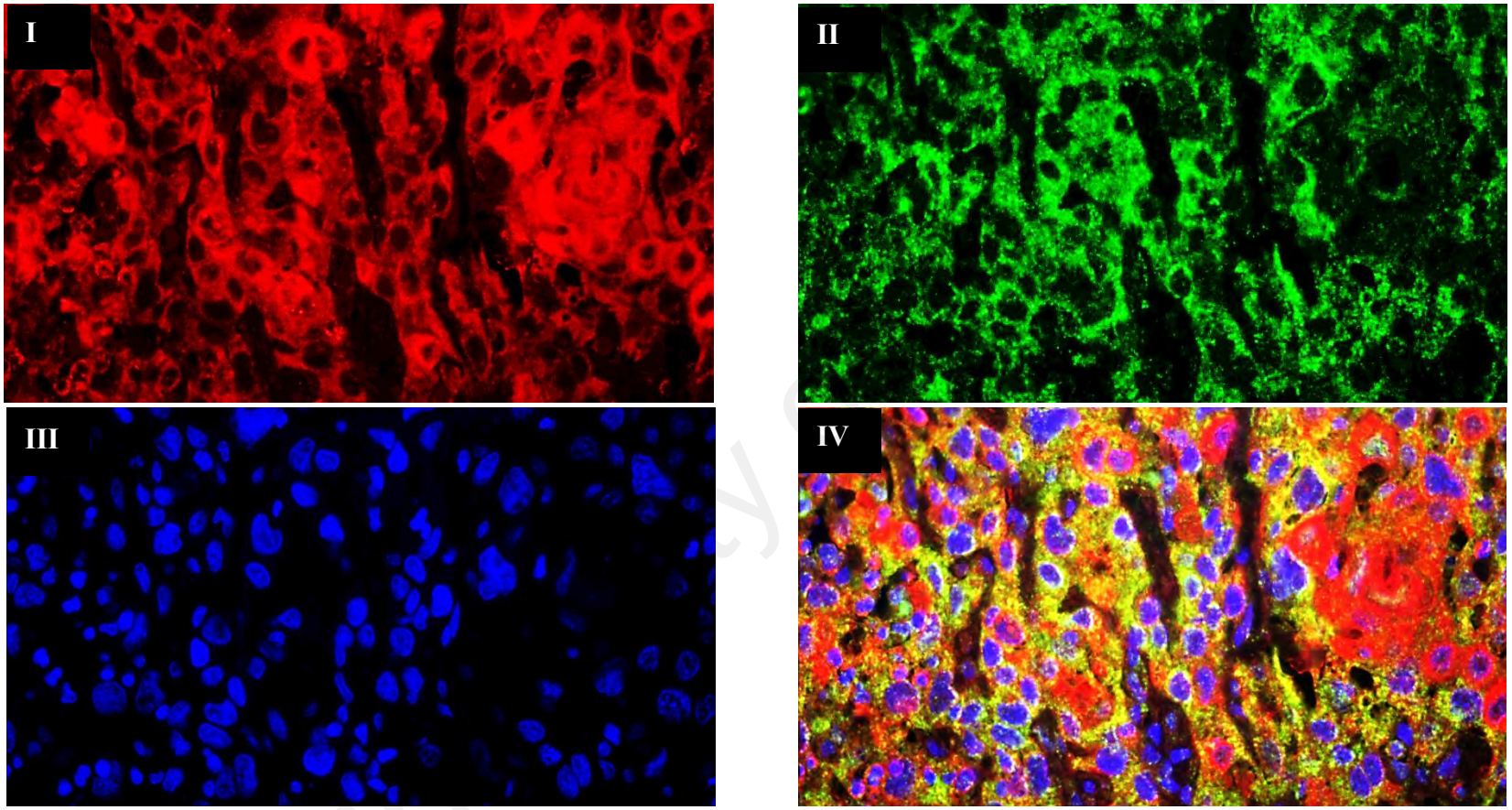

Figure 6.1: Representative images showing cytoplasmic and membranous DDR1 protein expression in OSCC tumour cells.

Tissues were multiplex-stained with **(I)** CK AE1/ AE3 (Cy3, red), **(II)** DDR1 (fluorescein, green) antibodies and **(III)** DAPI (blue) nuclear counterstain. **(IV)** Combined spectral composite image of CK and DDR1 shows strong DDR1 staining in malignant epithelium at magnification of 60X captured by Metamorph Pathology Imaging System (Nikon)**.**

Table 6.2: Association and correlation between DDR1 protein expression with socio-demographic and clinico-pathological parameters of OSCC patients.

Variables	Categories	DDR1 Expression (% of total cohort)		Pearson Chi Square	Spearman	Univariate ANOVA	Univariate Logistic Regression			Multiple Logistic Regression		
		Low	High	p-value	p-value	p-value	Odd ratio	95% CI	p-value	Odd ratio	95% CI	p-value
Age	30-50	7.1	14.3	0.402	0.836	0.421	1.00	-	-	1.00	-	-
	51-70	28.6	26.2				0.458	(0.09,2.29)	0.342	0.00	(0.00,-)	0.999
	71-90	7.1	16.7				1.167	(0.17,8.09)	0.876	0.00	(0.00,-)	0.999
Gender	Male	11.9	16.7	0.921	0.096	0.924	1.00	-	-	1.00	-	-
	Female	31.0	40.5				0.934	(0.24,3.63)	0.921	0.00	(0.00,-)	0.999
Etnic	Malay	7.1	9.5	0.941	0.826	0.945	1.00	-	-	1.00	-	-
	Chinese	7.1	11.9				1.250	(0.16,9.92)	0.833	0.00	(0.00,-)	0.999
	Indian	28.6	35.7				0.938	(0.18,5.02)	0.940	1.094E+156	(0.00,-)	0.999
Smoking	Yes	0.0	7.1	0.297	0.441	0.313	1.00	-	-	1.00	-	-
	No	31.0	35.7				0.00	(0.00,-)	0.999	0.00	(0.00,-)	0.999
	NA	11.9	14.3				0.00	(0.00,-)	0.999	0.00	(0.00,-)	0.999
Drink	Yes	0.0	4.8	0.455	0.557	0.474	1.00	-	-	1.00	-	-
	No	31.0	38.1				0.00	(0.00,-)	0.999	0.00	(0.00,-)	0.999
	NA	11.9	14.3				0.00	(0.00,-)	0.999	-	-	-
Betel quid chewing	Yes	21.4	26.2	0.957	0.838	0.960	1.00	-	-	1.00	-	-
	No	14.3	21.4				1.227	(0.32,4.77)	0.767	0.00	(0.00,-)	1.000
	NA	7.1	9.5				1.091	(0.19,6.20)	0.922	8.256E+130	(0.00,-)	0.999
Staging	Stage I	0.0	4.8	0.097	0486	0.099	1.00	-	-	1.00	-	-
	Stage II	11.9	11.9				0.00	(0.00,-)	0.999	1.108E+275	(0.00,-)	0.999
	Stage IV	31.0	28.6				0.00	(0.00,-)	0.999	-	(0.00,-)	0.999
	NA	0.0	11.9				1.00	(0.00,-)	1.000	5.594E+278	(0.00,-)	0.999
Vascular invasion	No	23.8	33.3	0.662	0.409	0.679	1.40	(0.37,5.27)	0.619	5.371E+33	(0.00,-)	0.999
	Yes	16.7	16.7				1.00	-	-	1.00	-	-
	NA	2.4	7.1				3.00	(0.25,36.33)	0.388	-	(0.00,-)	0.999

Table 6.2, continued.

Variables	Categories	DDR1 Expression (% of total cohort)		Pearson Chi Square	Spearman	Univariate ANOVA	Univariate Logistic Regression			Multiple Logistic Regression		
		Low	High	p-value	p-value	p-value	Odd ratio	95% CI	p-value	Odd ratio	95% CI	p-value
Histological Grade	Moderate	28.6	33.3	0.365	0.331	0.390	1.00	-	-	1.00	-	-
	Moderate to poor	2.4	0.0				0.00	(0.00,-)	1.000	1.068E+257	(0.00,-)	0.999
	Poor	4.8	2.4				0.429	(0.03,5.33)	0.510	0.00	(0.00,-)	0.999
	Well	7.1	16.7				2.000	(0.42,9.49)	0.383	6.772E+146	(0.00,-)	0.999
	NA	0.0	4.8				1384692741	(0.000,-)	0.999	0.00	(0.00,-)	1.000
Survival state	Alive	11.9	7.1	0.626	0.710	0.651	0.600	(0.03,13.58)	0.748	1.00	-	-
	Deceased	14.3	21.4				1.500	(0.08,28.89)	0.788	-	-	-
	Lost to follow up	2.4	2.4				1.00	-	-	0.00	(0.00,-)	0.999
	NA	14.3	26.2				1.833	(0.10,34.85)	0.687	0.00	(0.00,-)	1.000
Extent of primary tumour	T1	7.1	7.1	0.478	0.534	0.508	1.00	(0.15,6.77)	1.000	0.00	-	0.999
	T2	14.3	14.3				1.00	(0.21,4.67)	1.000	0.00	-	0.999
	T3	4.8	11.9				2.50	(0.36,17.50)	0.356	0.00	-	0.999
	T4	16.7	16.7				1.00	-	-	1.00	-	-
	NA	0.0	7.1				1615474864	(0.00,-)	0.999	3.844E+094	(0.00,-)	0.999
Extent of regional lymph node metastasis	N0	14.3	16.7	0.283	0.159	0.304	1.00	-	-	1.00	-	-
	N1	4.8	4.8				0.857	(0.09,8.08)	0.893	4.681E+191	(0.00,-)	0.999
	N2	2.4	0.0				0.000	(0.00,-)	1.000	317.782	(0.00,-)	1.000
	N2B	21.4	19.0				0.762	(0.18,3.24)	0.713	0.00	(0.00,-)	0.999
	N2C	0.0	2.4				1384692741	(0.00,-)	1.000	0.00	(0.00,-)	0.999
	N3	0.0	2.4				1384692741	(0.00,-)	1.000	0.00	(0.00,-)	0.999
	NA	0.0	11.9				1384692741	(0.00,-)	0.999	-	-	-

Table 6.2, continued.

Variables	Categories	DDR1 Expression (% of total cohort)		Pearson Chi Square	Spearman	Univariate ANOVA	Univariate Logistic Regression			Multiple Logistic Regression		
		Low	High	p-value	p-value	p-value	Odd ratio	95% CI	p-value	Odd ratio	95% CI	p-value
Tumour depth	1-10mm	14.3	21.4	0.411	0.447	0.438	1.50	(0.08,28.89)	0.788	80763325.43	(0.00,-)	1.000
	11-20mm	9.5	7.1				0.750	(0.03,17.51)	0.858	7.311E+071	(0.00,-)	1.000
	21-30mm	0.0	9.5				1615474864	(0.00,-)	0.999	0.00	(0.00,-)	0.999
	31-40mm	2.4	2.4				1.00	-	-	1.00	-	-
	NA	16.7	16.7				1.00	(0.05,19.36)	1.00	0.00	(0.00,-)	1.000
Perineural invasion	No	31.0	33.3	0.385	0.976	0.403	0.673	(0.18,2.59)	0.565	2.045E+12	(0.00,-)	1.000
	Yes	11.9	19.0				1.00	-	-	1.00	-	-
	NA	0.0	4.8				1009671790	(0.00,-)	0.999	0.00	(0.00,-)	1.000
Bone invasion	No	23.8	26.2	0.678	0.702	0.695	1.00	-	-	1.00	-	-
	Yes	14.3	19.0				1.212	(0.31,4.73)	0.782	-	(0.00,-)	0.999
	NA	4.8	11.9				2.273	(0.36,14.45)	0.384	9.630E+205	(0.00,-)	0.999
Extracapsular spread	No	31.0	33.3	0.385	0.295	0.403	0.673	(0.18,2.59)	0.565	0.00	(0.00,-)	1.000
	Yes	11.9	19.0				1.00	-	-	1.00	-	-
	NA	0.0	4.8				1009671790	(0.00,-)	0.999	-	-	-
Skip metastasis	No	33.3	40.5	0.455	0.536	0.474	0.971	(0.22,4.32)	0.970	3.027E+203	(0.00,-)	0.999
	Yes	9.5	11.9				1.00	-	-	1.00	-	-
	NA	0.0	4.8				1292379891	(0.00,-)	0.999	-	-	-

Multivariate Logistic Regression analyses was applied to adjust the confounders of age, gender, ethnic, smoking behaviour, drinking behaviour, betel quid chewing, staging, grading, survival status, extent of primary tumour, vascular invasion, extent of regional lymph node metastasis, tumour depth, perineural invasion and bone invasion, extracapsular spread and skip metastasis.

Abbreviation: NA, not available; Abbreviations: N0 (no regional lymph node metastasis); N1 (metastasis in single ipsilateral lymph node, ≤3cm); N2 (metastasis in single ipsilateral lymph node, 3-6cm); N2B (metastasis in single ipsilateral lymph node, ≤6cm); N2C (metastasis in bilateral/ contralateral lymph node, ≤6cm); N3 (metastasis in lymph node >6cm); T1 (tumour ≤2cm); T2 (tumour 2-4cm); T3 (tumour >4cm); T4 (tumour invades adjacent structures such as tongue, skin of neck and through cortical bone).

Survival data were available for 25 OSCC patients. Overall, the follow-up period ranged from 1 month to 65 months with a mean of 17 months and a median of 12 months. Among the 25 patients, 12 patients (48.0%) had low expression of DDR1, whilst 13 patients (52.0%) had high DDR1 expression. At last follow-up, 15 patients out of total 25 total patients (60%) were dead, whilst 10 patients (40%) were alive. Within the low DDR1 expression group, 6 patients (50% within low expression group) were dead whilst the remaining 6 patients (50% within low expression group) were alive. On the other hand, within the high DDR1 expression group, 9 patients (69.2% within high expression) were dead whilst 4 patients (38.8% within high expression) were alive. High DDR1 expression showed the trend of lower overall survival and lower 5-years survival rate (24.5%) compared to the low DDR1 expression group (36.0%). However, this comparison was not significant under the Log-Rank (Mantel Cox) (p= 0.170), Breslow (Generalised Wilcoxon) (p=0.074) and Tarone-Ware test (p=0.102) analyses (Figure 6.2).

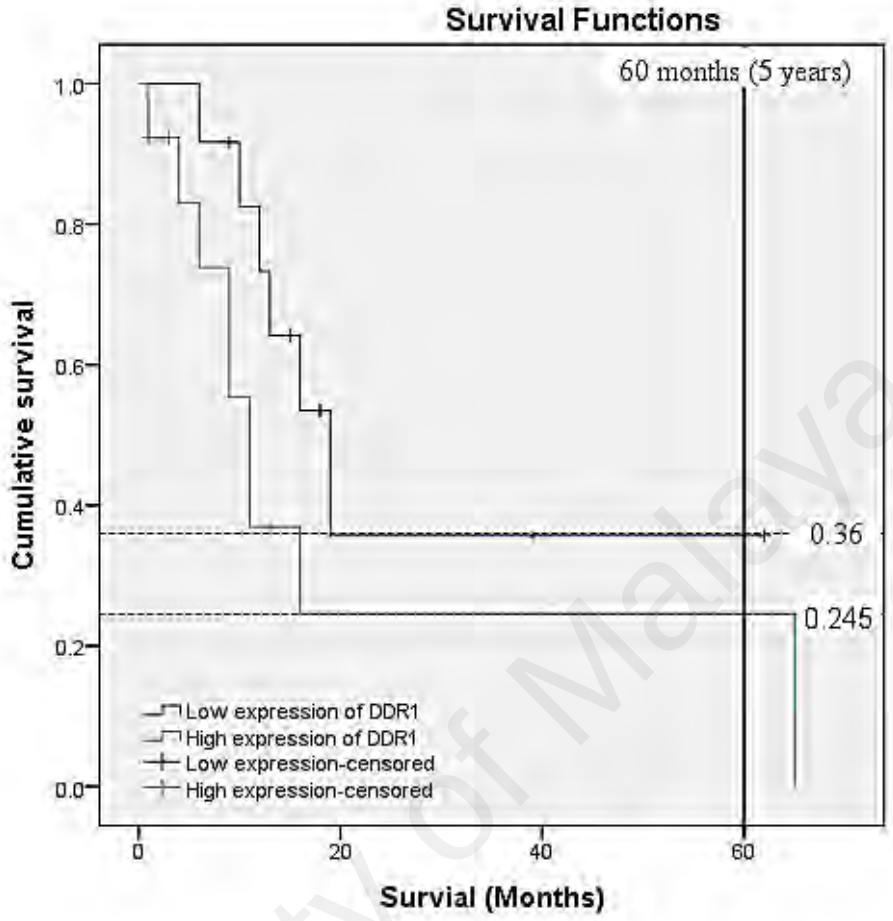

	Chi-Square	df	Sig.
Log Rank (Mantel-Cox)	1.885	1	.170
Breslow (Generalized Wilcoxon)	3.193	1	.074
Tarone-Ware	2.672	1	.102

Figure 6.2: Kaplan-Meir plot for Overall Survival of low and high DDR1 expression subsets in OSCC patients.

Patients with high DDR1 expression have lower 5-years survival rate (24.5%) than that of patients with low DDR1 expression (36.0%). However, no significant difference was found between the expression of DDR1 with the patients' overall survival in Log Rank (Mantel-Cox) test (p=0.170); Breslow (Generalised Wilcoxon) test (p=0.074); and Tarone-Ware test (p=0.102). Dashed line represents DDR1 low expression subset whilst straight line represents DDR1 high expression counterparts. Crosses indicate censored patients.

6.4 Expression of COL8a1 and association with socio-demographic and clinico-pathological parameters of OSCC patients

6.4.1 COL8a1 in tumour cells

Serial tissue sections from the same cohort were dual-stained for the presence of COL8a1 and the marker of fibroblasts activation, α-SMA. COL8a1 was found to be localised to the cytoplasm of the OSCC tumour cells (Figure 6.3).

The COL8a1 scores from fluorescence multiplex staining were transformed and recoded into low and high expression of COL8a1 in tumours by using the cut-off value (cut-off= 5008.5) obtained from Receiver Operating Characteristic Curve (AUC= 0.679) with the highest value of specificity and sensitive (85.7% sensitivity and 53.8% specificity) based on bone invasion status (Appendix I). Among the 44 cases, 16 cases (36.4% of total cohort) were recoded into low expression group whilst 24 cases (54.5% of total cohort) fell in high expression group. The remaining 4 cases (9.1% of total cohort) were excluded cases where the tissues were damaged after staining.

The majority of patients still alive had lower expression of COL8a1 in tumours (12.5% of total cohort) compared to higher expression of COL8a1 (5.0% of total cohort) (Pearson Chi Square, p=0.04; Univariate ANOVA, p= 0.036). Higher expression of COL8a1 in tumours was also found in patients with bone invasion (Pearson Chi Square, p=0.04; Univariate ANOVA, p=0.039; Logistic Regression, p=0.018), tumour of depth from 1-10mm (Pearson Chi Square, p=0.01; Univariate ANOVA, p=0.006). Patients with tumour extent of 2cm to 4cm showed lower expression of COL8a1 (Logistic Regression, p=0.040). There was no significant difference of the survival rates under the Kaplan-Meier Survival analysis.

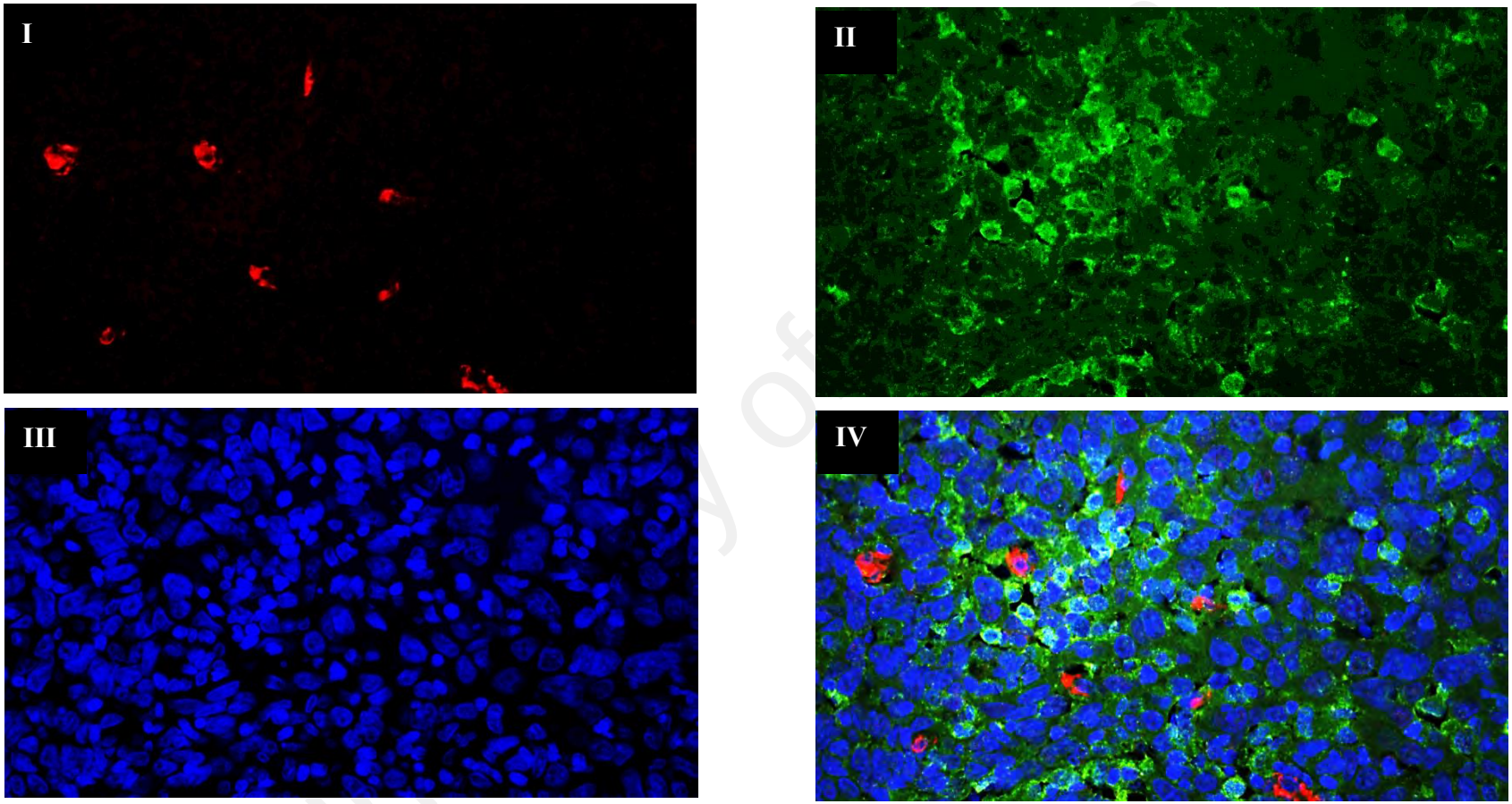

Figure 6.3: Representative images showing cytoplasmic COL8a1 protein expression in OSCC tumours.

The tumour cells expressed **(II)** COL8a1 (Fluorescein, green) when multiplex-stained with the **(I)** activated-CAFs marker, α-SMA (Cy3, red) and **(III)** DAPI (blue) nuclear counterstain. **(IV)** Combined spectral composite image of α-SMA and COL8a1 shows strong COL8a1 staining in malignant epithelium at magnification of 60X captured by Metamorph Pathology Imaging System (Nikon).

Table 6.3: Association and correlation between COL8a1 protein expression in tumour cells with socio-demographic and clinico-pathological parameters of OSCC patients.

Variables	Categories	COL8a1 Expression (% of total cohort)		Pearson Chi Square	Spearman	Univariate ANOVA	Univariate Logistic Regression			Multiple Logistic Regression		
		Low	High	p-value	p-value	p-value	Odd ratio	95% CI	p-value	Odd ratio	95% CI	p-value
Age	30-50	10.0	12.5	0.883	0.641	0.891	1.00	-	-	-	-	-
	51-70	22.5	32.5				1.156	(0.24,5.53)	0.856	-	-	-
	71-90	7.5	15.0				1.600	(0.25,10.81)	0.630	-	-	-
Gender	Male	12.5	17.5	0.888	0.891	0.891	1.00	-	-	-	-	-
	Female	27.5	42.5				1.104	(0.28,4.37)	0.888	-	-	-
Etnic	Malay	7.5	10.0	0.461	0.359	0.482	1.00	-	-	-	-	-
	Chinese	5.0	17.5				2.625	(0.30,23.0)	0.383	-	-	-
	Indian	27.5	32.5				0.886	(0.16,4.85)	0.889	-	-	-
Smoking	No	27.5	40.0	0.519	0.312	0.540	2.909	(0.23,36.16)	0.406	-	-	-
	Yes	5.0	2.5				1.00	-	-	-	-	-
	NA	7.5	17.5				4.667	(0.30,73.38)	0.273	-	-	-
Drink	No	27.5	42.5	0.181	0.206	0.191	2496640696	(0.00,-)	0.999	-	-	-
	Yes	5.0	0.0				1.00	-	-	-	-	-
	NA	7.5	17.5				3769437913	(0.00,-)	0.999	-	-	-
Betel quid chewing	No	15.0	22.5	0.262	0.141	0.277	1.500	(0.38,6.00)	0.566	-	-	-
	Yes	22.5	22.5				1.00	-	-	-	-	-
	NA	2.5	15.0				6.00	(0.60,60.44)	0.128	-	-	-
Staging	Stage I	2.5	2.5	0.610	0.222	0.636	1.00	-	-	-	-	-
	Stage II	12.5	10.0				0.800	(0.04,17.20)	0.887	-	-	-
	Stage IV A	0.0	0.0				2.125	(0.12,38.48)	0.610	-	-	-
	NA	5.0	5.0				1.00	(0.03,29.81)	1.000	-	-	-

Table 6.3, continued.

Variables	Categories	COL8a1 Expression (% of total cohort)		Pearson Chi Square	Spearman	Univariate ANOVA	Univariate Logistic Regression			Multiple Logistic Regression		
		Low	High	p-value	p-value	p-value	Odd ratio	95% CI	p-value	Odd ratio	95% CI	p-value
Histological Grade	Moderate	20.0	40.0	0.457	0.288	0.489	1.00	-	-	-	-	-
	Moderate to poor	2.5	0.0				0.00	(0.00,-)	1.000	-	-	-
	Poor	2.5	5.0				1.00	(0.08,12.76)	1.000	-	-	-
	Well	12.5	15.0				0.60	(0.14,2.58)	0.493	-	-	-
	NA	2.5	0.0				0.00	(0.00,-)	1.000	-	-	-
Survival state	Alive	12.5	5.0	*0.040	0.184	*0.036	1.00	-	-	1.00	-	-
	Deceased	20.0	17.5				2.188	(0.318,15.044)	0.426	5.565E+15	(0.00,-)	0.998
	Lost to follow up	0.0	5.0				4038687161	(0.00,-)	0.999	7.104E+14	(0.00,-)	0.999
	NA	7.5	32.5				10.833	(1.37,85.44)	0.024	2.225E+046	(0.00,-)	0.995
Extent of primary tumour	T1	5.0	10.0	0.309	0.172	0.332	0.545	(0.07,4.56)	0.576	4.912E+16	(0.00,-)	0.999
	T2	17.5	10.0				0.156	(0.03,0.92)	*0.040	0.294	(0.00,-)	1.000
	T3	7.5	10.0				0.364	(0.05,2.60)	0.314	0.00	(0.00,-)	1.000
	T4	7.5	27.5				1.00	-	-	1.00	-	-
	NA	2.5	2.5				0.273	(0.01,5.77)	1.000	0.00	(0.00,-)	1.000
Extent of regional lymph node metastasis	N0	10.0	20.0	0.757	0.528	0.796	1.00	-	-	-	-	-
	N1	5.0	5.0				0.500	(0.05,4.98)	0.554	-	-	-
	N2	0.0	2.5				807737432.1	(0.00,-)	1.000	-	-	-
	N2B	17.5	25.0				0.714	(0.15,3.33)	0.669	-	-	-
	N2C	0.0	2.5				807737432.1	(0.00,-)	1.000	-	-	-
	N3	2.5	0.0				0.00	(0.00,-)	1.000	-	-	-
	NA	5.0	5.0				0.500	(0.05,4.98)	0.554	-	-	-

Table 6.3, continued.

Variables	Categories	COL8a1 Expression (% of total cohort)		Pearson Chi Square	Spearman	Univariate ANOVA	Univariate Logistic Regression			Multiple Logistic Regression		
		Low	High	p-value	p-value	p-value	Odd ratio	95% CI	p-value	Odd ratio	95% CI	p-value
Vascular invasion	No	22.5	35.0	0.746	0.488	0.761	1.333	(0.34,5.27)	0.682	-	-	-
	Yes	15.0	17.5				1.00	-	-	-	-	-
	NA	2.5	7.5				2.571	(0.21,31.71)	0.461	-	-	-
Tumour depth	1-10mm	7.5	25.0	*0.010	0.053	*0.006	5384923212	(0.00,-)	0.999	6.928E+31	(0.00,-)	0.998
	11-20mm	0.0	15.0				2.610E+18	(0.00,-)	0.999	1.535E+078	(0.00,-)	0.996
	21-30mm	2.5	7.5				4846430891	(0.00,-)	0.999	2.439E+24	(0.00,-)	0.998
	31-40mm	5.0	0.0				1.00	-	-	1.00	-	-
	NA	25.0	12.5				807738481.8	(0.00,-)	0.999	1.030E+045	(0.00,-)	0.998
Perineural invasion	No	25.0	37.5	0.953	0.836	0.956	0.938	(0.24,3.71)	0.927	-	-	-
	Yes	12.5	20.0				1.00	-	-	-	-	-
	NA	2.5	2.5				0.625	(0.03,12.41)	0.758	-	-	-
Bone invasion	No	27.5	20.0	*0.040	0.062	*0.039	1.00	-	-	1.00	-	-
	Yes	5.0	30.0				8.250	(1.43,47.58)	*0.018	8.792E+21	(0.00,-)	0.999
	NA	7.5	10.0				1.833	(0.32,10.57)	0.498	3.637E+18	(0.00,-)	1.000
Extracapsular spread	No	22.5	37.5	0.908	0.875	0.090	1.250	(0.33,4.79)	0.745	-	-	-
	Yes	15.0	20.0				1.00	-	-	-	-	-
	NA	2.5	2.5				0.750	(0.04,14.58)	0.849	-	-	-

Table 6.3, continued.

Variables	Categories	COL8a1 Expression (% of total cohort)		Pearson Chi Square	Spearman	Univariate ANOVA	Univariate Logistic Regression			Multiple Logistic Regression		
		Low	High	p-value	p-value	p-value	Odd ratio	95% CI	p-value	Odd ratio	95% CI	p-value
Skip metastasis	No	27.5	45.0	0.901	0.876	0.908	1.309	(0.29,5.95)	0.727	-	-	-
	Yes	10.0	12.5				1.00	-	-	-	-	-
	NA	2.5	2.5				0.800	(0.04,17.20)	0.887	-	-	-

The parameter covariance matrix of all confounders cannot be computed, Multivariate Logistic Regression analyses was applied to adjust the selected confounders of survival status, extent of primary tumour, tumour depth and bone invasion which were significant either in Pearson Chi Square, Spearman correlation, Univariate ANOVA and Univariate Logistic Regression.

Abbreviation: NA, not available Abbreviation: NA, not available; Abbreviations: N0 (no regional lymph node metastasis); N1 (metastasis in single ipsilateral lymph node, ≤3cm); N2 (metastasis in single ipsilateral lymph node, 3-6cm); N2B (metastasis in single ipsilateral lymph node, ≤6cm); N2C (metastasis in bilateral/ contralateral lymph node, ≤6cm); N3 (metastasis in lymph node >6cm); T1 (tumour ≤2cm); T2 (tumour 2-4cm); T3 (tumour >4cm); T4 (tumour invades adjacent structures such as tongue, skin of neck and through cortical bone)

* denotes significant p-value, $p<0.05$.

6.4.2 COL8a1 in CAFs

COL8a1 was found to be co-expressed with α-SMA in the CAFs associated with OSCC and the protein was localised in the nuclei and cytoplasm (Figure 6.4). The scores of COL8a1 in CAFs were transformed and recoded into low and high expression by using the cut-off value (cut-off= 14712.5) obtained from Receiver Operating Characteristic Curve (AUC= 0.634) with the highest value of specificity and sensitive (77.8% sensitivity and 51.6% specificity) based on skip metastasis status (Appendix J). Cross-tabulation of the COL8a1 expression in CAFs also demonstrated that higher expression was seen in the patients who did not smoke, non-drinker, female, stage IV cancer, tumour invaded adjacent structures, metastasized in a single lateral lymph node less than 6cm, moderate histological grade, no bone invasion, no encapsulated spread, no skip metastasis and with deceased outcome. On the other hand, low expression was detected in patients with no vascular invasion and no perineural invasion (Table 6.4). However, none of these parameters were significant under statistical analyses. Similarly, there was no significant association between COL8a1 expression in CAFs and survival under the Kaplan-Meier Survival analyses.

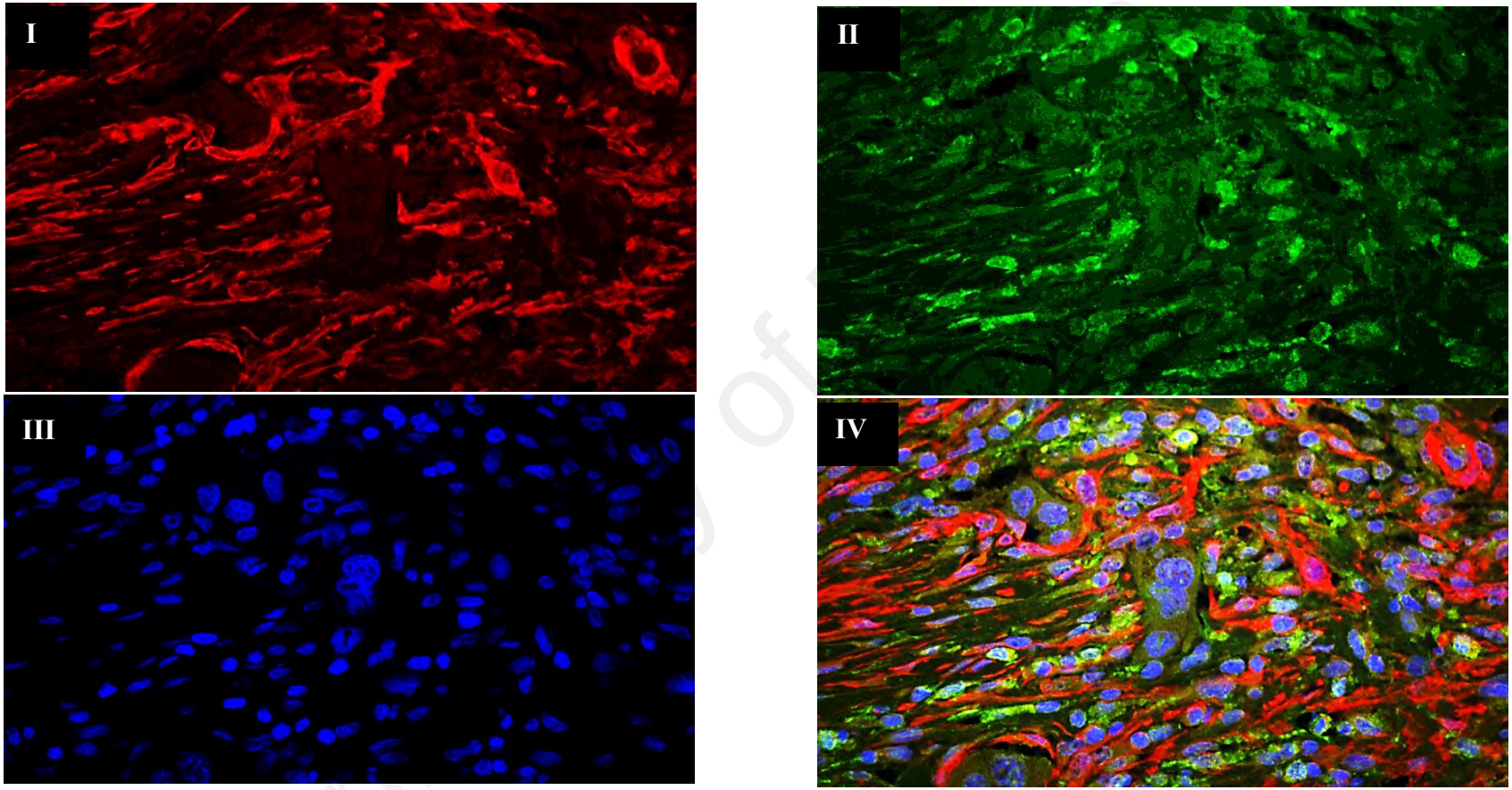

Figure 6.4: Representative images showing cytoplasmic and nuclear COL8a1 expression in OSCC CAFs.

Tissues were multiplex-stained with **(I)** activated-CAFs marker, α-SMA (Cy3, red), **(II)** COL8a1 (fluorescein, green) antibodies and **(III)** DAPI (blue) nuclear counterstain. **(IV)** Combined spectral composite image of α-SMA and COL8a1 shows strong COL8a1 staining in activated-CAFs at magnification of 60X captured by Metamorph Pathology Imaging System (Nikon).

Table 6.4: Association and correlation between COL8a1 protein expression in CAFs with socio-demographic and clinico-pathological parameters of OSCC patients.

Variables	Categories	COL8a1 Expression (% of total cohort)		Pearson Chi Square	Spearman	Univariate ANOVA	Univariate Logistic Regression			Multiple Logistic Regression		
		Low	High	p-value	p-value	p-value	Odd ratio	95% CI	p-value	Odd ratio	95% CI	p-value
Age	30-50	5.0	17.5	0.285	0.163	0.301	1.000	-	-	-	-	-
	51-70	27.5	27.5				0.286	(0.05,1.69)	0.168	-	-	-
	71-90	12.5	10.0				0.229	(0.03,1.77)	0.158	-	-	-
Gender	Male	12.5	17.5	0.781	0.788	0.788	1.000	-	-	-	-	-
	Female	32.5	37.5				0.824	(0.21,3.23)	0.782	-	-	-
Etnic	Malay	7.5	10.0	0.687	0.648	0.704	1.000	-	-	-	-	-
	Chinese	30.0	30.0				1.500	(0.20,11.54)	0.697	-	-	-
	Indian	7.5	15.0				0.750	(0.14,4.10)	0.740	-	-	-
Smoking	No	27.5	40.0	0.648	0.987	0.666	2.910	(0.23,36.16)	0.406	-	-	-
	Yes	5.0	2.5				1.000	-	-	-	-	-
	NA	12.5	12.5				2.000	(0.13,29.81)	0.615	-	-	-
Drink	No	27.5	42.5	0.233	0.816	0.247	2496640520	(0.00,-)	0.999	-	-	-
	Yes	5.0	0.0				1.000	-	-	-	-	-
	NA	12.5	12.5				1615473278	(0.00,-)	0.999	-	-	-
Betel Quid Chewing	No	10.0	27.5	0.140	0.147	0.147	4.321	(0.98,19.09)	0.054	-	-	-
	Yes	27.5	17.5				1.000	-	-	-	-	-
	NA	7.5	10.0				2.095	(0.36,12.32)	0.413	-	-	-
Staging	Stage I	2.5	2.5	0.631	0.620	0.657	1.000	-	-	-	-	-
	Stage II	10.0	12.5				1.250	(0.06,26.87)	0.887	-	-	-
	Stage IV	25.0	37.5				1.500	(0.08,26.86)	0.783	-	-	-
	NA	7.5	2.5				0.333	(0.01,11.94)	0.547	-	-	-

Table 6.4, continued.

Variables	Categories	COL8a1 Expression (% of total cohort)		Pearson Chi Square	Spearman	Univariate ANOVA	Univariate Logistic Regression			Multiple Logistic Regression		
		Low	High	p-value	p-value	p-value	Odd ratio	95% CI	p-value	Odd ratio	95% CI	p-value
Histological Grade	Moderate	22.5	37.5	0.469	0.200	0.501	1.000	-	-	-	-	-
	Moderate to poor	0.0	2.5				969284918.6	(0.00,-)	1.000	-	-	-
	Poor	5.0	2.5				0.300	(0.02,3.80)	0.353	-	-	-
	Well	15.0	12.5				0.500	(0.12,2.12)	0.348	-	-	-
	NA	2.5	0.0				0.000	(0.00,-)	1.000	-	-	-
Survival state	Alive	10.0	7.5	0.556	0.722	0.583	1.000	-	-	1.000		
	Deceased	17.5	20.0				1.524	(0.25,9.30)	0.648	12.753	(0.39,419.33)	0.153
	Lost to follow up	0.0	5.0				2153966488	(0.00,-)	0.999	19186329629	(0.00,-)	0.999
	NA	17.5	22.5				1.714	(0.29,10.30)	0.556	263.443	(2.61,26546.94)	0.018
Extent of primary tumour	T1	2.5	12.5	0.353	0.647	0.379	5.000	(0.46,54.51)	0.187	88.744	(0.52,15207.32)	0.087
	T2	17.5	10.0				0.571	(0.11,2.87)	0.497	1.321	(0.03,63.00)	0.888
	T3	5.0	12.5				2.500	(0.36,17.50)	0.356	16.484	(0.18,1497.47)	0.223
	T4	17.5	17.5				1.000	-	-	1.000	-	-
	NA	2.5	2.5				1.000	(0.05,19.36)	1.000	0.000	(0.00,-)	1.000
Extent of regional lymph node metastasis	N0	12.5	17.5	0.479	0.420	0.520	1.000	-	-	-	-	-
	N1	2.5	7.5				2.143	(0.17,27.10)	0.556	-	-	-
	N2	2.5	0.0				0.000	(0.00,-)	1.000	-	-	-
	N2B	17.5	25.0				1.020	(0.23,4.57)	0.979	-	-	-
	N2C	0.0	2.5				1153910618	(0.00,-)	1.000	-	-	-
	N3	2.5	0.0				0.000	(0.00,-)	1.000	-	-	-
	NA	7.5	2.5				0.238	(0.02,3.01)	0.268	-	-	-

Table 6.4, continued.

Variables	Categories	COL8a1 Expression (% of total cohort)		Pearson Chi Square	Spearman	Univariate ANOVA	Univariate Logistic Regression			Multiple Logistic Regression		
		Low	High	p-value	p-value	p-value	Odd ratio	95% CI	p-value	Odd ratio	95% CI	p-value
Vascular invasion	No	30.0	27.5	0.509	0.892	0.530	0.573	(0.14,2.29)	0.431	-	-	-
	Yes	12.5	20.0				1.000	-	-	-	-	-
	NA	2.5	7.5				1.875	(0.15,23.40)	0.625	-	-	-
Tumour depth	1-10mm	17.5	15.0	0.408	0.748	0.437	1384691006	(0.00,-)	0.999	17153752103	(0.00,-)	0.999
	11-20mm	5.0	10.0				3230945681	(0.00,-)	0.999	1241053254	(0.00,-)	0.999
	21-30mm	2.5	7.5				4846418522	(0.00,-)	0.999	29228286960	(0.00,-)	0.999
	31-40mm	5.0	0.0				1.000	-	-	1.000	-	-
	NA	15.0	22.5				2423209261	(0.00,-)	0.999	29277641684	(0.00,-)	0.999
Perineural invasion	No	35.0	27.5	0.152	0.075	0.160	0.236	(0.05,1.07)	0.061	-	-	-
	Yes	7.5	25.0				1.000	-	-	-	-	-
	NA	2.5	2.5				0.300	(0.01,6.38)	0.440	-	-	-
Bone invasion	No	22.5	25.0	0.960	0.931	0.963	1.000	-	-	1.000	-	-
	Yes	15.0	20.0				1.200	(0.30,4.82)	0.797	2.284	(0.04,147.56)	0.698
	NA	7.5	10.0				1.200	(0.21,6.88)	0.838	0.694	(0.01,77.31)	0.879
Extracapsular spread	No	22.5	37.5	0.497	0.374	0.517	2.222	(0.58,8.51)	0.244	-	-	-
	Yes	20.0	15.0				1.000	-	-	-	-	-
	NA	2.5	2.5				1.333	(0.07,25.91)	0.849	-	-	-

Table 6.4, continued.

Variables	Categories	COL8a1 Expression (% of total cohort)		Pearson Chi Square	Spearman	Univariate ANOVA	Univariate Logistic Regression			Multiple Logistic Regression		
		Low	High	p-value	p-value	p-value	Odd ratio	95% CI	p-value	Odd ratio	95% CI	p-value
Skip metastasis	No	37.5	35.0	0.296	0.161	0.313	0.267	(0.05,1.51)	0.135	-	-	-
	Yes	5.0	17.5				1.000	-	-	-	-	-
	NA	2.5	2.5				0.286	(0.01,6.91)	0.441	-	-	-

The parameter covariance matrix of all confounders cannot be computed, Multivariate Logistic Regression analyses was applied to adjust the selected confounders of survival status, extent of primary tumour, tumour depth and bone invasion which were significantly associated with COL8a1 in tumour either in Pearson Chi Square, Spearman correlation, Univariate ANOVA and Univariate Logistic Regression.

Abbreviation: NA, not available Abbreviation: NA, not available; Abbreviations: N0 (no regional lymph node metastasis); N1 (metastasis in single ipsilateral lymph node, ≤3cm); N2 (metastasis in single ipsilateral lymph node, 3-6cm); N2B (metastasis in single ipsilateral lymph node, ≤6cm); N2C (metastasis in bilateral/ contralateral lymph node, ≤6cm); N3 (metastasis in lymph node >6cm); T1 (tumour ≤2cm); T2 (tumour 2-4cm); T3 (tumour >4cm); T4 (tumour invades adjacent structures such as tongue, skin of neck and through cortical bone)

* denotes significant p-value, $p<0.05$.

6.5 Expression of COL11a1 and association with socio-demographic and clinico-pathological parameters of OSCC patients

6.5.1 COL11a1 in tumour cells

The tissue sections from the same cohort were dual-stained for the presence of another collagen subtype, COL11a1, and the marker of fibroblasts activation, α-SMA. The COL11a1 protein was found to be expressed in the OSCC tumour cells and expression was localised in the cytoplasm (Figure 6.5).

The area under curve of a Receiver Operating Characteristic Curve was below 0.6 and the skewness divided by standard deviation was less than 1.98 (skewness/ SD=-0.288) suggesting that the population was normally distributed. Therefore, the mean (μ= 100981.44) was used as the cut-off value in transforming the obtained COL11a1 scoring from fluorescence multiplex staining into low and high expression groups. Among the 44 cases, 17 cases (38.6% of total cohort) were recoded into the low expression group, whilst 22 cases (50.0% of total cohort) fell into the high expression group. The remaining 5 cases (11.4% of total cohort) were damaged during staining.

Cross-tabulation revealed higher expression of COL11a1 in patients aged between 51 to 70 years old, females, Indians, non-drinkers, non-smokers, tumours invading adjacent structures, betel quid chewers and patients with deceased outcome. Interestingly, high expression of COL11a1 was also seen in tumours of showing no regional lymph node metatstasis, no vascular and perineural invasion, no extracapsular spread and no skip metastasis. Lower expression was found in Stage IV tumours. However, the association and correlation of these factors were all not significant in the Pearson Chi Square and Spearman Correlation analyses, Univariate ANOVA, Logistic Regression and Multiple Logistic Regression. There was also no significant association between COL11a1 expression in tumour cells and survival rates under the Kaplan-Meier Survival analysis.

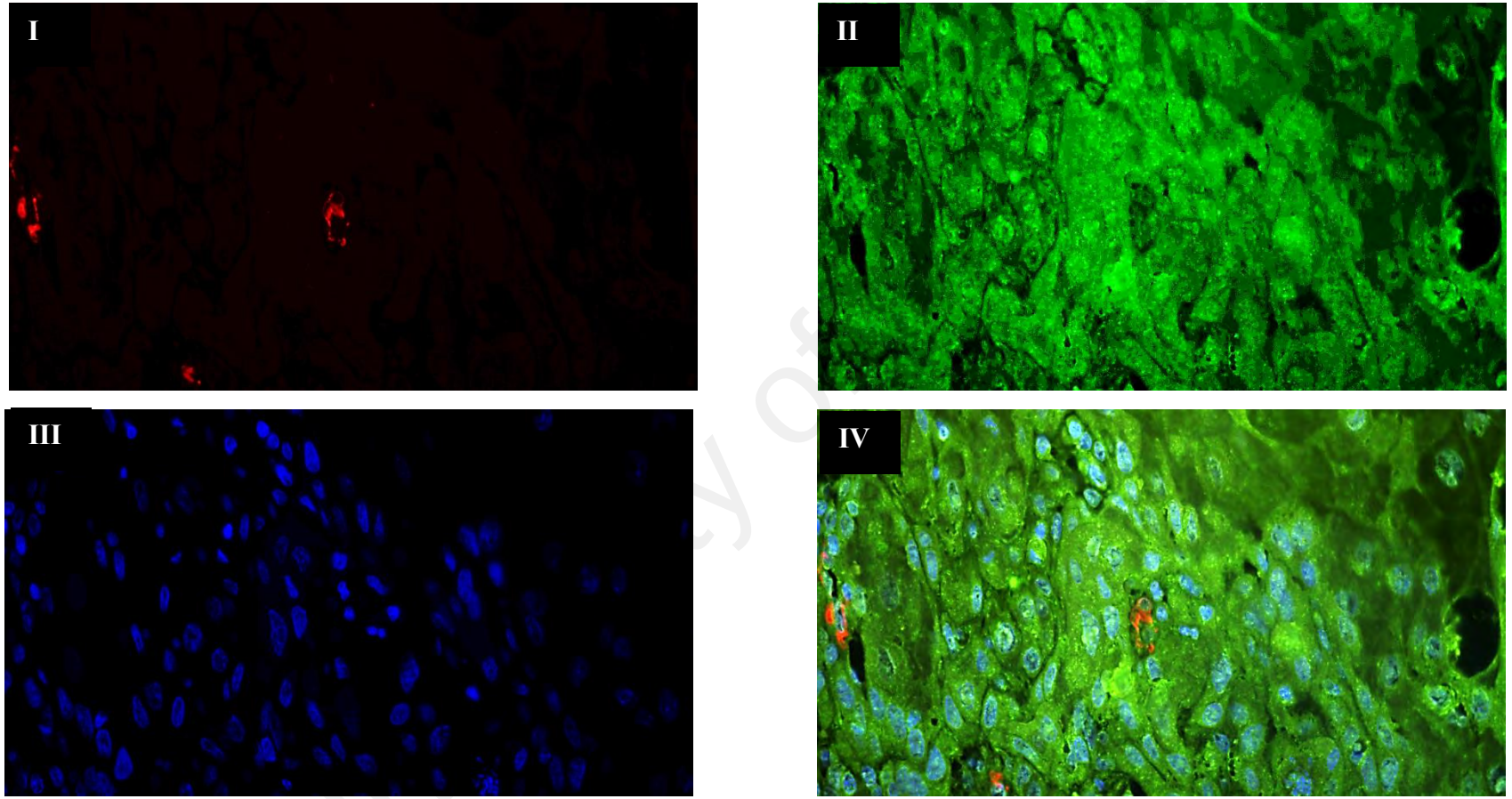

Figure 6.5: Representative images showing cytoplasmic COL11a1 protein expression in OSCC tumours.

The tumour cells (region indicated by arrows) expressed **(II)** COL11a1 (Fluorescein, green) when multiplex-stained with the **(I)** activated-CAFs marker, α-SMA (Cy3, red) and **(III)** DAPI (blue) nuclear counterstain. **(IV)** Combined spectral composite image of α-SMA and COL11a1 shows strong COL11a1 staining in malignant epithelium at magnification of 60X captured by Metamorph Pathology Imaging System (Nikon).

Table 6.5: Association and correlation between COL11a1 protein expression in tumour cells with socio-demographic and clinico-pathological parameters of OSCC patients.

Variables	Categories	COL11a1 Expression (% of total cohort)		Pearson Chi Square	Spearman	Univariate ANOVA	Univariate Logistic Regression			Multiple Logistic Regression		
		Low	High	p-value	p-value	p-value	Odd ratio	95% CI	p-value	Odd ratio	95% CI	p-value
Age	30-50	10.3	10.3	0.905	0.840	0.911	1.000	-	-	1.000	-	-
	51-70	23.1	33.3				1.444	(0.28,7.34)	0.658	0.000	(0.00,-)	0.999
	71-90	10.3	12.8				1.250	(0.19,8.44)	0.819	0.000	(0.00,-)	0.999
Gender	Male	12.8	17.9	0.872	0.876	0.876	1.000	-	-	1.000	-	-
	Female	30.8	38.5				0.893	(0.23,3.54)	0.872	-	(0.00,-)	0.999
Etnic	Malay	7.7	10.3	0.247	0.293	0.262	1.000	-	-	1.000	-	-
	Chinese	12.8	5.1				0.300	(0.03,2.76)	0.288	0.000	(0.00,-)	0.999
	Indian	23.1	41.0				1.333	(0.24,7.34)	0.741	-	(0.00,-)	0.999
Smoking	No	28.2	43.6	0.472	0.256	0.493	0.773	(0.06,9.58)	0.841	0.000	(0.00,-)	0.999
	Yes	2.6	5.1				1.000	-	-	1.000	-	-
	NA	12.8	7.7				0.300	(0.02,4.91)	0.398	0.000	(0.00,-)	0.999
Drink	No	28.2	46.2	0.455	0.340	0.476	1.636	(0.09,28.90)	0.737	0.000	(0.00,-)	0.999
	Yes	2.6	2.6				1.000	-	-	1.000	-	-
	NA	12.8	7.7				0.600	(0.03,13.58)	0.748	-	-	-
Betel Quid Chewing	No	15.4	17.9	0.635	0.361	0.654	0.681	(0.16,2.86)	0.599	0.000	(0.00,-)	0.999
	Yes	17.9	30.8				1.000	-	-	1.000	-	-
	NA	10.3	7.7				0.438	(0.08,2.55)	0.358	-	(0.00,-)	0.999
Staging	Stage I	0.0	5.1	0.319	0.096	0.340	1.000	-	-	1.000	-	-
	Stage II	7.7	17.9				0.00	(0.00,-)	0.999	0.000	(0.00,-)	0.999
	Stage IV	33.3	28.2				0.00	(0.00,-)	0.999	0.000	(0.00,-)	0.999
	NA	2.6	5.10				0.00	(0.00,-)	0.999	0.000	(0.00,-)	0.999

Table 6.5, continued.

Variables	Categories	COL11a1 Expression (% of total cohort)		Pearson Chi Square	Spearman	Univariate ANOVA	Univariate Logistic Regression			Multiple Logistic Regression		
		Low	High	p-value	p-value	p-value	Odd ratio	95% CI	p-value	Odd ratio	95% CI	p-value
Histological Grade	Moderate	30.8	30.8	0.474	0.281	0.506	1.000	-	-	1.000	-	-
	Moderate to poor	2.6	0.0				0.00	(0.00,-)	1.000	-	(0.00,-)	0.999
	Poor	2.6	5.1				2.000	(0.16,25.12)	0.591	-	(0.00,-)	0.999
	Well	5.1	17.9				3.500	(0.60,20.41)	0.164	-	(0.00,-)	0.999
	NA	2.6	2.6				1.000	(0.06,17.90)	1.000	0.000	(0.00,-)	0.999
Survival state	Alive	2.6	15.4	0.062	0.065	0.061	1.000	-	-	1.00	-	-
	Deceased	15.4	23.1				0.250	(0.02,2.64)	0.249	-	-	-
	Lost to follow up	0.0	5.1				269245810.7	(0.00,-)	0.999	-	-	-
	NA	25.6	12.8				0.083	(0.01,0.90)	0.040	0.000	(0.00,-)	0.999
Extent of primary tumour	T1	2.6	7.7	0.805	0.696	0.830	1.667	(0.14,20.58)	0.690	-	(0.00,-)	0.999
	T2	15.4	12.8				0.463	(0.09,2.32)	0.350	-	(0.00,-)	0.999
	T3	10.3	10.3				0.556	(0.10,3.25)	0.514	-	(0.00,-)	0.999
	T4	12.8	23.1				1.000	-	-	1.000	-	-
	NA	2.6	2.6				0.556	(0.03,10.93)	0.699	0.000	(0.00,-)	0.999
Extent of regional lymph node metastasis	N0	7.7	25.6	0.250	0.062	0.268	1.000	-	-	1.000	-	-
	N1	2.6	7.7				0.900	(0.07,12.18)	0.937	-	(0.00,-)	0.999
	N2	2.6	0.0				0.000	(0.00,-)	1.000	0.000	(0.00,-)	0.999
	N2B	23.1	17.9				0.233	(0.05,1.19)	0.079	0.000	(0.00,-)	0.999
	N2C	2.6	0.0				0.000	(0.00,-)	1.000	0.000	(0.00,-)	0.999
	N3	2.6	0.0				0.000	(0.00,-)	1.000	0.000	(0.00,-)	0.999
	NA	2.6	5.1				0.600	(0.04,9.16)	0.713	-	-	-

Table 6.5, continued.

Variables	Categories	COL11a1 Expression (% of total cohort)		Pearson Chi Square	Spearman	Univariate ANOVA	Univariate Logistic Regression			Multiple Logistic Regression		
		Low	High	p-value	p-value	p-value	Odd ratio	95% CI	p-value	Odd ratio	95% CI	p-value
Vascular invasion	No	28.2	30.8	0.688	0.426	0.706	0.545	(0.13,2.33)	0.413	0.000	(0.00,-)	0.999
	Yes	10.3	20.5				1.000	-	-	1.000	-	-
	NA	5.1	5.1				0.500	(0.05,4.98)	0.554	-	(0.00,-)	0.999
Tumour depth	1-10mm	17.9	17.9	0.396	0.738	0.425	1615478350	(0.00,-)	1.000	-	(0.00,-)	0.999
	11-20mm	2.6	15.4				9692870099	(0.00,-)	1.000	-	(0.00,-)	0.999
	21-30mm	5.1	5.1				1615478350	(0.00,-)	1.000	0.000	(0.00,-)	0.999
	31-40mm	2.6	0.0				1.000	-	-	1.000	-	-
	NA	15.4	17.9				1884724741	(0.00,-)	1.000	-	(0.00,-)	0.999
Perineural invasion	No	30.8	35.9	0.845	0.578	0.856	0.667	(0.16,2.84)	0.584	2.231E+278	(0.00,-)	0.999
	Yes	10.3	17.9				1.000	-	-	1.000	-	-
	NA	2.6	2.6				0.571	(0.03,11.85)	0.718	-	-	-
Bone invasion	No	23.1	25.6	0.882	0.762	0.890	1.000	-	-	1.000	-	-
	Yes	12.8	20.5				1.440	(0.34,6.05)	0.618	-	(0.00,-)	0.999
	NA	7.7	10.3				1.200	(0.21,6.88)	0.838	-	(0.00,-)	0.999
Extracapsular spread	No	23.1	38.5	0.621	0.453	0.641	1.944	(0.50,7.64)	0.341	0.00	(0.00,-)	0.999
	Yes	17.9	15.4				1.000	-	-	-	-	-
	NA	2.6	2.6				1.167	(0.06,22.94)	0.919	-	-	-

Table 6.5, continued.

Variables	Categories	COL11a1 Expression (% of total cohort)		Pearson Chi Square	Spearman	Univariate ANOVA	Univariate Logistic Regression			Multiple Logistic Regression		
		Low	High	p-value	p-value	p-value	Odd ratio	95% CI	p-value	Odd ratio	95% CI	p-value
Skip metastasis	Yes	5.1	15.4	0.492	0.279	0.514	1.000	-	-	-	-	-
	No	35.9	38.5				0.357	(0.06,2.07)	0.251	-	-	-
	NA	2.6	2.6				0.333	(0.01,8.18)	0.501	-	-	-

The parameter covariance matrix of all confounders cannot be computed, Multivariate Logistic Regression analyses was applied to adjust the confounders of age, gender, ethnic, smoking behaviour, drinking behaviour, betel quid chewing, staging, grading, extent of primary tumour, vascular invasion, extent of regional lymph node metastasis, tumour depth, perineural invasion and bone invasion, extracapsullar spread and survival status.

Abbreviation: NA, not available Abbreviation: NA, not available; Abbreviations: N0 (no regional lymph node metastasis); N1 (metastasis in single ipsilateral lymph node, ≤3cm); N2 (metastasis in single ipsilateral lymph node, 3-6cm); N2B (metastasis in single ipsilateral lymph node, ≤6cm); N2C (metastasis in bilateral/ contralateral lymph node, ≤6cm); N3 (metastasis in lymph node >6cm); T1 (tumour ≤2cm); T2 (tumour 2-4cm); T3 (tumour >4cm); T4 (tumour invades adjacent structures such as tongue, skin of neck and through cortical bone)

* denotes significant p-value, $p<0.05$.

6.5.2 COL11a1 in CAFs

COL11a1 also found to be expressed and localised in the nucleus and cytoplasm of CAFs associated with OSCC (Figure 6.6). The scoring of COL11a1 in CAFs were transformed and recoded into low and high expression by using the cut-off value (cut-off= 15267.5) obtained from Receiver Operating Characteristic Curve (AUC= 0.718) with the highest value of specificity and sensitive (100% sensitivity and 35% specificity) based on betel quid chewing status (Appendix K). Cross-tabulation of the COL11a1 expression in CAFs indicated high expressed in patients aged between 51 to 70 years old, females, Indians, non-smokers, non-drinkers, betel quid chewers, stage IV cancer, tumour size ranging from 1-10mm, moderate histological grade, tumour invaded adjacent structures, metastasized in a single ipsilateral lymph node less than 6cm, no vascular invasion, no perineural invasion and no bone invasion, no encapsulated spread, no skip metastasis and patients with deceased outcome. Among these clinico-pathological parameters, those that have significant association were Indian ethnicity (Pearson Chi Square, p=0.004; Univariate ANOVA, p=0.002), females (Pearson Chi Square, p=0.010; Spearman Correlation comparisons, p=0.009; Univariate ANOVA, p=0.009; Logistic Regression, p=0.020) and betel quid chewing behaviour (Pearson Chi Square, p=0.015; Spearman Correlation comparisons, p=0.011; Univariate ANOVA,p=0.013). However, none of these parameters was significant when Multivariate Logistic Regression analyses were applied to adjust for the confounders. Lastly, similarly to the COL11a1 expression in tumours, no significant association between the expression of COL11a1 in CAFs and survival was observed under the Kaplan-Meier Survival analyses.

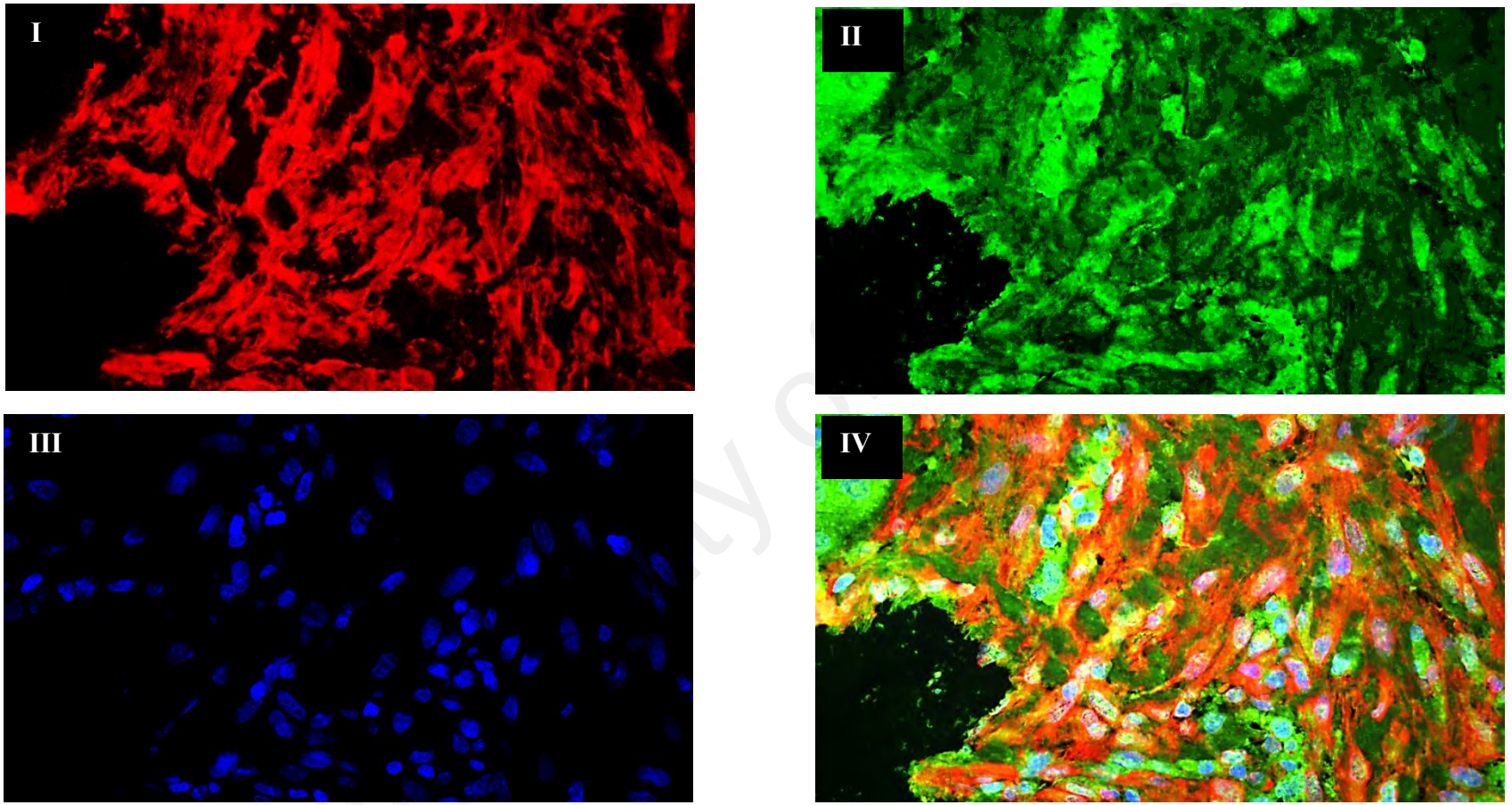

Figure 6.6: Representative images showing cytoplasmic and nuclei COL11a1 protein expression in OSCC CAFs.

Tissues were multiplex-stained with **(I)** activated-CAFs marker, α-SMA (Cy3, red), **(II)** COL11a1 (fluorescein, green) antibodies and **(III)** DAPI (blue) nuclear counterstain. **(IV)** Combined spectral composite image of α-SMA and COL11a1 shows strong COL11a1 staining in activated-CAFs at magnification of 60X captured by Metamorph Pathology Imaging System (Nikon).

Table 6.6: Association and correlation between COL11a1 protein expression in CAFs with socio-demographic and clinico-pathological parameters of OSCC patients.

Variables	Categories	COL11a1 Expression (% of total cohort)		Pearson Chi Square	Spearman	Univariate ANOVA	Univariate Logistic Regression			Multiple Logistic Regression		
		Low	High	p-value	p-value	p-value	Odd ratio	95% CI	p-value	Odd ratio	95% CI	p-value
Age	30-50	7.7	12.8	0.186	0.481	0.198	1.000	-	-	1.000	-	-
	51-70	5.1	51.3				6.000	(0.78,46.14)	0.085	81015949.01	(0.00,-)	1.000
	71-90	5.1	17.9				2.100	(0.25,17.59)	0.494	0.000	(0.00,-)	1.000
Gender	Male	12.8	17.9	*0.010	*0.009	*0.009	1.000	-	-	1.000	-	-
	Female	5.1	64.1				8.929	(1.42,56.31)	*0.020	0.000	(0.00,-)	1.000
Ethnic	Malay	5.1	12.8	*0.004	0.172	*0.002	1.000	-	-	1.000	-	-
	Chinese	10.3	7.7				0.300	(0.03,2.76)	0.288	0.000	(0.00,-)	0.999
	Indian	2.6	61.5				9.600	(0.72,127.53)	0.087	1.227E+21	(0.00,-)	0.999
Smoking	No	12.8	59.0	0.725	0.493	0.741	2.300	(0.17,30.60)	0.528	1.090E+14	(0.00,-)	1.000
	Yes	2.6	5.1				1.000	-	-	1.000	-	-
	NA	2.6	17.9				3.500	(0.15,84.69)	0.441	2.313E+054	(0.00,-)	0.999
Drink	No	12.8	61.5	0.457	0.394	0.742	4.800	(0.26,90.30)	0.295	698830416.8	(0.00,-)	1.000
	Yes	2.6	2.6				1.000	-	-	1.000	-	-
	NA	2.6	17.9				7.000	(0.22,226.01)	0.272	-	-	-
Betel Quid Chewing	No	12.8	20.5	*0.015	*0.011	*0.013	0.000	(0.00,-)	0.998	1785261.8	(0.00,-)	1.000
	Yes	0.0	48.7				1.000	-	-	1.000	-	-
	NA	5.1	12.8				0.000	(0.00,-)	0.998	0.000	(0.00,-)	1.000
Staging	Stage I	0.0	5.1	0.739	0.442	0.762	1.000	-	-	1.000	-	-
	Stage II	5.1	20.5				0.000	(0.00,-)	0.999	0.000	(0.00,-)	1.000
	Stage IV	12.8	48.7				0.000	(0.00,-)	0.999	0.000	(0.00,-)	1.000
	NA	0.0	7.7				1.000	(0.00,-)	1.000	2.880E+20	(0.00,-)	1.000

Table 6.6, continued.

Variables	Categories	COL11a1 Expression (% of total cohort)		Pearson Chi Square	Spearman	Univariate ANOVA	Univariate Logistic Regression			Multiple Logistic Regression		
		Low	High	p-value	p-value	p-value	Odd ratio	95% CI	p-value	Odd ratio	95% CI	p-value
Histological Grade	Moderate	15.4	46.2	0.077	0.092	0.074	1.000	-	-	-	-	-
	Moderate to poor	2.6	0.0				0.000	(0.00,-)	1.000	-	-	-
	Poor	0.0	7.7				538491621.4	(0.00,-)	0.999	-	-	-
	Well	0.0	23.1				538491621.4	(0.00,-)	0.999	-	-	-
	NA	0.0	5.1				538491621.4	(0.00,-)	0.999	-	-	-
Survival state	Alive	0.0	17.9	0.204	0.120	0.217	1.000	-	-	-	-	-
	Deceased	5.1	33.3				0.000	(0.00,-)	0.999	-	-	-
	Lost to follow up	0.0	5.1				1.000	(0.00,-)	1.000	-	-	-
	NA	12.8	25.6				0.000	(0.00,-)	0.999	-	-	-
Extent of primary tumour	T1	0.0	10.3	0.475	0.613	0.508	269245810.7	(0.00,-)	0.999	0.000	(0.00,-)	1.000
	T2	5.1	23.1				0.750	(0.09,6.39)	0.792	4.037E+11	(0.00,-)	1.000
	T3	7.7	12.8				0.278	(0.04,2.20)	0.225	2.751	(0.00,-)	1.000
	T4	5.1	30.8				1.000	-	-	1.000	-	-
	NA	0.0	5.1				269245810.7	(0.00,-)	0.999	0.000	(0.00,-)	0.999
Extent of regional lymph node metastasis	N0	5.1	28.2	0.438	0.879	0.478	1.000	-	-	-	-	-
	N1	2.6	7.7				0.545	(0.04,8.27)	0.662	-	-	-
	N2	0.0	2.6				293722702.6	(0.00,-)	1.000	-	-	-
	N2B	7.7	33.3				0.788	(0.11,5.60)	0.812	-	-	-
	N2C	2.6	0.0				0.000	(0.00,-)	1.000	-	-	-
	N3	0.0	2.6				293722702.6	(0.00,-)	1.000	-	-	-
	NA	5.1	28.2				293722702.6	(0.00,-)	0.999	-	-	-

Table 6.6, continued.

Variables	Categories	COL11a1 Expression (% of total cohort)		Pearson Chi Square	Spearman	Univariate ANOVA	Univariate Logistic Regression			Multiple Logistic Regression		
		Low	High	p-value	p-value	p-value	Odd ratio	95% CI	p-value	Odd ratio	95% CI	p-value
Vascular invasion	No	10.3	48.7	0.926	0.790	0.932	0.950	(0.15,6.12)	0.957	11157831.69	(0.00,-)	1.000
	Yes	5.1	25.6				1.000	-	-	1.000	-	-
	NA	2.6	7.7				0.600	(0.04,9.16)	0.713	10142884.33	(0.00,-)	1.000
Tumour depth	1-10mm	2.6	33.3	0.353	0.836	0.379	0.000	(0.00,-)	1.000	-	-	-
	11-20mm	2.6	15.4				0.000	(0.00,-)	1.000	-	-	-
	21-30mm	5.1	5.1				0.000	(0.00,-)	1.000	-	-	-
	31-40mm	0.0	2.6				1.000	-	-	-	-	-
	NA	7.7	25.6				0.000	(0.00,-)	1.000	-	-	-
Perineural invasion	No	10.3	56.4	0.548	0.293	0.569	2.062	(0.38,11.31)	0.404	0.000	(0.00,-)	1.000
	Yes	7.7	20.5				1.000	-	-	1.000	-	-
	NA	0.0	5.1				605803074.7	(0.00,-)	0.999	-	-	-
Bone invasion	No	10.3	38.5	0.884	0.938	0.892	1.000	-	-	1.000	-	-
	Yes	5.1	28.2				1.467	(0.23,9.49)	0.688	9.934E+24	(0.00,-)	0.999
	NA	2.6	15.4				1.600	(0.15,17.41)	0.700	0.000	(0.00,-)	1.000
Extracapsular spread	No	10.3	51.3	0.706	0.474	0.723	1.500	(0.28,8.04)	0.636	0.000	(0.00,-)	1.000
	Yes	7.7	25.6				1.000	-	-	1.000	-	-
	NA	0.0	5.1				484642459.3	(0.00,-)	0.999	-	-	-

Table 6.6, continued.

Variables	Categories	COL11a1 Expression (% of total cohort)		Pearson Chi Square	Spearman	Univariate ANOVA	Univariate Logistic Regression			Multiple Logistic Regression		
		Low	High	p-value	p-value	p-value	Odd ratio	95% CI	p-value	Odd ratio	95% CI	p-value
Skip metastasis	Yes	2.6	17.9	0.688	0.906	0.706	1.000	-	-	1.000	-	-
	No	15.4	59.0				0.548	(0.06,5.35)	0.605	0.000	(0.00,-)	1.000
	NA	0.0	5.1				230782123.5	(0.00,-)	0.999	-	-	-

The parameter covariance matrix of all confounders cannot be computed, Multivariate Logistic Regression analyses was applied to adjust the selected confounders of age, gender, ethnic, smoking behaviour, drinking behaviour, betel quid chewing, staging, extent of primary tumour, vascular invasion, tumour perineural invasion and bone invasion, extracapsullar spread and skip metastasis.

Abbreviation: NA, not available Abbreviation: NA, not available; Abbreviations: N0 (no regional lymph node metastasis); N1 (metastasis in single ipsilateral lymph node, ≤3cm); N2 (metastasis in single ipsilateral lymph node, 3-6cm); N2B (metastasis in single ipsilateral lymph node, ≤6cm); N2C (metastasis in bilateral/ contralateral lymph node, ≤6cm); N3 (metastasis in lymph node >6cm); T1 (tumour ≤2cm); T2 (tumour 2-4cm); T3 (tumour >4cm); T4 (tumour invades adjacent structures such as tongue, skin of neck and through cortical bone)

* denotes significant p-value, $p<0.05$.

6.6 Summary

The results of Chapter 4 and 5 demonstrated that DDR1 was expressed in HNSCC (OPSCC and OSCC) cell lines and tumours and that two of its ligands, COL8a1 and COL11a1, were expressed in CAFs. This study extended this work to examine the expression of these proteins in a Malaysian cohort of OSCCs. DDR1 was expressed in all the tumours examined. COL8a1 and COL11a1 expression was detected in a proportion of the OSCC tumour cells and their associated CAFs. The expression of these proteins was quantified using Metamorph Pathology Analysis Software. The pattern of expression of DDR1, COL8a1 and COL11a1 showed some similarities in that higher expression was detected in patients with similar demographic and clinical features, such as females, non-smokers, non-drinkers and no extracapsular spread characteristics, but most of these association were not statistically significant. In patients of Indian ethnicity, tumours from betel quid chewers had higher expression of DDR1 and statistically significantly higher expression of COL11a1 in tumour cells and CAFs, most of these associations were statistically significant. Further, patients with bone invasion, 1-10mm tumour depth and with a deceased outcome showed statistical significantly high expression of COL8a1 in tumour cells. Interestingly, OSCC patients who have higher expression of DDR1, COL8a1 and COL11a1 tend to have deceased survival outcome but this did not reach statistical significance using the Kaplan-Meir analyses. Collectively, these data show that DDR1 and its ligands are expressed in OSCCs and their expression levels might influence patient prognosis.

CHAPTER 7: THE PHENOTYPIC IMPACT OF DDR1 KNOCKDOWN AND EXOGENOUS COLLAGEN ON OPSCC HUMAN CELL LINES

7.1 Introduction

The results presented in Chapters 4-6 showed that the collagen-activated tyrosine kinase receptor, DDR1, was overexpressed in both OPSCC and OSCC and that high expression of DDR1 correlated with reduced survival in HPV-negative OPSCCs. It remains unclear how collagen-mediated activation of DDR1 influences the malignant phenotype, but recent data has shown that DDR1 induces proliferation in epithelial ovarian cancers (V. Y. Chung *et al.*, 2017), migration and metastasis in colon cancer (Yuge *et al.*, 2017) and regulates the cytotoxic effects of a therapeutic immunotoxin (Ali-Rahmani *et al.*, 2016) and the chemotherapeutic drug, 5-fluorouracil (Wei *et al.*, 2017). However, the effect of collagen-DDR1 signalling on the behaviour of HNSCC cells has not been examined.

The work in this chapter aimed to determine the functional effects of exogenous collagen and to investigate whether these roles are mediated specifically by DDR1 in HNSCC cell lines *in vitro*. The phenotypic consequences investigated included cell growth and proliferation, clonogenicity, migration, invasion and the cellular response to Cisplatin.

7.2 Effect of exogenous collagen on HNSCC cell proliferation

The effects of exogenous collagen on the growth of the OPSCC cell lines SCC040, SCC154, VU040T and VU147T cells was determined using cell growth assay over a 12-day period. The cells were grown in the absence and presence of collagen (100μg/mL, Merck Millipore) and cell growth was measured by cell counting using a Luna Automated Cell Counter (Logos, Biosystems) after 4, and 12 days. The exogenous addition of collagen significantly promoted the growth of all four cell lines compared to cells grown in the absence of collagen (Figure 7.1).

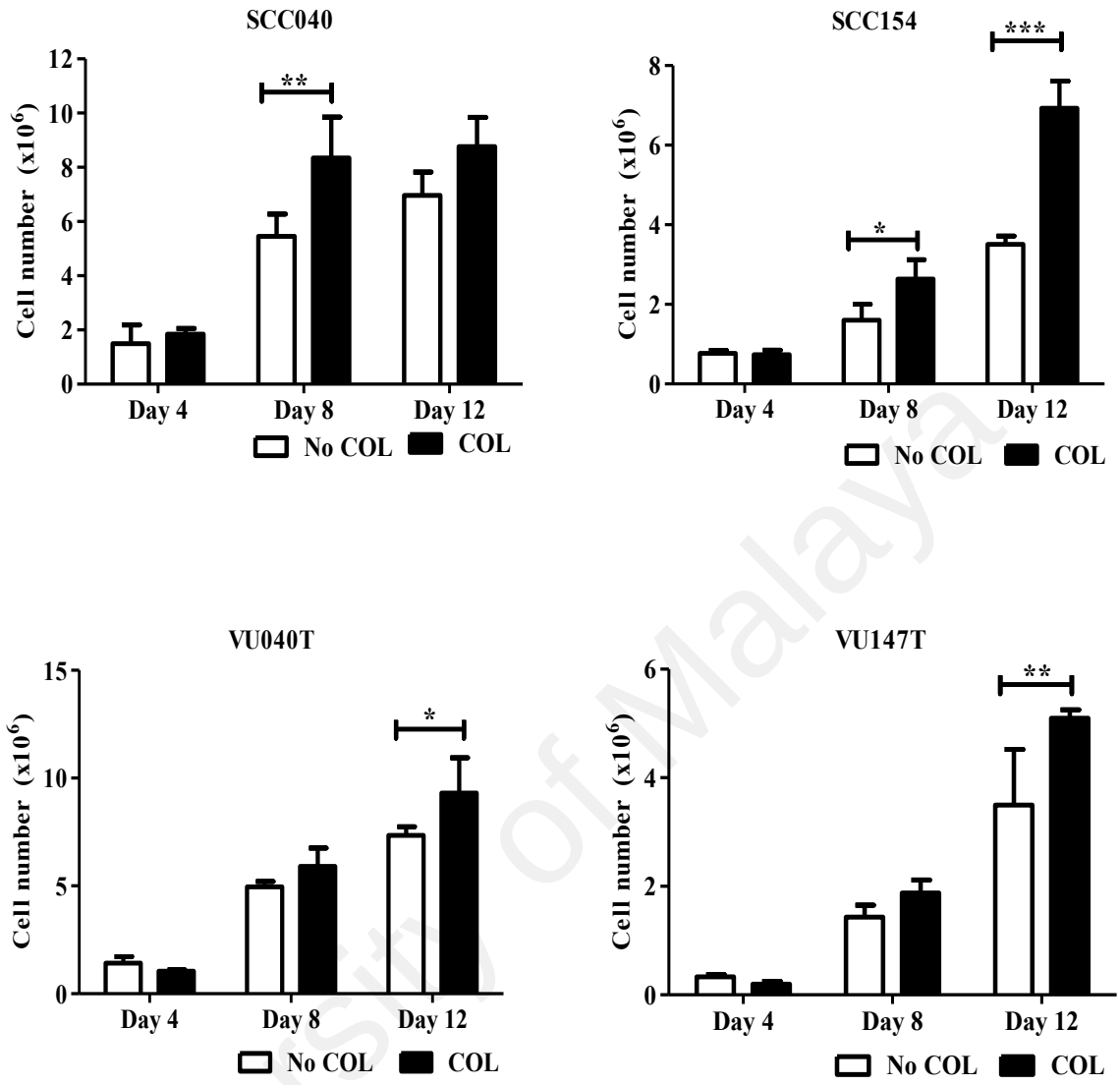

Figure 7.1: Exogenous collagen promoted the growth and proliferation of OPSCC cells.

The growth of SCC040, SCC154, VU040T and VU147T cell lines was examined in the absence or presence of collagen for 4-12 days. One-way ANOVA and Bonferroni Post Hoc Analyses showed that the exogenous addition of collagen significantly increased the growth of all four OPSCC cell lines. The data presented are representative of two independent experiments. *denotes $p<0.05$, ** denotes $p<0.01$, *** denotes $p<0.001$.

7.3 Effects of exogenous collagen on wound closure

The consequence of exogenous collagen on the wound closure response of SCC154 cells was examined using *in vitro* scratch assays. The denatured form of collagen, gelatin, which does not activate DDR1, was used as a negative control. The cells were grown in complete medium with or without or collagen (100μg/mL) or gelatin (100μg/mL) for 24 hours prior to the generation of the "wound" and images of the wound were captured at 24 hour intervals for 3 days. The ability of the cells to migrate and close the wound was enhanced by the addition of exogenous collagen in a time-dependent manner. Pre-treatment of SCC154 with collagen (100μg/mL) stimulated the wound healing process, whereby full closure of the wound was observed on after 2 days. Wound closure was not observed up to day 3 in cells grown in the absence of collagen or in the presence of gelatin (Figure 7.2).

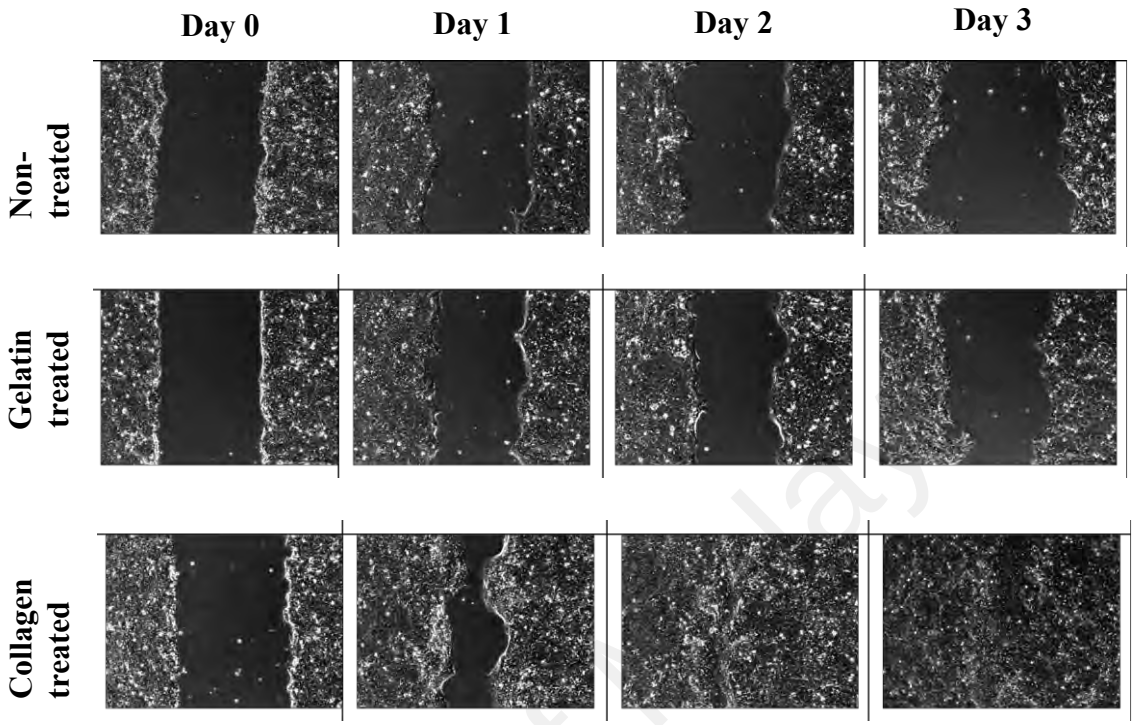

Figure 7.2: Stimulation of wound closure by exogenous collagen.

The wound closure/ scratch assay was performed in SCC154 cells grown on 6-well plates. SCC154 cells were treated with 100µg/mL gelatin, 100µg/mL collagen for 24 hours in serum-free medium before the wounds were scratched. Non-treated cells was used as a negative control. Photomicrographs were obtained at the indicated time points of Day 0, 1, 2 and 3 using 10X magnification on a Nikon Eclipse inverted microscope. Phase contrast images show the wound closure efficiency indicated by the distance that the cells moved from the edge of the scratch towards the centre of the scratch. Cells treated with collagen showed significant increase in wound closure rate compared to the control and cells treated with gelatin. The scratched area of cells treated with collagen was fully closed on Day 2 post-wounding but the wound remained unclosed over three days in the gelatin and non-treated controls. The data presented are representative of two independent experiments in duplicate wells each.

7.4 Effects of exogenous collagen on cell migration

The effect of exogenous collagen on the migratory ability of SCC040, SCC154, VU040T and VU147T cells was determined using Transwell migration assays. Cells were cultured in the presence or absence of collagen or gelatin (both 100μg/ mL) for 24 hours prior to seeding onto fibronectin-coated (10μg/mL) membranes. Media containing 20% FBS served as a chemo-attractant in the lower chamber and the number of migrated cells determined after 19 hours. The migration of the cells pre-treated with collagen was significantly ($p<0.001$) higher than cells pre-treated with gelatin or untreated controls (Figure 7.3).

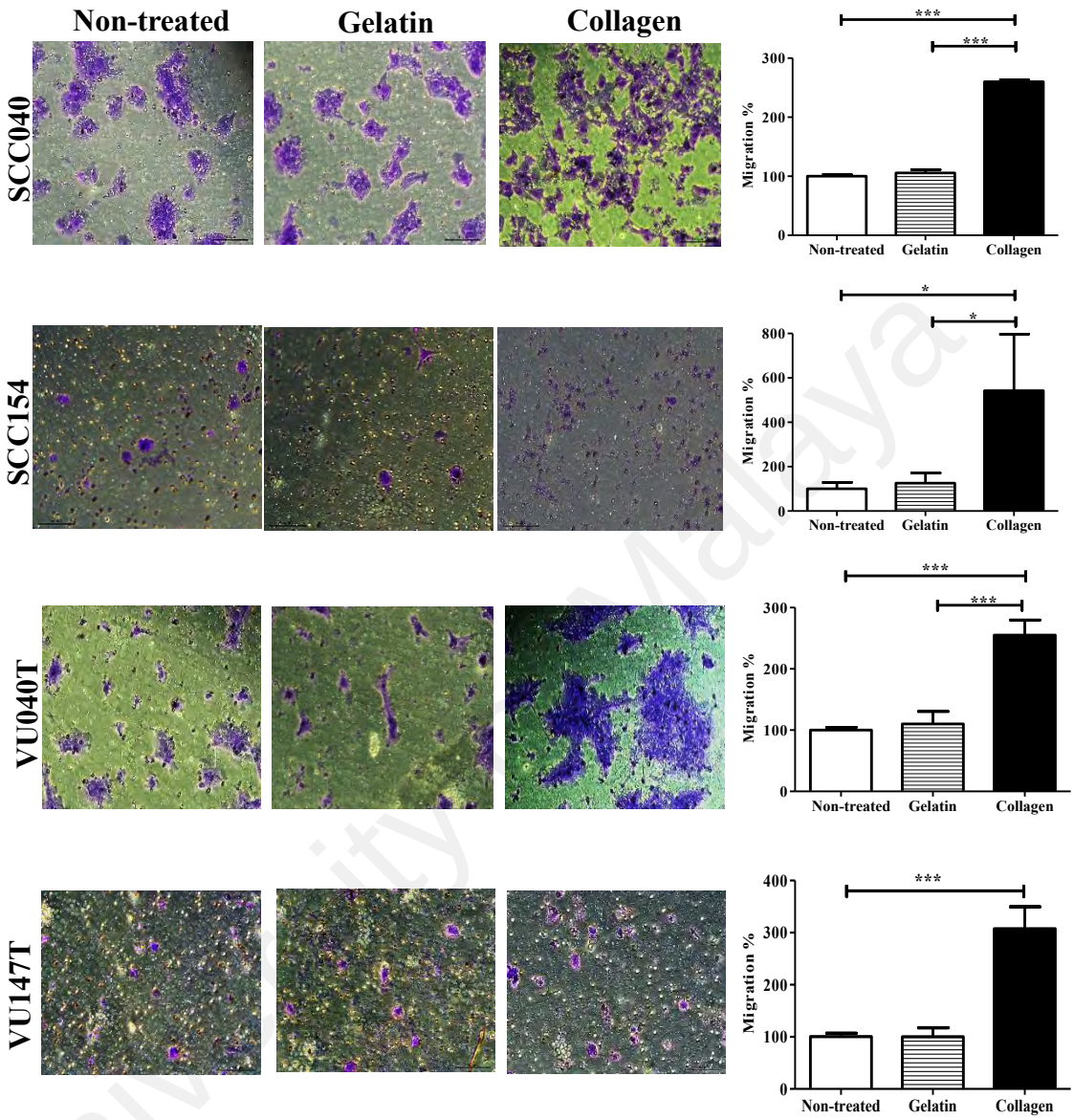

Figure 7.3: Collagen promoted OPSCC cell migration.

The migration of SCC040, SCC154, VU040T and VU147T cells was examined using Transwell assays in the absence or presence of gelatin and collagen (100µg/mL). Photomicrographs of migrated cells in each treatment groups were stained with 0.5% Crystal Violet and taken using 20X magnification on a Nikon Eclipse inverted microscope. Collagen but not denatured collagen (gelatin) significantly enhanced the migration of all the four cell lines examined. The data presented are representative of two independent experiments for each cell line. * denotes $p<0.05$ and *** denotes $p<0.0001$.

7.5 Effects of exogenous collagen on the response of OPSCC cells to Cisplatin

MTT assays were initially performed to test the effect of Cisplatin, on the OPSCC cell lines, SCC040, SCC154, VU040T and VU147T. Treatment of all the cell lines with Cisplatin for 72 hours resulted in a dose-dependent reduction in cell viability. VU040T and VU147T were selected as the representative cell lines for subsequent experiments due to similar IC_{50} values (50μM). A Cisplatin treatment dose of 50μM was chosen as the approximate IC_{50} to induce appropriate proportion of cell deaths as derived from the graph (Figure 7.4).

To study the effect of exogenous collagen on the response of cells to Cisplatin, VU040T and VU147T cells were grown with and without gelatin or collagen (100μg/mL) for 24 hours. Fluorescent Activated Cell Sorter (FACS; Becton Dickinson) flow cytometric analyses were carried out after 72 hours treatment with Cisplatin (50μM) or vehicle control (DMSO). Treatment of cells with DMSO induced a general 20%-30% early and late apoptosis. After 72 hours treatment with Cisplatin, collagen pre-treatment exerted significant inhibitory effect on the chemo-sensitivity of VU040T and VU147T in which the early and late apoptotic cells percentage were significantly reduced in the presence of collagen. In contrast, the early and late apoptotic percentages of VU040T grown in normal complete medium ($p<0.01$) and gelatin ($p<0.001$) were significantly higher than that of cells pre-treated with collagen. Similarly, the pre-treatment of another cell line, VU147T, with collagen also significantly suppressed the early and late apoptosis of cells towards Cisplatin compared to the non-pretreated control ($p<0.001$; Figure 7.5).

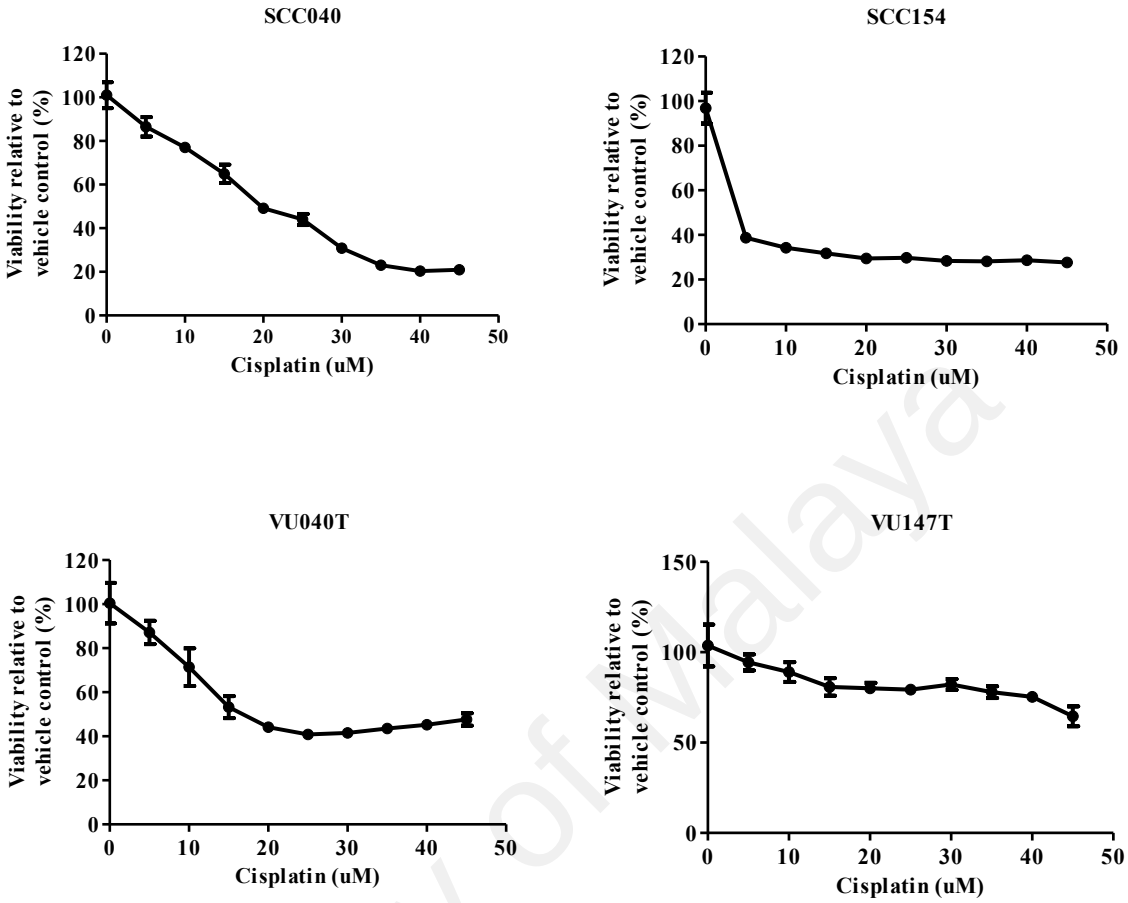

Cell line	IC_{50} (μM)
SCC040	20.0
SCC154	3.5
VU040T	46.0
VU147T	47.0

Figure 7.4: Cytotoxic effect of Cisplatin on OPSCC cell lines.

SCC040, SCC154, VU040T and VU147T were seeded for 24 hours before the 72 hours treatment of Cisplatin at the indicated concentrations in complete medium. MTT assays were performed following Cisplatin treatment. Results represent the percentage of cell viability expressed in relation to DMSO as the vehicle control for Cisplatin. The data presented are representative of two independent experiments. Data points, mean; error bars, SD of triplicates.

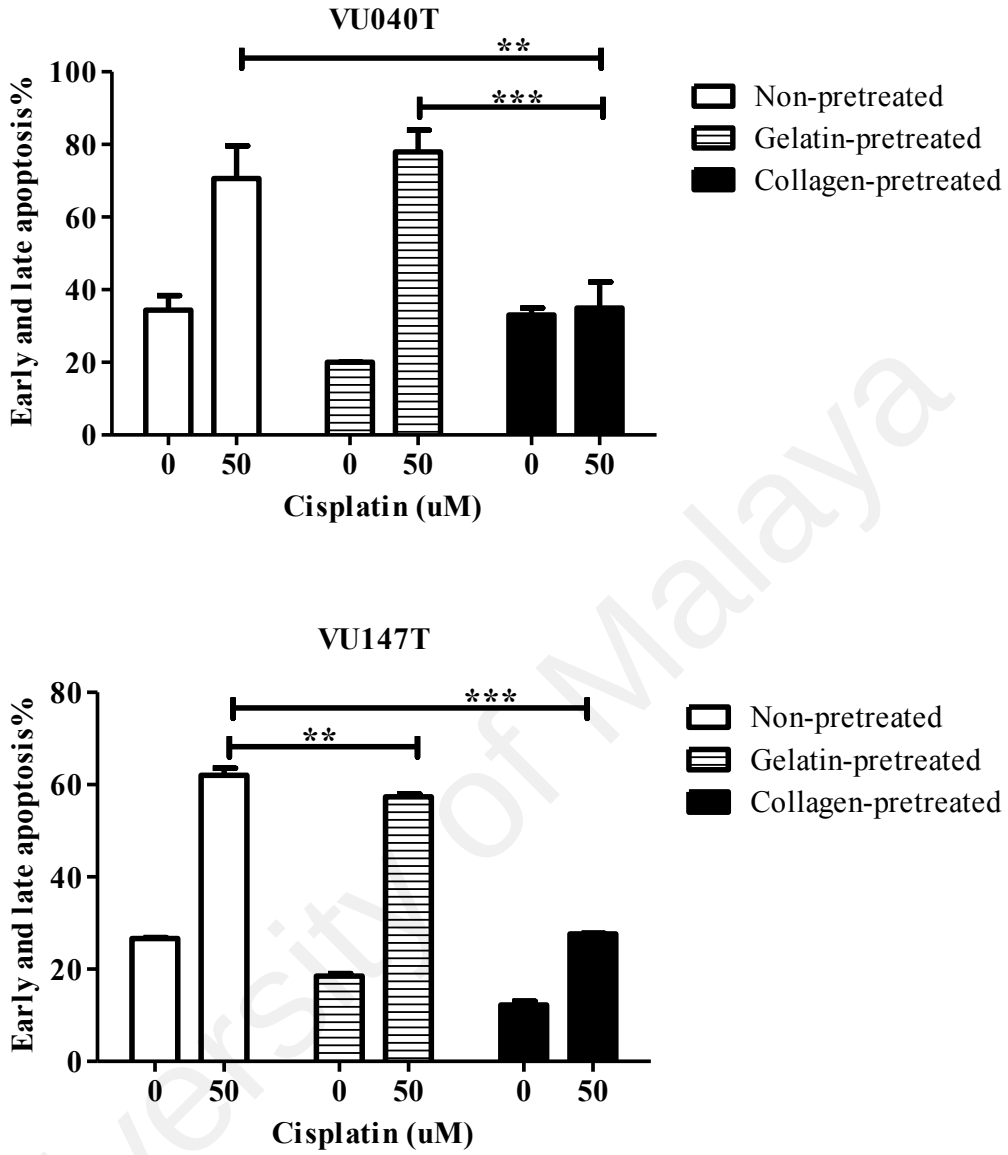

Figure 7.5: Exogenous collagen induced chemo-resistant response in OPSCC cells towards Cisplatin.

VU040T and VU147T were pre-treated with or without gelatin or collagen for 24 hours. Apoptosis was observed following treatment with 50μM Cisplatin for 72 hours as assessed by Annexin V-FITC/Propidium Iodide staining. DMSO was used as the vehicle control. The percentage of early and late apoptotic cells (Annexin V-FITC/ PI positive) were determined by fluorescent-activated cell sorter (FACS). Flow cytometer results showed the percentage of apoptotic cells were significantly reduced in cells pre-treated with collagen compared to the non-treated or gelatin-treated cells. The data presented are representative of two independent experiments. Data points, mean; error bars, SD of triplicates. ** denotes $p<0.01$; *** denotes $p<0.001$.

7.6 DDR1 isoform expression in HNSCC cell lines

Having shown that DDR1 is expressed in HNSCC cell lines and tissues (Chapters 4-6) reverse transcriptase polymerase chain reaction (RT-PCR) was performed to identify the major DDR1 isoforms expressed in OPSCC cell lines *in vitro*.

A set of primers to specifically amplify the juxtamembrane domain of the known 5 DDR1 isoforms (i.e. DDR1a-e) was used to examine DDR1 expression in HPV-positive and HPV-negative OPSCC cell lines. RT-PCR showed that the kinase active DDR1b isoform appeared to be the most highly expressed in all OPSCC cell lines. Two other kinase active forms, DDR1a and DDR1c, were detectable at lower levels, whilst the kinase inactive DDR1d and DDR1e isoforms were either absent or the bands were faint. In addition, the expression of the DDR1 transcripts in the OSCC cell line, H376, was determined using RNA-Seq. The RNA-Seq results revealed that amongst the known 58 DDR1 transcripts, 42 variants were expressed in H376 and 16 transcripts were missing (Appendix L). The top ten most abundant transcripts are listed in Table 7.1. Further sequence alignment was done by comparing the transcript table of DDR1 in Ensembl genome database with the five DDR1 known isoforms as reported by Valiathan *et al.* (2012). The sequence alignment results, based upon the number of amino acids, showed that the most abundant transcript encoded for the DDR1b isoform (Table 7.2). Subsequently, the PCR amplified products of OPSCC were ran in parallel with H376 by using primers that optimized to amplify only the DDR1 juxtamembraneous domain and subjected to gel electrophoresis. The strongest band present was found to correspond to the kinase-active DDR1b isoform (Figure 7.6).

Table 7.1: Top ten most abundant transcript isoforms of DDR1 in OSCC cell line

Transcript ID	Length	Average abundances from triplicates (%)
ENST00000452441 DDR1-208	3857	36.61
ENST00000446312 DDR1-207	3202	15.61
ENST00000376569 DDR1-003	3783	12.01
ENST00000396342 DDR1-013	675	5.28
ENST00000376568 DDR1-002	3894	4.71
ENST00000376570 DDR1-205	3820	4.67
ENST00000418800 DDR1-012	3588	3.84
ENST00000506573 DDR1-033	585	3.63
ENST00000412274 DDR1-031	496	2.48
ENST00000509639 DDR1-030	615	1.32

Table 7.2: Sequence alignment of DDR1 transcripts in Ensembl genome database with DDR1 isoforms

DDR1 isoforms	Number of amino acids	Corresponding transcripts in Ensembl
DDR1a	876	ENST00000454612 ENST00000376567 ENST00000376570 ENST00000376569 ENST00000418800
DDR1b	913	ENST00000324771 ENST00000376568 ENST00000452441
DDR1c	919	ENST00000513240
DDR1d	508	None
DDR1e	767	ENST00000446312

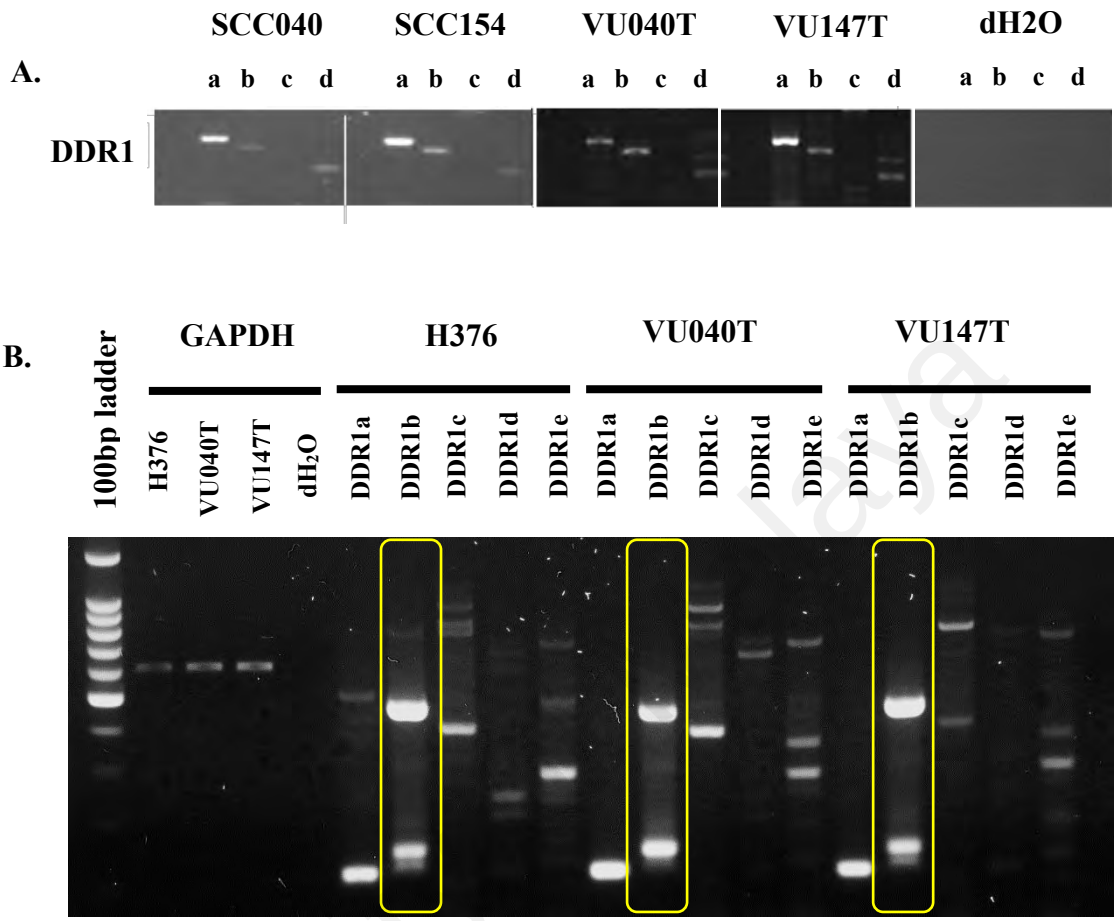

Figure 7.6: Identification of the major DDR1 isoform in HPV-negative and HPV-positive OPSCC cell lines.

A. Kinase active DDR1b isoform appeared to be the most highly expressed in all HPV-negative (SCC040 and VU040T) and HPV-positive (SCC154 and VU147T) OPSCC cell lines. Distilled water, dH2O, was used as the negative control. **B.** The sequence alignment results showed that the most abundant transcript in H376 obtained from Ensembl genome database was encoded for the DDR1b isoform in gel electrophoresis. With H376 as the reference control, representative HPV-negative (VU040T) and HPV-positive (VU147T) cell lines showed the similar trend with H376 suggesting the same most abundant transcript in these cell lines. Two other kinase active forms, DDR1a and DDR1c, were detectable at lower levels, whilst the kinase inactive DDR1d and DDR1e isoforms were either absent or the bands were faint. The data presented are representative of two independent experiments.

7.7 Biological significance of DDR1 knockdown

7.7.1 Stable knockdown of DDR1 in human OPSCC cell lines

The two HPV-negative (SCC040 and SCC154) and HPV-positive (VU040T and VU147T) OPSCC cell lines were used to perform the knockdown experiments. The cells were stably transduced with plasmids carrying three independent sequences of DDR1 shRNAs (shDDR1_10084, shDDR1_121163 and shDDR1_121293) or non-targeting shRNA (NS).

Compared to the parental cells, the DDR1 mRNA levels of all the cells transduced with shDDR1_10084 and shDDR1_121293 were significantly reduced by 65% to 95% ($p<0.001$) whereas the DDR1 mRNA levels of the cells transduced with shDDR1_121163 was reduced by 39.2% to 78% ($p<0.001$). The DDR1 mRNA level were remained high in the EV and NS controls of all cell lines. Therefore, cells transduced with shDDR1_10084 and shDDR1_121293 were selected for further study. Knockdown of DDR1 also led to a significant decrease in DDR1 protein of the selected shRNA clones compared to the parental, EV and NS controls. The knockdown also appeared to be specific for DDR1 with no noticeable effect on GAPDH levels (Figure 7.7).

The knockdown of DDR1 was checked regularly and appeared stable over time and after several passages.

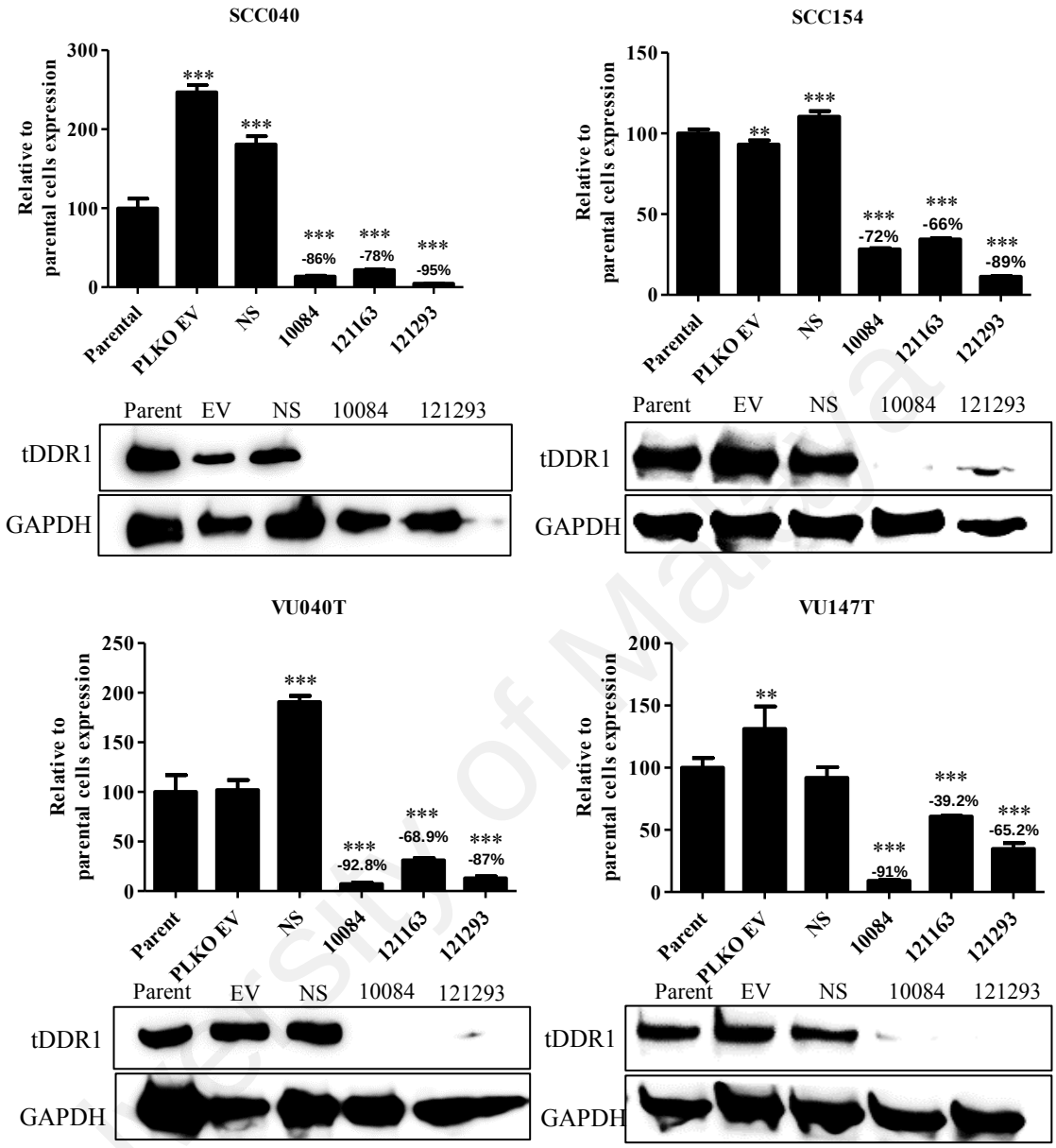

Figure 7.7: DDR1 mRNA expression and protein levels in SCC040, SCC154, VU040T and VU147T cells following knockdown of DDR1.

All the four OPSCC cell lines were stably transduced with plasmids carrying three independent sequences of DDR1 shRNAs or the empty vector (EV) and non-targeting shRNA sequence (NS). Compared to parental cells, transduction resulted in approximately 65.2%-95% reduction of DDR1 in two knockdown clones of 10084 and 121293. The data presented are representative of two independent experiments. Western blot analyses showed that the level of DDR1 proteins was decreased in the cells transduced with shRNA clones and results were in concordance with the Q-PCR results.

7.8 Effect of knock down of DDR1 on OPSCC cell growth and clonogenic survival

The consequence of DDR1 knockdown on the growth of OPSCC cells was determined using growth assays over a period of 12 days. Compared to the parental and NS controls, knockdown of DDR1 significantly inhibited the growth of all the four OPSCC cells from the fourth day onwards. One-way ANOVA and Bonferroni Post Hoc comparisons showed a significant difference in cell number between parental controls and cells following DDR1 knockdown (Figure 7.8).

As exogenous addition of collagen resulted in enhanced cell growth and DDR1 knockdown decreased cell growth, further experiments were carried out to determine the consequence of exogenous addition of collagen on the growth of cells following DDR1 knockdown for DDR1. In agreement with previous results (Figure 7.1), exogenous addition of collagen promoted the growth of parental and NS controls of all the four cell lines. In contrast, knockdown of DDR1 did not alter cell growth in either the absence or presence of exogenous collagen (Figure 7.9).

The colony surviving ability of VU040T and VU147T cells following knockdown of DDR1 was also determined by clonogenic assay. Single cell suspensions were seeded into each 60mm dish and media were replenished every four days. The counting of the colonies stained with 0.5% Crystal Violet after 14 days showed that DDR1 knockdown significantly reduced the number of surviving colonies compared to the parental controls ($p<0.001$; Figure 7.10).

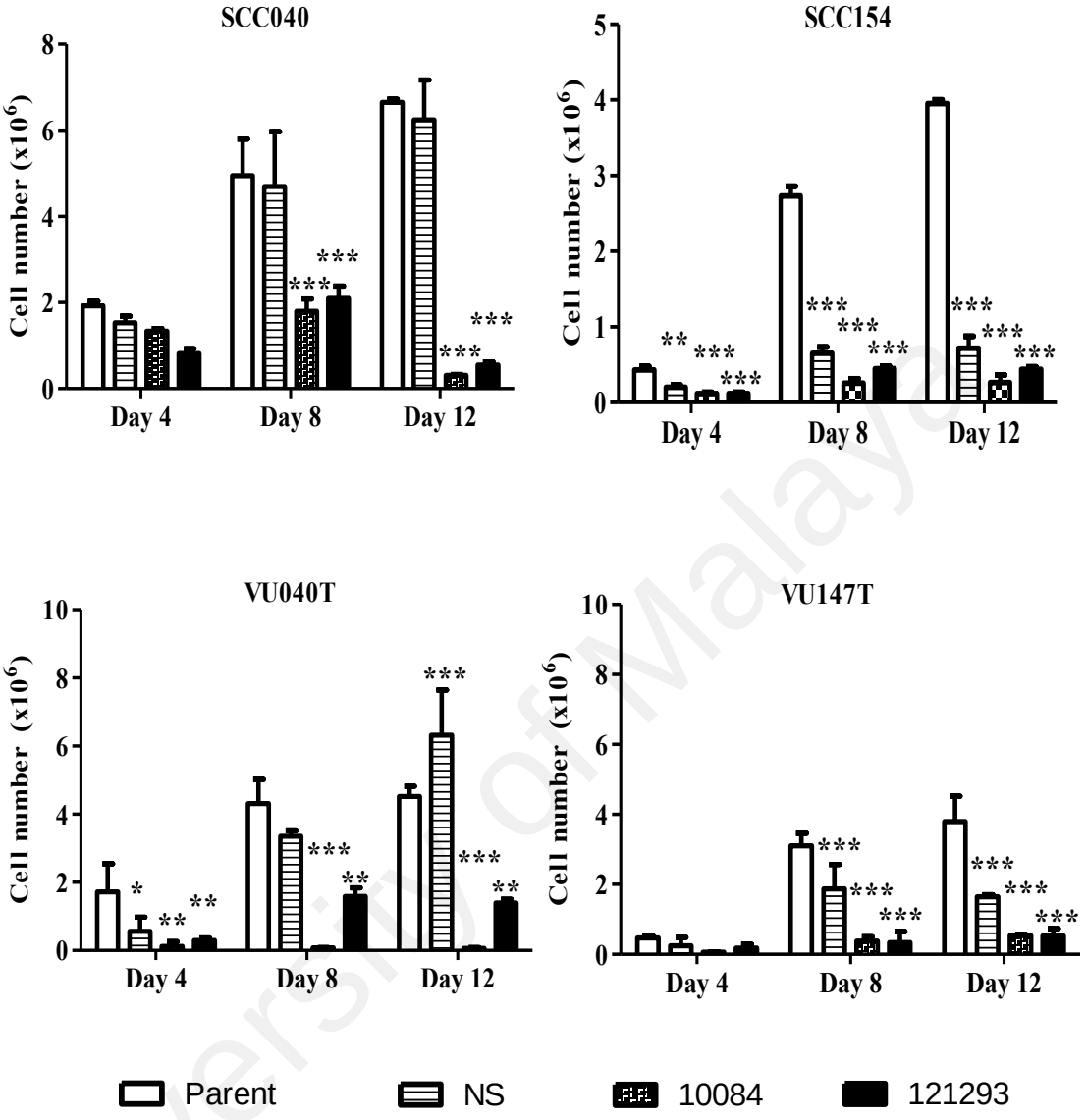

Figure 7.8: Knockdown of DDR1 decreased the growth of OPSCC cells.

Following DDR1 knockdown, SCC040, SCC154, VU040T and VU147T cells grew slower compared to the parental and NS controls. One-way ANOVA and Bonferroni Post Hoc Analyses comparing all the cells to the parental control showed a significant difference in cell number. The data presented are representative of two independent experiments. * denotes $p<0.05$, ** denotes $p<0.01$, *** denotes $p<0.001$.

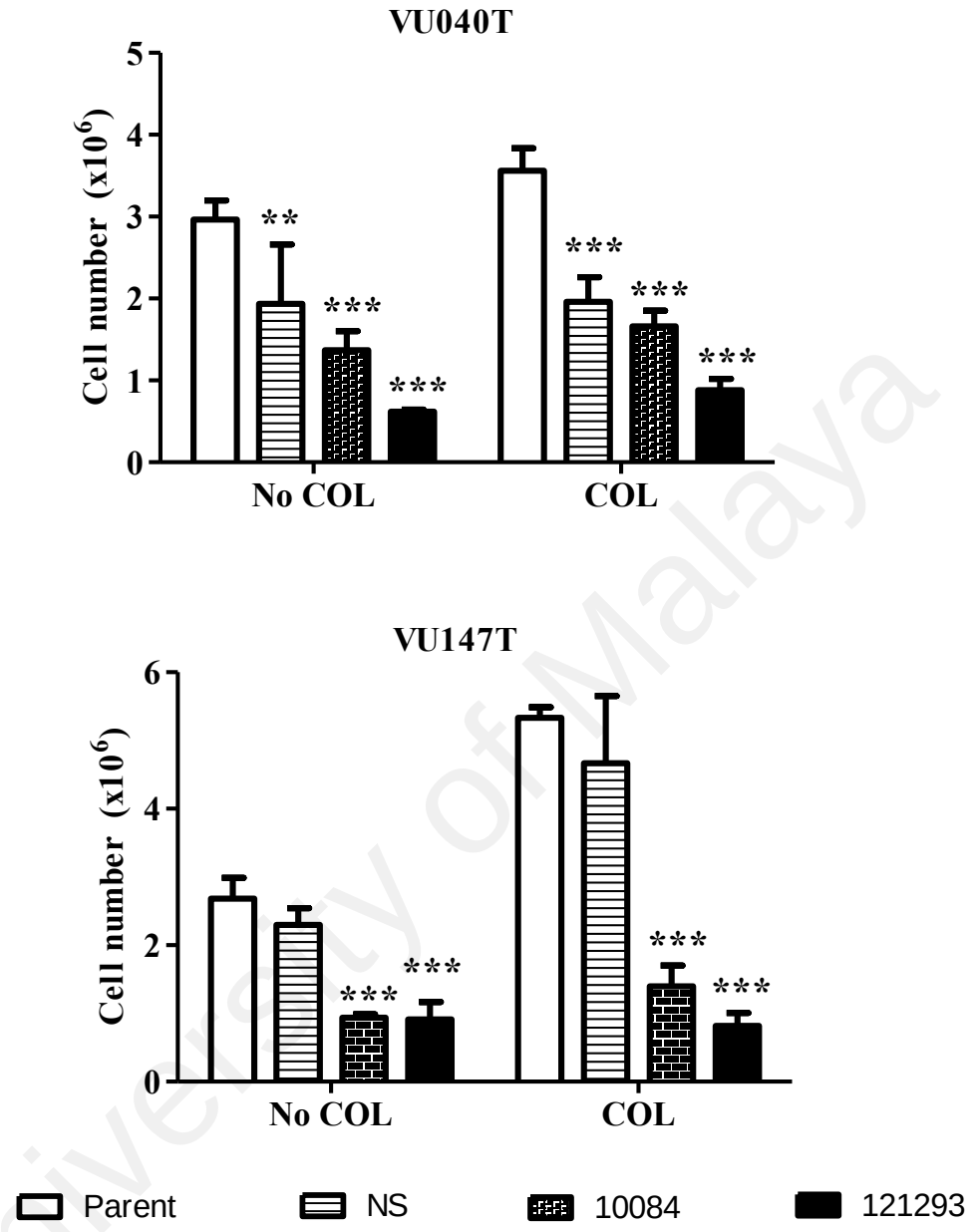

Figure 7.9: Knockdown of DDR1 inhibited the growth effect of exogenous collagen on OPSCC cells.

The growths of VU040T and VU147T cell lines were examined in the absence or presence of collagen for 8 days. One-way ANOVA and Bonferroni Post Hoc analyses showed that the knockdown of DDR1 significantly inhibited the growth of both cell lines despite the presence of exogenous collagen. The data presented are representative of two independent experiments. * denotes $p<0.05$, ** denotes $p<0.01$, *** denotes $p<0.001$.

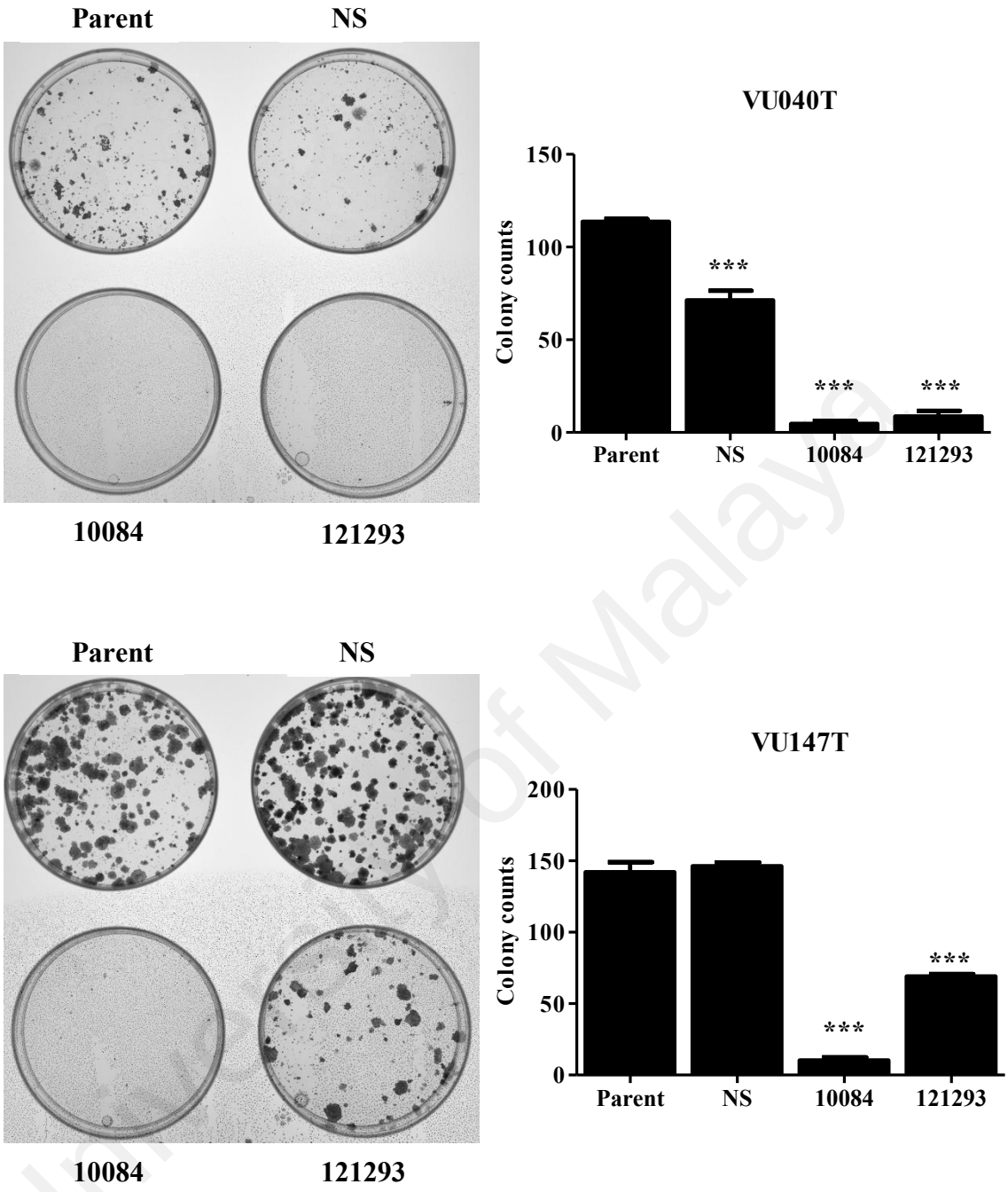

Figure 7.10: Knockdown of DDR1 reduced the surviving colonies of OPSCC cells.

A cluster of at least 20 cells stained by 0.5% Crystal Violet counted under 20X magnification was considered as a colony. Following DDR1 knockdown, less colonies of VU040T (top panel) and VU147T (bottom panel) formed and survived over a period of 14 days compared to the parental and NS controls. One-way ANOVA and Dunnett Post Hoc Analyses comparing all the cells to the parental control showed significant difference of colony survived after 14 days. The data presented are representative of two independent experiments. *** denotes $p<0.001$.

7.9 Effect of DDR1 knockdown on wound closure

The effect of DDR1 knockdown on the wound closure efficiency of HNSCC cells was examined. Addition of collagen (100μg/mL) to the parental cells and NS controls enhanced the closure of the wound area from Day 2 post-wounding. In contrast, following DDR1 knockdown, the SCC040 cells did not respond to the wounding at all compared to the parental and NS controls despite the presence or absence of collagen. These data indicated that DDR1 plays an important role in the wound closure effect stimulated by exogenous addition of collagen (Figure 7.11).

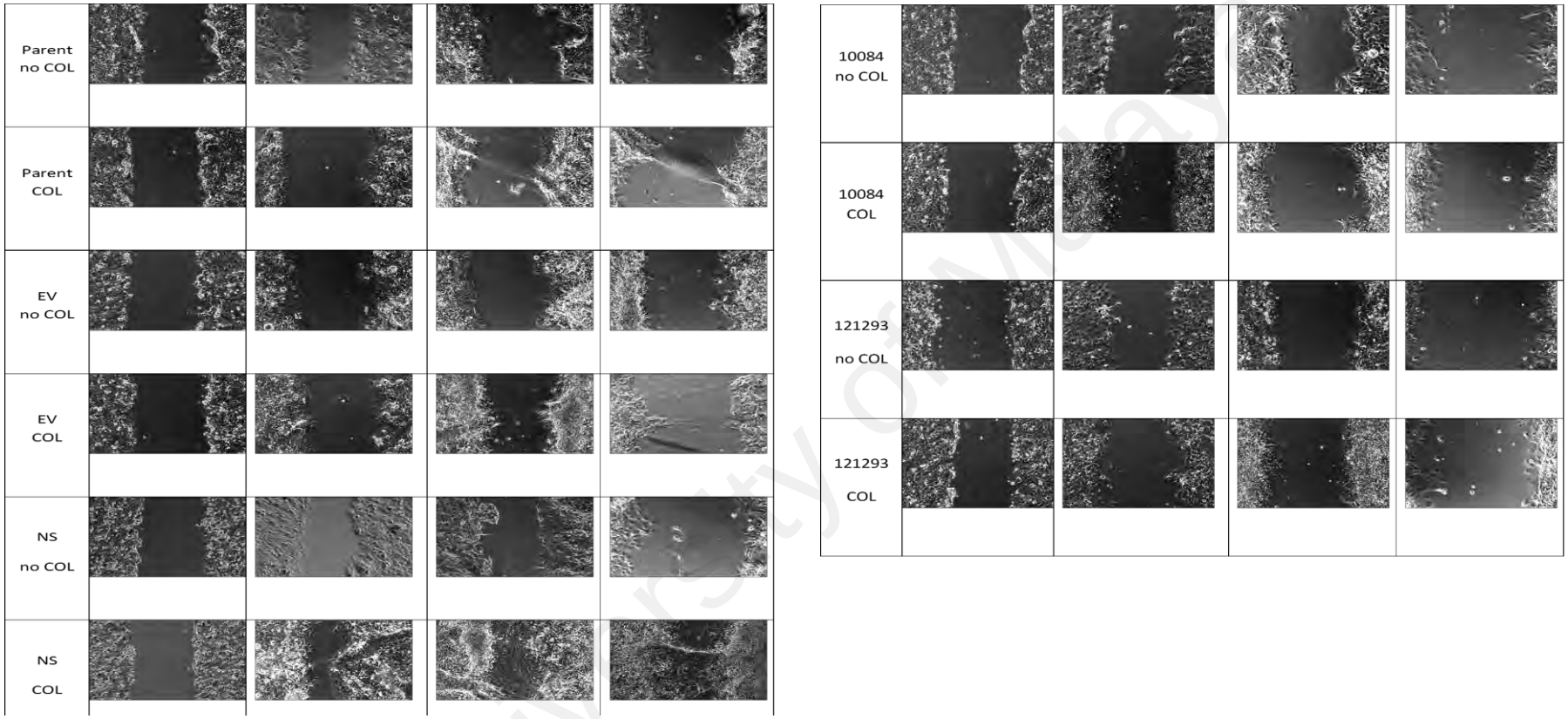

Figure 7.11: Knockdown of DDR1 inhibited HNSCC motility in wound closure.

The effect of DDR1 knockdown on the wound closure was performed in SCC040 seeded on 6-well plates in Day 0, 1, 2 and 3. The parental cells and NS controls showed cell motility to close the wound in the presence of collagen (100µg/ mL) but following DDR1 knockdown, the SCC040 cells did not respond to the wounding at all compared to the controls despite the presence or absence of collagen. The data presented are representative of one cell line from two independent experiments.

7.10 Effect of DDR1 knockdown on cell migration & invasion

Transwell migration assays were also performed to determine the migratory ability of VU040T and VU147T cells following DDR1 knockdown. The parental and NS controls showed increased migration ability following pre-treatment with collagen (100μg/mL). Compared to parental and NS controls, DDR1 knockdown significantly suppressed the migration of VU040T/DDR1_10084, VU040T/DDR1_121293, VU147T/DDR1_10084 and VU147T/DDR1_121293 cells by at least 90% ($p<0.0001$; Figure 7.12). These data were in agreement with the results obtained above (Figure 7.3) that addition of exogenous collagen enhanced the migration of OPSCC cells.

To investigate the effect of DDR1 knockdown and collagen on HNSCC cell invasion, the invasive ability of VU040T and VU147T cells were measured using matrigel-coated Transwells. The results showed that DDR1 knockdown markedly suppressed the invasion of the cells compared to parental and NS controls ($p<0.0001$; Figure 7.13).

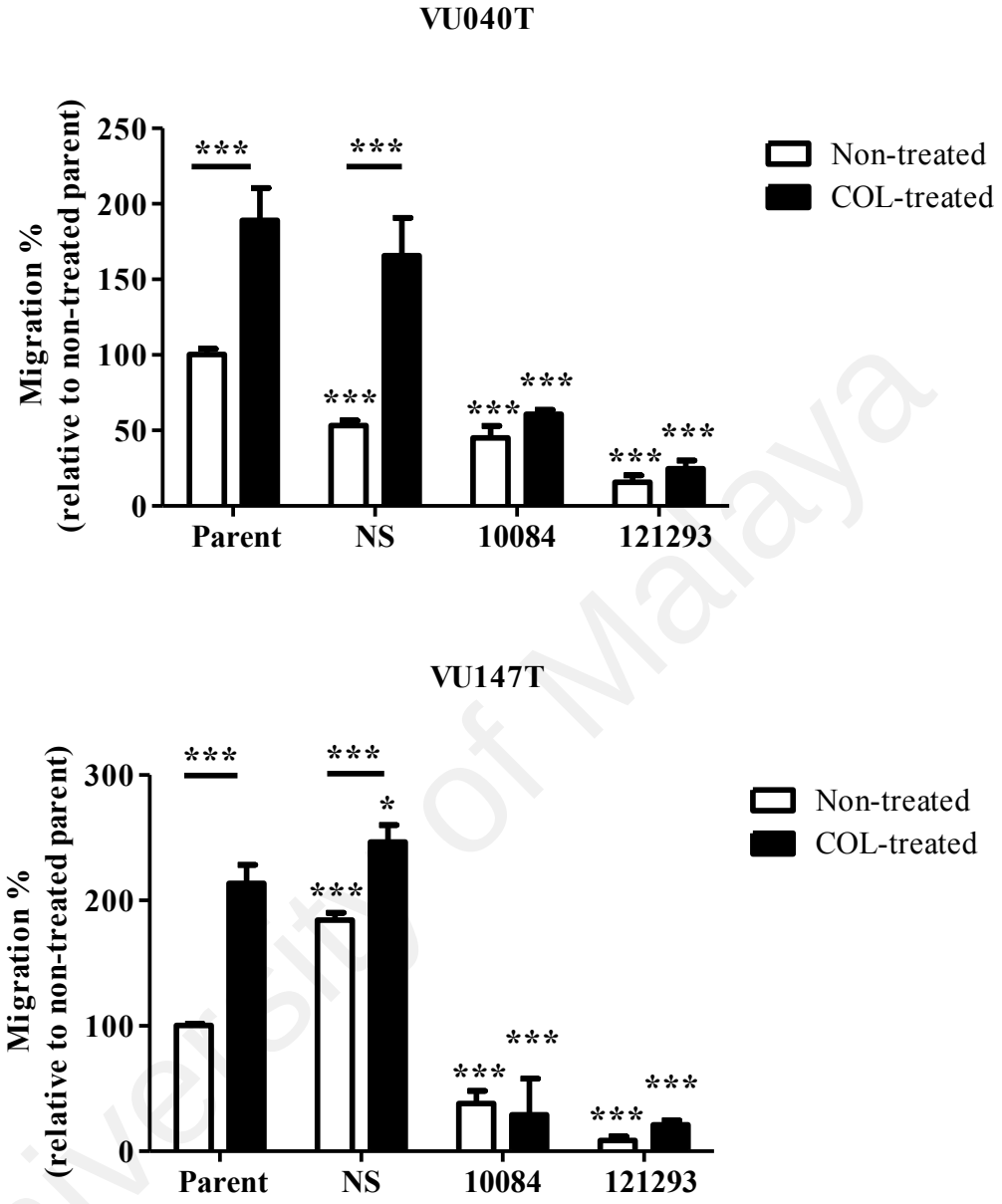

Figure 7.12: Knockdown of DDR1 inhibited HNSCC cell migration.

The effect of DDR1 knockdown on the migration of HNSCC cells was examined using Transwell assay in the presence of 20% FBS in the lower chamber as chemo-attractant. One-way ANOVA and Bonferroni Post Hoc Analyses showed that compared to parental control, knockdown of DDR1 significantly inhibited the migration of HNSCC cells. The data presented are representative of two independent experiments. * denotes $p<0.05$, *** denotes $p<0.001$.

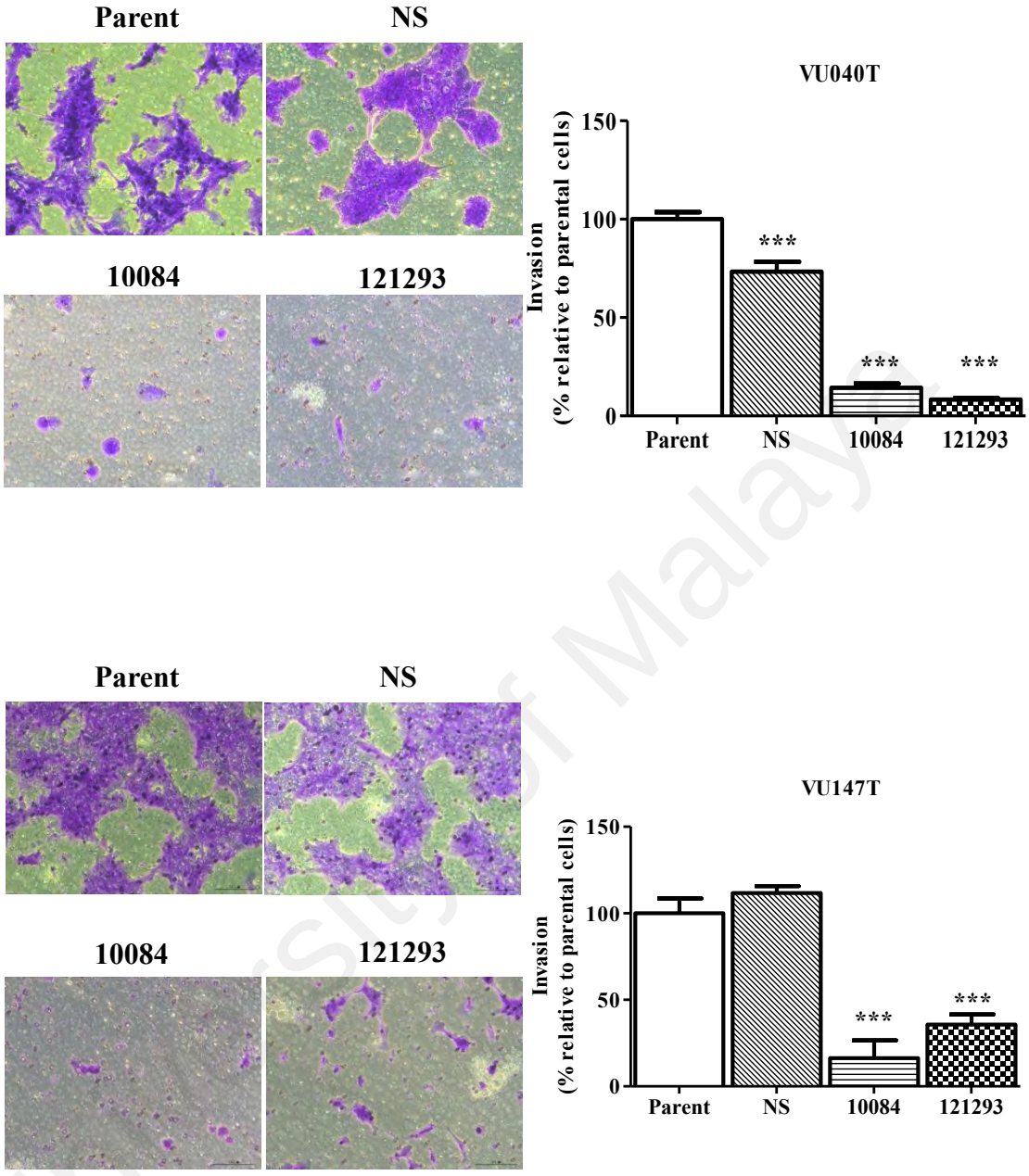

Figure 7.13: Knockdown of DDR1 inhibited HPV-negative and HPV-positive HNSCC cell invasion.

The effect of DDR1 knockdown on the invasion was performed on VU040T and VU147T cells seeded in 24-well plate growth factors reduced matrigel pre-coated invasion chamber in the presence of media containing 20% FBS in the lower chamber as chemo-attractant. One-way ANOVA and Dunnett Post Hoc analyses showed that compared to parental and NS controls, knockdown of DDR1 significantly inhibited the invasion of both HPV-negative and HPV-positive HNSCC cells. The data presented are representative of two independent experiments. *** denotes $p<0.0001$.

7.11 Effect of DDR1 knockdown on chemo-therapeutic response of HNSCC cells

To confirm the effects of collagen on Cisplatin sensitivity were mediated by DDR1, FACS analysis were performed using Cisplatin-treated VU040T and VU147T cells following knockdown of DDR1. The cells were grown in normal complete medium or collagen (100μg/mL) for 24 hours prior treated with Cisplatin (50μM). Collagen pre-treatment significantly inhibited the cytotoxicity of Cisplatin on the parental and NS cells compared to their controls grown in complete medium ($p<0.01$ and $p<0.001$ respectively). In contrast, these inhibitory effects of collagen were impaired in the VU147T/DDR1_10084 and VU147T/DDR1_121293 cells. Their early and late apoptosis percentage were even significantly higher than their counterparts grown in complete medium ($p<0.01$ and $p<0.001$ respectively; Figure 7.14).

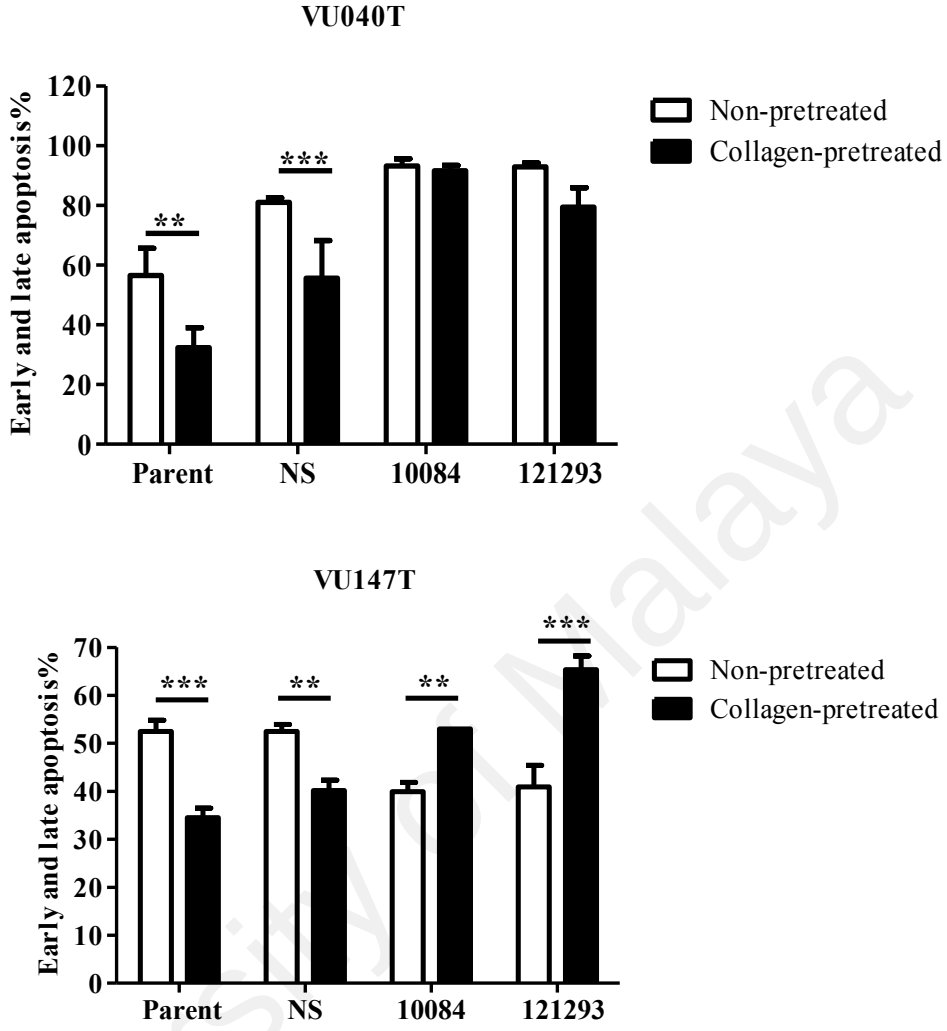

Figure 7.14: Knockdown of DDR1 enhanced the Cisplatin chemo-sensitivity response of HNSCC cells.

The parental cells, NS control and two clones knockdown for DDR1 of VU040T and VU147T were pre-treated with or without collagen for 24 hours. Apoptosis was observed following treatment with 50μM Cisplatin for 72 hours as assessed by Annexin V-FITC/Propidium Iodide staining. DMSO was used as the vehicle control. The percentage of early and late apoptotic cells (Annexin V-FITC/ PI positive) were determined by fluorescent-activated cell sorter (FACS; Becton Dickinson). Flow cytometer results showed the percentage of apoptotic cells were significantly decreased in the parental and NS cells pre-treated with collagen, but remained high in cells knockdown for DDR1. The data presented are representative of two independent experiments. Data points, mean; error bars, SD of triplicates. ** denotes $p<0.01$; *** denotes $p<0.001$.

7.12 Summary

In this chapter, the effects of collagen on the behaviour of HNSCC cells were investigated using *in vitro* assays of cell growth, clonogenic survival, wound healing, migration, invasion and cytotoxicity response to chemotherapeutic drug, Cisplatin. These effects were further confirmed to be mediated by DDR1 using shRNA-mediated knockdown.

In order to examine the contribution of collagen to the behaviour of HNSCC cells, the assays were carried out in the absence or presence of exogenous collagen. Exogenous treatment of HNSCC cells with collagen promoted growth and migration in all the cell lines examined. Further, treatment of cells with collagen reduced the amount of apoptosis induced in response to Cisplatin. These effects were specific because these cell behaviours were unaffected by denatured collagen (gelatin). The kinase active DDR1 isoform, DDR1b, was shown to be the predominant isoform expressed in HNSCC cells and is likely to mediate the effects of collagen.

Next, to confirm the involvement of DDR1 in mediating the effects of collagen, shRNA-mediated knockdown of DDR1 was employed. The growth, proliferation, clonogenic survival, migration, invasion and chemo-resistant were significantly inhibited following DDR1 knockdown and these phenotypes were markedly suppressed even in the presence of exogenous collagen.

Collectively, these data indicate that collagen plays a significant role in promoting the malignant phenotypes of HNSCC and DDR1 is the primary receptor involved in the collagen-mediated promotion of the malignant phenotype in these cells. This suggests that the DDR1/ collagen axis might be a novel therapeutic target for HNSCC patients.

CHAPTER 8: DISCUSSION

8.1 Introduction to discussion

It is becoming widely acknowledged that cross-talk between the tumour microenvironment (TME) and epithelial malignancies plays a crucial role in the pathogenesis of cancer and alters the behaviour of tumour cells. For example, the oncogenic function of CAFs has been shown to mediate bladder cancer invasion and progression (M. Miyake *et al.*, 2016), crosstalk between fibroblasts and liver tumours exacerbates hepatocarcinoma initiation (Luo *et al.*, 2017) and CAFs promote chemoresistance in ovarian cancer (Leung *et al.*, 2017). However, very little is known about the cross-talk between CAFs and tumour cells in HNSCC.

It is evident that DDR1 signalling plays an important role in promoting tumorigenesis in a wide range of cancer types by enhancing tumour progression (Barisione *et al.*, 2017), resistance to cell death (Fathima Zumla Cader *et al.*, 2013), migration and invasion (Zhaofeng Wang *et al.*, 2017; R. Xie *et al.*, 2016; Yuge *et al.*, 2017), angiogenesis (Raimondi *et al.*, 2014) and epithelial to mesenchymal transition (Song *et al.*, 2016). However, the expression of DDR1 and its collagen ligands and the biological consequences of DDR1 signalling in the pathogenesis of OPSCC and OSCC has never been studied. Hence, the present study was initiated to investigate biological significance of collagen-DDR1 signalling involved in the cross-talk of CAFs with OPSCC and OSCC tumour cells. The results of this study demonstrated that COL8a1 and COL11a1 are up-regulated in senescent CAFs derived from HNSCC compared to non-senescent CAFs and normal fibroblasts. By contrast, DDR1 was expressed in OPSCC and OSCC cell lines and tissues, but not CAFs. Next, COL8a1, COL11a1 and DDR1 were shown to be significantly associated and correlated with socio-demographic, clinico-pathological

parameters and most importantly with the patient survival. The function of collagen-DDR1 signalling was investigated *in vitro* and it was shown that exogenous collagen, acting via DDR1, enhanced HNSCC growth, colony survival, cell motility in wound closure, migration, invasion, as well as causing resistance to the chemotherapeutic drug, Cisplatin.

For ease of interpretation, the Discussion has been subdivided such that consideration is given to the data reported in each Results chapter. The following sections discuss the limitation of this study and present proposals for future work.

8.2 Identification of collagen subtypes and receptors that could mediate cross-talk between CAFs and HNSCCs

Evidence exists to show that cancer progression results in the induction of senescence in CAFs (Yazan Hassona *et al.*, 2013; E. K. Kim *et al.*, 2018) and, in turn, the paracrine signalling between CAFs and tumour cells can contribute to tumorigenesis in many malignancies (Ammirante *et al.*, 2014; Gascard & Tlsty, 2016; T. Wang *et al.*, 2017). For example, senescent CAFs have been reported to drive prostate cancer progression (Taddei *et al.*, 2014) and promote keratinocyte invasion and dis-cohesion relative to non-senescent fibroblasts (Y Hassona *et al.*, 2014). The present study attempted to identify the soluble ECM proteins which are up-regulated in senescent CAFs compared to non-senescent CAFs and normal fibroblasts. A previous transcriptomic expression profile reported by Lim *et al.* (2011b) identified two collagen subtypes, short chain collagen COL8a1 and fibrillar collagen COL11a1, that were up-regulated in senescent CAFs, indicating that these collagens are secreted ECM proteins produced by senescent CAFs and released into the tumour stroma. In the current study, the up-regulation of COL8a1 and COL11a1 mRNA level was validated in an independent panel of 6 HNSCC associated

senescent and non-senescent CAFs and 3 normal oral fibroblasts by Q-PCR. These results are in agreement with a previous study which found a distinguishable gene expression profile of oral senescent and non-senescent CAFs (Y Hassona *et al.*, 2014). Consistent with this report, RNA-sequencing studies have shown that collagen fibre organisation by senescent CAFs correlates with poor prognosis in HNSCC and oesophageal cancer and it impacts patients survival (Mellone *et al.*, 2017). However, the biological roles of COL8a1 and COL11a1 in the pathogenesis of HNSCC remain largely unexplored.

Collagens are the major constituent of the ECM and there are several types of receptors that interact with collagen to trigger intracellular signalling pathways. For example, some integrin family members (Lundgren-Åkerlund & Aszòdi, 2014; Raab-Westphal *et al.*, 2017), the immunoglobulin-like receptor (Fu *et al.*, 2017) and the mannose receptor (Jürgensen *et al.*, 2014) are activated following collagen binding. Another receptor is DDR1, which is a receptor tyrosine kinase that has been shown to be activated by a number of different collagen types (B Leitinger, 2016). DDR1 acts as an unique and specific receptor for collagens (C. Wang *et al.*, 2016; Yeung *et al.*, 2013), although the precise mechanism of activation by collagen is currently unknown. De-regulated DDR1 signalling contributes to diseases such as fibrotic disorders (Z. Wang *et al.*, 2016), inflammation (Dorison *et al.*, 2017) and arthritis (B Leitinger, 2016) and a number of studies have suggested a role for DDR1 in various cancer types (Rammal *et al.*, 2016a). However, the expression of DDR1 and its functional role in the pathogenesis of OPSCC and OSCC has not been investigated.

As COL8a1 and COL11a1 were found to be up-regulated in senescent CAFs in the present study, it was hypothesised that DDR1 would be expressed by tumour cells. Indeed, DDR1 was shown to be expressed at both the mRNA and protein levels in a panel

of OPSCC and OSCC cell lines but expression was undetectable in the fibroblasts strains. Further, a preliminary study indicated that DDR1 protein was over-expressed in both OPSCC and OSCC tissues. Taken together, these findings suggest that COL8a1 and COL11a1 are secreted by the CAFs into tumour microenvironment where they activate DDR1, which is expressed on tumour cells, to influence tumour cell behaviour.

Analysis of the RNAseq data in the Cancer Genome Atlas (TCGA) database, showed that DDR1 was up-regulated in HNSCCs compared to normal tissues. This is in line with the findings that DDR1 was aberrantly overexpressed in other cancer types, such as ovarian (Y. Deng *et al.*, 2017) and breast cancer (Belfiore *et al.*, 2018). However, the TCGA database analyses revealed no statistically significant difference of DDR1 between HPV-negative and HPV-positive HNSCC. This might be explained by a number of outliers in HPV-negative tumours which showed high expression of DDR1. High expression of DDR1 is associated with poor prognosis in bladder cancer patients (X. Xie *et al.*, 2017). However, in the present study, there was only a weak association of lower overall survival in HPV-negative HNSCC with high expression of DDR1 mRNA but this was not statistically significant. Further studies to examine DDR1 at the protein level were subsequently undertaken.

8.3. HPV status and clinico-pathological features of oropharyngeal OPSCC in Malaysia

The prevalence of HPV-related OPSCC in the developed world has been rising rapidly in recent years (Lewis *et al.*, 2015). However, there are very little data regarding the HPV status of OPSCCs in Asian countries and no data are available from Malaysia. Whilst the focus of the present study was to examine collagen-DDR1 signalling in HNSCC, including OPSCC, there was an opportunity as an adjunct to this study to investigate the

HPV status of archival OPSCC specimens from Malaysia. The present study examined p16 expression and the presence of high-risk HPV DNA in OPSCCs from 60 Malaysian patients identified over a 12-year period (2004-2015) from four different hospitals in two major cities, Kuala Lumpur and Penang. Overall, 15 tumours (25.0%) were p16 positive, 10 of which were also positive for HR-HPV ISH. However, between 2009 and 2015 where cases were available from all 4 hospitals, 13 of 37 cases (35.1%) where positive for p16 expression.

The prevalence of HPV positive OPSCC in this small cohort is much lower than the values reported elsewhere in Europe and America (35% vs 80%) (Hisham Mehanna *et al.*, 2013). A recent meta-analysis looking at the burden of HPV associated head and neck cancers in the Asia Pacific region reported an overall prevalence of 40.53% for oropharyngeal cancers (Shaikh *et al.*, 2015). However, there were considerable differences in the rates between regions and countries; the region with the highest prevalence was Oceania (49.32%) and the country with the lowest prevalence was China (9.50%) (Shaikh *et al.*, 2015). Our findings taken for cases diagnosed between 2009 and 2015 (35%) are comparable to the reported rates in East and South Asian regions (25.8% and 38.7% respectively) and Singapore (42%; Tan et al., 2016). In the present study, 80% of the p16 positive cases were from patients of Chinese ethnicity, whilst all the Indian patients had p16 negative OPSCC. This finding could be particularly relevant because according to the 2010 Population and Housing Census of Malaysia, the Chinese account for only 24.6% of the total population (Malaysia, 2011). Although this potentially alarming finding needs to be confirmed in a larger cohort, further research specifically into risk factors that predispose to HPV infection in the oropharynx are warranted in different populations.

Most epidemiological and clinical studies have indicated that patients with HPV positive OPSCC are relatively younger than patients with HPV negative disease (Gillison, 2006; Gillison *et al.*, 2008; Llewellyn *et al.*, 2001; Ryerson *et al.*, 2008; Shaikh *et al.*, 2015), although the present study findings do concur with those studies with the mean age of HPV positive patients being slightly lower than the mean age of HPV negative patients, the finding was not statistically significant. According to the recent meta-analysis by Shaikh et al (2015), the prevalence of HPV associated head and neck cancer is higher amongst males, however the studies involved in the meta-analysis involved small study samples as well as unequal gender distributions (Shaikh *et al.*, 2015). The findings from our study are also similar with the findings of the meta-analysis with a slight male predilection (55.6%).

The results from this study suggest that the occurrence of HPV-related OPSCC in Malaysia may not be as high as those reported in developed nations such as the USA and the UK, but the proportion of OPSCCs that are HPV positive appears to be increasing, particularly in patients of Chinese ethnicity. Further studies will be required to determine how these observations might impact upon Malaysian communities and the national healthcare system in the future.

8.4 COL8a1, COL11a1 and DDR1 expression, HPV status, socio-demographic and clinico-pathological features of OPSCC in United Kingdom

High expression of DDR1 has been reported in various types of cancer and is associated with a number of clinico-pathological parameters, including poor tumour differentiation and poor prognosis of pancreatic cancer (Huo *et al.*, 2015), and TNM stage, depth of tumour invasion and lymph node metastasis in renal clear cell carcinoma (Song *et al.*, 2016). However, DDR1 expression is thought to be cancer-type dependent

because malignancies can demonstrate a different profiles of DDR1 expression. For example, low expression of DDR1 and high expression of DDR2 protein has been observed in invasive triple negative breast carcinoma with worse prognosis (Toy *et al.*, 2015). COL8a1 is known to be expressed in mammalian osteoblasts (Aldea *et al.*, 2013) and overexpressed pancreatic tumours compared to normal pancreatic tissue (Badea *et al.*, 2008). The present study examined, for the first time, the expression of DDR1 together with the non-fibrillar collagen, COL8a1, and fibrillar collagen, COL11a1, in OPSCC biopsies from the United Kingdom, and assessed their utility as prognostic markers in HPV-negative and HPV-positive OPSCC patients.

8.4.1 Automated multispectral slide imaging and digital quantitative scoring of COL8a1, COL11a1 and DDR1 expression

DDR1, COL8a1 and COL11a1 protein expression levels in a total of 96 OPSCC biopsied tissues were determined by *in situ* Opal multiplex immunofluorescence staining. The analysis of COL11a1 and DDR1 proteins was first investigated using OPSCC tissues on a tissue microarray. The expression of COL8a1, COL11a1 and DDR1 were subsequently examined in whole-tissue serial sections, which facilitated the examination of protein expression in both the tumour and its stroma.

The assay and antibodies used in this project were all verified by trained pathologists prior to use. Staining was evaluated by digital multispectral imaging, scored and quantitated for cell type, subcellular localization, percentage positivity and intensity, and association with HPV subtypes and patient overall survival. Any background and auto-fluorescence staining were eliminated from threshold determined by the staining intensity of control slides and automated scoring softwares. A recently developed advanced multi-colour immunofluorescence assay based on Tyramide signal amplification was used to

interrogate α-SMA, COL8a1, COL11a1, CK AE1/AE3 and DDR1 expression in the FFPE tissues. Effective signal unmixing was successfully performed in the TMA by using the automated multispectral Vectra pathology system and inForm image analysis software in order to achieve precise image analyses. In addition, the Metamorph Microscopy Automation and Image Analysis software was used in conjunction with confocal scanning laser microscopy for imaging and analysis of whole-tissue sections. The imaging revealed that both COL8a1 and COL11a1 were expressed by CAFs in the tumour microenvironment and tumour cells, whilst DDR1 was predominantly expressed at the epithelium lining of OPSCC tumours. The COL8a1 staining was heterogeneous from strong to weak positively stained in the cytoplasm of tumours and CAFs. COL11a1 was strongly positive in the cytoplasm of tumours but found in the cytoplasm and nucleus of CAFs. On the other hand, strong DDR1 positive staining was cytoplasmic or appeared to be focally membranous. This study, for the first time, successfully detected the single cell co-localisation of both COL11a1 and DDR1 proteins in OPSCC tissues. There are no published studies reporting the expression of COL8a1 and COL11a1 in OPSCC. Similarly, the expression of DDR1 was previously unexplored in OPSCC. However, the cellular localization of DDR1 observed in the present study was in concordance with published studies in gastric (Hur *et al.*, 2017) and pancreatic cancer (Huo *et al.*, 2015).

8.4.2 Association and correlation of COL8a1, COL11a1 and DDR1 with HPV in OPSCC

HPV is estimated to cause up to 70% of OPSCC in Western countries (Saraiya *et al.*, 2015) and the incidence of HPV-positive OPSCC has increased more than 2-fold over the past two decades (D'Souza *et al.*, 2017). HPV has been recognised as an important and strong independent prognostic indicator for OPSCC patients (Dahlstrom *et al.*, 2016). Previous studies have reported that genes expressed in HPV-positive HNSCC may not be

significant in their HPV-negative counterparts (K. Y. Kim *et al.*, 2015). Hence, the present study investigated whether the expression of COL8a1, COL11a1 and DDR1 are related to the HPV status of OPSCC patients.

HPV DNA detection by *In Situ Hybridisation* (ISH) method is the most commonly applied detection method of HPV in clinical diagnostic histopathology laboratory (Coleman & Tsongalis, 2016). Despite that, owing to its extremely high sensitivity, there is a relatively high chance of HPV false-positive result due to transient infection or contaminations (Rietbergen *et al.*, 2014). Therefore, the present study incorporated the use of p16 IHC in addition to HPV DNA ISH in order to define the HPV status of all specimens (Bishop *et al.*, 2015; Ndiaye *et al.*, 2014b; Salazar *et al.*, 2014).

Interestingly, the per cell basis analyses on the tissue microarray in the present study showed a statistically significant single cell high co-expression of COL11a1 and DDR1 in p16-positive compared to p16-negative OPSCC. When the samples were stratified by combining the p16 and HPV DNA status, high co-expression of COL11a1 and DDR1 was predominantly found in intermediate (i.e. p16-positive/ HPV DNA-negative) and HPV-positive groups (i.e. p16 and HPV DNA-positive) group and the association was statistically significant. In light of the evidence that p16-positive/ HPV DNA-negative cancers in European cohorts have worse prognosis than p16 and HPV DNA-positive tumours(Rietbergen *et al.*, 2013), the findings of the present study where 60% within the intermediate group and 40% within the HPV positive group showed high co-expression implying that COL11a1 and DDR1 might explain the differences in prognosis between these two groups. This interesting result should be further explored in a larger number of samples in order to gain a higher level of statistical power.

On the other hand, both the analyses on tissue microarray and whole-tissue serial sections revealed there were no significant differences in the expression of COL8a1 and DDR1 in tumours and CAFs from HPV-negative and HPV-positive OPSCCs. These findings could be possibly due to the reason that present study only investigated a relatively small number of specimens in each HPV status discordant group that were available. Therefore, there may have been insufficient statistical power to detect significant differences of the COL8a1, COL11a1 and DDR1 expression between the groups. As no information is currently available regarding the expression and association of these proteins with HPV in any cancer type, the exact association of these proteins with HPV-status remains to be further investigated. The significant association found between COL11a1 with p16-negative patients in TMA was intriguing and could be further explored.

Recently, a collagen cleaver protein, ADAM23, was shown to be associated with HPV-mediated oral carcinogenesis (P. Yang, 2017). It is conceivable, therefore, that collagens might co-operate with HPV oncogenes to transform normal oral epithelial cells. Therefore, the study of this potential co-operation might be helpful in improving our understanding of the genetic differences between HPV-negative and HPV-positive tumours and aid in therapeutic management of these two categories of patients in the future.

8.4.3 Association and correlation of COL8a1, COL11a1 and DDR1 expression with OPSCC patients' clinico-pathological parameters

COL11a1 has been reported to be absent in pathologic process of benign lesions but highly expressed in activated stromal cells of gliomas and glioblastoma invasive carcinoma and importantly, its expression was correlated to carcinoma aggressiveness,

progression and lymph node metastasis (Vázquez-Villa *et al.*, 2015). However, in present study, COL11a1 expression in the whole-tissue sections was not associated with any of the clinico-pathological parameters.

OPSCC patients can be divided into three groups with regards to the risk of death (i.e. low, moderate and high), which takes into consideration various prognostic factors, including the tumour stage, nodal stage, pack years of tobacco smoking and HPV status (A. Hay & Ganly, 2015; Rietbergen *et al.*, 2013). In present study, there was no significant difference in COL11a1 expression between the three risk groups. However, DDR1 and COL8a1 protein expression showed significant associations with the risk of death groups. In particular, lower expression of DDR1 was associated with low risk patients compared to moderate or high risk patients, whilst higher expression of COL8a1 in tumour and CAFs was significantly associated with high-risk patients. In other words, the risk of death significantly increased with increasing expression of COL8a1 in tumours and CAFs, together with high levels of DDR1 in tumours. As moderate and high risk OPSCC patients are known to have an extremely poor prognosis (Ang *et al.*, 2010), it might be beneficial to incorporate COL8a1 and DDR1 expression in tumours and CAFs as additional determinants of risk classification, prognostic and therapy selection for patients in the future. The present study also suggests a novel pathological and prognostic role for the DDR1 and COL8a1 in moderate and high risk patients. These significant association and correlations with risk groups found in present study implies that DDR1 and COL8a1 might affect the patient survival since a previous study has reported that high risk patients possessed 3-years survival rate of only 33.5% compared to 88.1% of that in low risk patients (Rietbergen *et al.*, 2013). Thus, the results of the present study suggest that DDR1 and COL8a1 could be important determinants to survival. This warrants further investigation as it has been proposed that HNSCC categorised by high,

moderate and low risk of death groups have distinct molecular basis and clinical differences.

Smoking has been incorporated in prognostic classifications as there is published evidence for smoking being an adverse prognostic factor in HPV-associated OPSCC (Haigentz *et al.*, 2018). Interestingly, the present study showed a significant association of COL8a1 and DDR1 protein levels with smoking habits in OPSCC patients. Significantly higher expression of COL8a1 was found in both the tumour and CAFs of smokers. The significant association suggesting a novel role for COL8a1 in smoking-induced carcinogenesis. However, the smokers showed significantly lower expression of DDR1 whilst 72% of non-smokers with OPSCC highly expressed DDR1. This contradictory association of COL8a1 and DDR1 with smoking habit could be possibly due to the reason that other types of collagen receptor is involved in smoking-induced carcinogenesis rather than DDR1. However, this result is in agreement with the significant association of DDR1 with the moderate risk group as mentioned above. Moderate risk group comprised of HPV-negative T2 to T3 OPSCC patients with less than 10 pack-years of cigarette smoking (Lindel *et al.*, 2001), so it suggests that the role of DDR1 in OPSCC carcinogenesis is dependent on factors other than smoking, such as HPV status.

In addition, a significant association of COL8a1 expression in tumours and CAFs with lymph node metastasis was found in the present study. Significantly higher expression of COL8a1 was found in OPSCC with ipsilateral metastasis in lymph node which was less than 6cm (N1). In contrast, OPSCC with bilateral or contralateral metastasis in lymph node (N2) has significantly low expression of COL8a1 in tumours and CAFs. In light with the fact that HPV-positive OPSCC typically presents with smaller primary tumour

but more advanced nodal diseases with improved prognosis (Keane *et al.*, 2015), the present study suggests the role of COL8a1 as worse prognosis factor as its high expression was significantly associated with N1. It is well understood that lymph node metastasis is one of the most important established negative prognostic indicator for HNSCC (Layland *et al.*, 2005) and the nodal stage (N stage) has been a dominant prognostic factor in OPSCC (Keane *et al.*, 2015). The analysis of present study was done in corresponding to the latest OPSCC prognostic classification of 8th edition of American Joint Committee on Cancer/ Union for International Cancer Control (AJCC/ UICC) and International Collaboration on Oropharyngeal Cancer Network for Staging (ICON-S) newly announced in year 2017. In particular, N1 to N2b stages were now reassigned to N1 due to similar overall survival whist traditional N2c, bilateral or contralateral nodes is now N2 (S. Lee *et al.*, 2017). Since the present study found a significant difference in Univariate Logistic Regression analysis of COL8a1 expression between N1 and N2 groups, in this case COL8a1 might be a potential novel lymph node metastasis indicator in OPSCC and improve prognostic stratification.

8.4.4 Association and correlation of DDR1 expression with OPSCC patient survival

In the present study, survival analyses from Kaplan Meier, Log Rank (Mantel-Cox), Breslow (Generalised Wilcoxon) and Tarone-ware analyses revealed that OPSCC patients with high DDR1 expression had a strongly significant lower 5-years survival rate (33%) than those with low expression (78%). This is in agreement with the Multivariate Cox regression analysis which demonstrated that DDR1 expression was a statistically significant independent risk factor in prognosis of OPSCC patients after adjustment to other factors such as age, gender, p16, HPV DNA, HPV RNA, risk groups, smoking, T stage, N stage, overall survival time and disease recurrence free survival time. The results of the present study are in agreement with other studies which reported the positive

association of DDR1 with poor survival of patients in other solid tumours. For example, patients with high DDR1 expression was found to have significantly shorter survival time than those with low expression of DDR1 in pancreatic ductal adenocarcinoma (Huo *et al.*, 2015), up-regulation of DDR1 was showed in lung cancer tissues compared to normal tissues and associated with poor prognosis (Miao *et al.*, 2013) and significant association of DDR1 with poor prognosis and poor survival in gastric cancer (Hur *et al.*, 2017). However, the precise molecular mechanisms of how DDR1 negatively impacts the survival time of patients have yet to be elucidated and require further investigation. Taken together, these results suggest that DDR1 expression could be a novel prognostic marker for OPSCC patients and the use of DDR1 inhibitors could potentially represent a novel therapeutic strategy.

8.5 COL8a1, COL11a1 and DDR1 expression, socio-demographic and clinico-pathological features of OSCC in Malaysia

Overexpression of a few known collagen subtypes, such as type XVI collagen have been shown to enhance the proliferation of OSCC cells *in vitro* (Ratzinger *et al.*, 2011). However, the expression of COL8a1, COL11a1 and DDR1 receptor have never been reported in OSCC before. The present study, for the first time, provides the evidence of the expression of COL8a1, COL11a1 and DDR1 in a Malaysian OSCC cohort. Opal Multiplex Immunofluorescence staining was carried out and digitally scored using the Metamorph Pathology Analysis system and software under the guidance of head and neck pathologists.

8.5.1 Digital imaging and quantitative scoring of COL8a1, COL11a1 and DDR1 expression

Similar to the results with OPSCCs, the present study showed that COL8a1, COL11a1 and DDR1 proteins were expressed in the majority of OSCCs, suggesting a pathologic role for collagen-DDR1 signalling in this disease. The expression of COL8a1 and COL11a1 tended to be cytoplasmic in tumour cells, cytoplasmic and nuclear in CAFs. This is similar with a previous report regarding the localisation of other collagens in cutaneous squamous cell carcinoma, where COL18 was expressed in tumour cells whilst COL15 appeared as deposited in tumour stroma (Karppinen *et al.*, 2016). In contrast, the imaging of DDR1 revealed its membranous and cytoplasmic localization in tumours which suggests that it is secreted and expressed on the surface of tumour cells to interact with the collagens in the ECM produced by CAFs.

8.5.2 Association and correlation of COL8a1, COL11a1 and DDR1 expression with OSCC patients' clinico-pathological parameters

Although DDR1 was significantly up-regulated in OSCC at the mRNA and protein levels, no significant associations were observed between DDR1 expression with age, gender, ethnic, smoking, betel quid chewing, drinking, cancer staging, cancer grading, vascular invasion, perineural invasion, bone invasion, extent of primary tumour, extent of regional lymph node metastasis, extra-capsular spread, skip metastasis, tumour depths, patients outcome and survival months. OSCC patients with high DDR1 expression showed lower overall survival and lower 5-years survival rate (24.5%) compared to the low DDR1 expression (36%). However, this comparison was not statistically significant. These results suggest that DDR1 signalling is generally aberrant in OSCC and is independent of the cause and stage of the disease. However, this result does not exclude

the possibility of correlations between DDR1 expression and the socio-demographic and clinico-pathological characteristics.

In contradictory to a recent study reported that CAFs promoted bone invasion in OSCC (Elmusrati *et al.*, 2017), no significant association of COL8a1 expression in CAFs was found with socio-demographic and clinico-pathological characteristics in OSCC. Interestingly, high expression of COL8a1 in tumours showed a significant association with patients' survival state (deceased), tumour depth (1-10mm) and occurrence of bone invasion. The results of the present study suggest a novel role for COL8a1 in poor prognosis, bone invasion and survival of OSCC patients. This warrants further investigation as it has been proposed that OSCC with bone invasion has poor outcome (Johnson *et al.*, 2014). Therefore, COL8a1 might be a potential therapeutic target to improve patients' prognosis by inhibiting bone invasion.

The present study provides the first evidence showing strong significant association between high expression of COL11a1 with female gender, Indian ethnic and betel quid chewing in Malaysian OSCC patient cohort. A meta-analysis of 50 studies evaluated the causal role of these socio-demographic factors in OSCC carcinogensis where there is higher risk with increasing frequency of betel quid chewing and female than male in the Indian subcontinent (Guha *et al.*, 2014). Local recurrence rate is previously reported to be higher in patients with the positive history of betel quid chewing (Liao *et al.*, 2014). Therefore, it suggests the poor prognosis role of COL11a1 in OSCC patients.

8.6 Phenotypic impact of exogenous collagen and knockdown of DDR1 in HPV-negative and HPV-positive HNSCC cell lines

DDR1 has been shown to mediate matrix metalloproteinase production (Reel *et al.*, 2015), control linear invadosome (Juin *et al.*, 2014), mesenchymal to epithelial transition

(Koh *et al.*, 2015) and drive an aggressive phenotype in gastric cancer (Hur *et al.*, 2017), pointing a role for DDR1 as an oncogene. However, its biological roles in HNSCC have not been reported.

The present study examined the biological functions of exogenous collagen on HNSCC cell growth, motility in scratch wound and migration assays, invasion and response to Cisplatin were examined. Also, the effects of inhibiting endogenous DDR1 were examined by knocking down DDR1 in HNSCC cells using a lentiviral shRNA system to achieve a stable and long-term knockdown of DDR1.

Collagens are known to adopt a characteristic supercoiled triple helices structure (K. T. Walker *et al.*, 2017). Hydrolysis of collagen either by acidic or alkaline treatment produces gelatin, which has an almost identical amino acid content and composition with the collagen from which it is derived, but exists in a denatured, coiled structural form instead of a triple-helix (Kumar *et al.*, 2016; Nur *et al.*, 2016; Su & Wang, 2015). In the past 10 years, the role attributed to collagen has been a structural one (E. D. Hay, 2013). The fact that DDR1 is activated specifically by the collagens in triple helix structure but not the denatured, de-glycosylated or degraded forms (Boraschi-Diaz *et al.*, 2017), gelatin was used as a negative control in the functional experiments performed in this study.

8.6.1 Effects of collagen and DDR1 on cell growth and colony survival

To investigate the functional roles of collagen-DDR1 signalling in HNSCC, the present study used both HPV-positive and –negative HNSCC cell lines. HPV E6 and E7 expression was confirmed in the HPV-positive cell lines. Stable knockdown of DDR1 using two shRNA specific for DDR1 was used to confirm that any effects of collagen were mediated via DDR1.

Collagen is generally considered to stimulate the growth of cancer cells and this has been shown, for example, in pancreatic ductal adenocarcinoma (Rath *et al.*, 2016) and breast cancer (G. Huang *et al.*, 2017). Similarly, exogenous collagen increased the proliferation of all the HNSCC cell lines used in the present study. Knockdown of DDR1 resulted in a significant reduction in cell growth compared to parental and NS controls. Further, knockdown of DDR1 significantly reduced colony formation and survival. These results are consistent with other studies that reported that DDR1 signalling promoting the growth of mammary tumours (Sun *et al.*, 2018) and lung cancer (Xiao *et al.*, 2015) and increased colony forming capacity in gastric cancer (Hur *et al.*, 2017). Interestingly, the knockdown of DDR1 significantly abolished the growth promoting effect of collagen in both the HPV-negative and HPV-positive cell lines. Therefore, collagen promoted HNSCC growth in a DDR1-dependent manner in the present study. These data are supported by previous studies which showed that silencing of DDR1 but not β1-integrin decreased collagen induced survival in human breast cancer cells (Badaoui *et al.*, 2017), collagen promotes lung cancer growth and tumorigenesis through DDR1-mediated tumour autonomous and non-autonomous mechanisms (Xiao *et al.*, 2015) and the breast cancer proliferation regulation by collagen involved activation of DDR1 (Saby *et al.*, 2016).

Some possible mechanisms to explain how collagen-DDR1 signalling enhances cancer cell growth can be inferred from recent research findings. For example, activation of downstream ERK signalling cascade (Borza & Pozzi, 2014; Xiao *et al.*, 2015), regulating insulin receptor downstream signalling pathway including AKT and ERK1/2 cascades (Vella *et al.*, 2017), ERK1/2 and c-Myc activation (Badaoui *et al.*, 2017) and activation of Notch-1 signalling and pro-survival pathways (H.-G. Kim *et al.*, 2017).

8.6.2 Effects of collagen and DDR1 on *in vitro* wound closure, migration and invasion

Similarities between cancers and inflammatory responses associated with wound closure have been recognised and tumours have recently been regarded as wounds that do not heal (Schnittert *et al.*, 2018). It has been suggested that tumours adopted and assimilating the wound healing process to induce the tumour microenvironment required for cancer maintenance and growth (Dvorak, 2015). An *in vitro* model of monolayer scratch wound closure was used in the present study to investigate how collagen-DDR1 signalling influences cell motility *in vitro*. The results showed that collagen, but not gelatin, significantly enhanced wound closure. At the wound edge, the cells rearranged their membrane and cytoplasmic structure and leading to disassembly of cell-cell interaction for cell motility. This can be explained by the regulation of lamellipodia, filopodia and focal adhesions during wound healing process (Na *et al.*, 2017). Knockdown of DDR1 prevented wound closure in the presence or absence of collagen, suggesting that collagen contributed to the wound closure by promoting cells motility by activating DDR1. These data are supported by a study showing that DDR1 knockdown attenuated scratch wound closure on collagen matrix in A431 epidermoid carcinoma cells that was suggested to be ADAM10-dependent (Shitomi *et al.*, 2015). Furthermore, a recent study has demonstrated a functional link between collagen, DDR1 activation and cell contractility with regards to fibrosis in an *in vivo* wound healing model by showing that DDR1 interacts with non-muscle myosin IIA to cause collagen compaction by traction forces and DDR1 knockdown resulted in reduction of aligned collagen *in vitro* and *in vivo* (Coelho *et al.*, 2017).

In the present study cell migration was also assessed quantitatively using Transwell assays. The results showed that exogenous collagen significantly enhanced the migration of all HPV-negative and HPV-positive HNSCC cell lines and this migratory phenotype

was significantly attenuated by knockdown of DDR1. This finding is the first evidence reported using HNSCC cells but they are consistent with previous in other cancer types. For example, inhibition of DDR1 reduced cell migration and metastasis in colon cancer (Yuge *et al.*, 2017) and DDR1 promoted metastasis in pancreatic cancer (J.-c. Yang *et al.*, 2017).

Given that local regional recurrence, lymph node metastasis and poor five-years survival rate of patients are often associated and attributed to the invasive property of HNSCC (Jimenez *et al.*, 2015), the contribution of collagen-DDR1 to the invasive ability of cells using an *in vitro* Transwell assay was examined. In agreement with a previous study in gastric cancer (R. Xie *et al.*, 2016), knockdown of DDR1 significantly suppressed the invasive ability of HNSCC cells in the present study. These data are supported by the observation that overexpression of DDR1 resulted in osteosarcoma cell motility and invasiveness (Zhaofeng Wang *et al.*, 2017).

Although the mechanisms by which collagen-DDR1 signalling might promote invasion and metastasis in HNSCC are unknown, recent reports in other cancer types might offer some clues. For example, collagen cross-linking was shown to be induced by transforming growth factor 1 (TGF-β1) and enhanced invadosome formation via DDR activation in a Smad-4 dependent manner in hepatocellular carcinoma (Ezzoukhry *et al.*, 2016). Further, another DDR1 enables the activation of JAK/STAT3 signalling and drives metastatic reactivation of breast cancer cells in multiple target organs, such as lung, brain and bone (H. Gao *et al.*, 2016). Lastly, the overexpression of DDR1 in gastric carcinoma cells resulted in a significant decrease in epithelial markers with an up-regulation of in mesenchymal markers, suggesting that DDR1 promotes invasion and metastasis via the induction of an epithelial-mesenchymal transition (R. Xie *et al.*, 2016).

Taken together, the results of this study show for the first time that collagen promotes HNSCC cell motility, migration and invasion via the activation of DDR1. As HNSCC is a highly metastatic cancer and cervical lymph node metastasis is the most prominent prognostic factor in HNSCC (Irani, 2016), these data suggest that collagen-DDR1 signalling could be a promising therapeutic target to inhibit invasion and metastasis.

8.6.3 *In vitro* chemoresistance of HNSCC induced by collagen-DDR1 signalling

Cisplatin or cis-Diammineplatinum (II) dichloride, is the major chemotherapeutic drug to treat HNSCC. It acts as a DNA intercalator that binds the guanine residues of the DNA and leading to cell apoptosis by forming multiple inter- and intra-strand crosslinks. Drug resistance is a major hindrance for successful treatment of HNSCC and remains a major clinical problem (Qazi *et al.*, 2018). In the present study, collagen reduced the responsiveness of both the HPV-negative and -positive HNSCC cells to cisplatin and this effect was attenuated by the knockdown of DDR1. These results suggest a possible involvement of collagen-DDR1 signalling in the development of Cisplatin resistance in HNSCC. This finding is consistent with studies showing that chemoresistance is conferred by collagens in other cancer types (Rada, Eldred*, et al.*, 2017; H.-J. Wang *et al.*, 2017; Y. H. Wu *et al.*, 2017), and in line with a previous report that there is an association of DDR1 levels with resistance of breast carcinoma cells towards genotoxic drugs (Jing *et al.*, 2018). The inhibition of DDR1 has also been showed to improve the efficacy of chemotherapy in pancreatic ductal carcinoma (Aguilera *et al.*, 2017), exhibit the anti-tumour effects in nasopharyngeal cancer both *in vitro* and *in vivo* (Lu *et al.*, 2016) and the ectopic expression of DDR1 significantly increased the survival of lymphoma cells after chemotherapeutic drug treatment (Fathima Zumla Cader *et al.*, 2013).

The results of the present study indicate that DDR1 activation induced by collagen limits the response of HNSCC cells to chemotherapeutic drugs in both HPV-positive and –negative disease. The underlying molecular mechanisms responsible for this effect in HNSCC cells have yet to be elucidated, but chemoresistance resulting from DDR1 activation has been reported to be due to inhibition of the p53 mediated apoptosis, activation of Nucler Factor Kappa B (NFκB) and cyclooxygenase-2 (COX-2) (Rammal *et al.*, 2016a). Together, these data indicate that specific DDR1 inhibitors might be useful in combination with chemotherapy to improve the therapeutic outcome.

8.7 Opal multiplex staining

The present study is the first attempt to validate the reliability for quantitating spatially overlapping protein expression in HNSCC tissues by using multiplex immunofluorescence, fully-automated pathology system and digital analysis software. It demonstrated important information regarding the feasibility in digitalised scoring of multiple protein expression on a cellular level in tissue sections. Firstly, a digital method provides more reliable data in a way of producing continuous variable data and allows identification of IHC cut-off points with less significant prognostic relevance by visual scoring. Secondly, this digitalised automated approach improves the data quality and accuracy in a sense that digital algorithm standardised all the laser and measurement parameters so that whole batch of analysis was carried out under 'locked' and consistent condition. Thirdly, it overcomes the complications in analysis in the case where co-localisation of proteins occurred, even at single cell level in tissue sections. Notably, in order to assure the accuracy in automated region selection and warrant the quality of tissue segmentation and scoring, the whole process and post-scanning analyses in the present study were carried out under the supervision of expert pathologists who verified the data for every case. There was a minor setback in efficiency during the early phase of

training the system to recognise tumour and stroma areas. In spite of that, once the system was trained, the data analysis concordance with the pathologist evaluation reached agreement and eliminated possibility of false positive and negative results. Therefore, one of the key aspects of the present study is demonstrating the imagery in a workflow that significantly expands the range of metrics collectable from clinical tissue samples, whilst engaging the pathologist to utilise the strengths of human perception and professional judgment. This importantly provides a higher level of consistency and precision needed and prompts the colourful future in quantitative IHC and clinical research.

8.8 Study limitations

Although this study has been carefully designed to address specific research questions, there are a number of limitations that might influence the broader conclusions drawn from the data. Careful consideration of such limitations should be given before generalisation and application to practice.

Firstly, the analyses pertaining to the clinical data in Chapter 5 and 6 were subjected to the power of statistical analysis. Under ethical, time, cost and availability issues and considerations, as many as possible clinical samples from both United Kingdom and Malaysia were used in the present study. Therefore, in circumstances where no significant differences, associations or correlations were observed, this might be due to the small sample size.

Secondly, the analyses of the effects following exogenous collagen treatment was attributed to the activation of DDR1. However, the collagen might activate receptors other than DDR1, such as integrins. Therefore, the use of inhibitors to block other collagen-binding receptors would be beneficial to confirm that the effects of exogenous collagen were specifically due to DDR1 activation.

Lastly, the results reported in Chapter 7 were largely derived from pre-clinical, proof of concept *in vitro* studies. However, findings obtained from *in vitro* work were necessarily limited by the fact that the cells are treated outside their normal biological environment. There was lack of interaction with surrounding tissue and blood supply and the culture conditions do not absolutely mimic the *in vivo* situation. Therefore, it would be important to determine if these results could be recapitulated using relevant *in vivo* animal models.

8.9 Future work

The results and findings of this present study identified a number of areas of research for future investigations as described below. These future studies arising from the present study are likely to have fundamental implications for a better understanding of the contribution of collagen and DDR1 to the crosstalk between HNSCCs with its tumour microenvironment. It could potentially lead to a better understanding of the pathogenesis of HNSCC and subsequently aid in the development of new therapeutic strategies to target HPV-negative and –positive HNSCC.

The results of the present study convincingly show that DDR1 was overexpressed in primary clinical OPSCC and OSCC tissue samples, whilst collagens were expressed in CAFs. The aberrant activation of DDR1 signalling by collagens promotes the tumorigenic phenotypes of HPV-negative and –positive HNSCC cells. There are a number of other transmembrane receptors which are known to bind the extracellular matrix collagens. For example, integrins, immunoglobulin-like receptors and mannose receptors. The investigation collectively into the role of these receptors in mediating the effects of collagens would provide a fuller understanding of the contribution of aberrant collagen signalling with all their receptors to the pathogenesis of HNSCC.

Having shown that collagen and DDR1 promote the malignant phenotype of HNSCC, it would be informative to identify the precise molecular pathways and mechanisms involved in the regulation of the collagen-DDR1 signalling axis. Future work is suggested to explore the possible activation loops of DDR1 and its downstream targets or signalling crosstalk with other oncogenic pathways. For example, AKT, ERK and SMAD pathways. This might provide additional insights into the underlying tumorigenesis mechanism driven by DDR1 and help to explore the therapeutic potential of inhibitors or modulators of the signalling cascades.

Lastly, the development of specific DDR1 inhibitors might have the potential to circumvent tumour growth, metastasis, invasion and chemoresistance to improve treatment efficacy. Therefore, testing DDR1 inhibitors *in vitro* and *in vivo* in preclinical studies would be beneficial to explore whether DDR1 is a useful therapeutic target for HNSCC. For example, the efficacy of DDR1 inhibitors could be evaluated in preclinical animal models, which would also facilitate studying its use in combination therapies with Cisplatin.

CHAPTER 9: CONCLUDING REMARKS

HNSCCs are solid tumours which regarded as "organs" that are comprised of tumour cells and tumour microenvironment made up of extracellular matrix and non-malignant mesenchymal cells. The present study shows for the first time that collagen-DDR1 signalling promotes the malignant phenotype in HNSCCs and is significantly associated with worse overall survival, suggesting that this pathway could potentially be targeted for therapy (Figure 9.1).

This study showed that COL8a1 and COL11a1 were up-regulated in senescent CAFs and that the collagen receptor, DDR1, was over-expressed in tumours and cell lines. The results show for the first time that COL8a1, COL11a1 and DDR1 were highly expressed in HPV-negative and -positive HNSCC and that their expression was associated with various clinico-pathological parameters (e.g. bone invasion, tumour depth and lymph node metastasis) that might predict poor prognosis. It is noteworthy that high expression of DDR1 was significantly associated with a low survival rate in OPSCC patients. Collectively, these data show that DDR1 and its ligands are expressed in HPV-negative and -positive HNSCC and their expression levels might contribute to patients' poor prognosis.

To study the mechanisms by which collagen DDR1 signalling might affect the prognosis of HNSCC patients, the effect of this pathway on tumour behaviour was examined *in vitro.* The results demonstrated that collagen acting predominantly through the kinase active DDR1 isoform, i.e. DDR1b, profoundly promotes tumour growth, colony survival, cell motility in wound closure and migration, invasion and suppressed

chemo-sensitivity. Therefore, activated DDR1 signalling promotes the malignant phenotype of HNSCC in multiple ways.

Taken together, the results of this study indicate that specific DDR1 inhibitors might be useful as therapeutic agents for the treatment of HNSCCs, either alone or in combination with existing therapeutic drugs.

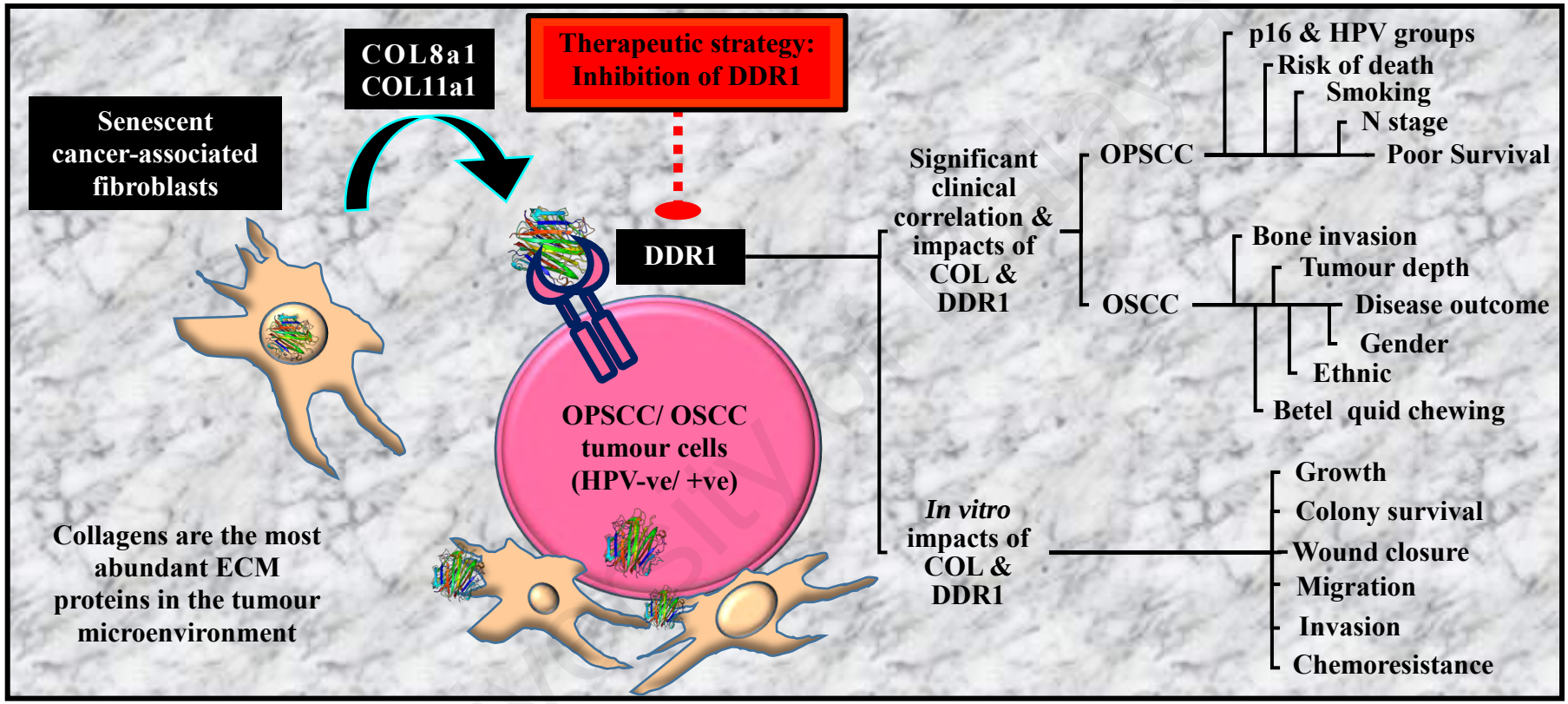

Figure 9.1: The roles of collagen-DDR1 signalling in HNSCC.

Collagens including COL8a1 and COL11a1 secreted into the tumour microenvironment by CAFs and tumour cells activates DDR1 on the cellular membrane of tumours and increases tumour growth, colony survival, migration, invasion and chemoresistance *in vitro* and significantly associated and correlated to socio-demographic risk factors and prognostic clinico-pathological parameters. Abrogation of collagen-DDR1 signalling by inhibition of DDR1 is suggested to be a potential therapeutic strategy for HNSCC patients.

REFERENCES

Adami, G. R., Schwartz, J. L., Zhou, Y., Tang, J. L., Markiewicz, M., Jefferson, G. D., . . . Kolokythas, A. (2017). Brush biopsy miRNA based OSCC detection and diagnosis: AACR.

Adiguzel, E., Hou, G., Sabatini, P. J., & Bendeck, M. P. (2013). Type VIII collagen signals via β1 integrin and RhoA to regulate MMP-2 expression and smooth muscle cell migration. *Matrix Biology, 32*(6), 332-341.

Aguilera, K. Y., Huang, H., Du, W., Hagopian, M. M., Wang, Z., Hinz, S., . . . Castrillon, D. H. (2017). Inhibition of discoidin domain receptor 1 reduces collagen-mediated tumorigenicity in pancreatic ductal adenocarcinoma. *Mol Cancer Ther*, molcanther. 0834.2016.

Al Salihi, K., Abdullah, I., & Ang, S. (2016). Histological implication of p53 gene expression in oral squamous cell carcinoma. *Journal of Cellular Cancer, 8*(1), 60-69.

Aldea, D., Hanna, P., Munoz, D., Espinoza, J., Torrejon, M., Sachs, L., . . . Marcellini, S. (2013). Evolution of the vertebrate bone matrix: an expression analysis of the network forming collagen paralogues in amphibian osteoblasts. *Journal of Experimental Zoology Part B: Molecular and Developmental Evolution, 320*(6), 375-384.

Ali-Rahmani, F., Fitzgerald, D., Martin, S., Patel, P., Prunotto, M., Ormanoglu, P., . . . Pastan, I. (2016). Tyrosine kinase discoidin domain receptor-1 (DDR1) regulates cytotoxicity of recombinant immunotoxin for cancer therapy: AACR.

Ammirante, M., Shalapour, S., Kang, Y., Jamieson, C. A., & Karin, M. (2014). Tissue injury and hypoxia promote malignant progression of prostate cancer by inducing CXCL13 expression in tumor myofibroblasts. *Proceedings of the National Academy of Sciences, 111*(41), 14776-14781.

Amtha, R., Razak, I. A., Basuki, B., Roeslan, B. O., Gautama, W., Puwanto, D. J., . . . Zain, R. B. (2014). Tobacco (kretek) smoking, betel quid chewing and risk of oral cancer in a selected Jakarta population. *Asian Pac J Cancer Prev, 15*(20), 8673-8678.

An, B., Abbonante, V., Xu, H., Gavriilidou, D., Yoshizumi, A., Bihan, D., . . . Leitinger, B. (2016). Recombinant collagen engineered to bind to discoidin domain receptor functions as a receptor inhibitor. *Journal of Biological Chemistry, 291*(9), 4343-4355.

Anantharaman, D., Marron, M., Lagiou, P., Samoli, E., Ahrens, W., Pohlabeln, H., . . . Richiardi, L. (2011). Population attributable risk of tobacco and alcohol for upper aerodigestive tract cancer. *Oral Oncol, 47*(8), 725-731.

Ang, K. K., Harris, J., Wheeler, R., Weber, R., Rosenthal, D. I., Nguyen-Tân, P. F., . . . Lu, C. (2010). Human papillomavirus and survival of patients with oropharyngeal cancer. *New England Journal of Medicine, 363*(1), 24-35.

Arcucci, A., Ruocco, M. R., Granato, G., Sacco, A. M., & Montagnani, S. (2016). Cancer: an oxidative crosstalk between solid tumor cells and cancer associated fibroblasts. *BioMed research international, 2016*.

Assent, D., Bourgot, I., Hennuy, B., Geurts, P., Noël, A., Foidart, J.-M., & Maquoi, E. (2015). A Membrane-Type-1 Matrix Metalloproteinase (MT1-MMP)–Discoidin Domain Receptor 1 Axis Regulates Collagen-Induced Apoptosis in Breast Cancer Cells. *PLoS One, 10*(3), e0116006.

Attieh, Y., & Vignjevic, D. M. (2016). The hallmarks of CAFs in cancer invasion. *European journal of cell biology, 95*(11), 493-502.

Aung, K. L., & Siu, L. L. (2016). Genomically personalized therapy in head and neck cancer. *Cancers of the Head & Neck, 1*(1), 2.

Badaoui, M., Mimsy-Julienne, C., Saby, C., Van Gulick, L., Peretti, M., Jeannesson, P., . . . Ouadid-Ahidouch, H. (2017). Collagen type 1 promotes survival of human breast cancer cells by overexpressing Kv10. 1 potassium and Orai1 calcium channels through DDR1-dependent pathway. *Oncotarget*.

Badea, L., Herlea, V., Dima, S. O., Dumitrascu, T., & Popescu, I. (2008). Combined gene expression analysis of whole-tissue and microdissected pancreatic ductal adenocarcinoma identifies genes specifically overexpressed in tumor epithelia-the authors reported a combined gene expression analysis of whole-tissue and microdissected pancreatic ductal adenocarcinoma identifies genes specifically overexpressed in tumor epithelia. *Hepato-gastroenterology, 55*(88), 2016.

Barcus, C. E., O'Leary, K. A., Brockman, J. L., Rugowski, D. E., Liu, Y., Garcia, N., . . . Schuler, L. A. (2017). Elevated collagen-I augments tumor progressive signals, intravasation and metastasis of prolactin-induced estrogen receptor alpha positive mammary tumor cells. *Breast Cancer Research, 19*(1), 9.

Barisione, G., Fabbi, M., Cutrona, G., De Cecco, L., Zupo, S., Leitinger, B., . . . Ferrini, S. (2017). Heterogeneous expression of the collagen receptor DDR1 in chronic lymphocytic leukaemia and correlation with progression. *Blood Cancer J, 6*(1), e513. doi: 10.1038/bcj.2016.121

Bates, A. L. (2015). *Roles of Fibroblast MMP2 in Breast to Lung Metastasis.* Vanderbilt University.

Belfiore, A., Malaguarnera, R., Nicolosi, M. L., Lappano, R., Ragusa, M., Morrione, A., & Vella, V. (2018). A novel functional crosstalk between DDR1 and the IGF axis and its relevance for breast cancer. *Cell adhesion & migration*(just-accepted), 01-31.

Berdiel-Acer, M., Sanz-Pamplona, R., Calon, A., Cuadras, D., Berenguer, A., Sanjuan, X., . . . Batlle, E. (2014). Differences between CAFs and their paired NCF from adjacent colonic mucosa reveal functional heterogeneity of CAFs, providing prognostic information. *Mol Oncol, 8*(7), 1290-1305.

Bernard, H.-U. (2013). Taxonomy and phylogeny of papillomaviruses: an overview and recent developments. *Infection, Genetics and Evolution, 18*, 357-361.

Bhattacharyya, I., Chehal, H. K., & Islam, M. N. (2017). Common Lesions in Oral Pathology for the General Dentist *The Dental Reference Manual* (pp. 227-289): Springer.

Bishop, J. A., Lewis Jr, J. S., Rocco, J. W., & Faquin, W. C. (2015). *HPV-related squamous cell carcinoma of the head and neck: an update on testing in routine pathology practice.* Paper presented at the Seminars in diagnostic pathology.

Blaszczak, W., Barczak, W., Wegner, A., Golusinski, W., & Suchorska, W. M. (2017). Clinical value of monoclonal antibodies and tyrosine kinase inhibitors in the treatment of head and neck squamous cell carcinoma. *Medical Oncology, 34*(4), 60.

Blatt, S., Voelxen, N., Sagheb, K., Pabst, A. M., Walenta, S., Schroeder, T., . . . Ziebart, T. (2016). Lactate as a predictive marker for tumor recurrence in patients with head and neck squamous cell carcinoma (HNSCC) post radiation: a prospective study over 15 years. *Clinical oral investigations, 20*(8), 2097-2104.

Boguslawska, J., Kedzierska, H., Poplawski, P., Rybicka, B., Tanski, Z., & Piekielko-Witkowska, A. (2016). Expression of genes involved in cellular adhesion and extracellular matrix remodeling correlates with poor survival of patients with renal cancer. *The Journal of urology, 195*(6), 1892-1902.

Boguslawska, J., Kedzierska, H., Rybicka, B., Poplawski, P., Tanski, Z., Nauman, A., & Piekielko-Witkowska, A. (2014). 281: A panel of 20 genes involved in cellular adhesion and ECM remodelling distinguishes renal cancer and control samples. *European journal of cancer, 50*, S66.

Bonnans, C., Chou, J., & Werb, Z. (2014). Remodelling the extracellular matrix in development and disease. *Nature reviews Molecular cell biology, 15*(12), 786-801.

Boraschi-Diaz, I., Wang, J., Mort, J. S., & Komarova, S. V. (2017). Collagen type I as a ligand for receptor-mediated signaling. *Frontiers in Physics, 5*, 12.

Borza, C. M., & Pozzi, A. (2014). Discoidin domain receptors in disease. *Matrix Biology, 34*, 185-192.

Bose, P., Brockton, N. T., & Dort, J. C. (2013). Head and neck cancer: from anatomy to biology. *Int J Cancer, 133*(9).

Burk, R. D., Harari, A., & Chen, Z. (2013). Human papillomavirus genome variants. *Virology, 445*(1), 232-243.

Burns, J., Baird, M., Clark, L., Burns, P., Edington, K., Chapman, C., . . . Parkinson, E. (1993). Gene mutations and increased levels of p53 protein in human squamous cell carcinomas and their cell lines. *Br J Cancer, 67*(6), 1274.

Bussu, F., Sali, M., Gallus, R., Petrone, G., Zannoni, G. F., Autorino, R., . . . Graziani, C. (2014). Human papillomavirus (HPV) infection in squamous cell carcinomas arising from the oropharynx: detection of HPV DNA and p16 immunohistochemistry as diagnostic and prognostic indicators—a pilot study. *International Journal of Radiation Oncology• Biology• Physics, 89*(5), 1115-1120.

Cader, F. Z., Vockerodt, M., Bose, S., Nagy, E., Brundler, M.-A., Kearns, P., & Murray, P. G. (2013). The EBV oncogene LMP1 protects lymphoma cells from cell death through the collagen-mediated activation of DDR1. *Blood, 122*(26), 4237-4245.

Cader, F. Z., Vockerodt, M., Bose, S., Nagy, E., Brundler, M. A., Kearns, P., & Murray, P. G. (2013). The EBV oncogene LMP1 protects lymphoma cells from cell death through the collagen-mediated activation of DDR1. [Research Support, Non-U.S. Gov't]. *Blood, 122*(26), 4237-4245. doi: 10.1182/blood-2013-04-499004

Campbell, C. M. P., Kreimer, A. R., Lin, H.-Y., Fulp, W., O'Keefe, M. T., Ingles, D. J., . . . Giuliano, A. R. (2015). Long-term persistence of oral human papillomavirus type 16: the HPV Infection in Men (HIM) study. *Cancer prevention research, 8*(3), 190-196.

Candotto, V., Lauritano, D., Nardone, M., Baggi, L., Arcuri, C., Gatto, R., . . . Carinci, F. (2017). HPV infection in the oral cavity: epidemiology, clinical manifestations and relationship with oral cancer. *ORAL & implantology, 10*(3), 209.

Canning, P., Tan, L., Chu, K., Lee, S. W., Gray, N. S., & Bullock, A. N. (2014). Structural mechanisms determining inhibition of the collagen receptor DDR1 by selective and multi-targeted type II kinase inhibitors. *J Mol Biol, 426*(13), 2457-2470.

Carafoli, F., & Hohenester, E. (2013). Collagen recognition and transmembrane signalling by discoidin domain receptors. *Biochimica et Biophysica Acta (BBA)-Proteins and Proteomics, 1834*(10), 2187-2194.

Carafoli, F., Mayer, M. C., Shiraishi, K., Pecheva, M. A., Chan, L. Y., Nan, R., . . . Hohenester, E. (2012). Structure of the discoidin domain receptor 1 extracellular region bound to an inhibitory Fab fragment reveals features important for signaling. *Structure, 20*(4), 688-697.

Carvalho, L. F. C., Bonnier, F., O'Callaghan, K., O'Sullivan, J., Flint, S., Byrne, H. J., & Lyng, F. M. (2015). Raman micro-spectroscopy for rapid screening of oral squamous cell carcinoma. *Experimental and molecular pathology, 98*(3), 502-509.

Chai, R. C., Lambie, D., Verma, M., & Punyadeera, C. (2015). Current trends in the etiology and diagnosis of HPV‐related head and neck cancers. *Cancer Med, 4*(4), 596-607.

Chen, W.-J., Ho, C.-C., Chang, Y.-L., Chen, H.-Y., Lin, C.-A., Ling, T.-Y., . . . Lin, C.-Y. (2014). Cancer-associated fibroblasts regulate the plasticity of lung cancer stemness via paracrine signalling. *Nat Commun, 5*, 3472.

Cheteh, E. H., Augsten, M., Rundqvist, H., Bianchi, J., Sarne, V., Egevad, L., . . . Wiman, K. G. (2017). Human cancer-associated fibroblasts enhance glutathione levels and antagonize drug-induced prostate cancer cell death. *Cell death & disease, 8*(6), e2848.

Chi, A. C., Day, T. A., & Neville, B. W. (2015). Oral cavity and oropharyngeal squamous cell carcinoma—an update. *CA Cancer J Clin, 65*(5), 401-421.

Chiasson-MacKenzie, C., & McClatchey, A. I. (2017). Cell–Cell Contact and Receptor Tyrosine Kinase Signaling. *Cold Spring Harbor perspectives in biology*, a029215.

Christensen, A., Kiss, K., Lelkaitis, G., Juhl, K., Persson, M., Charabi, B. W., . . . Jensen, D. H. (2017). Urokinase-type plasminogen activator receptor (uPAR), tissue factor (TF) and epidermal growth factor receptor (EGFR): tumor expression patterns and prognostic value in oral cancer. *BMC Cancer, 17*(1), 572.

Chua, L. S., Kim, H.-W., & Lee, J. H. (2016). Signaling of extracellular matrices for tissue regeneration and therapeutics. *Tissue Engineering and Regenerative Medicine, 13*(1), 1-12.

Chung, C. H., Zhang, Q., Kong, C. S., Harris, J., Fertig, E. J., Harari, P. M., . . . Trotti, A. (2014). p16 protein expression and human papillomavirus status as prognostic biomarkers of nonoropharyngeal head and neck squamous cell carcinoma. *Journal of clinical oncology, 32*(35), 3930-3938.

Chung, V. Y., Tan, T. Z., Huang, R.-L., Lai, H.-C., & Huang, R. Y.-J. (2017). Loss of discoidin domain receptor 1 (DDR1) via CpG methylation during EMT in epithelial ovarian cancer. *Gene, 635*, 9-15.

Clark, L., Edington, K., Swan, I., McLay, K., Newlands, W., Wills, L., . . . Robertson, G. (1993). The absence of Harvey ras mutations during development and progression of squamous cell carcinomas of the head and neck. *Br J Cancer, 68*(3), 617.

Coelho, N. M., Arora, P. D., van Putten, S., Boo, S., Petrovic, P., Lin, A. X., . . . McCulloch, C. A. (2017). Discoidin domain receptor 1 mediates myosin-dependent collagen contraction. *Cell reports, 18*(7), 1774-1790.

Coleman, W. B., & Tsongalis, G. J. (2016). *Diagnostic Molecular Pathology: A Guide to Applied Molecular Testing*: Academic Press.

Cooper, T., Biron, V., Adam, B., Klimowicz, A., Puttagunta, L., & Seikaly, H. (2014). Keratinization and Oropharyngeal Cancer Survival. *International Journal of Radiation Oncology• Biology• Physics, 88*(2), 516.

Cooper, T., Biron, V. L., Adam, B., Klimowicz, A. C., Puttagunta, L., & Seikaly, H. (2015). Association of keratinization with 5-year disease-specific survival in oropharyngeal squamous cell carcinoma. *JAMA Otolaryngology–Head & Neck Surgery, 141*(3), 250-256.

Crow, J. M. (2012). HPV: The global burden. *Nature, 488*(7413), S2-S3.

D'Souza, G., McNeel, T., & Fakhry, C. (2017). Understanding personal risk of oropharyngeal cancer: risk-groups for oncogenic oral HPV infection and oropharyngeal cancer. *Annals of oncology, 28*(12), 3065-3069.

Dahlstrom, K. R., Calzada, G., Hanby, J. D., Garden, A. S., Glisson, B. S., Li, G., . . . Sturgis, E. M. (2013). An evolution in demographics, treatment, and outcomes of oropharyngeal cancer at a major cancer center. *Cancer, 119*(1), 81-89.

Dahlstrom, K. R., Garden, A. S., William Jr, W. N., Lim, M. Y., & Sturgis, E. M. (2016). Proposed staging system for patients with HPV-related oropharyngeal cancer based on nasopharyngeal cancer N categories. *Journal of clinical oncology, 34*(16), 1848-1854.

Darby, I. A., Laverdet, B., Bonté, F., & Desmoulière, A. (2014). Fibroblasts and myofibroblasts in wound healing. *Clinical, cosmetic and investigational dermatology, 7*, 301.

Dart, A. (2017). Cell migration: Shall we travel together? *Nature Reviews Cancer*.

de Camargo Cancela, M., de Souza, D. L. B., & Curado, M. P. (2012). International incidence of oropharyngeal cancer: a population-based study. *Oral Oncol, 48*(6), 484-490.

Deng, Y., Zhao, F., Hui, L., Li, X., Zhang, D., Lin, W., . . . Ning, Y. (2017). Suppressing miR-199a-3p by promoter methylation contributes to tumor aggressiveness and cisplatin resistance of ovarian cancer through promoting DDR1 expression. *Journal of ovarian research, 10*(1), 50.

Deng, Z., Hasegawa, M., Yamashita, Y., Matayoshi, S., Kiyuna, A., Agena, S., . . . Suzuki, M. (2012). Prognostic value of human papillomavirus and squamous cell carcinoma antigen in head and neck squamous cell carcinoma. *Cancer Sci, 103*(12), 2127-2134.

Dissmann, P., Kansy, B., Bruderek, K., Dumitru, C., Lang, S., & Brandau, S. (2015). 24 Cross-talk of tumor cells with mesenchymal stromal cells enhances tumor progression in head and neck cancer. *Oral Oncol, 51*(5), e35.

Dong, J., Sarkar, A., Suhail, A., Fridman, R., & Hoffmann, P. (2016). SU‐F‐SPS‐08: Measuring the Interaction Of DDR Cell Receptors and Extracellular Matrix Collagen in Prostate Cells. *Medical physics, 43*(6), 3352-3352.

Doorbar, J. (2016). Model systems of human papillomavirus‐associated disease. *J Pathol, 238*(2), 166-179.

Dorison, A., Dussaule, J.-C., & Chatziantoniou, C. (2017). The Role of Discoidin Domain Receptor 1 in Inflammation, Fibrosis and Renal Disease. *Nephron, 137*(3), 212-220.

Dost, F., Le Cao, K., Ford, P., Ades, C., & Farah, C. (2014). Malignant transformation of oral epithelial dysplasia: a real-world evaluation of histopathologic grading. *Oral Surg Oral Med Oral Pathol Oral Radiol, 117*(3), 343-352.

Dvorak, H. F. (2015). Tumors: wounds that do not heal—redux. *Cancer immunology research, 3*(1), 1-11.

El Azreq, M.-A., Kadiri, M., Boisvert, M., Pagé, N., Tessier, P. A., & Aoudjit, F. (2016). Discoidin domain receptor 1 promotes Th17 cell migration by activating the RhoA/ROCK/MAPK/ERK signaling pathway. *Oncotarget, 7*(29), 44975.

Elmusrati, A., Pilborough, A., Khurram, S., & Lambert, D. (2017). Cancer-associated fibroblasts promote bone invasion in oral squamous cell carcinoma. *Br J Cancer, 117*(6), 867.

Ezzoukhry, Z., Henriet, E., Piquet, L., Boyé, K., Bioulac-Sage, P., Balabaud, C., . . . Saltel, F. (2016). TGF-β1 promotes linear invadosome formation in hepatocellular carcinoma cells, through DDR1 up-regulation and collagen I cross-linking. *European journal of cell biology, 95*(11), 503-512.

Fakhry, C., & D'Souza, G. (2015). *HPV and Head and Neck Cancers*: Springer.

Favreau, A. J., Vary, C. P., Brooks, P. C., & Sathyanarayana, P. (2014). Cryptic collagen IV promotes cell migration and adhesion in myeloid leukemia. *Cancer Med, 3*(2), 265-272.

Fischer, C. A., Zlobec, I., Green, E., Probst, S., Storck, C., Lugli, A., . . . Terracciano, L. M. (2010a). Is the improved prognosis of p16 positive oropharyngeal squamous cell carcinoma dependent of the treatment modality? *Int J Cancer, 126*(5), 1256-1262.

Fischer, C. A., Zlobec, I., Green, E., Probst, S., Storck, C., Lugli, A., . . . Terracciano, L. M. (2010b). Is the improved prognosis of p16 positive oropharyngeal squamous cell carcinoma dependent of the treatment modality? *International journal of cancer, 126*(5), 1256-1262.

Fischer, M., Uxa, S., Stanko, C., Magin, T. M., & Engeland, K. (2017). Human papilloma virus E7 oncoprotein abrogates the p53-p21-DREAM pathway. *Sci Rep, 7*(1), 2603.

Forman, D., de Martel, C., Lacey, C. J., Soerjomataram, I., Lortet-Tieulent, J., Bruni, L., . . . Plummer, M. (2012). Global burden of human papillomavirus and related diseases. *Vaccine, 30*, F12-F23.

Foy, J.-P., Bazire, L., Ortiz-Cuaran, S., Deneuve, S., Kielbassa, J., Thomas, E., . . . Bertolus, C. (2017). A 13-gene expression-based radioresistance score highlights the heterogeneity in the response to radiation therapy across HPV-negative HNSCC molecular subtypes. *BMC medicine, 15*(1), 165.

Fratzl, P. (2008). *Collagen: structure and mechanics*: Springer Science & Business Media.

Freire, J., Domínguez-Hormaetxe, S., Pereda, S., De Juan, A., Vega, A., Simón, L., & Gómez-Román, J. (2014). Collagen, type XI, alpha 1: an accurate marker for differential diagnosis of breast carcinoma invasiveness in core needle biopsies. *Pathology-Research and Practice, 210*(12), 879-884.

Fu, H.-L., Valiathan, R. R., Arkwright, R., Sohail, A., Mihai, C., Kumarasiri, M., . . . Agarwal, G. (2013). Discoidin domain receptors: unique receptor tyrosine kinases in collagen-mediated signaling. *Journal of Biological Chemistry, 288*(11), 7430-7437.

Fu, H. L., Valiathan, R. R., Arkwright, R., Sohail, A., Mihai, C., Kumarasiri, M., . . . Fridman, R. (2013). Discoidin domain receptors: unique receptor tyrosine kinases in collagen-mediated signaling. [Research Support, N.I.H., Extramural

Review]. *J Biol Chem, 288*(11), 7430-7437. doi: 10.1074/jbc.R112.444158

Fu, Q., Man, X., Yu, M., Chu, Y., Luan, X., Piao, H., . . . Jin, C. (2017). Human decidua mesenchymal stem cells regulate decidual natural killer cell function via interactions between collagen and leukocyte-associated immunoglobulin-like receptor 1. *Mol Med Rep, 16*(3), 2791-2798.

Fukusumi, T., Guo, T. W., Sakai, A., Ando, M., Ren, S., Haft, S., . . . Califano, J. A. (2018). The NOTCH4–HEY1 Pathway Induces Epithelial–Mesenchymal Transition in Head and Neck Squamous Cell Carcinoma. *Clinical cancer research, 24*(3), 619-633.

Gao, H., Chakraborty, G., Zhang, Z., Akalay, I., Gadiya, M., Gao, Y., . . . Akram, M. (2016). Multi-organ site metastatic reactivation mediated by non-canonical discoidin domain receptor 1 signaling. *Cell, 166*(1), 47-62.

Gao, M., Duan, L., Luo, J., Zhang, L., Lu, X., Zhang, Y., . . . Ren, X. (2013). Discovery and optimization of 3-(2-(Pyrazolo [1, 5-a] pyrimidin-6-yl) ethynyl) benzamides as novel selective and orally bioavailable discoidin domain receptor 1 (DDR1) inhibitors. *J Med Chem, 56*(8), 3281-3295.

García-Pravia, C., Galván, J. A., Gutiérrez-Corral, N., Solar-García, L., García-Pérez, E., García-Ocaña, M., . . . Juan, R. (2013). Overexpression of COL11A1 by cancer-associated fibroblasts: clinical relevance of a stromal marker in pancreatic cancer. *PLoS One, 8*(10), e78327.

Garnaes, E., Kiss, K., Andersen, L., Therkildsen, M., Franzmann, M., Filtenborg-Barnkob, B., . . . Specht, L. (2015). Increasing incidence of base of tongue cancers from 2000 to 2010 due to HPV: the largest demographic study of 210 Danish patients. *Br J Cancer, 113*(1), 131.

Gascard, P., & Tlsty, T. D. (2016). Carcinoma-associated fibroblasts: orchestrating the composition of malignancy. *Genes & development, 30*(9), 1002-1019.

Gil-Cayuela, C., Roselló-LLetí, E., Ortega, A., Tarazón, E., Triviño, J. C., Martínez-Dolz, L., . . . Rivera, M. (2016). New Altered Non-Fibrillar Collagens in Human Dilated Cardiomyopathy: Role in the Remodeling Process. *PLoS One, 11*(12), e0168130.

Gilkes, D. M., Chaturvedi, P., Bajpai, S., Wong, C. C., Wei, H., Pitcairn, S., . . . Semenza, G. L. (2013). Collagen prolyl hydroxylases are essential for breast cancer metastasis. *Cancer Res, 73*(11), 3285-3296.

Gillison, M. L. (2006). Human papillomavirus and prognosis of oropharyngeal squamous cell carcinoma: implications for clinical research in head and neck cancers: American Society of Clinical Oncology.

Gillison, M. L., Broutian, T., Pickard, R. K., Tong, Z.-y., Xiao, W., Kahle, L., . . . Chaturvedi, A. K. (2012). Prevalence of oral HPV infection in the United States, 2009-2010. *JAMA, 307*(7), 693-703.

Gillison, M. L., Chaturvedi, A. K., Anderson, W. F., & Fakhry, C. (2015). Epidemiology of human papillomavirus–positive head and neck squamous cell carcinoma. *Journal of clinical oncology, 33*(29), 3235.

Gillison, M. L., D'souza, G., Westra, W., Sugar, E., Xiao, W., Begum, S., & Viscidi, R. (2008). Distinct risk factor profiles for human papillomavirus type 16–positive and human papillomavirus type 16–negative head and neck cancers. *J Natl Cancer Inst, 100*(6), 407-420.

Giussani, M., Landoni, E., Merlino, G., Turdo, F., Veneroni, S., Cappelletti, V., . . . Triulzi, T. (2016). Extracellular matrix proteins derived from the tumor microenvironment as circulating breast cancer diagnostic markers. *European journal of cancer, 61*, S42.

Guo, W., Wang, S., Yu, X., Qiu, J., Li, J., Tang, W., . . . Wang, Z. (2016). Construction of a 3D rGO–collagen hybrid scaffold for enhancement of the neural differentiation of mesenchymal stem cells. *Nanoscale, 8*(4), 1897-1904.

Haigentz, M., Suarez, C., Strojan, P., Rodrigo, J. P., Rinaldo, A., Bradford, C. R., . . . Ferlito, A. (2018). Understanding Interactions of Smoking on Prognosis of HPV-Associated Oropharyngeal Cancers. *Advances in therapy*, 1-6.

Hansen, N., & Karsdal, M. (2016). Type VIII Collagen *Biochemistry of Collagens, Laminins and Elastin* (pp. 61-65): Elsevier.

Hansen, N. U. B., Willumsen, N., Sand, J. M. B., Larsen, L., Karsdal, M. A., & Leeming, D. J. (2016). Type VIII collagen is elevated in diseases associated with angiogenesis and vascular remodeling. *Clinical biochemistry, 49*(12), 903-908.

Hashibe, M., Brennan, P., Chuang, S.-c., Boccia, S., Castellsague, X., Chen, C., . . . Fabianova, E. (2009). Interaction between tobacco and alcohol use and the risk of head and neck cancer: pooled analysis in the International Head and Neck Cancer Epidemiology Consortium. *Cancer Epidemiology and Prevention Biomarkers, 18*(2), 541-550.

Hassona, Y., Cirillo, N., Heesom, K., Parkinson, E., & Prime, S. (2014). Senescent cancer-associated fibroblasts secrete active MMP-2 that promotes keratinocyte dis-cohesion and invasion. *Br J Cancer, 111*(6), 1230-1237.

Hassona, Y., Cirillo, N., Lim, K. P., Herman, A., Mellone, M., Thomas, G. J., . . . Prime, S. S. (2013). Progression of genotype-specific oral cancer leads to senescence of cancer-associated fibroblasts and is mediated by oxidative stress and TGF-β. *Carcinogenesis, 34*(6), 1286-1295.

Hay, A., & Ganly, I. (2015). Targeted therapy in oropharyngeal squamous cell carcinoma: the Implications of HPV for therapy. *Rare cancers and therapy, 3*(1-2), 89-117.

Hay, E. D. (2013). *Cell biology of extracellular matrix*: Springer Science & Business Media.

Hayes, D. N., Van Waes, C., & Seiwert, T. Y. (2015). Genetic landscape of human papillomavirus–associated head and neck cancer and comparison to tobacco-related tumors. *Journal of clinical oncology, 33*(29), 3227.

Hermsen, M. A., Joenje, H., Arwert, F., Welters, M. J., Braakhuis, B. J., Bagnay, M., . . . Slater, R. (1996). Centromeric breakage as a major cause of cytogenetic abnormalities in oral squamous cell carcinoma. *Genes, Chromosomes and Cancer, 15*(1), 1-9.

Hilgendorf, K. I., Leshchiner, E. S., Nedelcu, S., Maynard, M. A., Calo, E., Ianari, A., . . . Lees, J. A. (2013). The retinoblastoma protein induces apoptosis directly at the mitochondria. *Genes & development, 27*(9), 1003-1015.

Hiraki, A., Fukuma, D., Nagata, M., Shiraishi, S., Kawahara, K., Matsuoka, Y., . . . Yoshitake, Y. (2016). Sentinel lymph node biopsy reduces the incidence of secondary neck metastasis in patients with oral squamous cell carcinoma. *Molecular and clinical oncology, 5*(1), 57-60.

Holmes, B. J., Maleki, Z., & Westra, W. H. (2015). The fidelity of p16 staining as a surrogate marker of human papillomavirus status in fine-needle aspirates and core biopsies of neck node metastases: implications for HPV testing protocols. *Acta Cytol, 59*(1), 97-103.

Hong, A., Zhang, X., Jones, D., Veillard, A.-S., Zhang, M., Martin, A., . . . Rose, B. (2016). Relationships between p53 mutation, HPV status and outcome in oropharyngeal squamous cell carcinoma. *Radiotherapy and oncology, 118*(2), 342-349.

Hsia, L.-t., Ashley, N., Ouaret, D., Wang, L. M., Wilding, J., & Bodmer, W. F. (2016). Myofibroblasts are distinguished from activated skin fibroblasts by the expression of AOC3 and other associated markers. *Proceedings of the National Academy of Sciences, 113*(15), E2162-E2171.

Hu, Y., Liu, J., Jiang, B., Chen, J., Fu, Z., Bai, F., . . . Tang, Z. (2014). MiR-199a-5p loss up-regulated DDR1 aggravated colorectal cancer by activating epithelial-to-mesenchymal transition related signaling. *Dig Dis Sci, 59*(9), 2163-2172.

Hu, Y., Liu, J., Jiang, B., Chen, J., Fu, Z., Bai, F., . . . Tang, Z. (2014). MiR-199a-5p loss up-regulated DDR1 aggravated colorectal cancer by activating epithelial-to-mesenchymal transition related signaling. [Research Support, Non-U.S. Gov't]. *Dig Dis Sci, 59*(9), 2163-2172. doi: 10.1007/s10620-014-3136-0

Huang, G., Ge, G., Izzi, V., & Greenspan, D. S. (2017). α3 Chains of type V collagen regulate breast tumour growth via glypican-1. *Nat Commun, 8*, 14351.

Huang, H. (2016). Role of DDR1 in Pancreatic Cancer.

Huang, H., Svoboda, R. A., Lazenby, A. J., Saowapa, J., Chaika, N., Ding, K., . . . Johnson, K. R. (2016). Up-regulation of N-cadherin by Collagen I-activated Discoidin Domain Receptor 1 in Pancreatic Cancer Requires the Adaptor Molecule Shc1. *Journal of Biological Chemistry, 291*(44), 23208-23223.

Huang, S. H. (2013). Oral cancer: Current role of radiotherapy and chemotherapy. *Medicina oral, patologia oral y cirugia bucal, 18*(2), e233.

Huber, M. A., & Tantiwongkosi, B. (2014). Oral and oropharyngeal cancer. *Medical Clinics, 98*(6), 1299-1321.

Huo, Y., Yang, M., Liu, W., Yang, J., Fu, X., Liu, D., . . . Sun, Y. (2015). High expression of DDR1 is associated with the poor prognosis in Chinese patients with pancreatic ductal adenocarcinoma. *Journal of Experimental & Clinical Cancer Research, 34*(1), 88.

Hur, H., Ham, I.-H., Lee, D., Jin, H., Aguilera, K. Y., Oh, H. J., . . . Ding, K. (2017). Discoidin domain receptor 1 activity drives an aggressive phenotype in gastric carcinoma. *BMC Cancer, 17*(1), 87.

Idahosa, C. N., & Kerr, A. R. (2017). Clinical Evaluation of Oral Diseases. *Contemporary Oral Medicine*, 1-35.

Irani, S. (2016). miRNAs signature in head and neck squamous cell carcinoma metastasis: a literature review. *Journal of Dentistry, 17*(2), 71.

Iwai, L. K., Payne, L. S., Allam, D., & Huang, P. H. (2016). Discoidin Domain Receptor Signalling Networks *Discoidin Domain Receptors in Health and Disease* (pp. 201-216): Springer.

Jansma, A. L., Martinez-Yamout, M. A., Liao, R., Sun, P., Dyson, H. J., & Wright, P. E. (2014). The high-risk HPV16 E7 oncoprotein mediates interaction between the transcriptional coactivator CBP and the retinoblastoma protein pRb. *J Mol Biol, 426*(24), 4030-4048.

Jimenez, L., Jayakar, S. K., Ow, T. J., & Segall, J. E. (2015). Mechanisms of invasion in head and neck cancer. *Arch Pathol Lab Med, 139*(11), 1334-1348.

Jing, H., Song, J., & Zheng, J. (2018). Discoidin domain receptor 1: New star in cancer-targeted therapy and its complex role in breast carcinoma. *Oncology letters, 15*(3), 3403-3408.

Johansson, A. C., La Fleur, L., Melissaridou, S., & Roberg, K. (2016). The relationship between EMT, CD44high/EGFRlow phenotype, and treatment response in head and neck cancer cell lines. *Journal of Oral Pathology & Medicine, 45*(9), 640-646.

Johnson, N. W., & Amarasinghe, H. K. (2016). Epidemiology and aetiology of head and neck cancers *Head and Neck Cancer* (pp. 1-57): Springer.

Johnson, N. W., Quan, J., Gao, J., & Morrison, N. (2014). Bone invasion in oral squamous cell carcinoma (OSCC). *Pathology, 46*, S8-S9.

Jordan, R. C., Lingen, M. W., Perez-Ordonez, B., He, X., Pickard, R., Koluder, M., . . . Gillison, M. L. (2012). Validation of methods for oropharyngeal cancer HPV status determination in US cooperative group trials. *Am J Surg Pathol, 36*(7), 945-954.

Joshi, P., Dutta, S., Chaturvedi, P., & Nair, S. (2014). Head and neck cancers in developing countries. *Rambam Maimonides Med J, 5*(2).

Joshi, P. S., Hazarey, V., Prashant, M., Nagpal, N., Patil, A. A., Mathur, V., & Ahuja, R. (2015). DNA PLOIDY ANALYSIS OF ORAL SQUAMOUS CELL CARCINOMA-A RETROSPECTIVE FLOW CYTOMETRIC STUDY. *Journal of Advanced Medical and Dental Sciences Research, 3*(3), 16.

Jouhi, L., Hagström, J., Atula, T., & Mäkitie, A. (2017). Is p16 an adequate surrogate for human papillomavirus status determination? *Curr Opin Otolaryngol Head Neck Surg, 25*(2), 108-112.

Ju, G.-X., Hu, Y.-B., Du, M.-R., & Jiang, J.-L. (2015). Discoidin domain receptors (DDRs): potential implications in atherosclerosis. *European journal of pharmacology, 751*, 28-33.

Juin, A., Di Martino, J., Leitinger, B., Henriet, E., Gary, A.-S., Paysan, L., . . . Rosenbaum, J. (2014). Discoidin domain receptor 1 controls linear invadosome formation via a Cdc42–Tuba pathway. *J Cell Biol, 207*(4), 517-533.

Junaid, M. (2016). *A systematic review of survival outcomes for HPV/p16 sub-groups of oropharyngeal cancer, AND Drug re-purposing in head and neck cancer cell lines*. University of Birmingham.

Jürgensen, H. J., Johansson, K., Madsen, D. H., Porse, A., Melander, M. C., Sørensen, K. R., . . . Engelholm, L. H. (2014). Complex determinants in specific members of the mannose receptor family govern collagen endocytosis. *Journal of Biological Chemistry, 289*(11), 7935-7947.

Juskaite, V., Corcoran, D. S., & Leitinger, B. (2017). Collagen induces activation of DDR1 through lateral dimer association and phosphorylation between dimers. *Elife, 6*.

Justus, D. E., Hoffman, A., Mironova, E., Hartman, A., Goldsmith, J. G., Potts, J. D., & Goldsmith, E. C. (2016). Discoidin Domain Receptors in Cardiac Development *Discoidin Domain Receptors in Health and Disease* (pp. 331-347): Springer.

Kalluri, R. (2016). The biology and function of fibroblasts in cancer. *Nature Reviews Cancer, 16*(9), 582-598.

Kanwar, N., & Done, S. J. (2013). Metastatic Determinants: Breast Tumour Cells in Circulation *Cell and Molecular Biology of Breast Cancer* (pp. 191-209): Springer.

Karagiannis, G. S., Poutahidis, T., Erdman, S. E., Kirsch, R., Riddell, R. H., & Diamandis, E. P. (2012). Cancer-associated fibroblasts drive the progression of metastasis through both paracrine and mechanical pressure on cancer tissue. *Molecular cancer research, 10*(11), 1403-1418.

Karaglani, M., Toumpoulis, I., Goutas, N., Poumpouridou, N., Vlachodimitropoulos, D., Vasilaros, S., . . . Kroupis, C. (2015). Development of novel real-time PCR methodology for quantification of COL11A1 mRNA variants and evaluation in breast cancer tissue specimens. *BMC Cancer, 15*(1), 694.

Karppinen, S. M., Honkanen, H. K., Heljasvaara, R., Riihilä, P., Autio‐Harmainen, H., Sormunen, R., . . . Hurskainen, T. (2016). Collagens XV and XVIII show different expression and localisation in cutaneous squamous cell carcinoma: type XV appears in tumor stroma, while XVIII becomes upregulated in tumor cells and lost from microvessels. *Exp Dermatol, 25*(5), 348-354.

Kawana, K., Adachi, K., Kojima, S., Kozuma, S., & Fujii, T. (2012). Suppl 2: Therapeutic Human Papillomavirus (HPV) Vaccines: A Novel Approach. *The open virology journal, 6*, 264.

Keane, F. K., Chen, Y. H., Neville, B. A., Tishler, R. B., Schoenfeld, J. D., Catalano, P. J., & Margalit, D. N. (2015). Changing prognostic significance of tumor stage and

nodal stage in patients with squamous cell carcinoma of the oropharynx in the human papillomavirus era. *Cancer, 121*(15), 2594-2602.

Kempen, P. M., Noorlag, R., Braunius, W. W., Moelans, C. B., Rifi, W., Savola, S., . . . Willems, S. M. (2015). Clinical relevance of copy number profiling in oral and oropharyngeal squamous cell carcinoma. *Cancer Med, 4*(10), 1525-1535.

Kerawala, C., Roques, T., Jeannon, J., & Bisase, B. (2016). Oral cavity and lip cancer: United Kingdom national multidisciplinary guidelines. *The Journal of Laryngology & Otology, 130*(S2), S83-S89.

Kim, E. K., Moon, S., Kim, D. K., Zhang, X., & Kim, J. (2018). CXCL1 induces senescence of cancer-associated fibroblasts via autocrine loops in oral squamous cell carcinoma. *PLoS One, 13*(1), e0188847.

Kim, H.-G., Hwang, S. Y., Aaronson, S. A., Mandinova, A., & Lee, S. W. (2017). DDR1 receptor tyrosine kinase promotes prosurvival pathway through Notch1 activation. *J Biol Chem, 292*(17), 7162.

Kim, H.-G., Tan, L., Weisberg, E. L., Liu, F., Canning, P., Choi, H. G., . . . Wang, J. (2013). Discovery of a potent and selective DDR1 receptor tyrosine kinase inhibitor. *ACS chemical biology, 8*(10), 2145-2150.

Kim, K. Y., Zhang, X., & Cha, I. H. (2015). Identification of human papillomavirus status specific biomarker in head and neck cancer. *Head Neck, 37*(9), 1310-1318.

Kim, S.-J., Park, H.-J., Sagong, B., Bae, S.-H., Oh, S.-K., Baek, J.-I., . . . Kim, U.-K. (2016). Genetic analysis of COL11A2 in Korean patients with autosomal dominant non-syndromic hearing loss. *Genes & Genomics, 38*(10), 961-966.

Kirita, T., & Omura, K. (2015). *Oral cancer: diagnosis and therapy*: Springer.

Klingelhutz, A. J., & Roman, A. (2012). Cellular transformation by human papillomaviruses: lessons learned by comparing high-and low-risk viruses. *Virology, 424*(2), 77-98.

Knopf, A., Bahadori, L., Fritsche, K., Piontek, G., Becker, C.-C., Knolle, P., . . . Li, Y. (2017). Primary tumor-associated expression of CXCR4 predicts formation of local and systemic recurrency in head and neck squamous cell carcinoma. *Oncotarget, 8*(68), 112739.

Koh, M., Woo, Y., Valiathan, R. R., Jung, H. Y., Park, S. Y., Kim, Y. N., . . . Moon, A. (2015). Discoidin domain receptor 1 is a novel transcriptional target of ZEB1 in breast epithelial cells undergoing H‐Ras‐induced epithelial to mesenchymal transition. *Int J Cancer, 136*(6).

Koschut, D., Richert, L., Pace, G., Niemann, H. H., Mély, Y., & Orian-Rousseau, V. (2016). Live cell imaging shows hepatocyte growth factor-induced Met

dimerization. *Biochimica et Biophysica Acta (BBA)-Molecular Cell Research, 1863*(7), 1552-1558.

Kothiwale, S., Borza, C. M., Lowe, E. W., Pozzi, A., & Meiler, J. (2015). Discoidin domain receptor 1 (DDR1) kinase as target for structure-based drug discovery. *Drug Discov Today, 20*(2), 255-261.

Kothiwale, S., Borza, C. M., Lowe Jr, E. W., Pozzi, A., & Meiler, J. (2015). Discoidin domain receptor 1 (DDR1) kinase as target for structure-based drug discovery. *Drug Discov Today, 20*(2), 255-261.

Krishnamachary, B., Stasinopoulos, I., Kakkad, S., Penet, M.-F., Jacob, D., Wildes, F., . . . Bhujwalla, Z. M. (2017). Breast cancer cell cyclooxygenase-2 expression alters extracellular matrix structure and function and numbers of cancer associated fibroblasts. *Oncotarget, 8*(11), 17981.

Kumar, S., Tinson, A., Mulligan, B. P., & Ojha, S. (2016). Gelatin Binding Proteins in Reproductive Physiology. *Indian journal of microbiology, 56*(4), 383-393.

Lamandé, S. R., Cameron, T. L., Savarirayan, R., & Bateman, J. F. (2017). Molecular Genetics of the Cartilage Collagenopathies *Cartilage* (pp. 99-133): Springer.

Layland, M. K., Sessions, D. G., & Lenox, J. (2005). The influence of lymph node metastasis in the treatment of squamous cell carcinoma of the oral cavity, oropharynx, larynx, and hypopharynx: N0 versus N+. *Laryngoscope, 115*(4), 629-639.

Lechner, M., Fenton, T., West, J., Wilson, G., Feber, A., Henderson, S., . . . Butcher, L. (2013). Identification and functional validation of HPV-mediated hypermethylation in head and neck squamous cell carcinoma. *Genome medicine, 5*(2), 15.

Lee, H.-J., Kang, Y.-H., Lee, J.-S., Byun, J.-H., Kim, U.-K., Jang, S.-J., . . . Park, B.-W. (2015). Positive expression of NANOG, mutant p53, and CD44 is directly associated with clinicopathological features and poor prognosis of oral squamous cell carcinoma. *BMC oral health, 15*(1), 153.

Lee, S., Lee, S.-w., Park, S., Yoon, S. M., Park, J.-h., Song, S. Y., . . . Kim, S. S. (2017). Refining prognostic stratification of human papillomavirus-related oropharyngeal squamous cell carcinoma: different prognosis between T1 and T2. *Radiation oncology journal, 35*(3), 233.

Leemans, C. R., Braakhuis, B. J., & Brakenhoff, R. H. (2011). The molecular biology of head and neck cancer. *Nature Reviews Cancer, 11*(1), 9.

Leemans, C. R., Snijders, P. J., & Brakenhoff, R. H. (2018). The molecular landscape of head and neck cancer. *Nature Reviews Cancer*.

LeHew, C. W., Weatherspoon, D. J., Peterson, C. E., Goben, A., Reitmajer, K., Sroussi, H., & Kaste, L. M. (2017). The health system and policy implications of changing

epidemiology for oral cavity and oropharyngeal cancers in the United States from 1995 to 2016. *Epidemiologic Reviews, 39*(1), 132-147.

Leitinger, B. (2015). The DDR receptor family *Receptor Tyrosine Kinases: Family and Subfamilies* (pp. 79-106): Springer.

Leitinger, B. (2016). Collagen sensing: how do discoidin domain receptors transmit a signal across the membrane?

Leitinger, B. (2016). DDRs: Binding Properties, Cell Adhesion and Modulation of Integrin Function *Discoidin Domain Receptors in Health and Disease* (pp. 3-21): Springer.

Leung, C. S., Yeung, T.-L., Yip, K.-P., Wong, K.-K., Ho, S. Y., Mangala, L. S., . . . Wong, S. T. (2017). Cancer-associated fibroblasts regulate endothelial adhesion protein LPP to promote ovarian cancer chemoresistance. *J Clin Invest, 128*(2).

Lewis, A., Kang, R., Levine, A., & Maghami, E. (2015). The new face of head and neck cancer: the HPV epidemic. *Oncology, 29*(9), 616-616.

Li, A., Li, J., Lin, J., Zhuo, W., & Si, J. (2017). COL11A1 is overexpressed in gastric cancer tissues and regulates proliferation, migration and invasion of HGC-27 gastric cancer cells in vitro. *Oncol Rep, 37*(1), 333-340.

Li, C.-C., & Woo, S.-B. (2014). Understanding the pathobiology of head and neck squamous cell carcinoma. *Current Oral Health Reports, 1*(3), 196-203.

Li, H., & Grandis, J. R. (2015). Mutational profile of HPV-positive HNSCC *Human papillomavirus (HPV)-associated oropharyngeal cancer* (pp. 171-194): Springer.

Li, M., Li, M., Yin, T., Shi, H., Wen, Y., Zhang, B., . . . Wei, Y. (2016). Targeting of cancer-associated fibroblasts enhances the efficacy of cancer chemotherapy by regulating the tumor microenvironment. *Mol Med Rep, 13*(3), 2476-2484.

Li, R., Agrawal, N., & Fakhry, C. (2015). Anatomical sites and subsites of head and neck cancer *HPV and head and neck cancers* (pp. 1-11): Springer.

Lian, I.-B., Tseng, Y.-T., Su, C.-C., & Tsai, K.-Y. (2013). Progression of precancerous lesions to oral cancer: results based on the Taiwan National Health Insurance Database. *Oral Oncol, 49*(5), 427-430.

Liao, C.-T., Wallace, C. G., Lee, L.-Y., Hsueh, C., Lin, C.-Y., Fan, K.-H., . . . Tsao, C.-K. (2014). Clinical evidence of field cancerization in patients with oral cavity cancer in a betel quid chewing area. *Oral Oncol, 50*(8), 721-731.

Lim, K. P., Cirillo, N., Hassona, Y., Wei, W., Thurlow, J. K., Cheong, S. C., . . . Prime, S. S. (2011a). Fibroblast gene expression profile reflects the stage of tumour progression in oral squamous cell carcinoma. *J Pathol, 223*(4), 459-469.

Lim, K. P., Cirillo, N., Hassona, Y., Wei, W., Thurlow, J. K., Cheong, S. C., . . . Prime, S. S. (2011b). Fibroblast gene expression profile reflects the stage of tumour progression in oral squamous cell carcinoma. *The Journal of pathology, 223*(4), 459-469.

Lindel, K., Beer, K. T., Laissue, J., Greiner, R. H., & Aebersold, D. M. (2001). Human papillomavirus positive squamous cell carcinoma of the oropharynx. *Cancer, 92*(4), 805-813.

Lingen, M. W., Xiao, W., Schmitt, A., Jiang, B., Pickard, R., Kreinbrink, P., . . . Gillison, M. L. (2013). Low etiologic fraction for high-risk human papillomavirus in oral cavity squamous cell carcinomas. *Oral Oncol, 49*(1), 1-8.

Llewellyn, C., Johnson, N., & Warnakulasuriya, K. (2001). Risk factors for squamous cell carcinoma of the oral cavity in young people—a comprehensive literature review. *Oral Oncol, 37*(5), 401-418.

Lohavanichbutr, P., Houck, J., Fan, W., Yueh, B., Mendez, E., Futran, N., . . . Schwartz, S. M. (2009). Genomewide gene expression profiles of HPV-positive and HPV-negative oropharyngeal cancer: potential implications for treatment choices. *Archives of Otolaryngology–Head & Neck Surgery, 135*(2), 180-188.

Lopes, J., Adiguzel, E., Gu, S., Liu, S.-L., Hou, G., Heximer, S., . . . Bendeck, M. P. (2013). Type VIII collagen mediates vessel wall remodeling after arterial injury and fibrous cap formation in atherosclerosis. *Am J Pathol, 182*(6), 2241-2253.

Loughery, J., & Meek, D. (2013). Switching on p53: an essential role for protein phosphorylation? *BioDiscovery, 8*.

Loughran, O., Malliri, A., Owens, D., Gallimore, P., Stanley, M., Ozanne, B., . . . Parkinson, E. (1996). Association of CDKN2A/p16INK4A with human head and neck keratinocyte replicative senescence: relationship of dysfunction to immortality and neoplasia. *Oncogene, 13*(3), 561-568.

Lu, Q. P., Chen, W. D., Peng, J. R., Xu, Y. D., Cai, Q., Feng, G. K., . . . Guan, Z. (2016). Antitumor activity of 7RH, a discoidin domain receptor 1 inhibitor, alone or in combination with dasatinib exhibits antitumor effects in nasopharyngeal carcinoma cells. *Oncology letters, 12*(5), 3598-3608.

Lundgren-Åkerlund, E., & Aszòdi, A. (2014). Integrin α10β1: a collagen receptor critical in skeletal development *I Domain Integrins* (pp. 61-71): Springer.

Luo, Q., Wang, C.-Q., Yang, L.-Y., Gao, X.-M., Sun, H.-T., Zhang, Y., . . . Sheng, Y.-Y. (2017). FOXQ1/NDRG1 axis exacerbates hepatocellular carcinoma initiation via enhancing crosstalk between fibroblasts and tumor cells. *Cancer Lett*.

Lyford-Pike, S., Peng, S., Young, G. D., Taube, J. M., Westra, W. H., Akpeng, B., . . . Bishop, J. A. (2013). Evidence for a role of the PD-1: PD-L1 pathway in immune resistance of HPV-associated head and neck squamous cell carcinoma. *Cancer Res, 73*(6), 1733-1741.

Ma, Z.-H., Ma, J.-H., Jia, L., & Zhao, Y.-F. (2012). Effect of enhanced expression of COL8A1 on lymphatic metastasis of hepatocellular carcinoma in mice. *Experimental and therapeutic medicine, 4*(4), 621-626.

Maasland, D. H., van den Brandt, P. A., Kremer, B., Goldbohm, R. A. S., & Schouten, L. J. (2014). Alcohol consumption, cigarette smoking and the risk of subtypes of head-neck cancer: results from the Netherlands Cohort Study. *BMC Cancer, 14*(1), 187.

Madar, S., Goldstein, I., & Rotter, V. (2013). 'Cancer associated fibroblasts'–more than meets the eye. *Trends in molecular medicine, 19*(8), 447-453.

Malaysia, J. S. (2011). Population and housing census of Malaysia 2010: Population distribution and basic demographic characteristics.

Markopoulos, A. K. (2012). Current aspects on oral squamous cell carcinoma. *The open dentistry journal, 6*, 126.

Martinez-Zapien, D., Ruiz, F. X., Poirson, J., Mitschler, A., Ramirez, J., Forster, A., . . . Podjarny, A. (2016). Structure of the E6/E6AP/p53 complex required for HPV-mediated degradation of p53. *Nature, 529*(7587), 541.

Mathew, R. (2017). *The prognostic role of VEGF in head and neck squamous cell carcinoma.* Boston University.

Mathur, S., Conway, D. I., Worlledge-Andrew, H., Macpherson, L. M., & Ross, A. J. (2015). Assessment and prevention of behavioural and social risk factors associated with oral cancer: protocol for a systematic review of clinical guidelines and systematic reviews to inform Primary Care dental professionals. *Systematic reviews, 4*(1), 184.

McAlinden, A., Traeger, G., Hansen, U., Weis, M. A., Ravindran, S., Wirthlin, L., . . . Fernandes, R. J. (2014). Molecular properties and fibril ultrastructure of types II and XI collagens in cartilage of mice expressing exclusively the α1 (IIA) collagen isoform. *Matrix Biology, 34*, 105-113.

McIlwain, W. R., Sood, A. J., Nguyen, S. A., & Day, T. A. (2014). Initial symptoms in patients with HPV-positive and HPV-negative oropharyngeal cancer. *JAMA Otolaryngology–Head & Neck Surgery, 140*(5), 441-447.

Mehanna, H., Beech, T., Nicholson, T., El‐Hariry, I., McConkey, C., Paleri, V., & Roberts, S. (2013). Prevalence of human papillomavirus in oropharyngeal and nonoropharyngeal head and neck cancer—systematic review and meta‐analysis of trends by time and region. *Head Neck, 35*(5), 747-755.

Mehanna, H., Evans, M., Beasley, M., Chatterjee, S., Dilkes, M., Homer, J., . . . Sloan, P. (2016). Oropharyngeal cancer: United Kingdom national multidisciplinary guidelines. *The Journal of Laryngology & Otology, 130*(S2), S90-S96.

Mellone, M., Hanley, C. J., Thirdborough, S., Mellows, T., Garcia, E., Woo, J., . . . Moutasim, K. A. (2017). Induction of fibroblast senescence generates a non-fibrogenic myofibroblast phenotype that differentially impacts on cancer prognosis. *Aging (Albany NY), 9*(1), 114.

Meucci, S., Keilholz, U., Tinhofer, I., & Ebner, O. A. (2016). Mutational load and mutational patterns in relation to age in head and neck cancer. *Oncotarget, 7*(43), 69188.

Miao, L., Zhu, S., Wang, Y., Li, Y., Ding, J., Dai, J., . . . Song, Y. (2013). Discoidin domain receptor 1 is associated with poor prognosis of non-small cell lung cancer and promotes cell invasion via epithelial-to-mesenchymal transition. *Medical Oncology, 30*(3), 626.

Mienaltowski, M. J., & Birk, D. E. (2014). Structure, Physiology, and Biochemistry of Collagens. *Progress in Heritable Soft Connective Tissue Diseases, 802*, 2.

Minafra, L., Bravata, V., Forte, G. I., Cammarata, F. P., Gilardi, M. C., & Messa, C. (2014). Gene expression profiling of epithelial–mesenchymal transition in primary breast cancer cell culture. *Anticancer Res, 34*(5), 2173-2183.

Mirghani, H., Amen, F., Blanchard, P., Moreau, F., Guigay, J., Hartl, D., & Lacau St Guily, J. (2015). Treatment de‐escalation in HPV‐positive oropharyngeal carcinoma: Ongoing trials, critical issues and perspectives. *Int J Cancer, 136*(7), 1494-1503.

Mirghani, H., Amen, F., Moreau, F., & St Guily, J. L. (2015). Do high-risk human papillomaviruses cause oral cavity squamous cell carcinoma? *Oral Oncol, 51*(3), 229-236.

Miyake, K., Ishimoto, T., Izumi, D., Arima, K., Eto, T., Kuroda, D., . . . Yoshida, N. (2017). Interaction with extracellular matrix enhance the chemoresistance via CXCL12/CXCR4 and integrin signal activation by cancer-associated fibroblasts in gastric cancers: AACR.

Miyake, M., Hori, S., Morizawa, Y., Tatsumi, Y., Nakai, Y., Anai, S., . . . Rosser, C. (2016). 790 CXCL1 signalling is a crucial mediator between cancer cells and tumour-associated macrophages/cancer-associated fibroblasts for tumour invasion and progression in micro-environment of human bladder cancer. *European Urology Supplements, 15*(3), e790.

Momen-Heravi, F., Trachtenberg, A., Kuo, W., & Cheng, Y. (2014). Genomewide study of salivary microRNAs for detection of oral cancer. *J Dent Res, 93*(7_suppl), 86S-93S.

Monteiro, L., & Warnakulasuriya, S. (2017). Genetic Aberrations and Molecular Pathways in Head and Neck Cancer *Squamous cell Carcinoma* (pp. 97-111): Springer.

Mooren, J. J., Gültekin, S. E., Straetmans, J. M., Haesevoets, A., Peutz‐Kootstra, C. J., Huebbers, C. U., . . . Kremer, B. (2014). P16INK4A immunostaining is a strong indicator for high‐risk‐HPV‐associated oropharyngeal carcinomas and dysplasias, but is unreliable to predict low‐risk‐HPV‐infection in head and neck papillomas and laryngeal dysplasias. *Int J Cancer, 134*(9), 2108-2117.

Mostafa, B. E.-D., Abdelmageed, H. M., El-Begermy, M. M., Taha, M. S., Hamdy, T. A.-E., Omran, A., & Lotfy, N. (2016). Value of vitamin D assessment in patients with head and neck squamous cell cancer before treatment. *The Egyptian Journal of Otolaryngology, 32*(4), 279.

Moutasim, K. A., Robinson, M., & Thavaraj, S. (2015). Human papillomavirus testing in diagnostic head and neck histopathology. *Diagnostic Histopathology, 21*(2), 77-84.

Na, J., Shin, J. Y., Jeong, H., Lee, J. Y., Kim, B. J., Kim, W. S., . . . Ju, B.-G. (2017). JMJD3 and NF-κB-dependent activation of Notch1 gene is required for keratinocyte migration during skin wound healing. *Sci Rep, 7*(1), 6494.

Ndiaye, C., Mena, M., Alemany, L., Arbyn, M., Castellsagué, X., Laporte, L., . . . Trottier, H. (2014a). HPV DNA, E6/E7 mRNA, and p16 INK4a detection in head and neck cancers: a systematic review and meta-analysis. *The lancet oncology, 15*(12), 1319-1331.

Ndiaye, C., Mena, M., Alemany, L., Arbyn, M., Castellsagué, X., Laporte, L., . . . Trottier, H. (2014b). HPV DNA, E6/E7 mRNA, and p16INK4a detection in head and neck cancers: a systematic review and meta-analysis. *The lancet oncology, 15*(12), 1319-1331.

Network, C. G. A. (2015a). Comprehensive genomic characterization of head and neck squamous cell carcinomas. *Nature, 517*(7536), 576.

Network, C. G. A. (2015b). Comprehensive genomic characterization of head and neck squamous cell carcinomas. *Nature, 517*(7536), 576-582.

Ng, C., Lam, W., Chan, P. K., Lo, S., & Chong, W. (2015). Oropharyngeal squamous cell carcinoma (OPSCC), a practical prognostic immunophenotypic panel. *Pathology, 47*, S71.

Nguyen, N. P., Nguyen, L. M., Thomas, S., Hong-Ly, B., Chi, A., Vos, P., . . . Vinh-Hung, V. (2016). Oral sex and oropharyngeal cancer: The role of the primary care physicians. *Medicine, 95*(28).

Niaz, K., Maqbool, F., Khan, F., Bahadar, H., Ismail Hassan, F., & Abdollahi, M. (2017). Smokeless tobacco (paan and gutkha) consumption, prevalence, and contribution to oral cancer. *Epidemiology and Health, 39*, e2017009.

Nichols, A. C., Dhaliwal, S. S., Palma, D. A., Basmaji, J., Chapeskie, C., Dowthwaite, S., . . . Wehrli, B. (2013). Does HPV type affect outcome in oropharyngeal cancer? *Journal of Otolaryngology-Head & Neck Surgery, 42*(1), 9.

Nichols, A. C., Palma, D. A., Chow, W., Tan, S., Rajakumar, C., Rizzo, G., . . . Winquist, E. (2013). High Frequency of Activating PIK3CA Mutations in Human Papillomavirus–Positive Oropharyngeal Cancer. *JAMA Otolaryngology–Head & Neck Surgery, 139*(6), 617-622.

Nishida, N., & Shimada, I. (2016). DDR Structural Biology *Discoidin Domain Receptors in Health and Disease* (pp. 57-67): Springer.

Nune, S. K., Rama, K. S., Dirisala, V. R., & Chavali, M. Y. (2017). Electrospinning of collagen nanofiber scaffolds for tissue repair and regeneration *Nanostructures for Novel Therapy* (pp. 281-311): Elsevier.

Nur, H. Z., In, G., Caballero, B., Finglas, P., & Toldrá, F. (2016). This article was originally published in the Encyclopedia of Food and Health published by Elsevier, and the attached copy is provided by Elsevier for the author's benefit and for the benefit of the author's institution, for non-commercial research and educational use including without limitation use in instruction at your institution, sending it to specific colleagues who you know, and providing a copy to your institution's administrator.

O'rorke, M., Ellison, M., Murray, L., Moran, M., James, J., & Anderson, L. (2012). Human papillomavirus related head and neck cancer survival: a systematic review and meta-analysis. *Oral Oncol, 48*(12), 1191-1201.

Oguejiofor, K., Galletta-Williams, H., Dovedi, S. J., Roberts, D. L., Stern, P. L., & West, C. M. (2017). Distinct patterns of infiltrating CD8+ T cells in HPV+ and CD68 macrophages in HPV-oropharyngeal squamous cell carcinomas are associated with better clinical outcome but PD-L1 expression is not prognostic. *Oncotarget, 8*(9), 14416.

Oguejiofor, K., Hall, J., Slater, C., Betts, G., Hall, G., Slevin, N., . . . West, C. M. (2015). Stromal infiltration of CD8 T cells is associated with improved clinical outcome in HPV-positive oropharyngeal squamous carcinoma. *Br J Cancer, 113*(6), 886.

Ohshio, Y., Teramoto, K., Hanaoka, J., Tezuka, N., Itoh, Y., Asai, T., . . . Ogasawara, K. (2015). Cancer‐associated fibroblast‐targeted strategy enhances antitumor immune responses in dendritic cell‐based vaccine. *Cancer Sci, 106*(2), 134-142.

Ono, M., Sano, Y., & Suzuki, T. (2017). Anti-DDR1 antibody having anti-tumor activity: Google Patents.

Ota, I., Masui, T., Kurihara, M., Yook, J.-I., Mikami, S., Kimura, T., . . . Yamanaka, T. (2016). Snail-induced EMT promotes cancer stem cell-like properties in head and neck cancer cells. *Oncol Rep, 35*(1), 261-266.

Palladino, C., Matà, R., Nicolosi, M. L., Presti, A. R. L., Malaguarnera, R., Ragusa, M., . . . Vella, V. (2016). In breast cancer cells IGF-I induces upregulation of DDR1 by suppressing miR-199a-5p via the PI3K/Akt pathway: AACR.

Pannone, G., Rodolico, V., Santoro, A., Muzio, L. L., Franco, R., Botti, G., . . . Campisi, G. (2012). Evaluation of a combined triple method to detect causative HPV in oral and oropharyngeal squamous cell carcinomas: p16 Immunohistochemistry, Consensus PCR HPV-DNA, and In Situ Hybridization. *Infect Agent Cancer, 7*(1), 4.

Park, Y., Kim, W., Lee, J., Park, J., Cho, J., Pang, K., . . . Yang, K. (2015). Cytoplasmic DRAK1 overexpressed in head and neck cancers inhibits TGF-β1 tumor suppressor activity by binding to Smad3 to interrupt its complex formation with Smad4. *Oncogene, 34*(39), 5037.

Partlová, S., Bouček, J., Kloudová, K., Lukešová, E., Zábrodský, M., Grega, M., . . . Špíšek, R. (2015). Distinct patterns of intratumoral immune cell infiltrates in patients with HPV-associated compared to non-virally induced head and neck squamous cell carcinoma. *Oncoimmunology, 4*(1), e965570.

Patel, V., Wang, Z., Chen, Q., Rusling, J. F., Molinolo, A. A., & Gutkind, J. S. (2017). Emerging Cancer Biomarkers for HNSCC Detection and Therapeutic Intervention *Contemporary Oral Oncology* (pp. 281-308): Springer.

Paulsson, J., Rydén, L., Strell, C., Frings, O., Tobin, N. P., Fornander, T., . . . Östman, A. (2017). High expression of stromal PDGFRβ is associated with reduced benefit of tamoxifen in breast cancer. *The Journal of Pathology: Clinical Research, 3*(1), 38-43.

Petruzzi, M., Lucchese, A., Nardi, G. M., Lauritano, D., Favia, G., Serpico, R., & Grassi, F. R. (2014). Evaluation of autofluorescence and toluidine blue in the differentiation of oral dysplastic and neoplastic lesions from non dysplastic and neoplastic lesions: a cross-sectional study. *J Biomed Opt, 19*(7), 076003-076003.

Petti, S., Masood, M., & Scully, C. (2013). The magnitude of tobacco smoking-betel quid chewing-alcohol drinking interaction effect on oral cancer in South-East Asia. A meta-analysis of observational studies. *PLoS One, 8*(11), e78999.

Pickup, M. W., Mouw, J. K., & Weaver, V. M. (2014). The extracellular matrix modulates the hallmarks of cancer. *EMBO reports, 15*(12), 1243-1253.

Pidelaserra Martí, G., & Bassols Teixidó, A. M. (2015). Cancer-associated fibroblasts, key drivers of tumorigenesis.

Pollock, N., Wang, L., Wallweber, G., Gooding, W. E., Huang, W., Chenna, A., . . . Li, H. (2015). Increased expression of HER2, HER3, and HER2: HER3 heterodimers in HPV-positive HNSCC using a novel proximity-based assay: implications for targeted therapies. *Clinical cancer research*, clincanres. 3338.2014.

Polo, V., Pasello, G., Frega, S., Favaretto, A., Koussis, H., Conte, P., & Bonanno, L. (2016). Squamous cell carcinomas of the lung and of the head and neck: new insights on molecular characterization. *Oncotarget, 7*(18), 25050.

Posner, M., Lorch, J., Goloubeva, O., Tan, M., Schumaker, L., Sarlis, N., . . . Cullen, K. (2011). Survival and human papillomavirus in oropharynx cancer in TAX 324: a subset analysis from an international phase III trial. *Annals of oncology, 22*(5), 1071-1077.

Poundarik, A. A., Wu, P.-C., Evis, Z., Sroga, G. E., Ural, A., Rubin, M., & Vashishth, D. (2015). A direct role of collagen glycation in bone fracture. *Journal of the mechanical behavior of biomedical materials, 52*, 120-130.

Prabhu, P. R., & Pillai, M. R. (2017). Human Papillomaviruses and Squamous Cell Carcinomas of Head and Neck Region *Contemporary Oral Oncology* (pp. 77-101): Springer.

Puram, S. V., & Rocco, J. W. (2015). Molecular aspects of head and neck cancer therapy. *Hematology/Oncology Clinics, 29*(6), 971-992.

Pytynia, K. B., Dahlstrom, K. R., & Sturgis, E. M. (2014). Epidemiology of HPV-associated oropharyngeal cancer. *Oral Oncol, 50*(5), 380-386.

Pytynia, K. B., Dahlstrom, K. R., & Sturgis, E. M. (2014). Epidemiology of HPV-associated oropharyngeal cancer. [Review]. *Oral Oncol, 50*(5), 380-386. doi: 10.1016/j.oraloncology.2013.12.019

Qazi, A. K., Siddiqui, J. A., Jahan, R., Chaudhary, S., Walker, L. A., Syed, Z., . . . Macha, M. A. (2018). Emerging therapeutic potential of graviola and its constituents in cancers. *Carcinogenesis, 1*, 12.

Quail, D. F., & Joyce, J. A. (2013). Microenvironmental regulation of tumor progression and metastasis. *Nat Med, 19*(11), 1423.

Qureishi, A., Mawby, T., Fraser, L., Shah, K. A., Møller, H., & Winter, S. (2017). Current and future techniques for human papilloma virus (HPV) testing in oropharyngeal squamous cell carcinoma. *European Archives of Oto-Rhino-Laryngology, 274*(7), 2675-2683.

Raab-Westphal, S., Marshall, J. F., & Goodman, S. L. (2017). Integrins as therapeutic targets: successes and cancers. *Cancers, 9*(9), 110.

Rada, M., Cha, J., Sage, J., Orsulic, S., & Cheon, D.-J. (2017). Collagen type XI alpha 1 confers cisplatin chemoresistance in ovarian cancer through inhibitor of apoptosis proteins (IAPs): AACR.

Rada, M., Eldred, C., Sage, J., Orsulic, S., & Cheon, D.-J. (2017). Abstract TMEM-017: COLLAGEN TYPE XI ALPHA 1 (COL11A1) IS A NOVEL STROMAL MEDIATOR OF CHEMORESISTANCE: AACR.

Raimondi, L., Amodio, N., Di Martino, M. T., Altomare, E., Leotta, M., Caracciolo, D., . . . D'Aquila, P. (2014). Targeting of multiple myeloma-related angiogenesis by miR-199a-5p mimics: in vitro and in vivo anti-tumor activity. *Oncotarget, 5*(10), 3039.

Rammal, H., Saby, C., Magnien, K., Van-Gulick, L., Garnotel, R., Buache, E., . . . Morjani, H. (2016a). Discoidin domain receptors: potential actors and targets in cancer. *Frontiers in pharmacology, 7*.

Rammal, H., Saby, C., Magnien, K., Van-Gulick, L., Garnotel, R., Buache, E., . . . Morjani, H. (2016b). Discoidin domain receptors: potential actors and targets in cancer. *Frontiers in pharmacology, 7*, 55.

Rao, S. V. K., Mejia, G., Roberts-Thomson, K., & Logan, R. (2013). Epidemiology of oral cancer in Asia in the past decade-an update (2000-2012). *Asian Pacific journal of cancer prevention, 14*(10), 5567-5577.

Rath, N., Morton, J. P., Julian, L., Helbig, L., Kadir, S., McGhee, E. J., . . . Pinho, A. V. (2016). ROCK signaling promotes collagen remodeling to facilitate invasive pancreatic ductal adenocarcinoma tumor cell growth. *EMBO molecular medicine*, e201606743.

Ratzinger, S., Grässel, S., Dowejko, A., Reichert, T. E., & Bauer, R. J. (2011). Induction of type XVI collagen expression facilitates proliferation of oral cancer cells. *Matrix Biology, 30*(2), 118-125.

Rautava, J., & Syrjänen, S. (2012). Biology of human papillomavirus infections in head and neck carcinogenesis. *Head Neck Pathol, 6*(1), 3-15.

Ravenda, P. S., Zampino, M. G., Fazio, N., Barberis, M., Bottiglieri, L., & Chiocca, S. (2015). Human papillomavirus in anal squamous cell carcinoma: an angel rather than a devil? *ecancermedicalscience, 9*.

Reel, B., Korkmaz, C. G., Arun, M. Z., Yildirim, G., Ogut, D., Kaymak, A., . . . Ergur, B. U. (2015). The regulation of matrix metalloproteinase expression and the role of discoidin domain receptor 1/2 signalling in zoledronate-treated PC3 cells. *Journal of Cancer, 6*(10), 1020.

Regezi, J. A., Sciubba, J. J., & Jordan, R. C. (2016). *Oral pathology: clinical pathologic correlations*: Elsevier Health Sciences.

Reyes-Uribe, E., Serna-Marquez, N., & Salazar, E. P. (2015). DDRs: receptors that mediate adhesion, migration and invasion in breast cancer cells. *AIMS Biophysics, 2*(3), 303-317.

RIBEIRO, F. A. P., Noguti, J., OSHIMA, C. T. F., & Ribeiro, D. A. (2014). Effective targeting of the epidermal growth factor receptor (EGFR) for treating oral cancer: a promising approach. *Anticancer Res, 34*(4), 1547-1552.

Richters, A., Nguyen, H. D., Phan, T., Simard, J. R., Grüt er, C., Engel, J., & Rauh, D. (2014). Identification of type II and III DDR2 inhibitors. *J Med Chem, 57*(10), 4252-4262.

Rieckmann, T., Tribius, S., Grob, T. J., Meyer, F., Busch, C.-J., Petersen, C., . . . Kriegs, M. (2013). HNSCC cell lines positive for HPV and p16 possess higher cellular radiosensitivity due to an impaired DSB repair capacity. *Radiotherapy and oncology, 107*(2), 242-246.

Rietbergen, M. M., Brakenhoff, R. H., Bloemena, E., Witte, B., Snijders, P., Heideman, D., . . . Leemans, C. (2013). Human papillomavirus detection and comorbidity: critical issues in selection of patients with oropharyngeal cancer for treatment De-escalation trials. *Annals of oncology, 24*(11), 2740-2745.

Rietbergen, M. M., Snijders, P. J., Beekzada, D., Braakhuis, B. J., Brink, A., Heideman, D. A., . . . Jong, B. D. (2014). Molecular characterization of p16 ‐ immunopositive but HPV DNA ‐ negative oropharyngeal carcinomas. *Int J Cancer, 134*(10), 2366-2372.

Ritchie, J. M., Smith, E. M., Summersgill, K. F., Hoffman, H. T., Wang, D., Klussmann, J. P., . . . Haugen, T. H. (2003). Human papillomavirus infection as a prognostic factor in carcinomas of the oral cavity and oropharynx. *Int J Cancer, 104*(3), 336-344.

Rivera, C. (2015). Essentials of oral cancer. *International journal of clinical and experimental pathology, 8*(9), 11884.

Rivera, C., González-Arriagada, W. A., Loyola-Brambilla, M., de Almeida, O. P., Della Coletta, R., & Venegas, B. (2014). Clinicopathological and immunohistochemical evaluation of oral and oropharyngeal squamous cell carcinoma in Chilean population. *International journal of clinical and experimental pathology, 7*(9), 5968.

Rivera, C., Oliveira, A. K., Costa, R. A. P., De Rossi, T., & Leme, A. F. P. (2017). Prognostic biomarkers in oral squamous cell carcinoma: a systematic review. *Oral Oncol, 72*, 38-47.

Rivera, C., & Venegas, B. (2014). Histological and molecular aspects of oral squamous cell carcinoma. *Oncology letters, 8*(1), 7-11.

Robinson, M., Schache, A., Sloan, P., & Thavaraj, S. (2012). HPV specific testing: a requirement for oropharyngeal squamous cell carcinoma patients. *Head Neck Pathol, 6*(1), 83-90.

Robinson, M. D., McCarthy, D. J., & Smyth, G. K. (2010). edgeR: a Bioconductor package for differential expression analysis of digital gene expression data. *Bioinformatics, 26*(1), 139-140.

Romayor, I., Herrero-Alonso, A., Hernandez-Unzueta, I., Benedicto, A., Marquez, J., & Arteta, B. (2017). 45PRole of discoidin domain receptors in extracellular matrix remodeling during tumor-host interaction in liver metastasis. *Annals of oncology, 28*(suppl_5).

Rudra-Ganguly, N., Lowe, C., Mattie, M., Chang, M. S., Satpayev, D., Verlinsky, A., . . . Challita-Eid, P. (2014). Discoidin domain receptor 1 contributes to tumorigenesis through modulation of TGFBI expression. *PLoS One, 9*(11), e111515.

Ruiz-Castro, P. A., Shaw, D., & Jarai, G. (2016). Discoidin Domain Receptor Signaling and Pharmacological Inhibitors *Discoidin Domain Receptors in Health and Disease* (pp. 217-238): Springer.

Ryerson, A. B., Peters, E. S., Coughlin, S. S., Chen, V. W., Gillison, M. L., Reichman, M. E., . . . Kawaoka, K. (2008). Burden of potentially human papillomavirus‐associated cancers of the oropharynx and oral cavity in the US, 1998–2003. *Cancer, 113*(S10), 2901-2909.

Saby, C., Rammal, H., Magnien, K., Pasco-Brassart, S., Maquoi, E., Jeannesson, P., & Morjani, H. (2016). Regulation of breast carcinoma cell proliferation and apoptosis by type I collagen aging and 3D confinement involves differential activation of DDR1.

Salazar, C. R., Anayannis, N., Smith, R. V., Wang, Y., Haigentz, M., Garg, M., . . . Belbin, T. J. (2014). Combined P16 and human papillomavirus testing predicts head and neck cancer survival. *Int J Cancer, 135*(10), 2404-2412.

Samman, M., Wood, H. M., Conway, C., Stead, L., Daly, C., Chalkley, R., . . . Egan, P. (2015). A novel genomic signature reclassifies an oral cancer subtype. *Int J Cancer, 137*(10), 2364-2373.

Saraiya, M., Unger, E. R., Thompson, T. D., Lynch, C. F., Hernandez, B. Y., Lyu, C. W., . . . Hopenhayn, C. (2015). US assessment of HPV types in cancers: implications for current and 9-valent HPV vaccines. *J Natl Cancer Inst, 107*(6), djv086.

Sarkar, A., Fridman, R., Sohail, A., & Hoffmann, P. (2015). Measurement of DDR-Collagen interaction Forces with Atomic force Microscopy. *Bulletin of the American Physical Society, 60*.

Sarmento, D. J. d. S., Godoy, G. P., Miguel, M. C. d. C., & Silveira, É. J. D. d. (2016). Link between immunoexpression of hMLH1 and hMSH2 proteins and clinical-epidemiological aspects of actinic cheilitis. *Anais brasileiros de dermatologia, 91*(4), 463-467.

Schaal, C., & Chellappan, S. P. (2014). Nicotine-mediated cell proliferation and tumor progression in smoking-related cancers. *Molecular cancer research, 12*(1), 14-23.

Schiegnitz, E., Kaemmerer, P. W., & Al-Nawas, B. (2017). Quality Assessment of Systematic Reviews and Meta-analyses on Biomarkers in Oral Squamous Cell Carcinoma. *Oral Health & Preventive Dentistry, 15*(1).

Schiffman, M., & Wentzensen, N. (2013). Human papillomavirus infection and the multistage carcinogenesis of cervical cancer: AACR.

Schiller, J. T., & Lowy, D. R. (2012). Understanding and learning from the success of prophylactic human papillomavirus vaccines. *Nature Reviews Microbiology, 10*(10), 681-693.

Schnittert, J., Bansal, R., Storm, G., & Prakash, J. (2018). Integrins in wound healing, fibrosis and tumor stroma: High potential targets for therapeutics and drug delivery. *Advanced drug delivery reviews*.

Schoepp, M., Ströse, A. J., & Haier, J. (2017). Dysregulation of miRNA Expression in Cancer Associated Fibroblasts (CAFs) and Its Consequences on the Tumor Microenvironment. *Cancers, 9*(6), 54.

Screening, P., & Board, P. E. (2017). Oral Cavity and Oropharyngeal Cancer Prevention (PDQ®).

Seguin, L., Desgrosellier, J. S., Weis, S. M., & Cheresh, D. A. (2015). Integrins and cancer: regulators of cancer stemness, metastasis, and drug resistance. *Trends in cell biology, 25*(4), 234-240.

Seiwert, T. Y., Zuo, Z., Keck, M. K., Khattri, A., Pedamallu, C. S., Stricker, T., . . . Cho, J. (2015). Integrative and comparative genomic analysis of HPV-positive and HPV-negative head and neck squamous cell carcinomas. *Clinical cancer research, 21*(3), 632-641.

Serrano, M. A., Li, Z., Dangeti, M., Musich, P. R., Patrick, S., Roginskaya, M., . . . Zou, Y. (2013). DNA-PK, ATM and ATR collaboratively regulate p53–RPA interaction to facilitate homologous recombination DNA repair. *Oncogene, 32*(19), 2452-2462.

Shabestari, S. B., Shirinbak, I., & Azadarmaki, R. (2017). A Comprehensive Look at Oromaxillofacial and Laryngopharyngeal Cancers *Cancer Genetics and Psychotherapy* (pp. 531-587): Springer.

Shaikh, M. H., McMillan, N. A., & Johnson, N. W. (2015). HPV-associated head and neck cancers in the Asia Pacific: A critical literature review & meta-analysis. *Cancer Epidemiol, 39*(6), 923-938.

Shakir, N. (2014). *An investigation into mechanisms of action of colchicine, zinc acetate and paracetemol-potential candidates for drug repurposing in head and neck cancer therapy.* University of Birmingham.

Shen, L., Yang, M., Lin, Q., Zhang, Z., Zhu, B., & Miao, C. (2016). COL11A1 is overexpressed in recurrent non-small cell lung cancer and promotes cell proliferation, migration, invasion and drug resistance. *Oncol Rep, 36*(2), 877-885.

Shitomi, Y., Thøgersen, I. B., Ito, N., Leitinger, B., Enghild, J. J., & Itoh, Y. (2015). ADAM10 controls collagen signaling and cell migration on collagen by shedding the ectodomain of discoidin domain receptor 1 (DDR1). *Mol Biol Cell, 26*(4), 659-673.

Singhi, A. D., & Westra, W. H. (2010). Comparison of human papillomavirus in situ hybridization and p16 immunohistochemistry in the detection of human papillomavirus - associated head and neck cancer based on a prospective clinical experience. *Cancer, 116*(9), 2166-2173.

Sivasithamparam, J., Visk, C. A., Cohen, E. E., & King, A. C. (2013). Modifiable risk behaviors in patients with head and neck cancer. *Cancer, 119*(13), 2419-2426.

Skrbic, B., Engebretsen, K. V., Strand, M. E., Lunde, I. G., Herum, K. M., Marstein, H. S., . . . Christensen, G. (2015). Lack of collagen VIII reduces fibrosis and promotes early mortality and cardiac dilatation in pressure overload in mice. *Cardiovascular research, 106*(1), 32-42.

Slebos, R. J., Yi, Y., Ely, K., Carter, J., Evjen, A., Zhang, X., . . . Burkey, B. B. (2006). Gene expression differences associated with human papillomavirus status in head and neck squamous cell carcinoma. *Clinical cancer research, 12*(3), 701-709.

Smyth, G. K. (2004). Linear models and empirical bayes methods for assessing differential expression in microarray experiments. *Statistical applications in genetics and molecular biology, 3*(1), 1-25.

Sok, J., Lee, J., Dasari, S., Joyce, S., Contrucci, S., Egloff, A., . . . Grandis, J. (2013a). Collagen type XI α1 facilitates head and neck squamous cell cancer growth and invasion. *Br J Cancer, 109*(12), 3049-3056.

Sok, J., Lee, J., Dasari, S., Joyce, S., Contrucci, S., Egloff, A., . . . Grandis, J. (2013b). Collagen type XI α1 facilitates head and neck squamous cell cancer growth and invasion. *Br J Cancer, 109*(12), 3049.

Somaiah, C., Kumar, A., Mawrie, D., Sharma, A., Patil, S. D., Bhattacharyya, J., . . . Jaganathan, B. G. (2015). Collagen promotes higher adhesion, survival and proliferation of mesenchymal stem cells. *PLoS One, 10*(12), e0145068.

Song, J., Chen, X., Bai, J., Liu, Q., Li, H., Xie, J., . . . Zheng, J. (2016). Discoidin domain receptor 1 (DDR1), a promising biomarker, induces epithelial to mesenchymal transition in renal cancer cells. *Tumor Biology, 37*(8), 11509-11521.

Songock, W. K., Kim, S.-m., & Bodily, J. M. (2017). The human papillomavirus E7 oncoprotein as a regulator of transcription. *Virus research, 231*, 56-75.

Soria-Céspedes, D., Canchola, A. G., Lara-Torres, C., Sánchez-Marle, J., Hernández-Peña, R., & Ortiz-Hidalgo, C. (2012). Metastatic oropharyngeal squamous cell carcinoma in cervical lymph nodes associated to HPV infection type 16 and 45; clinical, morphological and molecular study of two cases. *Gaceta medica de Mexico, 149*(6), 673-679.

Spranger, J. (1998). The type XI collagenopathies. *Pediatr Radiol, 28*(10), 745-750.

Stanley, M. A. (2012). Epithelial cell responses to infection with human papillomavirus. *Clinical microbiology reviews, 25*(2), 215-222.

Stats, F. (2011). An interactive tool for access to SEER cancer statistics. *Surveillance Research Program, National Cancer Institute. Accessed on April, 11*.

Stein, A. P., Saha, S., Kraninger, J. L., Swick, A. D., Yu, M., Lambertg, P. F., & Kimple, R. (2015). Prevalence of human papillomavirus in oropharyngeal cancer: a systematic review. *Cancer journal (Sudbury, Mass.), 21*(3), 138.

Stransky, N., Egloff, A. M., Tward, A. D., Kostic, A. D., Cibulskis, K., Sivachenko, A., . . . McKenna, A. (2011). The mutational landscape of head and neck squamous cell carcinoma. *Science, 333*(6046), 1157-1160.

Su, K., & Wang, C. (2015). Recent advances in the use of gelatin in biomedical research. *Biotechnology letters, 37*(11), 2139-2145.

Sun, X., Gupta, K., Wu, B., Zhang, D., Yuan, B., Zhang, X., . . . Bendeck, M. P. (2018). Tumor-extrinsic discoidin domain receptor 1 promotes mammary tumor growth by regulatingadipose stromal interleukin 6 production in mice. *Journal of Biological Chemistry*, jbc. RA117. 000672.

Taberna, M., Mena, M., Pavón, M., Alemany, L., Gillison, M., & Mesía, R. (2017). Human papillomavirus related oropharyngeal cancer. *Annals of oncology*.

Taddei, M. L., Cavallini, L., Comito, G., Giannoni, E., Folini, M., Marini, A., . . . Raspollini, M. R. (2014). Senescent stroma promotes prostate cancer progression: The role of miR‐210. *Mol Oncol, 8*(8), 1729-1746.

Tafe, L. J. (2017). The Molecular Pathology of Head and Neck Squamous Cell Carcinoma *The Molecular Basis of Human Cancer* (pp. 589-601): Springer.

Tandon, P., Dadhich, A., Saluja, H., Bawane, S., & Sachdeva, S. (2017). The prevalence of squamous cell carcinoma in different sites of oral cavity at our Rural Health Care Centre in Loni, Maharashtra–a retrospective 10-year study. *Contemporary Oncology, 21*(2), 178.

Tang, X., Hou, Y., Yang, G., Wang, X., Tang, S., Du, Y., . . . Zhou, M. (2016). Stromal miR-200s contribute to breast cancer cell invasion through CAF activation and ECM remodeling. *Cell Death & Differentiation, 23*(1), 132-145.

Tangsadthakun, C., Kanokpanont, S., Sanchavanakit, N., Banaprasert, T., & Damrongsakkul, S. (2017). Properties of collagen/chitosan scaffolds for skin tissue engineering. *Journal of Metals, Materials and Minerals, 16*(1).

Team, R. C. (2016). R: A language and environment for statistical computing. R Foundation for Statistical Computing, Vienna, Austria. 2014.

Thavaraj, S., Stokes, A., Guerra, E., Bible, J., Halligan, E., Long, A., . . . Robinson, M. (2011). Evaluation of human papillomavirus testing for squamous cell carcinoma of the tonsil in clinical practice. *J Clin Pathol, 64*(4), 308-312.

Theocharis, A. D., Skandalis, S. S., Gialeli, C., & Karamanos, N. K. (2016). Extracellular matrix structure. *Advanced drug delivery reviews, 97*, 4-27.

Thibault, B., Castells, M., Delord, J.-P., & Couderc, B. (2014). Ovarian cancer microenvironment: implications for cancer dissemination and chemoresistance acquisition. *Cancer and Metastasis Reviews, 33*(1), 17-39.

Tinhofer, I., Budach, V., Saki, M., Konschak, R., Niehr, F., Jöhrens, K., . . . Krause, M. (2016). Targeted next-generation sequencing of locally advanced squamous cell carcinomas of the head and neck reveals druggable targets for improving adjuvant chemoradiation. *European journal of cancer, 57*, 78-86.

Torre, L. A., Bray, F., Siegel, R. L., Ferlay, J., Lortet‐Tieulent, J., & Jemal, A. (2015). Global cancer statistics, 2012. *CA Cancer J Clin, 65*(2), 87-108.

Toy, K. A., Valiathan, R. R., Núñez, F., Kidwell, K. M., Gonzalez, M. E., Fridman, R., & Kleer, C. G. (2015). Tyrosine kinase discoidin domain receptors DDR1 and DDR2 are coordinately deregulated in triple-negative breast cancer. *Breast Cancer Res Treat, 150*(1), 9-18.

Tseng, R. S. (2016). *High-risk HPV: From infection to cerivcal cancer progression*: The University of Arizona.

Ukpo, O. C., Thorstad, W. L., & Lewis, J. S. (2013). B7-H1 expression model for immune evasion in human papillomavirus-related oropharyngeal squamous cell carcinoma. *Head Neck Pathol, 7*(2), 113-121.

Valencia, K., Ormazabal, C., Zandueta, C., Luis-Ravelo, D., Anton, I., Pajares, M. J., . . . Lecanda, F. (2012). Inhibition of collagen receptor discoidin domain receptor-1 (DDR1) reduces cell survival, homing, and colonization in lung cancer bone metastasis. [Research Support, Non-U.S. Gov't]. *Clin Cancer Res, 18*(4), 969-980. doi: 10.1158/1078-0432.CCR-11-1686

Valiathan, R. R., Marco, M., Leitinger, B., Kleer, C. G., & Fridman, R. (2012). Discoidin domain receptor tyrosine kinases: new players in cancer progression. *Cancer and Metastasis Reviews, 31*(1-2), 295-321.

Van Bockstal, M., Lambein, K., Van Gele, M., De Vlieghere, E., Limame, R., Braems, G., . . . Bracke, M. (2014). Differential regulation of extracellular matrix protein expression in carcinoma-associated fibroblasts by TGF-β1 regulates cancer cell spreading but not adhesion. *Oncoscience, 1*(10), 634.

Van, J. A., Scholey, J. W., & Konvalinka, A. (2017). Insights into Diabetic Kidney Disease Using Urinary Proteomics and Bioinformatics. *Journal of the American Society of Nephrology, 28*(4), 1050-1061.

van Kempen, P. M., Noorlag, R., Braunius, W. W., Stegeman, I., Willems, S. M., & Grolman, W. (2014). Differences in methylation profiles between HPV-positive and HPV-negative oropharynx squamous cell carcinoma: a systematic review. *Epigenetics, 9*(2), 194-203.

Vázquez-Villa, F., García-Ocaña, M., Galván, J. A., García-Martínez, J., García-Pravia, C., Menéndez-Rodríguez, P., . . . Juan, R. (2015). COL11A1/(pro) collagen 11A1 expression is a remarkable biomarker of human invasive carcinoma-associated stromal cells and carcinoma progression. *Tumor Biology, 36*(4), 2213-2222.

Vella, V., Malaguarnera, R., Nicolosi, M. L., Palladino, C., Spoleti, C., Massimino, M., . . . Morrione, A. (2017). Discoidin domain receptor 1 modulates insulin receptor signaling and biological responses in breast cancer cells. *Oncotarget, 8*(26), 43248.

Vigneswaran, N., & Williams, M. D. (2014). Epidemiologic trends in head and neck cancer and aids in diagnosis. *Oral and Maxillofacial Surgery Clinics, 26*(2), 123-141.

Virdee, J. T., & Kalavrezos, N. (2016). Oral and Oropharyngeal Cancer. *Textbook of Plastic and Reconstructive Surgery*, 77.

Wahyudi, H., Reynolds, A. A., Li, Y., Owen, S. C., & Yu, S. M. (2016). Targeting collagen for diagnostic imaging and therapeutic delivery. *Journal of Controlled Release, 240*, 323-331.

Walden, M. J., & Aygun, N. (2013). *Head and neck cancer.* Paper presented at the Seminars in roentgenology.

Walker, D. M., Boey, G., & McDonald, L. A. (2003). The pathology of oral cancer. *Pathology, 35*(5), 376-383.

Walker, K. T., Nan, R., Wright, D. W., Gor, J., Bishop, A. C., Makhatadze, G. I., . . . Perkins, S. J. (2017). Non-linearity of the collagen triple helix in solution and implications for collagen function. *Biochemical Journal, 474*(13), 2203-2217.

Wang, B., Zhang, S., Yue, K., & Wang, X.-D. (2013). The recurrence and survival of oral squamous cell carcinoma: a report of 275 cases. *Chin J Cancer, 32*(11), 614.

Wang, C., Yeung, D., Wellerming, J., Herr, A., Miller, J., Fridman, R., & Agarwal, G. (2016). Role of DDR2 ECD Oligomerization in Binding to Collagen. *Microscopy and Microanalysis, 22*(S3).

Wang, H.-J., Li, M.-Q., Liu, W.-W., Hayashi, T., Fujisaki, H., Hattori, S., . . . Ikejima, T. (2017). Collagen gel protects L929 cells from TNFα-induced death by activating NF-κB. *Connective tissue research, 58*(5), 456-463.

Wang, T., Notta, F., Navab, R., Joseph, J., Ibrahimov, E., Xu, J., . . . Tsao, M.-S. (2017). Senescent carcinoma-associated fibroblasts upregulate IL8 to enhance prometastatic phenotypes. *Molecular cancer research, 15*(1), 3-14.

Wang, Z., Bian, H., Bartual, S. G., Du, W., Luo, J., Zhao, H., . . . Xu, Y. (2016). Structure-based design of tetrahydroisoquinoline-7-carboxamides as selective discoidin domain receptor 1 (DDR1) inhibitors. *J Med Chem, 59*(12), 5911-5916.

Wang, Z., Chen, G., Wang, Q., Lu, W., & Xu, M. (2017). Identification and validation of a prognostic 9-genes expression signature for gastric cancer. *Oncotarget, 8*(43), 73826.

Wang, Z., Sun, X., Bao, Y., Mo, J., Du, H., Hu, J., & Zhang, X. (2017). E2F1 silencing inhibits migration and invasion of osteosarcoma cells via regulating DDR1 expression. *Int J Oncol, 51*(6), 1639-1650.

Wei, Z.-W., Zhang, C.-H., & He, Y. (2017). P-0187rh, a novel selective discoidin domain receptor 1 (DDR1) inhibitor, enhances 5-fluorouracil response in gastric cancer. *Annals of oncology, 28*(suppl_3).

Welters, M. J., Ma, W., Santegoets, S. J., Goedemans, R., Ehsan, I., Jordanova, E. S., . . . van Egmond, S. I. (2017). Intratumoral HPV16-specific T-cells constitute a type 1 oriented tumor microenvironment to improve survival in HPV16-driven oropharyngeal cancer. *Clinical cancer research*, clincanres. 2140.2017.

Wenig, B. M. (2015). *Atlas of Head and Neck Pathology E-Book*: Elsevier Health Sciences.

Williams, C., Kinshuck, A., Derbyshire, S., Upile, N., Tandon, S., Roland, N., . . . Lancaster, J. (2014). Transoral laser resection versus lip-split mandibulotomy in the management of oropharyngeal squamous cell carcinoma (OPSCC): a case match study. *European Archives of Oto-Rhino-Laryngology, 271*(2), 367-372.

Wolff, K.-D., Follmann, M., & Nast, A. (2012). The diagnosis and treatment of oral cavity cancer. *Dtsch Arztebl Int, 109*(48), 829.

Woolgar, J. A., & Triantafyllou, A. (2009). Pitfalls and procedures in the histopathological diagnosis of oral and oropharyngeal squamous cell carcinoma and a review of the role of pathology in prognosis. *Oral Oncol, 45*(4), 361-385.

Wu, C. L., Roz, L., McKown, S., Sloan, P., Read, A. P., Holland, S., . . . Tavassoli, M. (1999). DNA studies underestimate the major role of CDKN2A inactivation in

oral and oropharyngeal squamous cell carcinomas. *Genes, Chromosomes and Cancer, 25*(1), 16-25.

Wu, L., Deng, W.-W., Yu, G.-T., Mao, L., Bu, L.-L., Ma, S.-R., . . . Sun, Z.-J. (2016). B7-H4 expression indicates poor prognosis of oral squamous cell carcinoma. *Cancer Immunology, Immunotherapy, 65*(9), 1035-1045.

Wu, Y. H., Huang, Y. F., Chang, T. H., & Chou, C. Y. (2017). Activation of TWIST1 by COL11A1 promotes chemoresistance and inhibits apoptosis in ovarian cancer cells by modulating NF‐κB‐mediated IKKβ expression. *Int J Cancer, 141*(11), 2305-2317.

Xiao, Q., Jiang, Y., Liu, Q., Yue, J., Liu, C., Zhao, X., . . . Ge, G. (2015). Minor Type IV Collagen α5 Chain promotes cancer progression through discoidin domain receptor-1. *PLoS genetics, 11*(5), e1005249.

Xie, R., Wang, X., Qi, G., Wu, Z., Wei, R., Li, P., & Zhang, D. (2016). DDR1 enhances invasion and metastasis of gastric cancer via epithelial-mesenchymal transition. *Tumor Biology, 37*(9), 12049-12059.

Xie, X., Rui, W., He, W., Shao, Y., Sun, F., Zhou, W., . . . Zhu, Y. (2017). Discoidin domain receptor 1 activity drives an aggressive phenotype in bladder cancer. *American journal of translational research, 9*(5), 2500.

Yang, J.-c., Zhang, Y., He, S.-j., Li, M.-m., Cai, X.-l., Wang, H., . . . Cao, J. (2017). TM4SF1 Promotes Metastasis of Pancreatic Cancer via Regulating the Expression of DDR1. *Sci Rep, 7*, 45895.

Yang, P. (2017). *Suppression of ADAM23 is functionally associated with HPV-mediated carcinogenesis.* University of California, Los Angeles.

Yap, L. F., Lai, S. L., Patmanathan, S. N., Gokulan, R., Robinson, C. M., White, J. B., . . . Liew, Y. T. (2016). HOPX functions as a tumour suppressor in head and neck cancer. *Sci Rep, 6*, 38758.

Ye, J., Wu, D., Wu, P., Chen, Z., & Huang, J. (2014). The cancer stem cell niche: cross talk between cancer stem cells and their microenvironment. *Tumor Biology, 35*(5), 3945-3951.

Yeudall, W., Paterson, I., Patel, V., & Prime, S. (1995). Presence of human papillomavirus sequences in tumour-derived human oral keratinocytes expressing mutant p53. *Oral Oncol, 31*(2), 136-143.

Yeudall, W., Torrance, L., Elsegood, K., Speight, P., Scully, C., & Prime, S. (1993). Ras gene point mutation is a rare event in premalignant tissues and malignant cells and tissues from oral mucosal lesions. *European Journal of Cancer Part B: Oral Oncology, 29*(1), 63-67.

Yeung, D., Chmielewski, D., Mihai, C., & Agarwal, G. (2013). Oligomerization of DDR1 ECD affects receptor–ligand binding. *Journal of structural biology, 183*(3), 495-500.

Young, D., Xiao, C. C., Murphy, B., Moore, M., Fakhry, C., & Day, T. A. (2015). Increase in head and neck cancer in younger patients due to human papillomavirus (HPV). *Oral Oncol, 51*(8), 727-730.

Yuge, R., Kitadai, Y., Takigawa, H., Tanaka, S., Chayama, K., & Yasui, W. (2017). Inhibition of collagen receptor discoidin domain receptor-1 (DDR1) reduces gastric cancer cell motility and metastasis: AACR.

Zaravinos, A. (2014). An updated overview of HPV-associated head and neck carcinomas. *Oncotarget, 5*(12), 3956.

Zevallos, J. P., Mazul, A. L., Rodriguez, N., Weissler, M. C., Brennan, P., Anantharaman, D., . . . Olshan, A. F. (2016). Previous tonsillectomy modifies odds of tonsil and base of tongue cancer. *Br J Cancer, 114*(7), 832-838.

Zhang, C., Deng, Z., Pan, X., Uehara, T., Suzuki, M., & Xie, M. (2015). Effects of methylation status of CpG sites within the HPV16 long control region on HPV16-positive head and neck cancer cells. *PLoS One, 10*(10), e0141245.

Zhang, D., Zhu, H., & Harpaz, N. (2016). Overexpression of α1 chain of type XI collagen (COL11A1) aids in the diagnosis of invasive carcinoma in endoscopically removed malignant colorectal polyps. *Pathology-Research and Practice, 212*(6), 545-548.

Zhang, J., & Liu, J. (2013). Tumor stroma as targets for cancer therapy. *Pharmacology & therapeutics, 137*(2), 200-215.

Zhang, X., Wu, J., Luo, S., Lechler, T., & Zhang, J. Y. (2016). FRA1 promotes squamous cell carcinoma growth and metastasis through distinct AKT and c-Jun dependent mechanisms. *Oncotarget, 7*(23), 34371.

Zhu, C.-c., Tang, B., Su, J., Zhao, H., Bu, X., Li, Z., . . . Yao, L.-b. (2015). Abnormal accumulation of collagen type I due to the loss of Discoidin domain receptor 2 (Ddr2) promotes testicular interstitial dysfunction. *PLoS One, 10*(7), e0131947.

Zhu, Y., Shen, J., & Xiao, Z. (2017). B7 Gene Family: Promising Immunotherapeutic Checkpoint in Cancers. *Clin Oncol, 2*, 1199.

Ziaee, S., Chu, G. C.-Y., Huang, J.-M., Sieh, S., & Chung, L. W. (2015). Prostate cancer metastasis: roles of recruitment and reprogramming, cell signal network and three-dimensional growth characteristics. *Translational andrology and urology, 4*(4), 438.

Zum Gottesberge, A. M., & Hansen, S. (2014). The collagen receptor DDR1 co-localizes with the non-muscle myosin IIA in mice inner ear and contributes to the

cytoarchitecture and stability of motile cells. *Cell and tissue research, 358*(3), 729-736.

LIST OF PUBLICATIONS

Articles published:

1. Patmanathan SN, Johnson SP, **Lai SL**, Panja Bernam S, Lopes V, Wei W, Ibrahim MH, Torta F, Narayanaswamy P, Wenk MR, Herr DR, Murray PG, Yap LF, Paterson IC. Aberrant expression of the S1P regulating enzymes, SPHK1 and SGPL1, contributes to a migratory phenotype in OSCC mediated through S1PR2. Scientific Reports (ISI Journal). 2016 May 10; 10.1038/srep25650.
2. Lee Fah Yap, **Sook Ling Lai**, Patmanathan SN, Gokulan Ravindran, C Max Robinson, Joe White, SJ Chai, Pathmanathan Rajadurai, Wenbin Wei, Robert J Hollows, Paul G Murray, Daniel W Lambert, Keith D Hunter, Ian C Paterson. HOPX functions as a tumour suppressor in head and neck cancer. Scientific Reports (ISI Journal). 2016 Dec 9; 10.1038/srep38758.

Articles in progress for submission:

1. Lee Fah Yap, **Sook Ling Lai**, Anthony Rhodes, Hans Prakash Sathasivam, Maizaton Atmadini Abdullah, Kin-Choo Pua, Pathmanathan Rajadurai, Selvam Thavaraj, C. Max Robinson, Ian C. Paterson. HPV status and clinico-pathological features of oropharyngeal squamous cell carcinomas in Malaysia. Submitted to Infectious Agent and Cancer (ISI Journal).
2. **Sook Ling Lai**, Maha Ibrahim, Paul G Murray, Hisham Mehanna, Neeraj Lal, C Max Robinson, Robert J Hollows, Wenbin Wei, Rachel J Watkins, Adnan Ramanathan, Mohammad Zain, Ivy Chung, Lee Fah Yap, Ian C Paterson. The

Role of DDR1 in Head and Neck Cancer. Manuscript will be submitted to The Journal of Pathology (ISI Journal).

www.nature.com/scientificreports

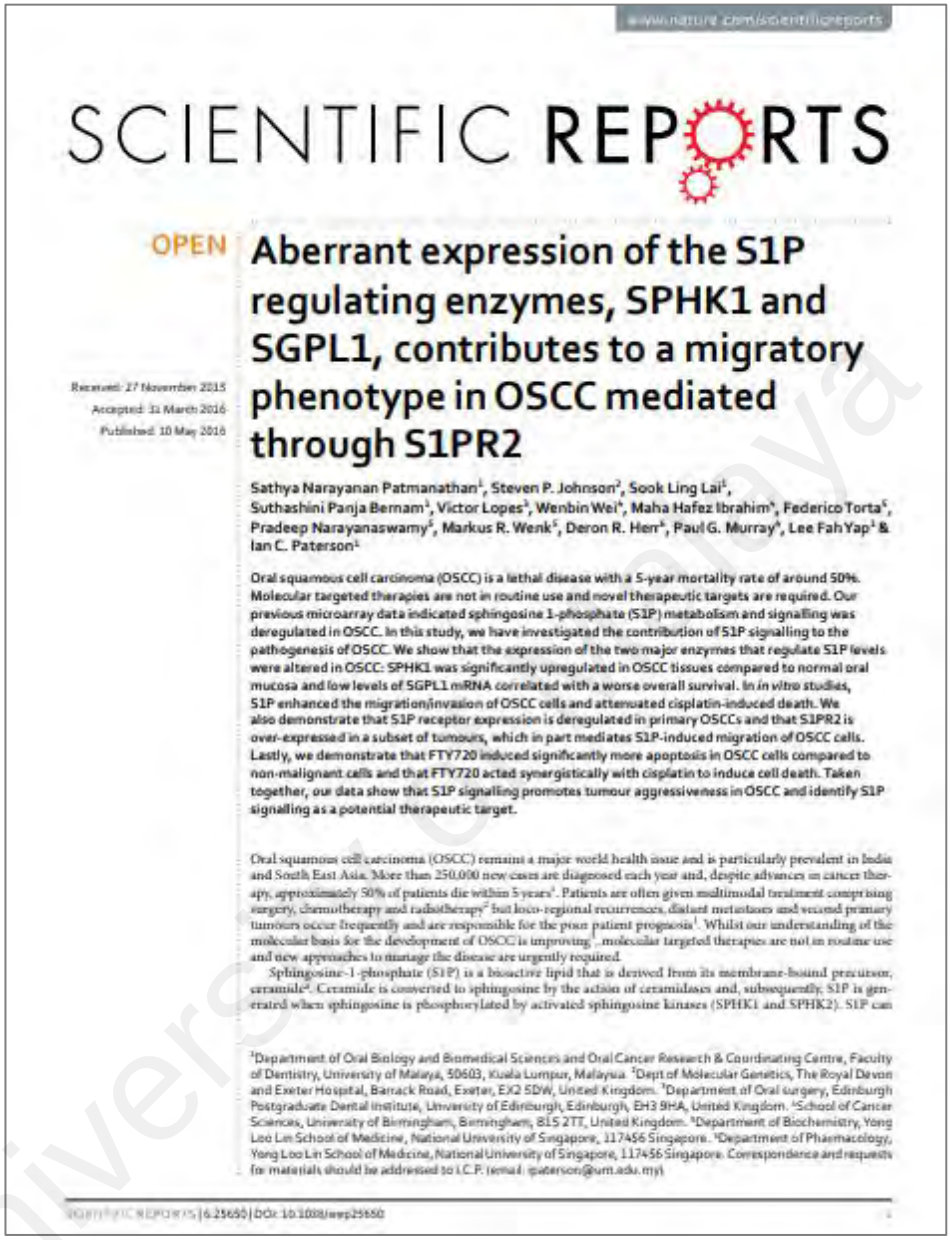

SCIENTIFIC REPORTS

OPEN

Aberrant expression of the S1P regulating enzymes, SPHK1 and SGPL1, contributes to a migratory phenotype in OSCC mediated through S1PR2

Received: 27 November 2015
Accepted: 31 March 2016
Published: 10 May 2016

Sathya Narayanan Patmanathan[1], Steven P. Johnson[2], Sook Ling Lai[1], Suthashini Panja Bernam[1], Victor Lopes[3], Wenbin Wei[3], Maha Hafez Ibrahim[4], Federico Torta[5], Pradeep Narayanaswamy[5], Markus R. Wenk[5], Deron R. Herr[4], Paul G. Murray[6], Lee Fah Yap[1] & Ian C. Paterson[1]

Oral squamous cell carcinoma (OSCC) is a lethal disease with a 5-year mortality rate of around 50%. Molecular targeted therapies are not in routine use and novel therapeutic targets are required. Our previous microarray data indicated sphingosine 1-phosphate (S1P) metabolism and signalling was deregulated in OSCC. In this study, we have investigated the contribution of S1P signalling to the pathogenesis of OSCC. We show that the expression of the two major enzymes that regulate S1P levels were altered in OSCC: SPHK1 was significantly upregulated in OSCC tissues compared to normal oral mucosa and low levels of SGPL1 mRNA correlated with a worse overall survival. In *in vitro* studies, S1P enhanced the migration/invasion of OSCC cells and attenuated cisplatin-induced death. We also demonstrate that S1P receptor expression is deregulated in primary OSCCs and that S1PR2 is over-expressed in a subset of tumours, which in part mediates S1P-induced migration of OSCC cells. Lastly, we demonstrate that FTY720 induced significantly more apoptosis in OSCC cells compared to non-malignant cells and that FTY720 acted synergistically with cisplatin to induce cell death. Taken together, our data show that S1P signalling promotes tumour aggressiveness in OSCC and identify S1P signalling as a potential therapeutic target.

Oral squamous cell carcinoma (OSCC) remains a major world health issue and is particularly prevalent in India and South East Asia. More than 250,000 new cases are diagnosed each year and, despite advances in cancer therapy, approximately 50% of patients die within 5 years[1]. Patients are often given multimodal treatment comprising surgery, chemotherapy and radiotherapy[2] but loco-regional recurrences, distant metastases and second primary tumours occur frequently and are responsible for the poor patient prognosis[1]. Whilst our understanding of the molecular basis for the development of OSCC is improving[3], molecular targeted therapies are not in routine use and new approaches to manage the disease are urgently required.

Sphingosine-1-phosphate (S1P) is a bioactive lipid that is derived from its membrane-bound precursor, ceramide[4]. Ceramide is converted to sphingosine by the action of ceramidases and, subsequently, S1P is generated when sphingosine is phosphorylated by activated sphingosine kinases (SPHK1 and SPHK2). S1P can

[1]Department of Oral Biology and Biomedical Sciences and Oral Cancer Research & Coordinating Centre, Faculty of Dentistry, University of Malaya, 50603, Kuala Lumpur, Malaysia. [2]Dept of Molecular Genetics, The Royal Devon and Exeter Hospital, Barrack Road, Exeter, EX2 5DW, United Kingdom. [3]Department of Oral surgery, Edinburgh Postgraduate Dental Institute, University of Edinburgh, Edinburgh, EH3 9HA, United Kingdom. [4]School of Cancer Sciences, University of Birmingham, Birmingham, B15 2TT, United Kingdom. [5]Department of Biochemistry, Yong Loo Lin School of Medicine, National University of Singapore, 117456 Singapore. [6]Department of Pharmacology, Yong Loo Lin School of Medicine, National University of Singapore, 117456 Singapore. Correspondence and requests for materials should be addressed to I.C.P. (email: ipaterson@um.edu.my)

www.nature.com/scientificreports

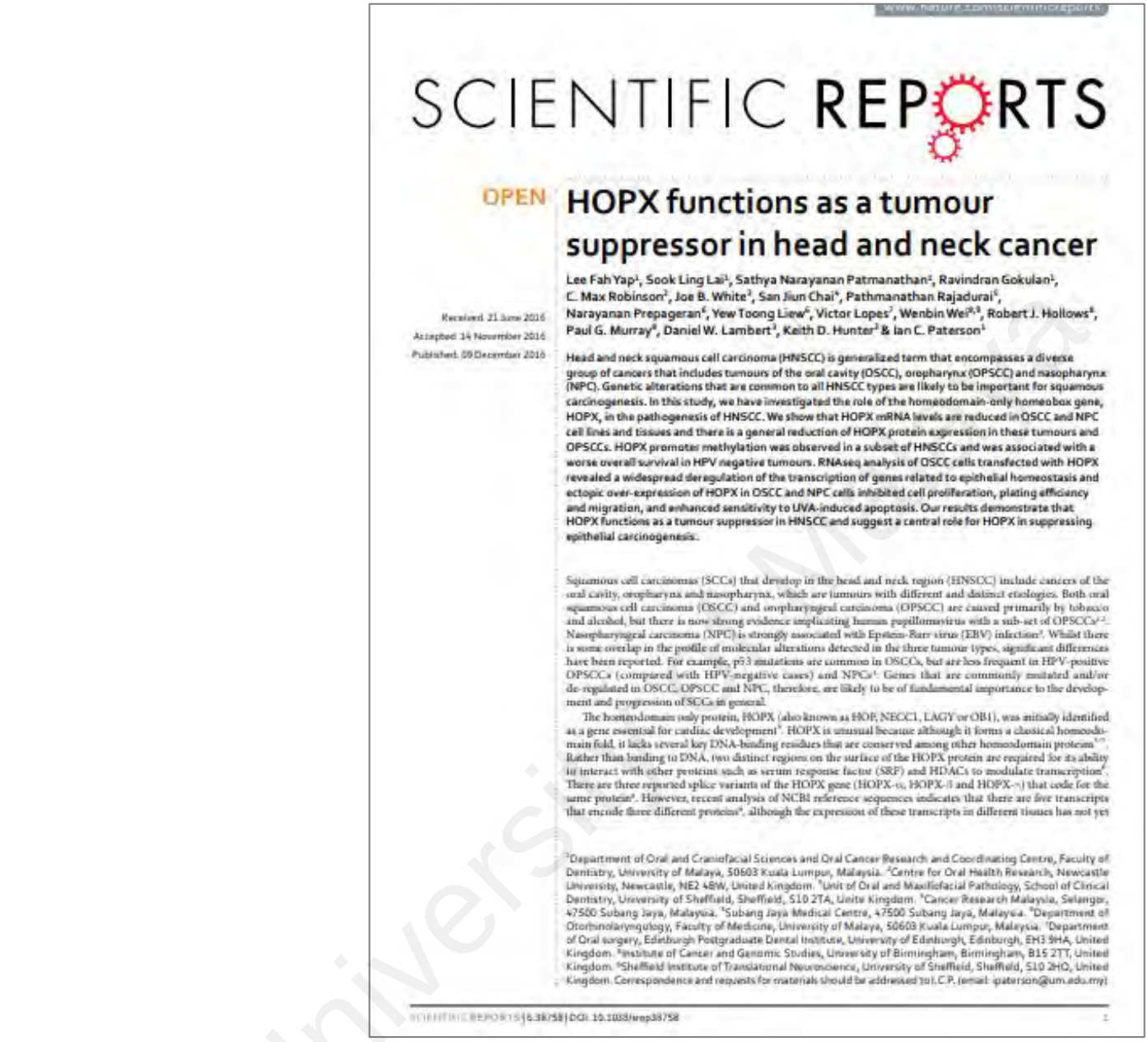

OPEN

HOPX functions as a tumour suppressor in head and neck cancer

Lee Fah Yap[1], Sook Ling Lai[1], Sathya Narayanan Patmanathan[1], Ravindran Gokulan[1], C. Max Robinson[2], Joe B. White[3], San Jiun Chai[4], Pathmanathan Rajadurai[5], Narayanan Prepageran[6], Yew Toong Liew[6], Victor Lopes[7], Wenbin Wei[8,9], Robert J. Hollows[8], Paul G. Murray[8], Daniel W. Lambert[3], Keith D. Hunter[3] & Ian C. Paterson[1]

Received: 21 June 2016
Accepted: 14 November 2016
Published: 09 December 2016

Head and neck squamous cell carcinoma (HNSCC) is generalized term that encompasses a diverse group of cancers that includes tumours of the oral cavity (OSCC), oropharynx (OPSCC) and nasopharynx (NPC). Genetic alterations that are common to all HNSCC types are likely to be important for squamous carcinogenesis. In this study, we have investigated the role of the homeodomain-only homeobox gene, HOPX, in the pathogenesis of HNSCC. We show that HOPX mRNA levels are reduced in OSCC and NPC cell lines and tissues and there is a general reduction of HOPX protein expression in these tumours and OPSCCs. HOPX promoter methylation was observed in a subset of HNSCCs and was associated with a worse overall survival in HPV negative tumours. RNAseq analysis of OSCC cells transfected with HOPX revealed a widespread deregulation of the transcription of genes related to epithelial homeostasis and ectopic over-expression of HOPX in OSCC and NPC cells inhibited cell proliferation, plating efficiency and migration, and enhanced sensitivity to UVA-induced apoptosis. Our results demonstrate that HOPX functions as a tumour suppressor in HNSCC and suggest a central role for HOPX in suppressing epithelial carcinogenesis.

Squamous cell carcinomas (SCCs) that develop in the head and neck region (HNSCC) include cancers of the oral cavity, oropharynx and nasopharynx, which are tumours with different and distinct etiologies. Both oral squamous cell carcinoma (OSCC) and oropharyngeal carcinoma (OPSCC) are caused primarily by tobacco and alcohol, but there is now strong evidence implicating human papillomavirus with a sub-set of OPSCCs[1,2]. Nasopharyngeal carcinoma (NPC) is strongly associated with Epstein-Barr virus (EBV) infection[3]. Whilst there is some overlap in the profile of molecular alterations detected in the three tumour types, significant differences have been reported. For example, p53 mutations are common in OSCCs, but are less frequent in HPV-positive OPSCCs (compared with HPV-negative cases) and NPCs[4]. Genes that are commonly mutated and/or de-regulated in OSCC, OPSCC and NPC, therefore, are likely to be of fundamental importance to the development and progression of SCCs in general.

The homeodomain only protein, HOPX (also known as HOP, NECC1, LAGY or OB1), was initially identified as a gene essential for cardiac development[5]. HOPX is unusual because although it forms a classical homeodomain fold, it lacks several key DNA-binding residues that are conserved among other homeodomain proteins[6,7]. Rather than binding to DNA, two distinct regions on the surface of the HOPX protein are required for its ability to interact with other proteins such as serum response factor (SRF) and HDACs to modulate transcription[8]. There are three reported splice variants of the HOPX gene (HOPX-α, HOPX-β and HOPX-γ) that code for the same protein[9]. However, recent analysis of NCBI reference sequences indicates that there are five transcripts that encode three different proteins[9], although the expression of these transcripts in different tissues has not yet

[1]Department of Oral and Craniofacial Sciences and Oral Cancer Research and Coordinating Centre, Faculty of Dentistry, University of Malaya, 50603 Kuala Lumpur, Malaysia. [2]Centre for Oral Health Research, Newcastle University, Newcastle, NE2 4BW, United Kingdom. [3]Unit of Oral and Maxillofacial Pathology, School of Clinical Dentistry, University of Sheffield, Sheffield, S10 2TA, Unite Kingdom. [4]Cancer Research Malaysia, Selangor, 47500 Subang Jaya, Malaysia. [5]Subang Jaya Medical Centre, 47500 Subang Jaya, Malaysia. [6]Department of Otorhinolaryngology, Faculty of Medicine, University of Malaya, 50603 Kuala Lumpur, Malaysia. [7]Department of Oral surgery, Edinburgh Postgraduate Dental Institute, University of Edinburgh, Edinburgh, EH3 9HA, United Kingdom. [8]Institute of Cancer and Genomic Studies, University of Birmingham, Birmingham, B15 2TT, United Kingdom. [9]Sheffield Institute of Translational Neuroscience, University of Sheffield, Sheffield, S10 2HQ, United Kingdom. Correspondence and requests for materials should be addressed to I.C.P. (email: ipaterson@um.edu.my)

LIST OF PRESENTATIONS AND AWARDS

1. S.L. Lai, M.H. Ibrahim, P.G. Murray, H. Mehanna, N. Lal, A. Ramanathan, R. Zain, I. Chung, L.F. Yap, I.C. Paterson. Differential expression of the collagen receptor, DDR1, and collagens XIa1 andVIIIa1 in HPV-negative and –positive oropharyngeal papillomavirus. Presented: 2nd ICGEB Workshop on "Human papillomavirus: From Basic Biology to Cancer Prevention", Prince of Wales Hospital, Hong Kong (8th – 10th Nov 2016). **Award: Best Oral Presentation**.
2. S.L. Lai, M.H. Ibrahim, P.G. Murray, H. Mehanna, N. Lal, A. Ramanathan, R. Zain, I. Chung, L.F. Yap, I.C. Paterson. Is collagen a culprit in Oropharnygeal Cancer? Presented: 3-Minutes-Thesis Competition of Inter-faculty of Dentistry & Institute of Graduate Studies Level Year 2017. Institute of Graduate Studies, University of Malaya (6th March 2017). **Award: Champion**.
3. S.L. Lai, M.H. Ibrahim, P.G. Murray, H. Mehanna, N. Lal, A. Ramanathan, R. Zain, I. Chung, L.F. Yap, I.C. Paterson. Collagen-DDR1 Signalling in HPV-negative and –positive Oropharnygeal Cancer. Presented: 3-Minutes-Thesis Competition of University Level Year 2017. University of Malaya (22nd March 2017). **Award: Champion**.
4. S.L. Lai, M.H. Ibrahim, P.G. Murray, H. Mehanna, N. Lal, A. Ramanathan, R. Zain, I. Chung, L.F. Yap, I.C. Paterson. Is collagen a culprit in Oropharnygeal Cancer? Presented: 3-Minutes-Thesis Competition of National Level Year 2017. University Sains Malaya (16th May 2017). **Award: 3rd Prize.**
5. S.L. Lai, I. Chung, I.C. Paterson. CAFs as the chemoresistance mediator in oral squamous cell carcinoma. Presented: PhD Proposal Seminar, University of Malaya (3rd September 2014).

6. S.L. Lai, M.H. Ibrahim, P.G. Murray, H. Mehanna, N. Lal, I. Chung, L.F. Yap, I.C. Paterson. Investigation of the role of tumour microenvironment in pathogenesis of head and neck cancer. Presented: Mini-seminar, University of Birmingham, United Kingdom (30th May 2015).
7. S.L. Lai, M.H. Ibrahim, P.G. Murray, H. Mehanna, N. Lal, A. Ramanathan, R. Zain, I. Chung, L.F. Yap, I.C. Paterson. Analysis of the collagens-DDR1 signalling pathway in oropharyngeal cancer. Poster presented: PHD Candidature Defence, University of Malaya (29th Spet 2016).
8. S.L. Lai, M.H. Ibrahim, P.G. Murray, H. Mehanna, N. Lal, A. Ramanathan, R. Zain, I. Chung, L.F. Yap, I.C. Paterson. Analysis of the collagens-DDR1 signalling pathway in oropharyngeal cancer. Poster presented: Dental Congregation 2016, Hotel Royale Chulan Damansara (13th & 14th August 2016).
9. S.L. Lai, M.H. Ibrahim, P.G. Murray, H. Mehanna, N. Lal, A. Ramanathan, R. Zain, I. Chung, L.F. Yap, I.C. Paterson. Analysis of the collagens-DDR1 signalling pathway in oropharyngeal cancer. Poster presented: IADR MalSec 16th Annual Scientific Meeting 2017, Royale Chulan Damansara (18th March 2017).
10. S.L. Lai, I. Chung, I.C. Paterson. Collagen-DDR1 Signalling in HPV-positive and –negative Head and Neck Cancer. Presented: PhD Thesis Seminar, University of Malaya (9th April 2018).